AUTOMATIC GENERATION CONTROL OF INTERCONNECTED MULTI AREA POWER SYSTEM

A Thesis Submitted in Partial Fulfillment of the Requirements
for the Award of the Degree of

DOCTOR OF PHILOSOPHY

Submitted by

NIDHI GUPTA
(Enrollment No. 2K11/PhD/EE/09)

Under the Supervision of

Prof. NARENDRA KUMAR
(Professor, Department of Electrical Engineering, DTU, Delhi)

Prof. T. S. BHATTI
(Professor, Centre of Energy Studies, IIT, Delhi)

Department of Electrical Engineering

Delhi Technological University
Bawana Road, Delhi-110042
May, 2022

CANDIDATE'S DECLARATION

I hereby certify that the work which is being presented in this thesis entitled **"Automatic Generation Control of Interconnected Multi Area Power System"** submitted in partial fulfilment of the requirements for the award of the degree of Doctor of Philosophy in the Department of Electrical Engineering, Delhi Technological University, Delhi. This is an authentic record of my own work carried out under the supervision of Dr. Narendra Kumar, Professor, Department of Electrical Engineering. The matter presented in this thesis has not been submitted elsewhere for the award of a degree.

Place: Delhi

(NIDHI GUPTA
(Enrollment No. 2K11/PhD/EE/09)

Date: 10-05-2022

CERTIFICATE

On the basis of candidate"s declaration, I hereby certify that the thesis entitled **"Automatic Generation Control of Interconnected Multi Area Power System"** submitted to the Department of Electrical Engineering, Delhi Technological University, Delhi in partial fulfilment of the requirements for the award of degree of Doctor of Philosophy, is an original contribution with the existing knowledge and faithful record of the research work carried out by her under my guidance and supervision.

To the best of my knowledge, this work has not been submitted in part or full for the award of any degree elsewhere.

Dr. Narendra Kumar-I
Former Head & Professor
Department of Electrical Engineering
Delhi Technological University
Bawana road, Delhi-110042, India

The Ph.D. viva-voce of Ms. Nidhi Gupta, research scholar has been held on ……………

Prof. Narendra Kumar
Supervisor

External
Examiner

Prof. Uma Nagia
Head, Dept. of Electrical
Engg.

ACKNOWLEDGEMENTS

I am at a deficiency of words to depict sufficiently the inspiration and backing I have got from Prof. Pramod Kumar all through my exploration work. He and his unrestricted help were consistently with me during this exploration work.

I thank the college management of my institute for deputing me to pursue Ph.D. degree.

The completion of this work came at the expense of my long hours of absence from home. No words are adequate to express my indebtedness to my family to bring me up to this stage. I am extremely thankful to all my friends and special thanks to my cousin grand mother and grand father for their sincere good wishes.

Nidhi Gupta
(Enrollment No. 2K11/PhD/EE/09)

ABSTRACT

Currently, power system operation and control with AGC are undergoing fundamental changes due to rapidly increasing amount of renewable sources, energy storage system, restructuring and emerging of new types of power generation, consumption and power electronics technologies. Continuous growth in size and complexity, stochastically changing power demands, system modeling errors, alterations in electric power system structures and variations in the system parameters over the time has turned AGC task into a challenging one. Infrastructure of the intelligent power system should effectively support the provision of auxiliary services such as an AGC system from various sources through intelligent schemes. Literature survey shows that performance of AGC of interconnected power system with diverse sources gets improved by changing in controller structure, using intelligent optimization techniques for controller parameters, adding storage system and by considering different participation of diverse sources in multi area power systems. Hence, proposing and implementing new controller approaches using high performance heuristic optimization algorithms to real world problems are always welcomed. Researchers are devising various optimization Algorithms with different behaviors in various systems. Widespread review of the taxonomy of optimization algorithms in power system is explored in this study. Most popular nature inspired algorithm is population based algorithm which has a set of solution which moves towards the goal all together. Meta-Heuristic Algorithm is divided into two important groups as trajectory based and population based. Population based algorithm are further divided into six groups depending on bio-inspired, physics, chemistry, social human behavior, plant

characteristics. Review of various population based algorithm in application to frequency control is studied. Also, critical review of AGC schemes in interconnected multi area power system with diverse sources is done. Performance of many controllers depends on proper selection of certain algorithms and specific control parameters. Hence, the goal of the present study is to propose different types of new supplementary controller to achieve better dynamic performances in multi-area interconnected power system with diverse sources. Based on the extensive literature review on the control designs of AGC of interconnected power system, it has been felt that new control techniques for design of AGC regulators for interconnected power system especially for renewable sources is always welcome and challenging for researchers. The problem of nonlinearity in interconnected power system with diverse sources has also been addressed with suitable control algorithms. The study is conducted by proposing novel human based nature inspired artificial intelligence (AI) technique - Jaya for AGC of two area interconnected thermal-hydro-gas power system with varying participation of sources. Comparative analysis of proposed Jaya based AGC with bio-inspired AI technique like BAT and recently published Bacterial Forging Optimization (BFO) technique justify the stability of controller. The controllers are compared in terms of dynamic response, performance index value and performance. Regular increase in energy demand made the researchers to work towards the realistic hybrid interconnected multi source power system. Undesirable behavior of renewable sources likes hydro and wind is regularly amended by researchers through incorporating different artificial techniques, energy sources, varying participation of sources etc.To make the system realistic, researchers studied nonlinearities and participation factors incorporation in power system. Novel Jaya

based AI technique is further employed on realistic power system by considering non linearities like Governor Dead band (GDB), Generation Rate Constraint (GRC) and Boiler dynamics. The study is done on Jaya based AGC of two area interconnected thermal-hydro-wind and thermal-hydro-diesel power system with and without nonlinearities by considering step load and random perturbation at different control areas. By proper selection of AI technique based controller for AGC of interconnected multi area multi source power system gives the opportunity to works well with nonlinearities also. Using novel Jaya based PID parameter values, two area interconnected multi source power system without nonlinearities are simulated and set against other bio-inspired based AI techniques like bio inspired IPSO, PSO and BFA and social human behavior based TLBO algorithm.

Modern control theory helps in achieving the main objectives of AGC by effective design strategy. Design of optimal AGC regulator is explored for three area interconnected multi source power system with suitable structures of weighting matrices. Linear quadratic regulator (LQR) owns the top spot for Optimal AGC regulator design. The choice of weighting matrices propels the improvement in dynamic performance and stability of system. Designing of optimal AGC regulator for three different three-area interconnected multi source power systems has been planned. In each power system, optimal AGC regulators have been designed by using different structures of cost weighting matrices (Q an R). Three different structures of cost weighting matrices have been inspected for the design of optimal AGC regulators. One of the novel approaches for design of cost weighting matrices is based on the scaling method. To validate the effectiveness of optimal AGC regulator with structures of control and state cost weighting matrices, dynamic response of system for frequency

and tie line power deviation is procured with 1% slp in each area. Optimal feedback gain matrix, eigen values, dynamic response characteristics and dynamic responses are the assessment to examine the stability of power system. The investigation carried out reveal that optimal AGC regulator based on structures of control and state cost weighting matrices with scaling method offer remarkable improvement in dynamic stability as compared to other designed regulators.

Implementation of Superconducting Magnetic Energy Storage System (SMES) in operation and control of AGC of three-area multi source power systems has been studied. Analysis of PSO tuned Integral controller for AGC of three area interconnected multi source power systems with and without SMES by considering step load perturbation at different control areas has bee done. Comparative performance of different bio-inspired artificial technique has been presented on AGC of three area interconnected power system with SMES. With the use of SMES in power system, significant improvement in the dynamic responses of power system has been observed .Degradation of system due to the presence of hydro sources in interconnected multi source power system with SMES is noticeably reduced by considering 1% slp in all area as compared to 1% slp in individually areas.

Battery Energy Storage System (BESS) has the feature are to provide and absorb power at the time of load disturbances and have ability to charge and discharge in short span. AGC of three area multi source interconnected power systems by including and excluding Battery Energy Storage System (BESS) at step load perturbation in different control areas has been studied. Application of BESS in power system certainly helps the power system to achieve AGC objectives in astonishingly quick response time even with reneweable sources.

CONTENTS

LIST OF FIGURES

xiv

xvii

LIST OF TABLES

NOMENCLATURE

Symbols   **Name of the parameter/constant**

ΔF_n System frequency deviation of nth area

R_n Speed regulation of generator of nth area

P_{rn} Rated power system capacity of nth area

T_{gn} Time constant of speed governor of nth area

T_{tn} Time constant of reheat thermal turbine of nth area

T_{Pn} Power system Time constant of nth area

T_{Wn} Water turbine for hydraulic turbine

K_{pn} Power system gain of nth area

ΔP_{Gn} Change in generated power of nth area

ΔP_{Dn} Change in load demand of nth area

ΔP_{Cn} Change in speed governor of nth area

ΔX_{RH} Incremental change in mechanical governor

ΔP_{tie} Tie-line power deviation

T_{ij} Synchronizing coefficient for tie-line

ACE_n Area Controller Error of nth area

b_n Bias constant of nth area

s Laplace operator

n Control area

ΔX_{En} Incremental change in governor valve position change.

ΔX_{hn} Incremental change in hydraulic governor

ΔP_{FCn} Incremental change in Fuel system and combustor

ΔP_{Vn} Incremental change in Gas valve position

ΔX_{gn} Incremental change in Gas turbine speed governor

iter   Maximum number of iteration

K_{pn} Proportional parameters of nth area

K_{In} Integral parameters of nth area

K_{Dn} Derivative parameters of nth area

p   Population size

m   Design variables

rand   Random number lies between [0,1]

x_i , v_i Position and velocity at i^{th} iteration

Q_i Pulse frequency of bat at i^{th} iteration

r_i Pulse rate at i^{th} iteration

A_i Loudness at i^{th} iteration

X   State vector of system

U   Control vector of system

P_d Disturbance vector of system

Y   Output vector of system

A   System matrix

B   Control matrix

Γ Disturbance matrix

C   Output matrix

Q   Positive semi-definite symmetric state cost weighting matrix

R   Positive definite symmetric control cost weighting matrix

K   Optimal feedback gain matrix

J   Performance Index

r_{bl} Overvoltage resistance in BESS

r_{bp} Self discharge resistance in BESS

$\propto$ Firing angle of converter

C_{bp} Battery capacitance

X_{c0} Commutating resistance

K_{BESS} Control gain parameter of BESS

T_{BESS} Time constant of control loop in BESS

R_{Ds} Equivalent commutating resistance in SMES

ΔE_{ds} Voltage deviation across inductor in SMES

ΔI_{ds} Current deviation across inductor in SMES

ΔPSM Power flow deviation in SMES

T_{dcs} Converter time delay

K_{so} Gain of the control loop in SMES

L Coil inductance

I_{dso} Inductor current

E_{dso} Inductor voltage

K_{Ids} Negative current feedback gain

CHAPTER 1

INTRODUCTION

1.1   General

Electrical energy plays a vital role in human life. One of the most important functions in maintaining the quality of electrical power other than storing electricity is to maintain the required operating level of frequency under variable load conditions called load frequency control. A balance between energy demand and energy production is needed to provide electricity to consumers reliably. These days it has become a very difficult task to achieve the required levels of energy due to the increasing demand for electricity together with environmental problems. The interconnection of the various generating plants through the power system grid stabilizes the variation in frequency to a great extent by enhancing the system inertia [1]. Power system consists of interconnected multi area diverse power sources which offer power to the consumers at rated voltage and frequency. So, interconnected power system enables benefits in terms of both economic and environment issues [2]. Further, power system is interconnected with other areas for better operation and control, minimization of reserve capacity and reliability in power transmission and distribution.

Multi areas are interconnected by network of transmission lines and each control area represents coherent groups of generators of diverse sources which are also

associated with local production stations and local load areas. The main purpose of power system is to deliver reliable energy to the load centres.

Modern power system has become highly complex with the uncertainty deterministic system [3]. Also, it comprises of multi sources such as conventional fossil fuel plants, hydro plants, pumped storage plants, gas turbine plants, and non-conventional plants such as photo-voltaic, wind turbine, etc. Dynamism in power system due to load variations and other types of transient disturbances cause the frequency variations continuously. However, if the frequency variation of the deficit area continues to grow then automatic generation control (AGC) needs to be operated to stabilize the frequency and tie line power of the interconnected system.

1.2   Automatic generation control (AGC)

Automatic Generation Control (AGC) is defined by IEEE as the regulation of the power output of electric generators within a prescribed area in response to changes in system frequency, tie-line loading or the regulation of these to each other, so as to maintain the scheduled system frequency or the established interchange with other areas within predetermined limits [4]. General problems associated with power system can be defined as peak load coverage, spinning reserve, load frequency control and voltage regulation [5,6]. Effect of all these problems depends on the size of input supply system, interconnected system and system load variation. First three problems are related to active power change and voltage regulation depends on reactive power changes. AGC function can be recognized as a control function that attempts to match the generation process within a controlled environment to track the need for random loading in primary governor control and provide a good arrangement of local frequency after the deviation of the loads in secondary control as shown in Fig.1.1. So,

the purpose of AGC in a control area, is to frequent the power supply from load sharing areas, so as to monitor the frequency of the power supply and tie lines to be in prescribed limits as defined in [7-9].
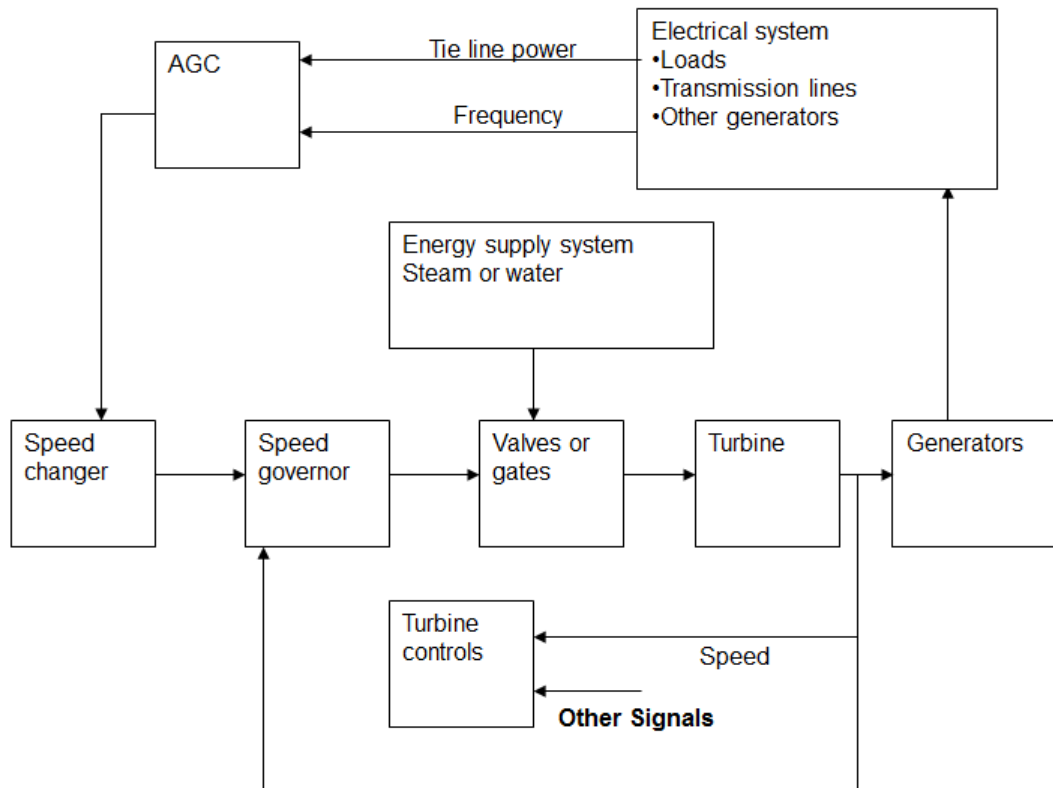
Fig.1.1:   Power System Operation and Control

1.3   Controllers for Power System

With the uncertainty deterministic system, real power system has grown extremely complex. Real power system are interconnected with different power generation sources such as thermal plants, hydraulic plants, pumped storage, gas turbines, photovoltaics, wind turbines etc. Controllers for power system support in maintaining less variation in frequency caused by load variations or other types of transients [10,11]. A large number of research papers reported in the literature presented a rich contribution of different performance index [19,308] , optimization techniques [20-86] and different type of controllers like optimal [12,176,177,178,213,214], fuzzy

[13,155,160], sliding mode controller [14,15,172,314], neural [16] , hybrid controllers [219] and intelligent technique [17,18] based controllers. Brief review of optimal controller and intelligent technique based proportional controllers are described in next chapter. Intelligent technique based controller in power system consists of controller, plant and feedback system. Error achieved by the difference of required and achieved data is fed to the intelligent technique based controller of plant in the system as shown in Fig.1.2.
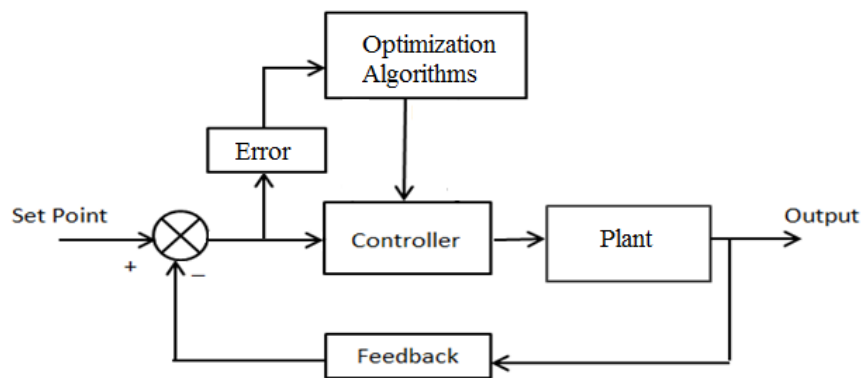
Fig.1.2:   Optimization Algorithm based Control scheme for power system.

Standard controllers such as Proportional (P), Proportional-Integral (PI) or Proportional-Integral-Derivative (PID) controller are commonly applied in power system and prove to be useful [19]. These days, parameters of controllers are being enhanced by the use of newly developed AI techniques and control techniques in AGC to control the frequency and tie line power of the productive interconnected power system within the allowable limit.
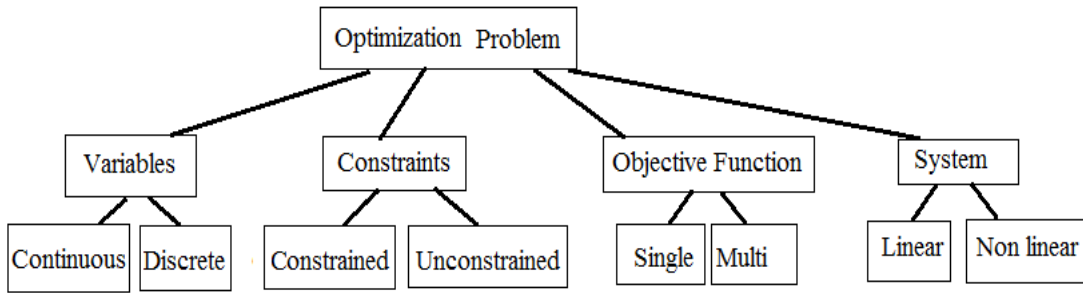
Fig.1.3:   Classification of optimization problem

However, optimizing the value of parameters of these controllers has always been a challenging task for researchers, who are working on various Artificial Intelligent (AI) techniques. The job of optimization algorithm is to find best possible solution for constraint/ unconstrained system, linear/ non-linear system, discrete/continuous variable and single or multi problems as shown in Fig.1.3. Optimization means finding the best solution among many feasible solutions that are available to us in a wider global space with reduced computation time. Feasible solutions are those that satisfy all the constraints in the optimization problem. By using proper optimization technique, the performance of non- linear or linear dynamic systems can be improved.

1.4   Taxonomy of Optimization Algorithms

Researchers are devising various Optimization Algorithms with different behaviors in various systems. In general, basic Taxonomy of Optimization starts with two important groups as Deterministic and Non-Deterministic as shown in Fig.1.4. Deterministic methods are mathematical programming methods which provide accurate solution for problems in continuous space [20-22]. It requires suitable initial point and difficulty increases with increase in problem size. Some of the recognized Deterministic are Linear Programming, Nonlinear Programming, Simplex, Hooke-

5

Jeeves Pattern and Gradient Descent. Non-Deterministic is also popular known as Stochastic Algorithms. It is more computational efficient as compared to deterministic. It searches randomization with local search to global search. Stochastic method gives numerous solutions at several runs. Further, stochastic is divided into two different criteria namely Heuristic and Meta-Heuristic Algorithm [23-25]. Meta-Heuristic Algorithm solves complex problems and gives a better solution than Heuristic Algorithm. Meta-Heuristic Algorithm is divided into two important groups as trajectory based and population based [26-28]. Trajectory based or neighborhood based algorithms have the feature to evaluate only one solution at a time and solution moves through a trajectory in the solution space. Some of the famous trajectory based algorithms are tabu Search [29,30] and hill climbing [31] . Most popular nature inspired algorithm is population based algorithm which has a set of solution which moves towards the goal all together. Population based algorithm are further divided into six groups depending on bio-inspired, physics, chemistry, social human behavior, plant and miscellaneous characteristics [32-38]. Review of various optimization technique applied to frequency control is presented in [35]. Bio-inspired are probabilistic algorithms and divided in two popular groups as evolutionary based and swarm based algorithms. Some of the well-known evolutionary based meta-heuristic algorithms are genetic algorithm -1970 [39, 45,147,148,155,216], differential evolution -1997 [40-42], evolution strategies - 2002 [43], earth worm optimization – 2018 [44, 45]. Some of the recognized swarm based algorithms are particle swarm optimization – 1995 [46, 47], BAT -2012 [48-50], harris hawks optimization-2020 [38], bald eagle search-2019 [51], Bacteria Foraging Optimization- 2009 [52,173,174], cuckoo search [149,175,297,159], grasshopper algorithm [171], grey wolf algorithm

[87,88 ,143], firefly algorithm [145,246], ant colony [152] and whale optimization [263]. During last two decades, this group has grown largely in size. It depends on the collective behavior of species. Species like flying, terrestrial, aquatic and microorganism animals studied in swarm based algorithm. Some of familiar physics phenomenon based algorithms are artificial electric field algorithm-2019 [53], black hole- 2013 [54, 55], sonar inspired -2017 [56] , wind driven algorithm [168] and big bang big crunch-2006 [57-59].
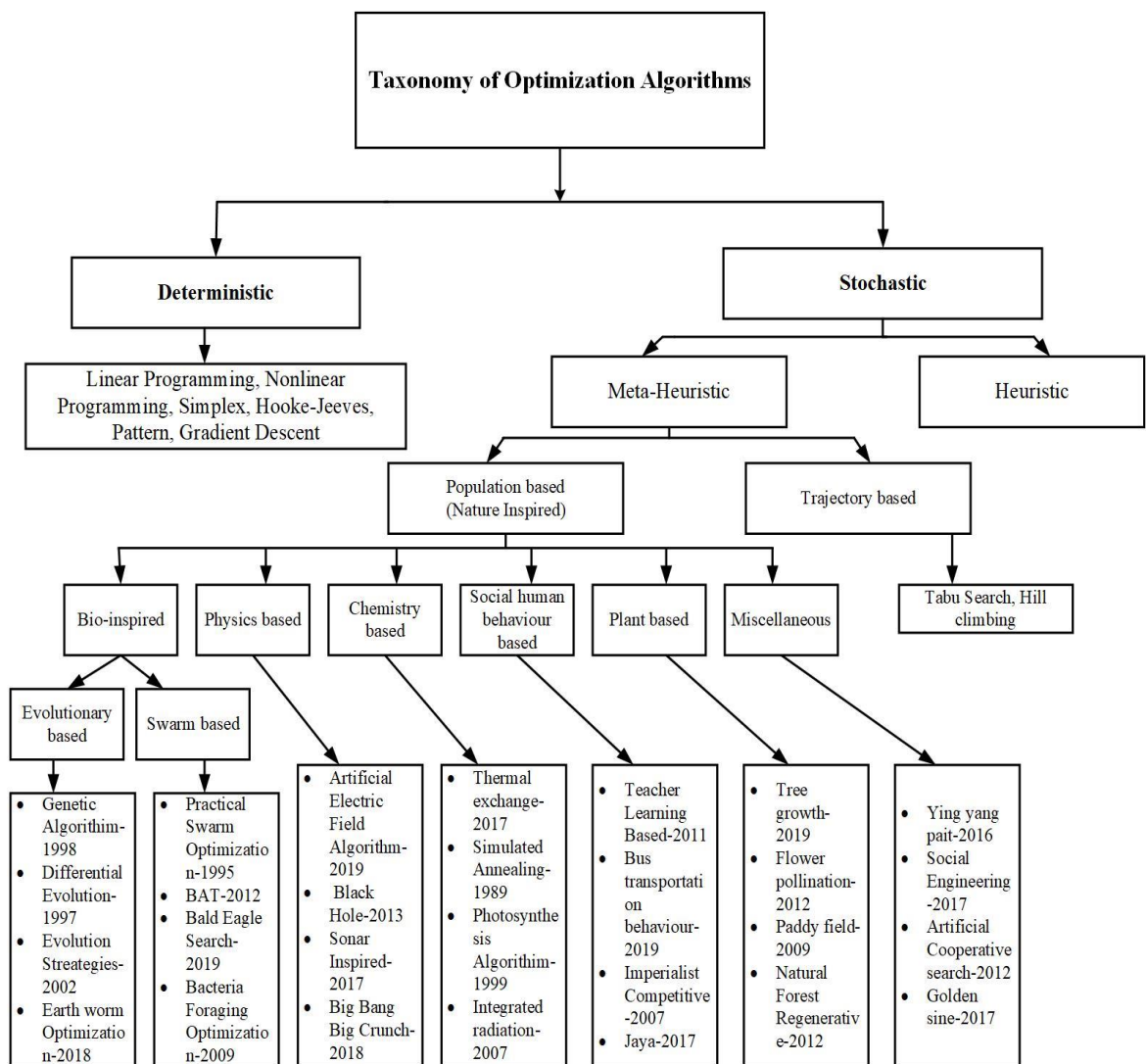
Fig.1.4:   Taxonomy of Optimization Algorithm

Some of the common chemistry phenomenon based algorithms are thermal exchange -2017 [60, 61], simulated annealing-1989 [62-64], photosynthesis algorithm-1999 [65], integrated radiation- 2007 [66] and water cycle algorithm [142]. Some of the social human behavior based algorithms are teacher learning based – 2011 [67,144,330], bus transportation behavior – 2019 [68], volley ball premier league-2017 [69], imperialist competitive algorithm – 2007 [70-72], Jaya -2017 [215,73-75]. These algorithms are dependent on the ideologies with the competition or development of society.

Some of the Plant based algorithms are tree growth -2019 [76,77], flower pollination – 2012 [30, 78, 79], paddy field – 2009 [80], natural forest regenerative - 2012 [81] and sunflower algorithm [232]. This plant type algorithm does not have communication between agents. Some of the miscellaneous algorithms are ying yang pair – 2016 [82], social engineering-2017 [83], artificial cooperative search- 2012 [84,85], golden sine – 2017 [86], sine cosine algorithm [217]. This category does not have some uniformly that's why it is kept under miscellaneous group.

1.5   Intelligent Techniques under consideration

In this study, artificial intelligent algorithm like evolutionary based algorithm (GA, DE), swarm based algorithm (PSO, BAT, BFA) and social human behavior based algorithm (TLBO, Jaya) are studied. A brief description of some of the algorithm are explained in this section.

1.5.1   Particle swarm optimization technique -

Modern meta-heuristic methods are big support to the problems of real power system. unlike heuristic methods, population based meta-heuristic algorithm has set of solution

which moves towards the goal all together. PSO belong to one of the popular group of swarm based algorithms. In the literature, researchers studied that power system with linear or nonlinear, continuous or discrete performs well with swarm algorithms. Kennedy [47] developed visual simulation of bird flock behavior. Flock of birds has the nature of socializing and cooperating. They share and learn with there and other experiences.
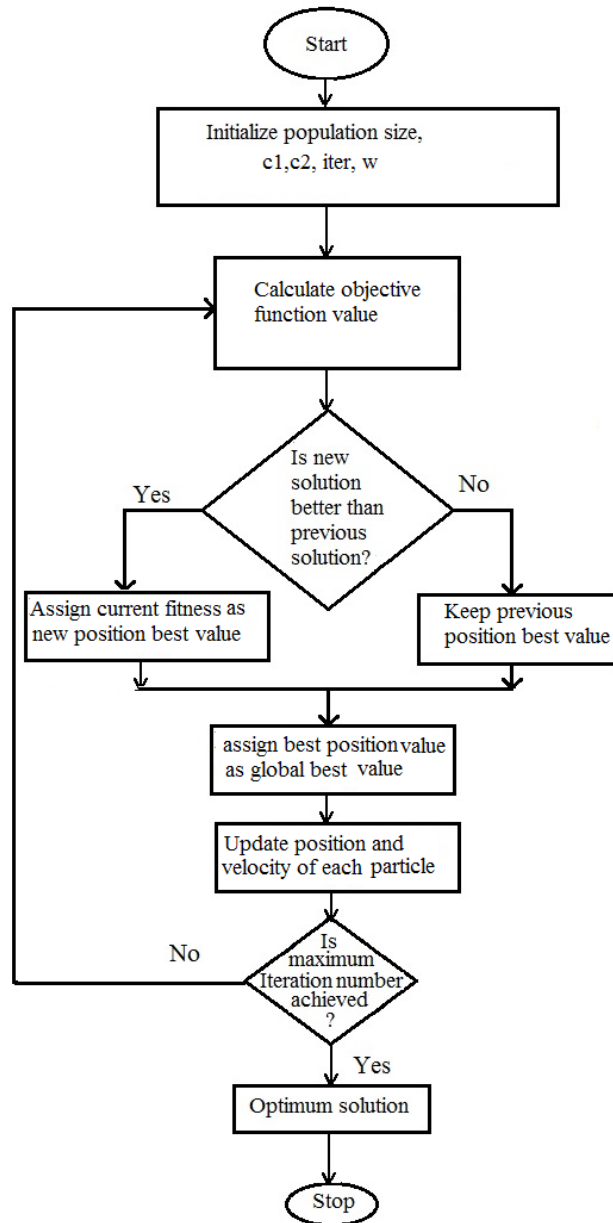
Fig.1.5:   Flowchart of PSO Algorithm.

9

Accordingly they adjust their velocity and position. Each particle saves recent best fitness value of the objective function. Value of position best (X_{pbest}), global best (X_{gbest}) helps each individual to adjust individual velocity by considering their and other experiences in each iteration of the optimization algorithm by using Eqns. (1.1-1.3). The flowchat of PSO algorithm is given in Fig.1.5.

$$V_n^{m+1} = w * V_n^m + c_1 * ran_1 * \left(X_{pbest\,n} - X_n^m\right) + c_2 * ran_2 * \left(X_{gbest\,n} - X_n^m\right) \quad (1.1)$$

Where, ran is uniformly distributed random numbers in the range of 0 to 1, w_{mx} is maximum weight , n is current iteration number and w_{mn} is minimum weight.

$$w = w_{mx} - [(w_{mx} - w_{mn}) * n]/Iterm \quad (1.2)$$

If value of w is large then it facilitates the global search, whereas if the value is small then it facilitates a local search. Now the position of particle is updated

$$X_n^{m+1} = X_n^m + V_n^{m+1} \quad (1.3)$$

1.5.2 Jaya Optimization Technique

Rao developed Jaya algorithm [215] which is sturdy and fits well to give solution. This algorithm is named Jaya as it strives for reaching the best solution. This is a specific algorithm with less parameter whereas other algorithm demands specific control parameters. The gains of PID controllers for two power system model are optimized using Jaya algorithm as described in Fig.2. Jaya begins with an initial population and maximum number of iteration just like any other algorithm. In Jaya algorithm, failure is tried to be avoided so that success can be obtained. After

considering the objective function given in Eqn. no.1, population is updated by using following Eqn. (1.4)

$$X'_{k,p,i} = X_{k,p,i} + r_{1k,i}\left(X_{k,best,i} - \left|X_{k,p,i}\right|\right) - r_{2k,i}\left(X_{k,worst,i} - \left|X_{k,p,i}\right|\right) \tag{1.4}$$

Where $X_{k,p,i}$ is k^{th} variable value for p^{th} population at i^{th} iteration, $r_{1k,i}$ and $r_{2k,i}$ are random variables, $X_{k,best,i}$ and $X_{k,worst,i}$ are k^{th} variable value for best and worst population.
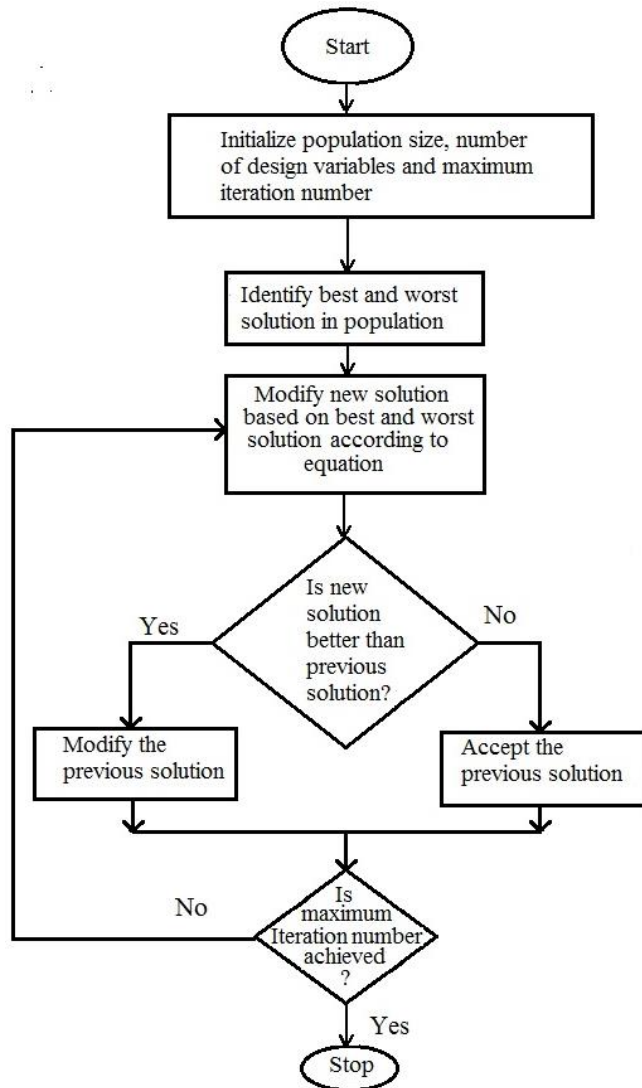
Fig.1.6: Flowchart of Jaya Algorithm.

This procedure is repeated till the last iteration and designing of PID controller is accomplished with parameter values of PID controller. The flowchat of Jaya algorithm is given in Fig.1.6.

1.5.3   Genetic algorithm (GA) John developed GA on the basis of biological processes by using the concept of natural selection. The stochastic algorithm based on Darwin's principle is inherently discrete [216]. GA belongs to a group of evolutionary based meta-heuristic algorithm with randomized operators. In genetic, strings of DNA are called chrosomes of each cell. Genes set are different in different chromosomes. It has high computation cost. It works on three operators namely selection or reproduction, crossover and mutation. Speed of GA depends on the population size of the problem. After calculating fitness value of objective function, select parent strings pair to generate new string with crossover. The probability of ith string can be calculated by using Eqn. (1.5). The flowchat of GA algorithm is given in Fig.1.7.

$$p_{b\alpha} = OF_{\alpha}/\sum_{j=1}^{\gamma} OF_{\beta} \qquad\qquad (1.5)$$

Expected count $= \gamma \times p_{b\alpha}$

Where $p_{b\alpha}$ probability of the αth string in population is, OF_{α} is the fitness value of object function, γ is population size.
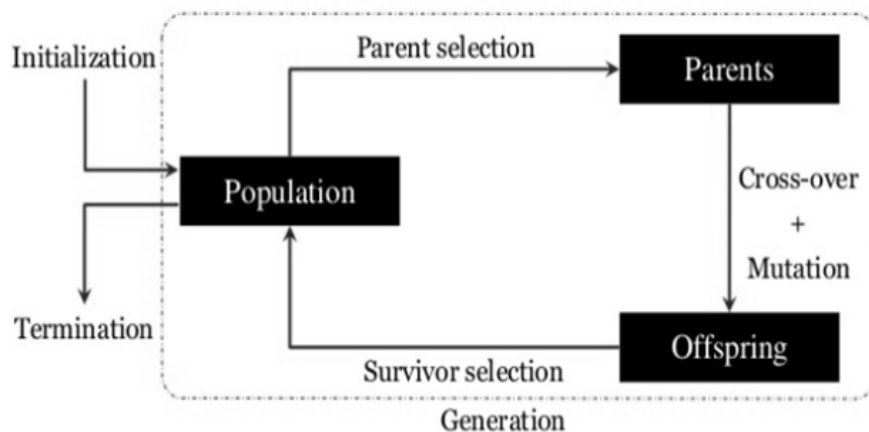
Fig.1.7:   Genetic algorithm

Crossover with bigger expected count will be selected more and produce new chromosomes by one point, two point or uniform techniques. Mutation changes one or more value in chromosome from its first state. Randomly mutation can be done in fit-bit, boundary, uniform or non- uniform technique. Till the completion of iteration, fitness value of objective function is calculated. Parameter values of controller are obtained after completion of iteration.

1.5.4 BAT Algorithm – Bat algorithm belongs to most popular group of bio-inspired optimization algorithm and developed by Yang [48].
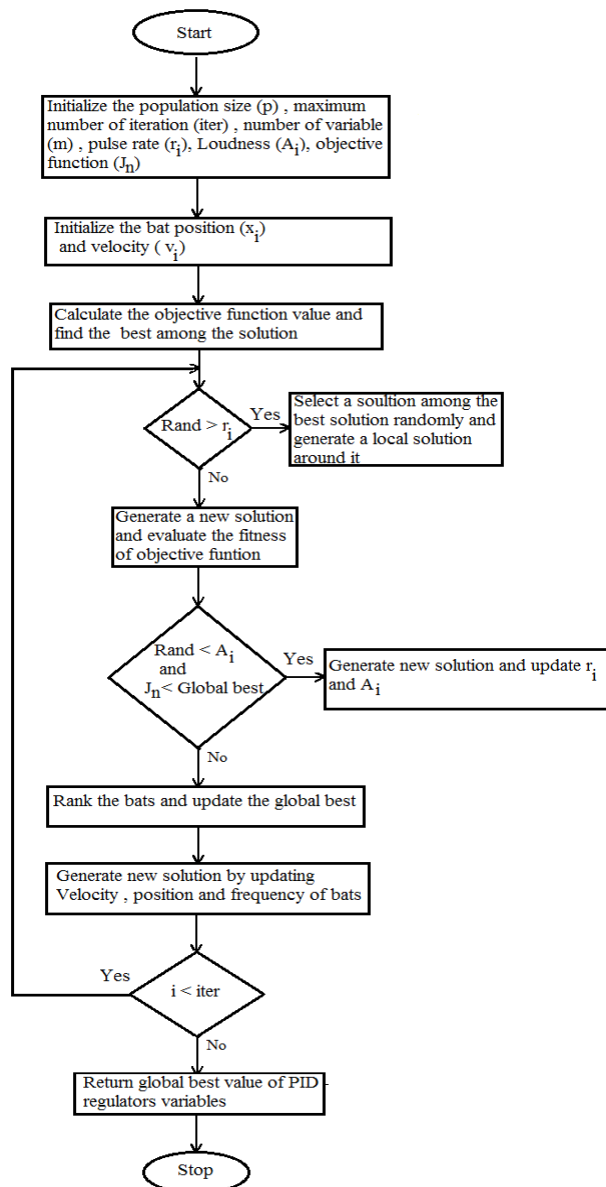
Fig.1.8: Flowchart for BAT optimization technique

Parameters like loudness, pulse rate and frequency along with PSO parameters namely position and velocity are explored in BAT algorithm. It works on the echolocation behavior of bats for finding food and hunting prey. Notorious bat adjusted sound produces sonar frequency differently for both. Micro bats use the replica of sonar as echolocation. In a second, they emit ten to twenty sounds which last for 10 to 20 ms. Typical range of frequency lie in the range of 20 to 100 kHz. The Effect of the ultrasonic sound increases in vicinity of prey. When the echoes of sound produced by bat returns back after striking the target, they start adjusting the sound. This approach is used to find the parameter values of controller after minimizing the value of objective function in considered power system. Fig.1.8 explains the steps for BAT algorithm. In a power system, Position, velocity and frequency of bat during optimization is updated according to the following Eqns. (1.6-1.8), which are given as:-

$$Q_i = Q_{min} + (Q_{max} - Q_{min}) \times rand \qquad (1.6)$$

$$v_i^{iter} = v_i^{iter-1} + (x_i^{iter} - x_{best}) \times Q_i \qquad (1.7)$$

$$x_i^{iter} = x_i^{iter-1} + v_i^{iter} \qquad (1.8)$$

Where x_i is position, v_i is velocity, Q_i is frequency of bat population at i^{th} iteration and rand is the random number between 0 and 1.

1.6 Objective Of The Thesis

The excellent inspiration of the interconnected framework is to get monetary advantages of large scale generation at planned topographical areas. The interconnection additionally works on the unwavering quality of the general framework through shared provision during crises and diminishes the save limit prerequisite of reserves at the individual power stations. Gathering of generators in a power system structured a control area. Power systems of various control areas today are integrated with neighbouring regions, and the issue of AGC turns into a joint endeavour. An unexpected burden misfortune in a standalone or single area system

will leads to deviation in rated frequency and results in complete power outage. In the event, a similar burden disappointment would address a lesser amount of precent misfortune if the similar framework were part of pool. These control regions are interconnected through tie lines for exchanging power under ordinary working conditions. Structure sizes lessen the requirement for saving power among the pool individuals. The deviation in frequency and tie line power will be diminished through interconnected tie lines in multi area power system.

Subsequently, control issue in power system is to keep up these deviated values in control areas. Stores of articles have seemed in regards to the examination of AGC in multi area power system. Different control methodologies have been proposed to accomplish better framework dynamic execution. Realistic power system of two area / three area has been explored with nonlinearities or energy sources. AGC controller designing has been done every now and then by considering traditional, modern and optimization techniques. To deal with certain important issues in future, there is a possibility to do the inspections in two / three area power system with diverse sources.

Literature survey shows that performance of power system depends on the controller structure and optimization techniques employed to optimize controller parameters. Hence, proposing and implementing new controller approaches using high performance heuristic optimization algorithms to real world problems are always welcomed. Performance of integral, proportional integral and proportional integral derivative controller depends on proper selection of certain algorithm specific control parameters. Critical review of literature shows that very less work is done in the area of AGC of interconnected multi area power system with diverse sources. So, latest

developed human based and swarm based AI techniques like Jaya, PSO, BAT algorithm are applied on two /three area interconnected power system with diverse sources and nonlinearity.

One of the revolutionary optimal control concepts for AGC regulator designs of interconnected power system which leads to betterment of dynamic stability of the power system was initiated by Elgerd [15]. Important aspect in the design of optimal controller is the formulation of performance index and the choice of weighting matrices. Very little work in literature is related to optimal control of three area interconnected multi source power system with different structures of cost weighting matrices. In this study, different structures are applied to design AGC regulators for three area interconnected power system with diverse sources.

Keeping in view the foregoing discussion and the motivation, the main objectives of the thesis are stated as follows:

1. To propose Jaya based PID controller for AGC of two area interconnected thermal-hydro-gas power system with varying participation of sources at step load purturbation and random load perturbation.

2. To suggest Jaya based PID controller for AGC of two area interconnected thermal-hydro-wind and thermal-hydro-diesel power system with and without nonlinearities by considering step load and random perturbation at different control areas. The nonlinearities considered are Governor Dead band (GDB), Generation Rate Constraint (GRC) and Boiler dynamics.

3. To develop optimal AGC of three area interconnected multi source power systems with new structures of control cost weighting matrix (R) and state cost weighting matrix (Q).

4. To compare AGC for three area interconnected multi source power systems with Superconducting Magnetic Energy Storage System (SMES) by considering step load perturbation at different control areas.

5. To compare AGC for three area interconnected multi source power systems with Battery Energy Storage System (BESS) by considering step load perturbation at different control areas.

1.7 Outline Of Chapters

The presented work is divided into nine chapters.

Chapter-1 presents a brief introduction to the various power system issues and their solutions. One of the feasible solutions for active power control is to use an AGC in power system. The importance of interconnected multi area power system is conferred. Stability in dynamic performances after using different controllers for AGC in interconnected multi area power system with diverse sources. Widespread review of the taxonomy of optimization algorithms is presented. A brief description of optimization algorithms under consideration is presented in chapter-1. Objective and organization of thesis is given at the end of this chapter.

Chapter-2 includes an extensive literature review AGC schemes in interconnected multi area diverse source power systems. Exhaustive literature survey on the AGC regulator design and control techniques for the interconnected multi area power system is given in this chapter. Moreover, interconnected multi area power system with

17

nonlinearities is discussed. Literature survey on the AGC of interconnected multi area diverse source power system with energy storage systems has been made.

Chapter-3 deals with the development of transfer function models of single area power system with diverse sources. Mathematical modeling of AGC of single area power system is presented. Dynamic models of two area and three area interconnected power systems with diverse sources under consideration is shown. The main simulation work starts from Chapter 4.

Chapter 4 - latest human based AI technique is adopted to conduct the study for AGC of two area interconnected multi source power system. The novel impact of varying participation of diverse power sources in Jaya based AGC of interconnected two area power system is presented. Moreover, to check the robustness of system it has been perturbed to random varying load. Further, a comparative analysis has been done to show a significant impact of varying participation of diverse source on dynamic responses.

Chapter 5- To make the system realistic, nonlinearities and participation factors are incorporated in multi-source power system. Design of novel Jaya based PID controller for Jaya optimized AGC of two-area multi source power system with and without system nonlinearities is endeavored at step load and random varying load. The dynamic performances of power system are studied including the nonlinearities like Governor Dead band (GDB), Generation Rate Constraint (GRC) and boiler dynamics.

Chapter 6 – presents the designing of Optimal AGC regulator for three different three-area interconnected multi source power systems. In each power system, optimal AGC regulators have been designed by using different structures of cost

weighting matrices (Q an R) and then performance of all three types of regulators has been compared in each of the power systems. Eigenvalue study of optimal AGC regulators has been done. The uncertainty of available resources and desire to achieve minimal frequency and tie line power deviation developed the need of energy storage system in power system. Effect of energy storage devices on AGC of three area power system has been studied in chapter 7 and chapter 8.

Chapter 7 - presents the implementation of Superconducting Magnetic Energy Storage System (SMES) in operation and control of AGC of three-area multi source power systems. SMES has the capability of rapid response with high energy efficiency as it converts directly from one form to another and take less time for discharging and charging. This chapter gives deep analysis of PSO tuned Integral controller for AGC of three area interconnected multi source power systems by including and excluding SMES at step load perturbation in different control areas. Comparative performance of different bio-inspired artificial technique has been accomplished on AGC of three area interconnected power system with multi sources.

Chapter 8 – Battery energy storage systems (BESS) provide fast active power compensation and manage sudden demand of power requirement in load, thus effectively dampening the frequency oscillations due to large disturbances in load. Chapter 8 presents AGC of three area multi source interconnected power systems by including and excluding Battery Energy Storage System (BESS) at step load perturbation in different control areas.

Chapter 9 - summarizes the performance of different control techniques presented for AGC of multi area interconnected multi source power system and

highlights the main conclusions of the proposed work. The scope of future work in this area is also listed at the end of this chapter.

<div align="right">

CHAPTER 2

</div>

LITERATURE SURVEY

2.1   Introduction

This chapter emphasizes a brief review of literature pertaining to the AGC of interconnected multi area power system with diverse sources over a period of past eight decades.

The review of literature has been organized in five categories.

- AGC design and implementation

- AGC of interconnected multi area multi sources power system

- AGC of interconnected multi area multi sources with nonlinearities.

- Optimal AGC of interconnected multi area power systems.

- AGC for interconnected multi area power system with Superconducting Magnetic Energy Storage System (SMES)

- AGC for interconnected multi area multi source power system with Battery Energy Storage Systems (BESS)

Transfer of continuous electric power supply within an acceptable quality from the source to consumers is the main purpose of power system. With increase in demand and technology development, researchers face challenges to control real and reactive power under physical constraints of diverse generation sources. The generation sources consist of conventional fossil fuel plants such as thermal, hydro plant, pumped

storage, gas turbine plant, diesel plant and non-conventional plants such as Photo-Voltaic, bio-gas, wind plant etc. After considering uncertainty or non-linearity in power system, complexity increases.The basic important works on frequency control and tie line power control in interconnected power system has been discussed [89-91].

2.2 Brief review of AGC schemes

Intelligent AGC issues and several control strategies have been developed for simultaneous minimization of system frequency deviation and tie-line power deviation to match total generation and load demand, which is required for successful operation of two area/ three area interconnected multi source power system at realistic situation. Moreover, with the advancement in energy sources, intelligent AGC of interconnected multi area multi source power systems have also been well studied with energy storage system in this problem. Currently, power system operation and control with AGC are undergoing changes due to rapidly increasing amount of renewable sources, energy storage system, restructuring and emerging of new types of control strategies, power generation, consumption, and power electronic technologies. A different issue on multilevel frequency control has been explored [92]. Some aspects of economic load dispatch in a power system have been solved [93, 94,312,313]. Infrastructure of the future intelligent power system should effectively support the services to AGC through intelligent schemes [95]. Cyber security is the important issue wherever intelligent control comes in power system [96, 315]. Some researchers discussed various challenging issues like regulation, optimization and stabilization of interconnected power system control [97-100]. Few studies show solution of voltage control in interconnected system by using FACTS controller [101]. Discussion on planning of

distributed generation has been conducted [102]. Some of the issues related to frequency and tie line power are solved by considering multi area power system with diverse source altogether with intelligent controllers and various control methods is well reviewed in [103-109]. The power system control analysis depends on simulation of system dynamic behavior. Initially, researchers studied the effect of changing frequency bias parameter in frequency control [110-113,129-131].

2.3   AGC schemes in interconnected power systems

Most of the studies focussed on AGC of single or two area thermal or hydro thermal power systems [114-145]. With the demand of renewable sources in existing power system, there is a need to add novelty in design of AGC regulator to achieve better dynamic performances in multi area with diverse source power systems.

The preliminary studies on single area power system have been conducted on thermal, hydro, gas, wind or diesel generation sources [114-127]. Adaptive controller for single area thermal power system has been designed in [114,115]. Further, a delay dependent criterion for frequency control of thermal power system has been analyzed in [116-118]. Further, different control techniques for single area hydro power system have been described [119-121]. Novel technique of reducing dumped load size for frequency control of small hydro single area power system [119] has been discussed. Generally, AGC studies show that the control area of interconnected or isolated power system consists of single type of thermal or combination of hydro and thermal systems. Wind-diesel model for isolated electric power system has been introduced in [122]. Further, AGC of wind-diesel-micro hydro isolated power system has been presented in [123]. Some researchers have investigated different controllers by

considering thermal-hydro-gas as a control area. Single area with AGC of thermal-hydro-gas power system has been described in [124,125,126,127,285]. The linearized mathematical model of wind turbine generators and its effect on frequency response when integrated with thermal-hydro-gas single area power system has been described in [127].

Since three decades, researchers are utilizing the concept of interconnected tie-line power system with more than one area [131,132,135,139,151,153,159]. AGC of two-area interconnected power system with thermal source has been considered by [89,128,131,132,133]. AC and AC/DC interconnected power system with reheat thermal sources has been explored by [133-135]. Further for hydro and thermal as energy sources, various control techniques have been proposed by [136,137]. PID controller for two-area hydro-hydro power system has been designed [138-140]. Nichols chart proves to be effective method for improving the stability and the dynamics of the system [138]. Different type of two area power system with all thermal, all hydro and mixed thermal hydro sources has been analyzed by [140]. AGC of power system with multi sources as thermal, hydro and gas sources has been analyzed [141,142]. Authors [141] presented Bacterial Foraging Algorithm (BFA) tuned AGC and modelling of power system with thermal, hydro and gas energy sources. Frequency control of two area power system at random load has been inspected [142]. AGC of power system with renewable sources create challenges. Grey wolf optimization based AGC of two area interconnected power system with thermal, hydro and wind sources has been studied in [143]. Further, PSO and Iteration Particle Swam Optimization (IPSO) based AGC of thermal-hydro-wind and thermal-hydro-diesel interconnected power system has been explored [144]. Authors [145]

presented Firefly algorithm (FA) tuned PI controller for PV grid and thermal in two area interconnected power system.

The three area thermal power system has been shown in [146,147,148,150,175]. Study on three unequal area of reheat thermal system has been done [175]. The combination of thermal and hydro sources in three area power system has been considered for frequency control [149]. Multi sources as thermal, gas, distributed generation-electric vehicle has been considered in AGC of three area power system by [117,263,229]. The frequency control of four area thermal power system has been considered by [135,152,153,177]. To study the effect of multi area, analysis of AGC of four, three, two and one area thermal power systems has been done [152]. State estimation of four area thermal power system has been considered by [154]. Combination of thermal and hydro in four area power system has been described in [155]. Frequency control of four area power system with thermal and wind source has been presented in [151].

2.4   AGC of interconnected power system with nonlinearities

Realistic power system consists of nonlinearities like Governor Dead band (GDB), Generation Rate Constraint (GRC) and boiler dynamics. The influence of GRC in one area of thermal power system has been proposed [114,115]. GRC in multi area thermal power system is studied [311]. Further, impact of GRC in multi-source power system with thermal hydro and gas sources has been explored [125]. Effect of one of the non-linearity like GDB in thermal-thermal interconnected power system has been studied [7,126,156,157,158]. The two area power system incorporating GRC has

been further explored [111,161,162,163,166,330]. Stability and dynamics of Hydro-hydro two-area power system takes more time than thermal system. Hydro-hydro power system with nonlinearity like GDB has been inspected [95]. Combination of thermal and hydro sources in two area power system with nonlinearity has been presented in [127,137, 164,165, 167,169,210]. Amalgamation of renewable sources and nonlinearities in realistic power system makes the modern power system challenging. Wind integrated two area multi source power systems with nonlinearities has been observed [127,143,151,170]. Effect of wind integrated system to modified Jaya tuned AGC of thermal-hydro with nonlinearities has been studied [127]. The effect of different loads on firefly algorithm optimized AGC of two area reheat thermal, hydro and gas interconnected power system including non-linearity, time delay, SMES and unified power flow controller (UPFC) has been analyzed [246]. Nonlinearities like boiler dynamics and GDB on reheat thermal-hydro-wind and reheat thermal-hydro-diesel interconnected power system has been investigated [171]. Power system including non-linearities with thermal-hydro-nuclear and thermal-hydro-gas has been studied by [172]. AGC of thermal-hydro-dish stirling solar thermal system and thermal-hydro-nuclear with GRC as nonlinearity has been investigated [170]. The effect of GRC on frequency control of three area thermal power system has been explored [108,150,173,175]. The decentralized frequency control of four area power system with nonlinearity has been considered in [154].

A large interconnected power system may be viewed as an interconnection of several lower order systems. Few types of multi-level control schemes in an interconnected power system have been suggested by [92,146]. Eigen value technique analysis is performed on power system [207, 239].

26

2.5 Optimal AGC schemes in interconnected power system

One of the revolutionary optimal control concepts of AGC regulator designs for interconnected power system which leads to betterment of dynamic stability of the multi-variable power system has been initiated by [90]. Various optimal control schemes are applied in power system [200,203]. H infinity concept of optimal design on several systems has been applied [210-213]. Application of optimal H − infinity criterion for rotating inverse pendulum has been deliberated [212]. In a modern optimal control theory, state variable model helps the multi-variable power system for easy computation.

Initially, optimal control for dual area interconnected non-reheat thermal power systems has been examined. It has been studied that the greater stability margins can be achieved with regulators designed using optimal control strategies as compared to that obtained with conventional/ classical control techniques for multi variable system [179,181,194,195]. Various application of riccati equation in optimal control system to develop a secure system is designed [196,197,200,201,204,205,208]. Optimal LQR controller for single-area power system by considering different parameters has been studied [202]. Further, design of LQR for power system with time delay system has been considered [197,200]. Linear quadratic regulator (LQR) for two area thermal power system has been designed by [205]. Various application of LQR in multi machine is explored [190,198,199]. Recently, procedure for Genetic Algorithm based LQR controller for improving fuel cell voltage regulation has been proposed [185]. Participating neural network with LQR design for frequency control of AC / DC interconnected power system has been used by [188,189]. Moreover, optimal control

shows successful results in renewable source power system [208, 209]. Also, LQR works well with UPFC and RFB for hydro power system [209]. Important aspect in the design of optimal AGC regulator is the availability of all state variables, minimization of performance index and the choice of weighting matrices [180, 204]. A procedure for finding the structure of weighting matrices by the use of pole placement with optimal regulator has been suggested in [182,183]. Various techniques for designing of structures of control cost weighting matrix for two-area thermal interconnected power system has been formulated by [186,187,189]. A new criterion for selection of the weight matrices Q and R is proposed which will lead to the desired natural frequency and damping ratio of the closed-loop system.

Selection of weighting matrices using fractional order integral performance index has been explained in [184]. Very less work related to optimal control of three-area interconnected multi source power system with different structures of cost weighting matrices has been found in literature. Structures based on scaling method for power system has been proposed by [190,191]. By using the concept of controllability, different structures of weighting matrices has been designed in [193,206].

2.6   AGC with energy storage system

Energy sources require battery management system (BMS) to screen and keep up with protected, ideal activity of every battery pack [218]. Batteries are dynamic in nature, continually working external the balance state during cycling and gets debase. This degradation can be sped up by expanded temperature or overcharging. BMS controls to fulfil power need and diminish the reason of degradation [220-223]. BMS

have the information on condition of charge and condition of wellbeing in battery during demand response. Energy sources are classified in terms of mechanical, chemical and electromechanical energy sources [224-230]. Various energy storage systems are used in AGC of power system [232-235]. The appropriateness and helpfulness of recurrence stabilizers in the types of superconducting attractive energy storing (SMES), battery energy storage system (BESS), capacitive energy storing (CES), thyristor control series capacitor (TCSC), static coordinated series compensator (SSSC) and thyristor control stage shifter (TCPS) is widely concentrated in [231,248,301] and result shows critical improvement in power framework steadiness.

Recent advancement in distributed generations, DC systems, superconducting technologies and power electronics spurred technical and economic growth of high temperature SMES in the demanding power system. The problems faced by power systems with other energy sources like low discharge rate, increased power flow reversal time and more maintenance requirement has led to the growth of SMES [236]. It has better performances in terms of rapid response, high efficiency and control as compared to hydro pumped or chemical storage [236,237]. SMES of small rating offer protection to critical or fluctuating loads or used as storage [261]. However, SMES of large rating with power system increases voltage stability, offer load leveling, and provides load frequency control [238]. Also, brief review of SMES configuration with six pulse bridge converter, voltage source converter and current source converter is considered by [238]. The usage of an IGBT convertor rather than thyristor convertor with the SMES for AGC of power system is presented in [243]. A Superconducting Magnetic Energy Storage (SMES) which is capable of controlling active and reactive power simultaneously has been expected as one of the most effective and significant

stabilizer of frequency oscillations. The design of SMES by considering thermal stability, initial current and power conditioning system is discussed in [240]. Study on single area power system with SMES for load frequency control in thermal power system is considered in [241]. Moreover, the frequency control for thermal-hydro and wind-diesel power systems is presented in [239,242] respectively. Photo voltaic power system with SMES of voltage source converter is considered in [244]. The influence of SMES in AGC of two area power systems is revealed in [245-259]. The preliminary studies on frequency control problem for two area thermal power system is carried by [140, 245-248]. Further, effect of SMES is studied with incorporation of non linearities like GRC, GDB or boiler dynamics in thermal power systems [249-253]. The influences of SMES in each area of dual reheat thermal power system including GRC and GDB is analyzed by [252,254]. Frequency control of two area reheat-thermal power system with nonlinearities like GRC and boiler dynamics are effective in damping oscillations by incorporating SMES [253]. SMES with fuzzy logic controller for two area thermal power system is considered in [253]. The frequency control of two area thermal-hydro power system with SMES is considered in [255-259]. Effective use of SMES for sudden load changes includes two area hydro-hydro interconnected power systems has been explained in [140]. Further, influence of SMES in AGC of multi source including thermal-hydro-gas power system in [260].

Moreover, frequency challenges with SMES in three area power systems are considered in [262-264]. Combination of various sources like thermal-thermal, thermal-hydro and thermal-gas are considered in three area power system with SMES [262]. AGC of three area power system with thermal-gas including non-linearity, electric vehicle, distributed generation and SMES is studied in [263,264].

AGC of four-area power system with SMES by using neural technique is presented by [264]. Moreover, SMES helps in improving the power issues in wind farms [265,266]. Literature review shows that less attention has been devoted to the AGC of interconnected three area multi source power systems with SMES.

Literature survey exhibits that very less work have been witnessed about the AGC of interconnected three area thermal-hydro-gas power system with SMES. However, no literature is available to show the effect of SMES in three area thermal-hydro-gas power system on load perturbation in different control areas. Moreover, such comparative study is not witnessed within multi area multi sources of thermal-hydro-gas making it further important to practice investigations on the same.

For large scale applications of renewable power source, there is a need of advanced energy storage devices for storage energy [267,269,270]. Battery energy storage system (BESS) is composed only of static elements. So, it has a very fast dynamic response as compared to other generators or storing devices. BESS covers a wide spectrum of application ranging from short term power applications to long term energy management in various fields. Study reveals that there are various battery technologies, which include Li-ion, lead acid, fuel cell, redox flow etc [276,269,271,281]. Among them lead acid battery is considered a promising energy storage solution, which is suitable for generating utilities including spinning reserve, frequency control, load leveling, modular construction and deferral of investments in new generation and transmission equipment [268,293,302,303]. Nowadays, it is present as an outstanding advantage for frequency control of fossil fuel power system and photo voltaic system and in Electric Vehicle applications [279,280]. The preliminary article on BESS as a form of Renewable Energy integration has been

registered in 1982. Various types of battery technology, modeling, issues, and challenges of existing technology are described in various review articles [261,273,274,275,277,300]. The review article is based on a battery system where five types of batteries such as lead acid, flooded type, sodium sulphur, redox-flow and lithium-ion are compared following their application, construction, and cost for the grid. The production of electrical energy in BESS varies with state of charge, storing capacity, rate of charge or discharge, environmental temperature and self-life [304]. BESS performs well with an efficient Battery Management System which is responsible for safe operation and consider all the aforementioned conditions depending on load profile [272,281,296,299]. Various researchers have highlighted BESS in Electric Vehicle technology, their challenges and issues [293]. The stability studies of power system are usually expressed in two axis frame. So, the quantities of BESS are configured in d-q axis which can be linked with other devices in same frame [277]. It has been clearly analyzed that the BESS system is not only limited to replacing fuel-efficient appliances but also is used as backup power and power or frequency where one technology is not enough to allow a future grid. Review of intelligent approach highlights the importance of BESS study in AGC of power system. BESS helps in improving supply reliability and performance of the AGC of power system during peak load periods.

In this section, a group of articles handiest on AGC of diverse area multi-source power system with BESS has been discussed. BESS with island system or microgrid system are described in [278,279,282,298]. PV with BESS improves power system quality [305-308]. DC microgrid with PV, wind and different energy storage like BESS, fuel cell are considered in [297,299]. Frequency control of isolated or single

area power system with BESS is studied in [280,283,284,285,287,288]. Single area with thermal power system with BESS is simulated in [286]. Effect of BESS in reheat thermal power system with non-linearity (GRC) has been explored [274]. Combination of Thermal, hydro and gas sources as diverse sources of practically single area power system incorporating redox flow batteries is well described in [285]. In the past, studies have reintroduced the application of BESS in AGC of two area interconnected power system. A two area power system consisting of thermal or combination with other sources is studied in [286,289,290,292,294,295]. Moreover, thermal sources with nonlinearity like GRC and GDB are explored in [274]. Effect of BESS in two area power system, where, reheat thermal source as one area and hydro sources as second area is studied in [291]. Effect of BESS is studied in thermal-wind two area power system [294]. Amalgamation of various sources like thermal, hydro and nuclear sources with GDB and time delay has been investigated [295]. Effect of BESS in microgrid with hydro, photo voltaic and wind unit is considered in [296]. With the advancement in renewable sources, BESS is well applied in individual solar units or combination with other units [278,279,280,282,296,298]. Frequency control of thermal and hydro unit in three area interconnected power system with BESS is studied in [291]. To our knowledge, very less work for AGC of three area multi source interconnected power system with BESS has been seen.

2.7 Conclusion

Based on the extensive literature review on the control designs of AGC of interconnected multi area power system, it has been felt that new control techniques are required for design of AGC regulators for interconnected multi area power system including renewable sources. The main objectives of the proposed research work are to

achieve better dynamic performances in multi-area with diverse source power systems, namely two area power system with and without non-linearity and three area power system with optimal and energy storage system. New AGC regulators are designed and developed which are simple, robust and easy to implement as compared to available control techniques. The problem of nonlinearity in interconnected power system with diverse sources has also been addressed with suitable controller.

CHAPTER 3

DEVELOPMENT OF MATHEMATICAL MODELS FOR AGC OF POWER SYSTEMS

3.1 Introduction

Modern power system comprises of various power generation sources such as fossil fuel plants, hydraulic plant, gas turbine, and non-conventional energy sources etc. The dynamism in power system due to load variation or other type of transients cause the frequency variation continuously. The interconnection of the various generative plants through the power system grid stabilizes the frequency variation to a great extent by enhancing the system inertia. Further, the power system is divided into various control areas for better operation and control. In present power demand, the application of diverse source in interconnected multi area power system provides a good design of AGC system. In this chapter, mathematical modeling of thermal, hydro and gas power system as a single control area is carried out. In each system, the dynamic model is expressed in terms of state variable form. Transfer function model for the reheat turbine, speed governor, load and tie line power deviation for thermal, hydro and gas power system are expressed in this chapter. The transfer function block diagrams of two area interconnected thermal-hydro-gas power system, two-area interconnected power system including nonlinearities, optimal control of three area interconnected multi source power systems, three area interconnected multi source power system with SMES and three area interconnected multi source power systems with BESS are shown in Fig. 3.8-3.19. The study of dynamic response at load disturbances using linearized models of various multi area power systems has been widely accepted [316-329]. Lot of research has been reported on the modeling of thermal, hydro and gas dynamics for AGC

studies of power system [319-324]. Also, modeling of diesel and wind plant is presented [325-329].

3.2 Mathematical modeling of power system

The power system consists of a large number of generators interconnected by network of transmission lines which provide power to the consumers at rated voltage and frequency. The prime movers convert these sources of energy into mechanical energy that is, in turn, converted to electrical energy by synchronous generators. In this study, various sources like thermal, hydro, gas, diesel, wind are explored in different combinations in two area or three area power systems. Mathematical modelling of various sources like thermal, reheat thermal, hydro, gas, diesel, wind are well explained by many researchers [320-330]. The prime mover governing system offer a method through which turbine can be started and operate to meet power demand. The load damping constant (D_n) in p.u. MW/Hz, rated frequency (F_n) in Hz, rated power of power system (P_{rn}) in MW, power system gain constant (K_{Pn}) in Hz/p.u. MW, load (P_d) in MW, power system time constant (T_{Pn}) in s, inertia constant (H_n) in s and area frequency response characteristic (β_n) are defined in Eqns. (3.1-3.4) [2]:

$$D_n = \frac{\partial P_{dn}}{\partial F_n} \times \frac{1}{P_{rn}} \quad \text{p.u. MW/Hz} \tag{3.1}$$

$$K_{Pn} = \frac{1}{D_n} \quad \text{Hz/p.u. MW} \tag{3.2}$$

$$T_{Pn} = \frac{2H_n}{F_n D_n} \, s \tag{3.3}$$

$$\beta_n = D_n + \frac{1}{R_n} \, \text{p.u. MW/Hz} \tag{3.4}$$

Where, n is control area of power system.

3.2.1   Modeling of thermal power system

The main resource of electrical power is thermal power derived from fossil fuels. The stored energy of steam is transformed to mechanical energy and then to electrical energy by the generator. Steam turbines may be categorized as non-reheat or reheat turbines. The mathematical model for single area thermal power system is defined in Eqn. (3.5-3.7). The transfer function block diagram for thermal power system including steam turbine and governing system is shown in Fig. 3.1 [390-321]. It is a mechanical speed governor system.
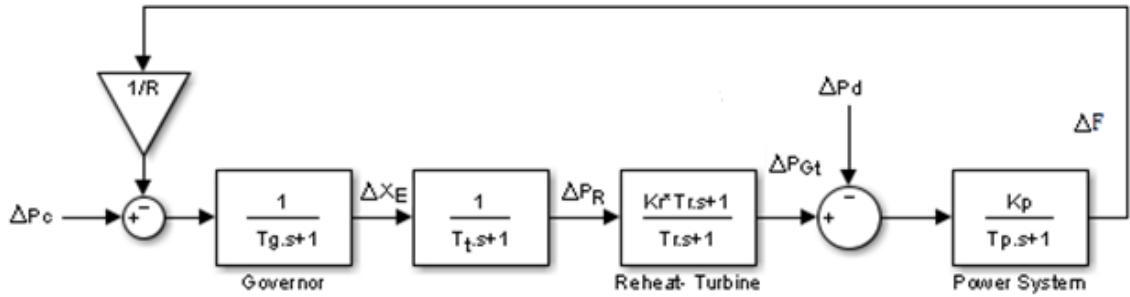
Fig. 3.1:   Transfer function block diagram of single area thermal power system.

$$\Delta X_t(s) = \frac{1}{(1+sT_g)} \left(\Delta P_c(s) - \frac{\Delta F(s)}{R} \right) \tag{3.5}$$

Time constant of speed governor is Tg , thermal turbine is Tt, reheat-thermal turbine is Tr and power system is T_P . Steam turbine power deviation is expressed in Eqn. (3.6) [141].

$$\Delta P_{Gt}(s) = \frac{(1+sK_rT_r)}{(1+sT_t)(1+sT_r)} \Delta X_t(s) \tag{3.6}$$

Where, K_r is reheat coefficient due to high pressure steam and K_P is power system gain. Frequency deviation of single area thermal power system in response of change in speed governor (ΔPC) and load demand (ΔPd) is developed in Eqn. (3.7).

$$\Delta F(s) = (\Delta P_{Gt}(s) - \Delta P_d(s)) \frac{K_P}{(1+sT_P)} \qquad (3.7)$$

3.2.2 Modeling of hydro power system

Hydro units differ from thermal units in that the relatively large inertia of water used as a source of energy causes a considerable greater time lag in the response of changes of prime mover torque to changes in gate position, and also an initial tendency for the torque to change in a direction opposite to that finally produced [322,323]. The speed governor characteristics of the hydro units are widely different from that of turbo governor due to the effects of water inertia. The mathematical model for single area hydro power system is defined in Eqn. (3.8-3.10). The transfer function block diagram for power system with hydro turbine and governing system is shown in Fig. 3.2 [141, 321].

$$\Delta X_h(s) = \frac{(1+sT_R)}{(1+sT_{RH})(1+sT_{GH})} \left(\Delta P_c(s) - \frac{\Delta F(s)}{R}\right) \qquad (3.8)$$
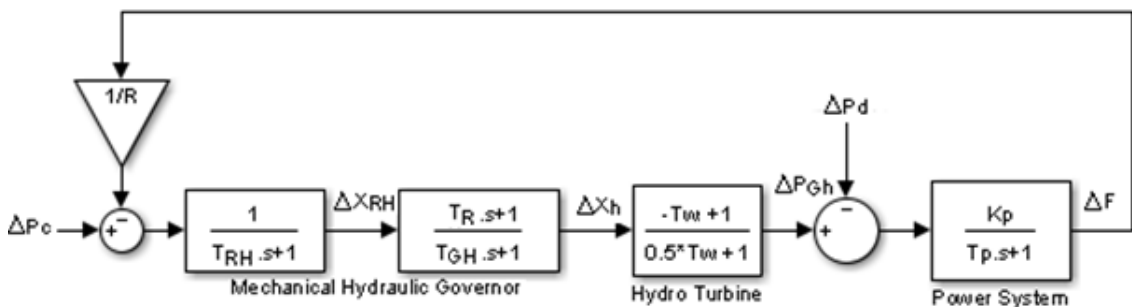
Fig. 3.2:   Transfer function block diagram of single area hydro power system.

Time constant of hydro speed governor is T_{RH}, dashpot is T_R, turbine is T_W, main servo is T_{GH} and power system is T_P. Hydro turbine power deviation is expressed in Eqn. (3.9).

$$\Delta P_{Gh}(s) = \frac{(1-sT_{Ws})}{(1+0.5sT_{Ws})} \Delta X_h(s) \qquad (3.9)$$

Frequency deviation of single area hydro power system in response of change in speed governor (ΔP_C) and load demand (ΔP_d) is developed in Eqn. (3.10).

$$\Delta F(s) = (\Delta P_{Gh}(s) - \Delta P_d(s)) \frac{K_P}{(1+sT_P)} \qquad (3.10)$$

3.2.3 Modeling of gas power system

Interconnected power system generally contains thermal and hydro power generation. In an interconnected power system, gas turbine is getting popular as air is used as the source. Gas power system comprises of compressor, combustion chamber and turbine. The transfer function block diagram for gas power system with gas turbine and governing system is shown in Fig. 3.3 [324].
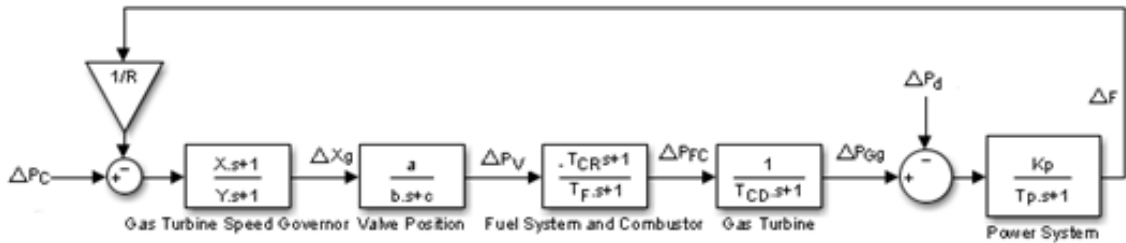
Fig. 3.3:   Transfer function block diagram of single area gas power system.

The transfer function for gas turbine governing system is expressed in Eqn.3.11 [141].

$$\Delta X_g(s) = \frac{(1+sX)}{(1+sY)}\left(\Delta P_c(s) - \frac{\Delta F(s)}{R}\right) \tag{3.11}$$

Time constant of speed governor as lead and lag are (X) and (Y), fuel and combustion reaction are T_F and T_{CR}, and combustion discharge volume is T_{CD}. Changes of power in valve, fuel and combustor system are expressed in Eqn. (3.12, 3.13).

$$\Delta P_{Vp}(s) = \frac{a}{(c+sb)}\Delta X_g(s) \tag{3.12}$$

$$\Delta P_{FC}(s) = \frac{(1-sT_{CR})}{(1+sT_F)}\Delta P_{Vp}(s) \tag{3.13}$$

Gas turbine power deviation is expressed in Eqn. (3.14).

$$\Delta P_{Gg}(s) = \frac{1}{(1+sT_{CD})}\Delta P_{FC}(s) \tag{3.14}$$

Frequency deviation of single area gas power system in response of change in speed governor (ΔP_C) and load demand (ΔP_d) is developed in Eqn. (3.15).

$$\Delta F(s) = (\Delta P_{Gg}(s) - \Delta P_d(s))\frac{K_P}{(1+sT_P)} \tag{3.15}$$

3.2.4 Modeling of interconnected tie-line

Nowadays, power system is divided into various areas for better operation and control. During a transient event, the two areas exchange the power supply through tie-lines as shown in Fig. 3.4 [1,6].
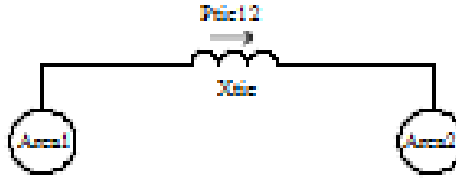
Fig. 3.4:   Two-area interconnected system
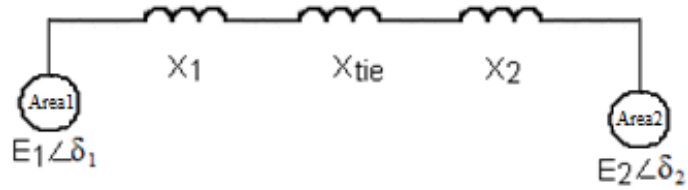
Fig. 3.5:   Electrical equivalent of two area interconnected system

Electrical equivalent of two area interconnected system circuit is shown in Fig. 3.5. In two area interconnected system, tie-line power is calculated by considering each area voltage as expressed in Eqn. (3.16)

$$P_{tie12} = (E_1 E_2 / X_T) \operatorname{Sin} (\delta_1 - \delta_2) \tag{3.16}$$

Where, $X_T = X_1 + X_{tie} + X_2$

$$\Delta P_{tie12} = T_{12} \Delta \delta_{12} \tag{3.17}$$

Where, $\Delta \delta_{12} = \Delta \delta_1 - \Delta \delta_2,$

Synchronizing torque coefficient can be given as,

$$T_{12} = (E_1 E_2 / X_T) \operatorname{Cos} (\delta_{10} - \delta_{20}) \tag{3.18}$$

Where, $\delta_1 = \delta_{10}$ and $\delta_2 = \delta_{20}$ at initial operating point.

Transfer Function of two area interconnected tie-lines in a system is shown in Fig. 3.6. Deviation in tie-line power is expressed in terms of deviation in frequency of two areas in an interconnected system as shown in Eqn. (3.19, 3.20).

$$\Delta P_{tie12} = 2 \pi T_{12} \int (\Delta F_1 - \Delta F_2) \, dt \tag{3.19}$$

$$\Delta P_{tie12} = \frac{2\Pi T_{12}}{s} (\Delta F_1 - \Delta F_2) \tag{3.20}$$
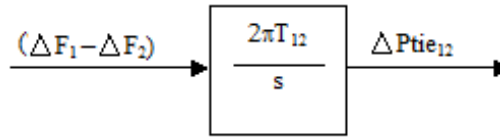
Fig. 3.6:   Transfer function of two area interconnected system

During transient period, sudden change of load causes each area generation to react according to its power characteristic which effects steady state frequency of each area of and tie-line power in primary control. In secondary control, system frequency and tie-line power are tried to restore at scheduled value by considering area control error (ACE). The control signal made up of tie-line flow deviation added to frequency deviation weighted by a bias factor (b) would accomplish the desired objective of secondary control is shown in Eqn.3.21.

$$ACE = \Delta P_{tie12} + b \, \Delta F \text{ , in MW} \tag{3.21}$$

The different intelligent controller with ACE regulates the speed changer and helps in achieving the preferred output in power system as shown in Fig.3.7.
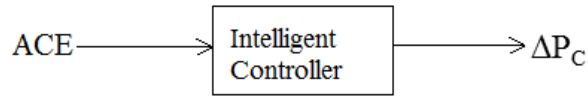
Fig. 3.7:   Intelligent controller with area control error

3.3   Power system models under investigation

Simulation of interconnected multi area multi source power system is conducted by using different intelligent controllers namely GA, DE, BAT, PSO, BFO, TLBO and JAYA.

1. AGC of two area interconnected reheat thermal-hydro-gas power systems.

In this two area interconnected diverse source power system, each area consist of thermal, hydro and gas sources as shown in Fig.3.8.
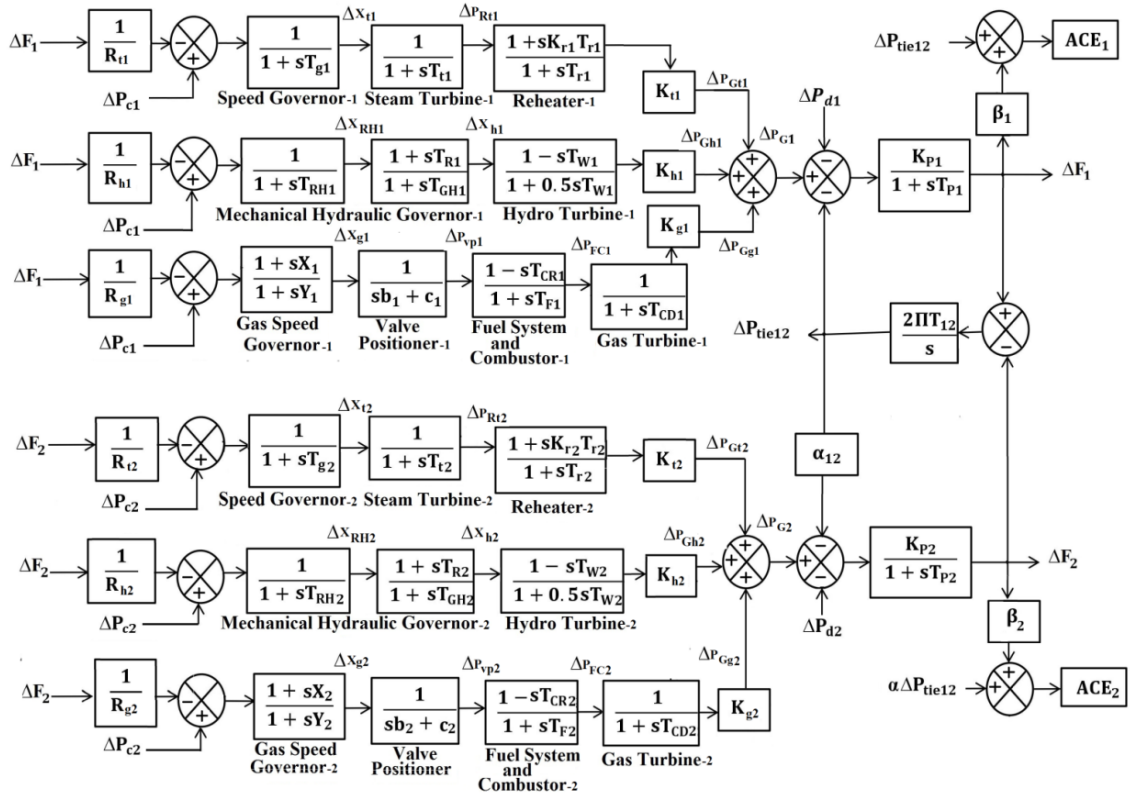
Fig. 3.8:   Transfer function model of power system under study.

The power system performance is studied by using different intelligent controller at 1% slp and random load perturbation.

2. Jaya based AGC of two area interconnected multi source Power System incorporating non-linearity

In this power system, first area consist of thermal, hydro, wind and second area consist of thermal, hydro, diesel energy sources as shown in Fig.3.9. The power system performance is studied by including boiler dynamics, governor deadband and Generation Rate Constraint in an interconnected power system at different loads.
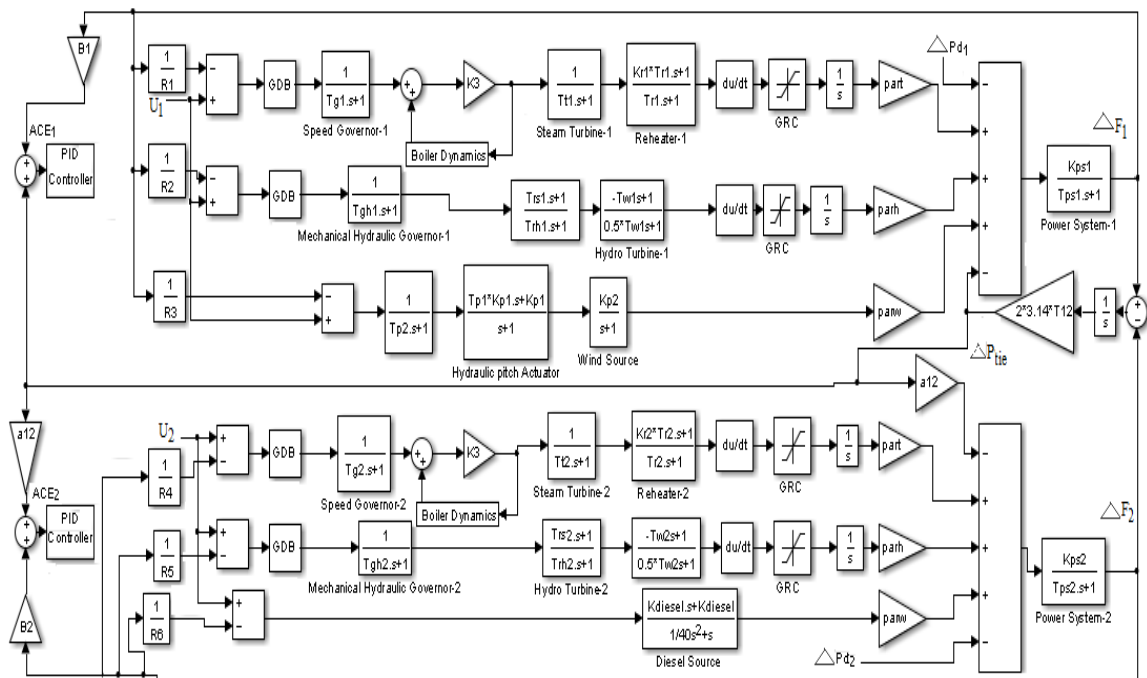
Fig. 3.9:   Two area interconnected power system including nonlinearities

3. Optimal Automatic generation control of three area interconnected multi source power systems by considering new structures of matrix Q and R. Different cases of Optimal AGC of three area interconnected multi source power system.

In this study, Optimal AGC of three power systems is considered. The power system performance is studied by considering various case study of developing cost weighting matrices at 1% slp.

a) Non-reheat thermal, hydro and gas power system

First power system has non-reheat thermal as first, hydro as second and gas as third control area as shown in Fig.3.10. The power system performance is studied by considering various case study of developing cost weighting matrices at 1% slp.
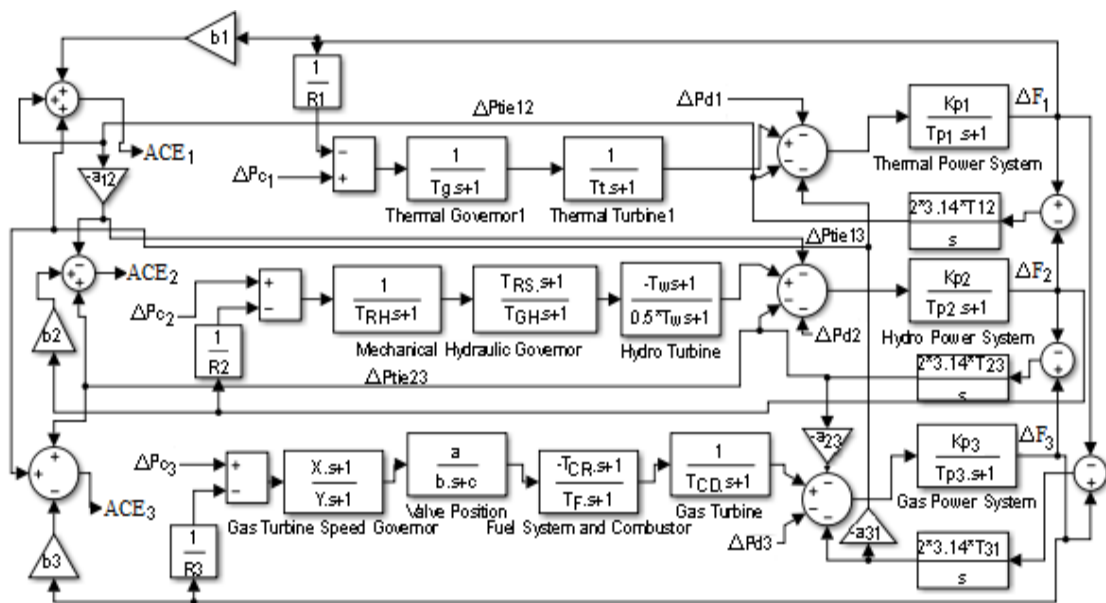
Fig. 3.10: Three area controlled non-reheat thermal-hydro-gas power system model

b)   Non-reheat thermal power system

Second power system has non-reheat thermal as control area as shown in Fig.3.11. The power system performance is studied by considering various case study

45

of developing cost weighting matrices at 1% slp.
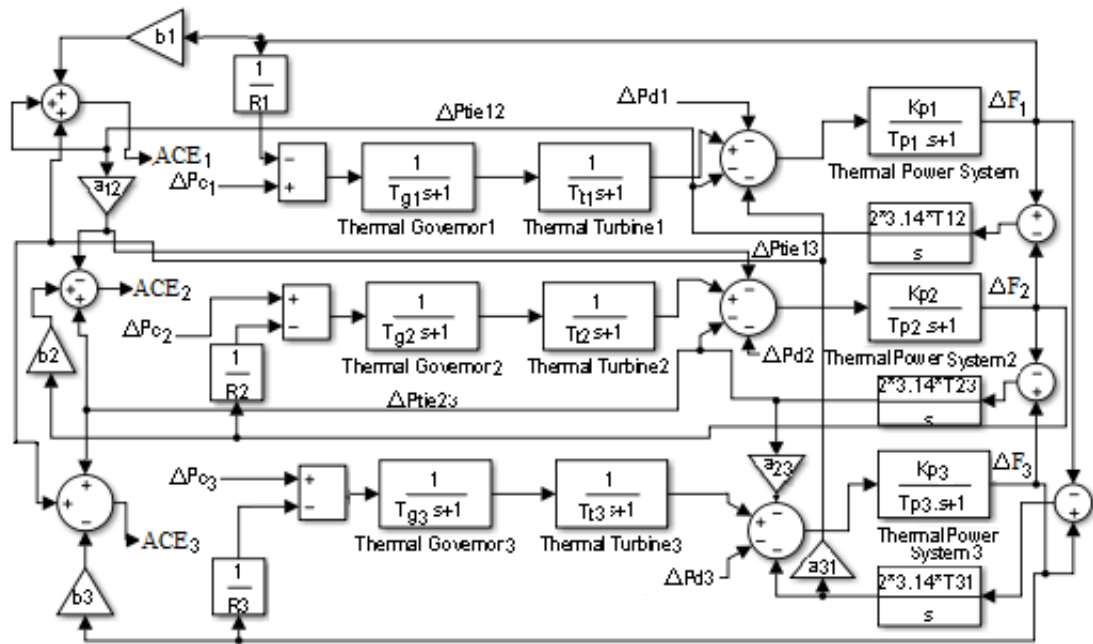
Fig. 3.11:   Three area controlled non-reheat thermal power system model

c) Non-reheat thermal, hydro and Non-reheat thermal power system
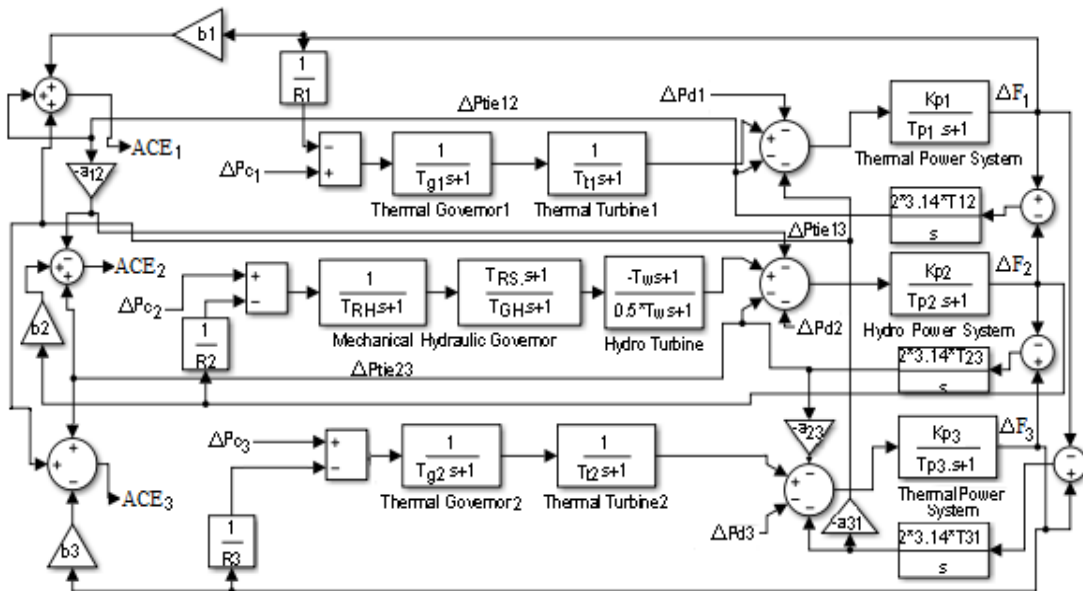
Fig. 3.12:   Three area controlled non-reheat thermal-hydro- non-reheat thermal power system model

In this study, power system has non-reheat thermal as first, hydro as second and non-reheat thermal as third control area as shown in Fig.3.12. The power system performance is studied by considering various case study of developing cost weighting matrices at 1% slp.

4. AGC Of Interconnected Multi Area Multi Source Power System With SMES

a) Non-reheat thermal-hydro-gas power system model with SMES

First power system with SMES has non-reheat thermal as first, hydro as second and gas as third control area as shown in Fig.3.13. The performance of power system with SMES is studied by considering load at 1% slp.
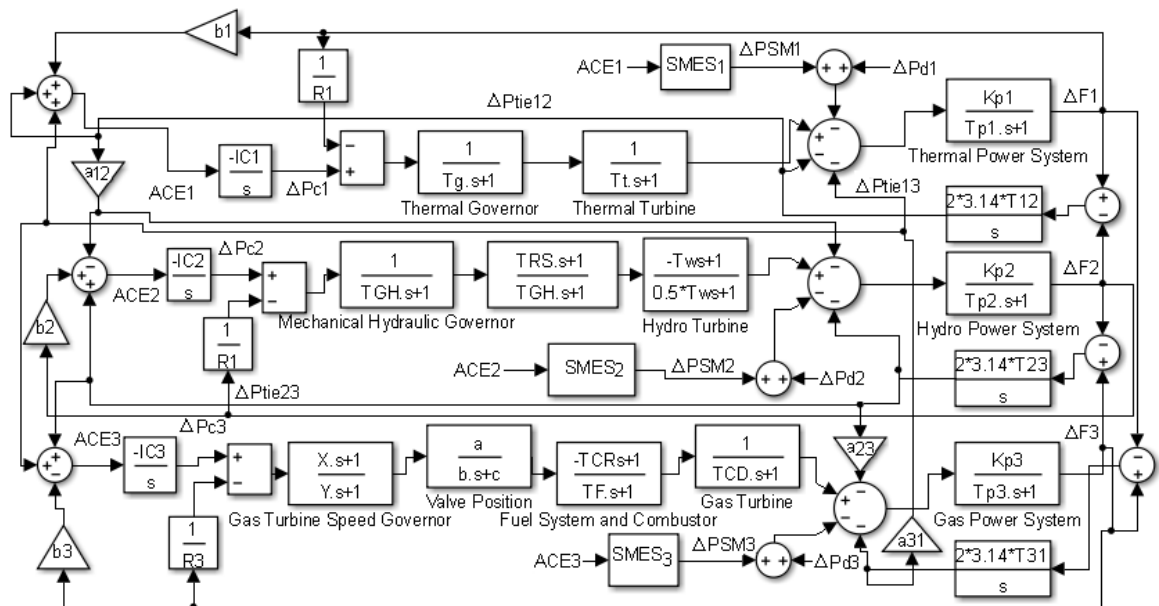
Fig. 3.13:   Three area controlled non-reheat thermal-hydro-gas power system model with SMES

b) Three area controlled non-reheat thermal power system model

Second power system with SMES has non-reheat thermal source as both control area as shown in Fig.3.14. The performance of power system with SMES is studied by considering load at 1% slp.
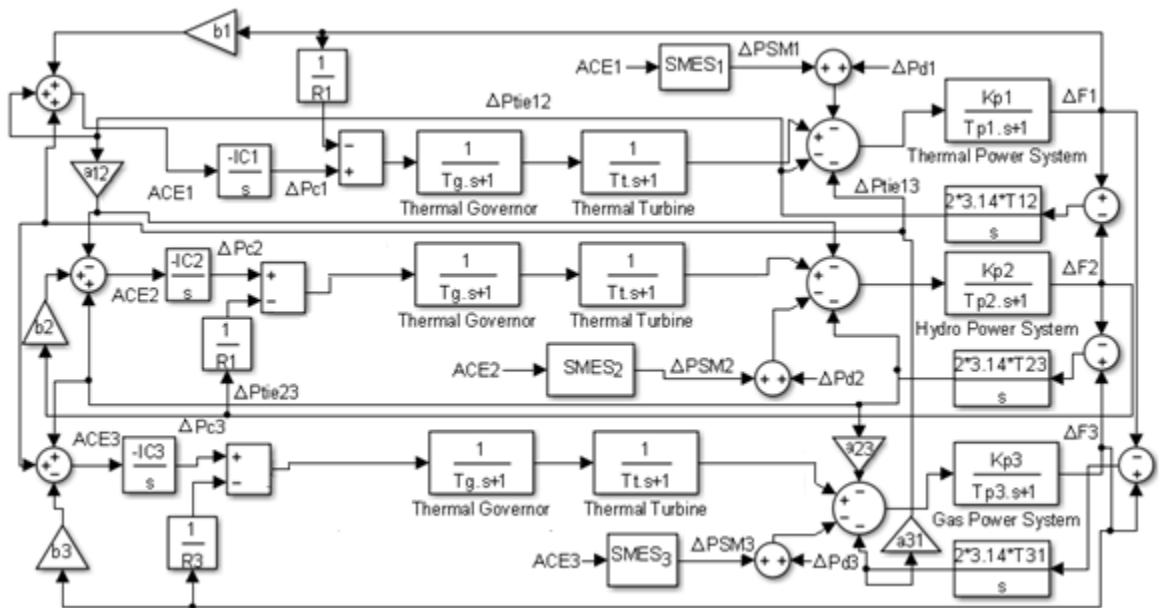
Fig. 3.14:   Three area controlled non-reheat thermal power system model with SMES

c) Non-reheat thermal-hydro-non-reheat thermal power system model with SMES

First power system with SMES has non-reheat thermal as first, hydro as second and non-reheat thermal as third control area as shown in Fig.3.15. The performance of power system with SMES is studied by considering load at 1% slp.

48
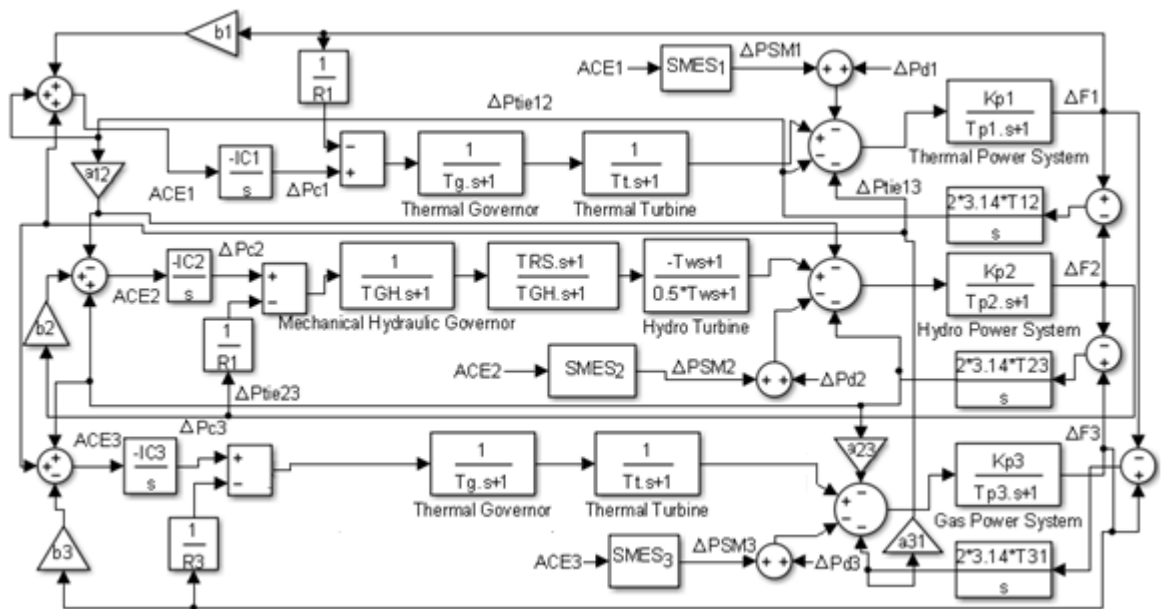
Fig. 3.15: Three area controlled non-reheat thermal-hydro- thermal power system model with SMES

5. AGC Of Interconnected Multi Area Multi Source Power System With BESS

a) Reheat thermal, hydro and gas power system
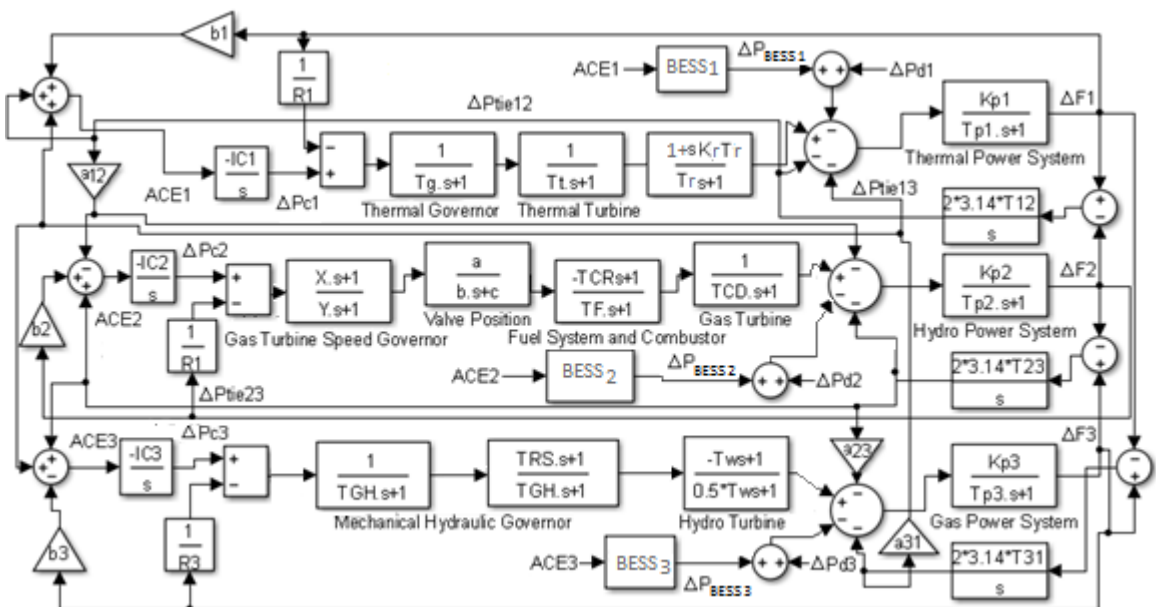
Fig. 3.16: Three area controlled reheat thermal-gas-hydro power system model with BESS

49

First power system with BESS has reheat thermal as first, hydro as second and gas as third control area as shown in Fig.3.16. The performance of power system with BESS is studied by considering load at 1% slp.

b) Non-reheat thermal, hydro and gas power system

Second power system with BESS has non-reheat thermal as first, hydro as second and gas as third control area as shown in Fig.3.17. The performance of power system with BESS is studied by considering load at 1% slp.
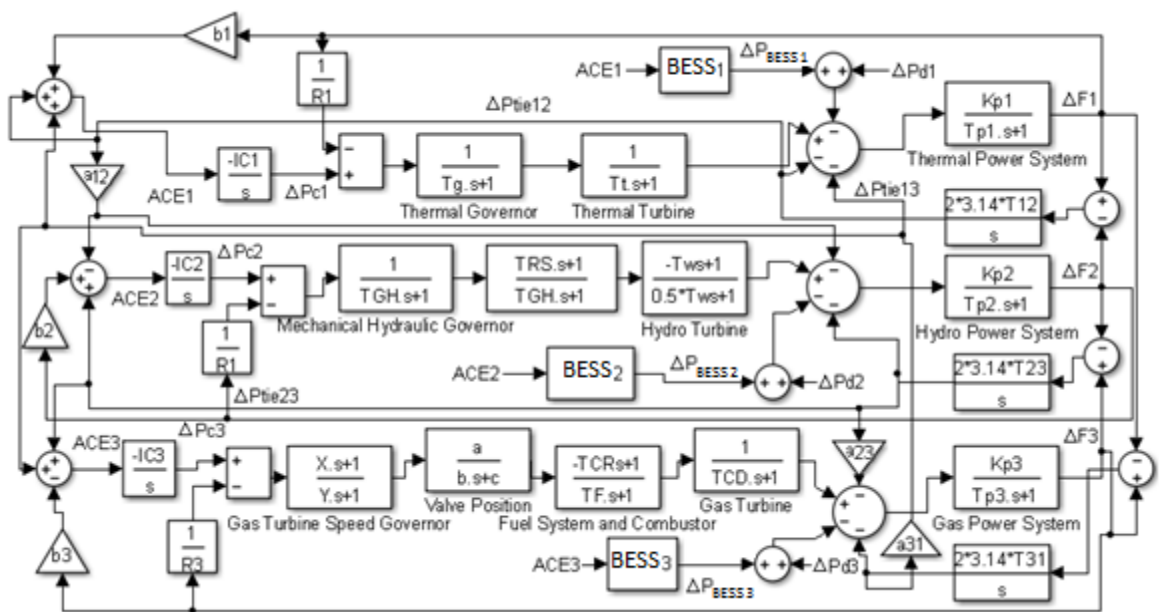
Fig. 3.17:   Three area controlled non-reheat thermal-hydro-gas power system model with BESS

c) Non-reheat thermal interconnected power system

Third power system with BESS has non-reheat thermal source as both control area as shown in Fig.3.18. The performance of power system with SMES is studied by considering load at 1% slp.
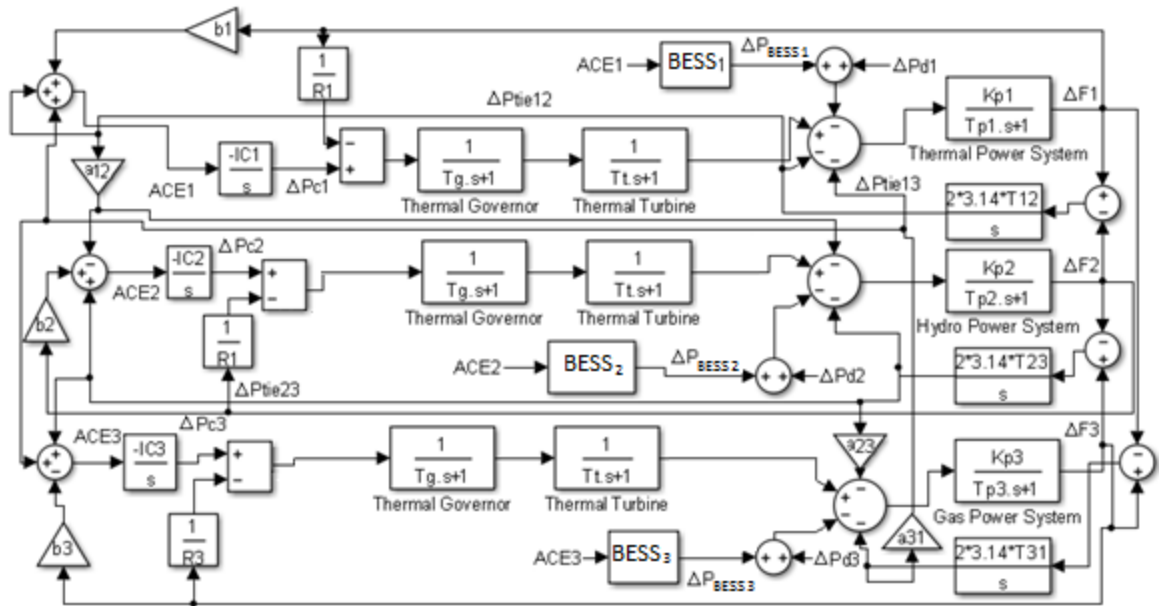
Fig. 3.18:   Three area controlled non-reheat thermal power system model with BESS

d) Non-reheat thermal, hydro and non-reheat thermal power system

Fourth power system with BESS has non-reheat thermal as first, hydro as second and non-reheat thermal as third control area as shown in Fig.3.19. The performance of power system with BESS is studied by considering load at 1% slp.
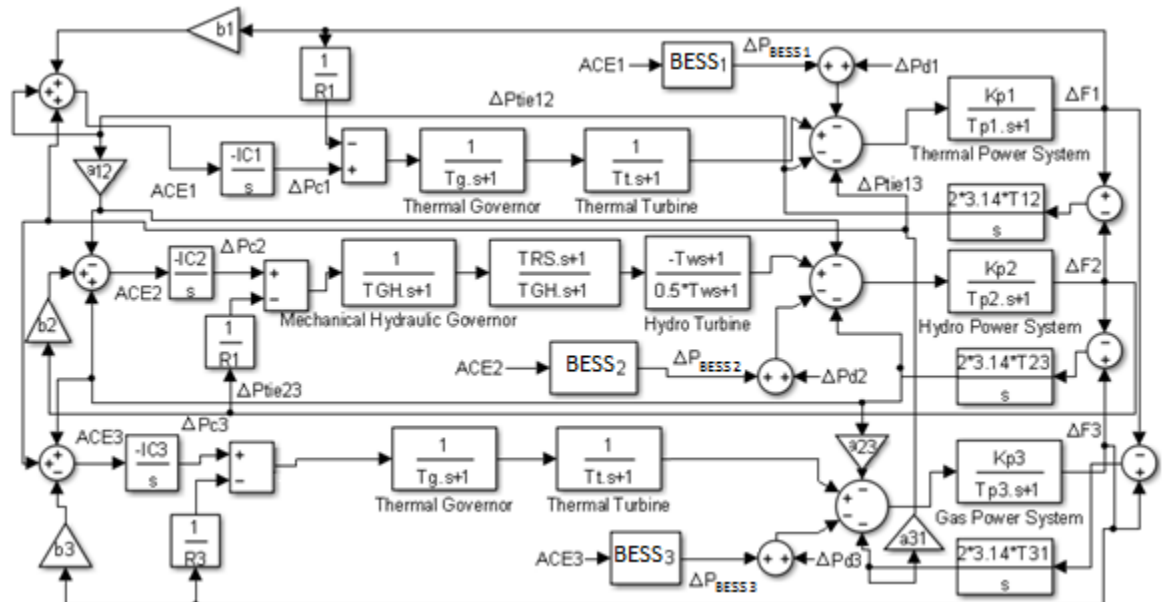
Fig. 3.19:   Three area controlled non-reheat thermal-hydro- non-reheat thermal power system model with BESS

3.4   Conclusion

In this third chapter, modeling of single area thermal, single area hydro, and single area gas power system including governing systems, interconnected AC tie-line, and other used components is done. The transfer function model of two-area and three-area interconnected multi source power system with various controllers, nonlinearities or energy sources is also developed.

CHAPTER 4

JAYA BASED AGC OF TWO-AREA INTERCONNECTED DIVERSE SOURCE POWER SYSTEM WITH VARYING PARTICIPATION

4.1   Introduction

In today's modern power system, AGC is actively operated in interconnected power system with diverse sources. Since last decades various sources like thermal, hydro and gas are considered as one of the reliable interconnected powers system. However, hydro power system diminished dynamic responses of power system at load disturbances. To operate power system successfully, the role of AGC in renewable sources like hydro power system requires amendment. This behavior of hydro power system is quiet suppressed by using different artificial techniques or by using energy storage system. Since, energy storage system increases the cost of the plant when applied in interconnected power system.   So, there is a need to explore artificial techniques for the unstable effect of hydro sources in an interconnected power system with diverse sources. A new Artificial Intelligence (AI) technique known as Jaya algorithm is used to design Proportional-Integral-Derivative (PID) controllers for AGC of two area interconnected diverse source power system. The superiority of proposed Jaya based AGC has been demonstrated by contrasting its dynamic response, performance index value and performance parameters in terms of settling time, peak time and first peak undershoot value with BAT and recently published Bacterial Forging Optimization (BFO) technique. The robustness analysis of the proposed

controller in terms of system dynamic responses with random load disturbances in control area-1 has been done. The study is further extended to analyze the effect of varying participation of diverse sources. In this chapter the novel impact of varying participation of diverse power sources in Jaya based AGC strategy for interconnected two area power system is presented. Further, a comparative analysis has been done to show a significant impact of varying participation of diverse source on dynamic response in terms of frequency deviation and tie line power deviation, settling time, first peak undershoot and performance index value of the system at 1% slp in one of the area. It has been shown that the sluggishness of dynamic response due to the use of hydro source can be significantly improved by decreasing the participation of hydro source and increasing the participation of thermal and gas source in an interconnected power system.

4.2   Power system under investigation

In this chapter, novel human based nature inspired artificial intelligence (AI) technique - Jaya is used to design PID controllers for AGC of interconnected two control areas diverse source power system. First of all, comparison of proposed Jaya based AGC has been shown by comparing its dynamic response, performance index value and performance parameters in terms of ST, FPu and FPt with bio-inspired AI technique like BAT and recently published Bacterial Forging Optimization (BFO) technique. Modeling of individual power system is explained in Chapter 3. The transfer function model of two area interconnected power system having diverse sources is indicated in Fig. 4.1. Each control area of considered power system model comprises of a combination of reheat thermal, hydro and gas power source. Each

control area are of same capacity of 2000MW is studied. The nominal parameters of the reheat thermal, hydro and gas power sources are specified in Appendix B.
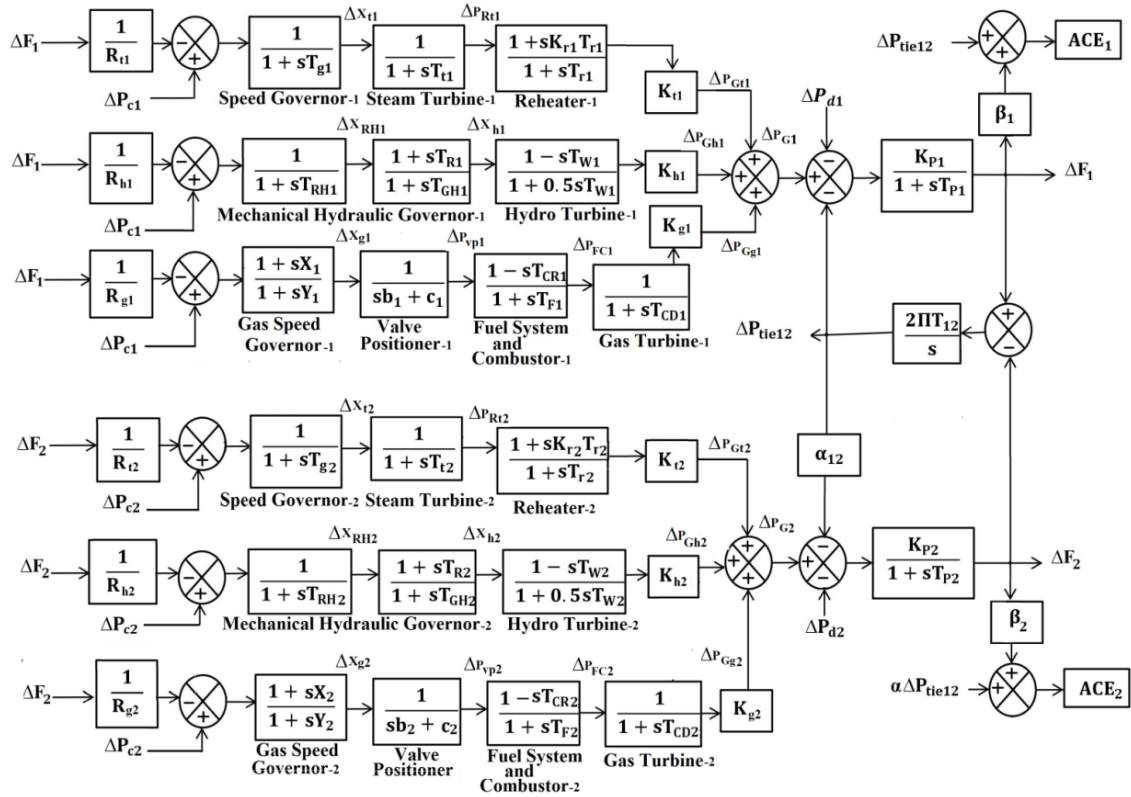
Fig. 4.1:   Transfer function block diagram of power system under study.

TABLE 4. 1   Different cases of two area diverse source power system

S.No.	Participation of diverse sources for scheduled generation in Area-1			Participation of diverse sources for scheduled generation in Area-2		
	K_{t1}	K_{h1}	K_{g1}	K_{t2}	K_{h2}	K_{g2}
1	0.33	0.33	0.33	0.33	0.33	0.33
2	0.5	0.25	0.25	0.5	0.25	0.25
3	0.6	0.1	0.3	0.6	0.1	0.3
4	0.25	0.5	0.25	0.25	0.5	0.25
5	0.6	0.3	0.1	0.6	0.3	0.1

Further, the approach of varying participation of energy sources in AGC of interconnected power system with diverse sources is simulated and scrutinized. Five different cases of two area interconnected diverse sources power system are categorized on the basis of varying participation of energy sources is shown in Table 4.1. Initialy comparative performance parameters of different AI optimized generation control strategy for considered power system at 1% slp in area-1 is presented in Table 4.2. Further for various cases of two area diverse source power system with varying participation, designing of PID controller is accomplished by using proposed Jaya optimization technique.

4.3   Optimization problem

The main problem formation is to minimize the objective function for considered power system having specific performance index (J_n) for two control area. Area control error (ACE) of the control area is considered as a base for the formulation of the objective function in AGC of interconnected diverse source power system. For considered power system, the integral square error criterion is formulated for performance index design of PID controller by using social human behavior based nature inspiresd optimization algorithm and swarm based bio inspired optimization algorithms.

The performance index is given by Eqn. (4.1)

$$J_n = \int_0^T ACE_n^2 dt \tag{4.1}$$

Where, n = 1 to 2 , ACE is the combination of frequency and tie-line power deviations.

Minimizing J_n is subject to the constraints of PID controller as given in Eqn. (4.2-4.4)

$$K_{pn}^{min} \leq K_{pn} \leq K_{pn}^{max} \qquad\qquad\qquad (4.2)$$

$$K_{In}^{min} \leq K_{In} \leq K_{In}^{max} \qquad\qquad\qquad (4.3)$$

$$K_{Dn}^{min} \leq K_{Dn} \leq K_{Dn}^{max} \qquad\qquad\qquad (4.4)$$

Where, K_{pn}, K_{In} and K_{Dn} are the proportional, integral and derivative parameters, min and max stand for the minimum and maximum values of the respective PID controller for each area.

Consequently, in each power system model PID controller has been designed with six parameters which are optimized by AI techniques are presented in Table 4.2. Social human behavior based nature inspired like Jaya optimization technique and swarm based bio inspired optimization technique like BAT and BFO are applied to optimize PID controller.

4.4   Simulation results and discussions

4.4.1   Different AI techniques at 1% slp and random load perturbation in control area-1

Effect of different artificial techniques for designing of PID controller for AGC of interconnected two area diverse source power system at 1% slp in area-1 is simulated. Social human behavior based nature inspiresd AI technique like Jaya is compared with swarm based bio inspired AI technique like BAT and recently published BFO for the same system [141]. Each control area of equal rating comprises of reheat thermal, hydro and gas power sources as depicted in Fig.4.1. The comparison of frequency and tie line power deviation of interconnected power system at 1% slp in

area-1 is shown in Fig. 4.2 (a-c). Critical scruitning of Fig. 4.2 (a-c) clears that dynamic responses of nature inspiresd AI technique like Jaya tuned PID controller for AGC of interconnected reheat thermal, hydro and gas power system gives better responses than bio inspired AI technique like BAT and BFO based power system. Performance of dynamic responses are numerically evaluated in terms of settling time (ST), first peak undershoot (FPu), first peak time (FPt), performance index value (PIv) and percentage improvement of ST as indicated in Table. Even though parameters of PID incase of Jaya is more than BAT and BFO but PIv for Jaya based AGC of interconnected power system (PIv = 0.51×10^{-5}) is comparatively better than BAT tuned AGC power system (PIv = 2.6×10^{-5}). Critical inspection of performance parameters given in Table 4.2, shows that the settling time of frequency deviation in area-1 gets improved with Jaya based AGC approach to around 6.25s as compared to BAT and BFO technique which has settling time around 8.24 s and 8.21 s. In case of frequency deviation in area-1, it is quite clear that the FPu is (-0.0063Hz) for the proposed optimized AI technique which is quite less as compared to BAT and BFO optimized technique where FPu is (-0.001 Hz) and (-0.0084 Hz) from steady state values. Similar inclination can be seen for frequency deviation of area-2 and tie-line power deviation between area-1 and area-2. It has been clearly seen that Jaya based AGC strategy at 1% slp in area-1 gives better performance parameters in terms of ST, FPu and FPt. This is justified by comparing values of Jaya approach with BAT and BFO approach in terms of percentage improvement in ST as 24.15% and 23.8% in frequency deviation of area-1, 33.1% and 18.25% in frequency deviation of area-2 and 10.55% and 22.81% in tie-line power deviation between area-1 and area-2. Moreover, the system has been perturbed to random load disturbances in area-1 as shown in

Fig.4.3(a). Comparison of dynamic responses of Jaya based AGC concepts with BAT based AGC concepts at random load disturbances in area-1 are shown in Fig. 4.3(b-d). At random load disturbances, Jaya technique gives PIv as 0.0003772 and BAT technique gives PIv as 0.0003821 with simulation time of 150 s. This comparison strengthens the fact that Jaya based AGC strategy proves to be robustness for two area interconnected diverse source power system.

4.4.2 Different participation of diverse sources at 1% slp in control area-1 and control area-2

Jaya based AGC of two area interconnected power system has been applied to study and analyze the dynamic performances of numerous cases with varying participation of diverse sources. Different cases of Jaya based AGC of two area interconnected reheat thermal-hydro-gas power systems with different participation of energy sources are illustrated in Table 4.1. Comparison of dynamic responses for five cases at 1% slp in area-1 and area-2 has been demonstrated in Fig. 4.4 (a-c) and Fig. 4.5 (a-c) respectively.

(a)
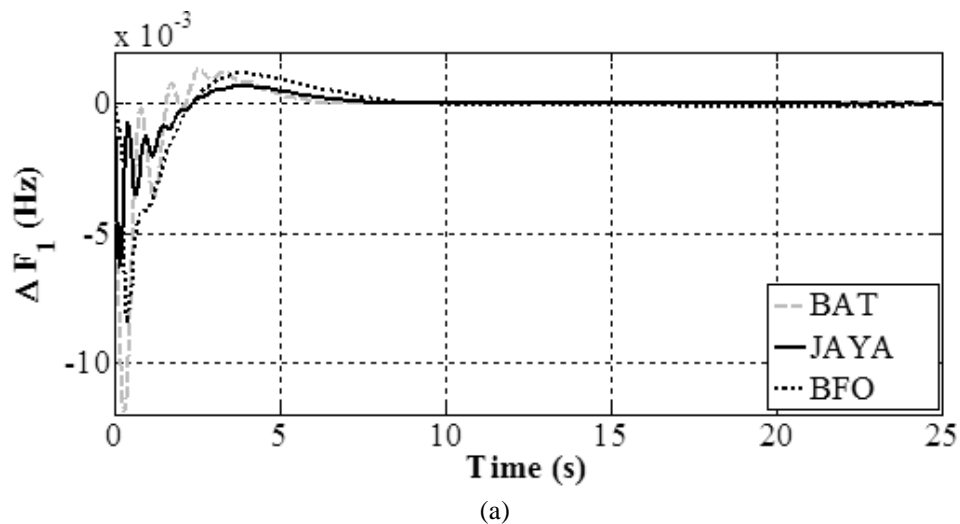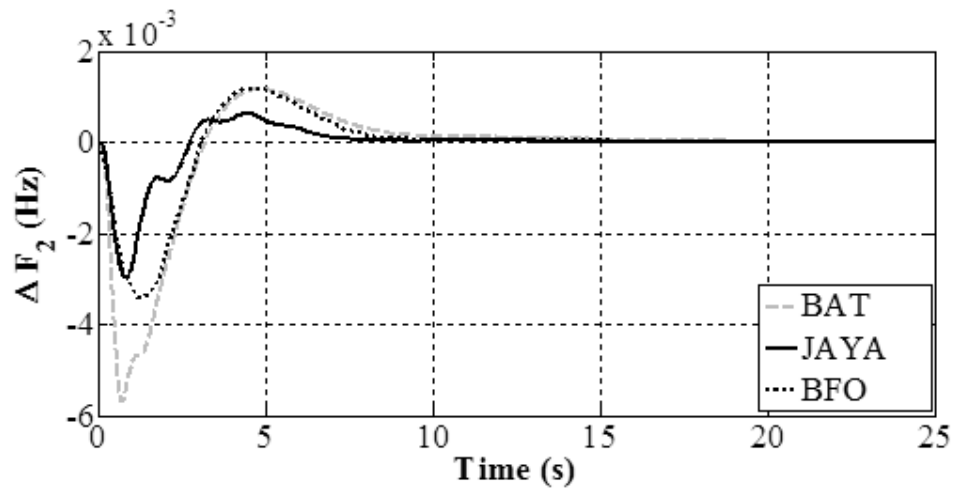
(b)
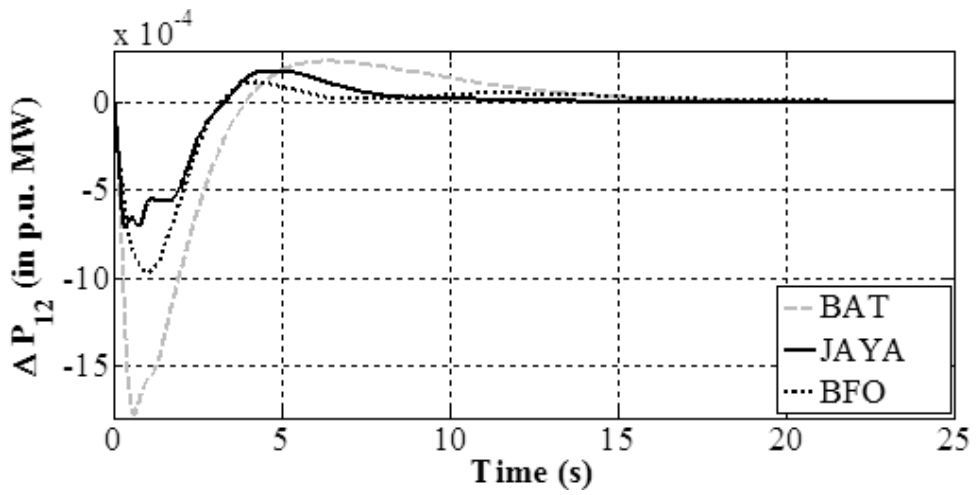
(c)

Fig. 4.2: Comparison of dynamic responses of power system with various AI techniques (a) ΔF_1 versus time (b) ΔF_2 versus time (c) ΔP_{12} versus time, at 1% slp in the control area-1.

(a)
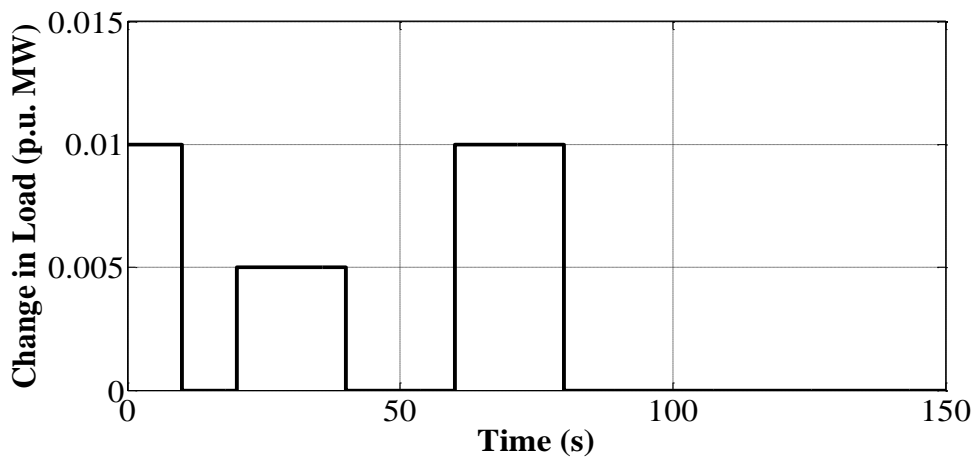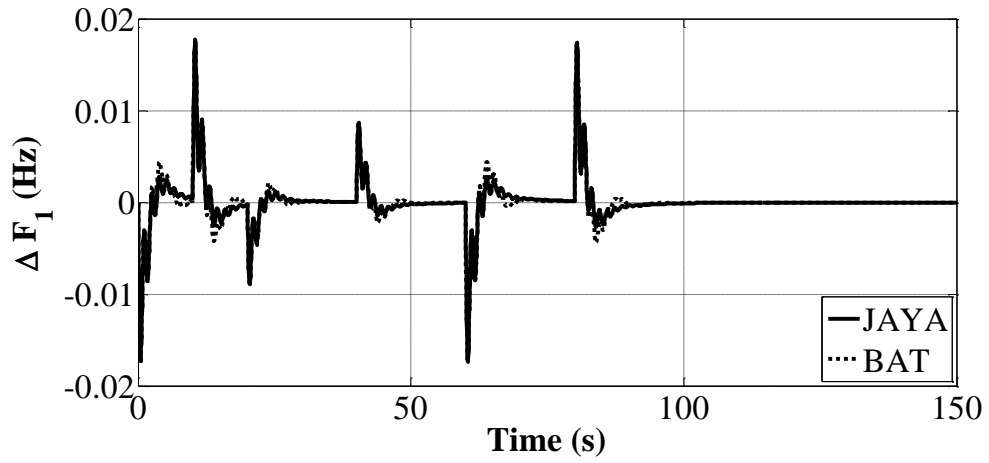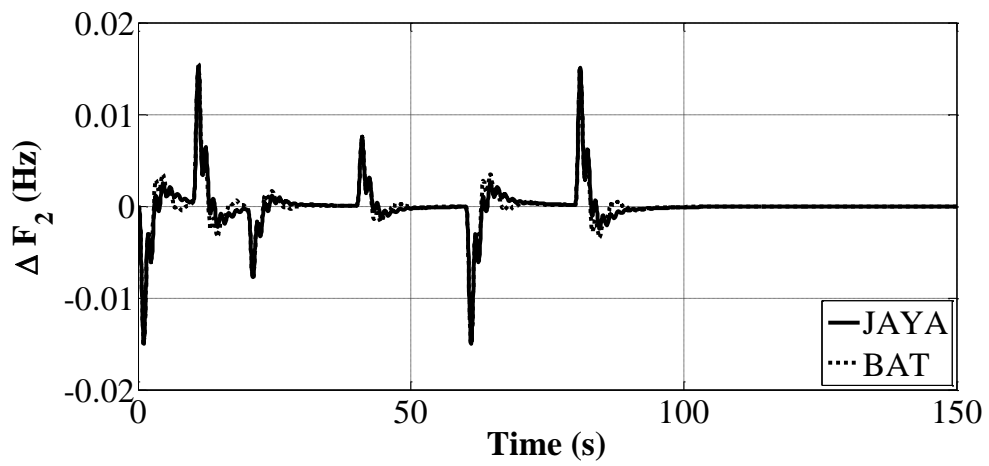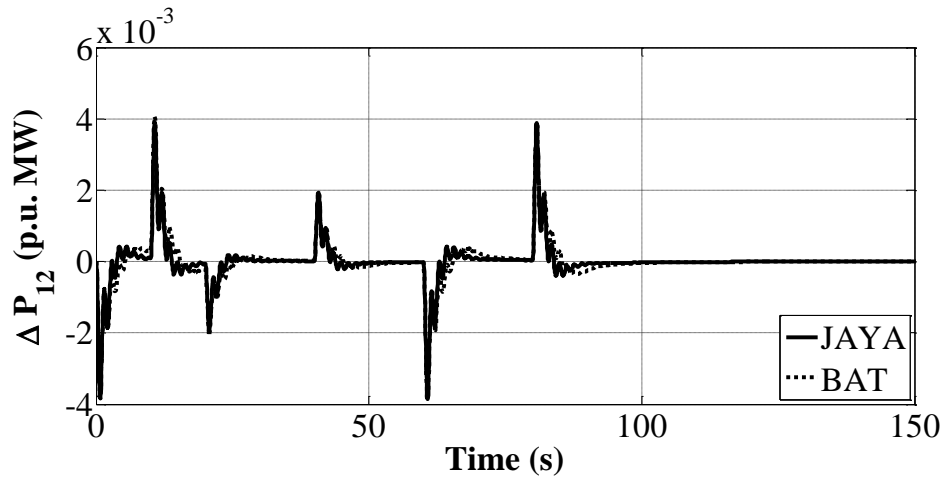
Fig. 4.3:   Two area interconnected power system at random load disturbance in area-1 (a) Change in load disturbance, (b) ΔF_1 versus time (c) ΔF_2 versus time (d) ΔP_{12} versus time.

61

The investigation of Table 4.3 and Table 4.4 clearly reveals that Jaya based AGC approach for varying participation of diverse sources have a significant impact on value of ST, FPu and PIv of the system. It is well studied by researchers that dynamic performances degrades more in hydro sources, this is due to the presence of water inertia of hydro source in power system.

TABLE 4. 2 **Comparative performance parameters of different AI optimized generation control strategy for considered power system at 1% slp in area-1**

		JAYA	BAT	BFO
ST (s)	ΔF_1	6.25	8.24	8.21
	ΔF_2	7.70	11.51	9.42
	ΔP_{12}	13.13	14.68	17.01
FPu (Hz) $\times$ 10^{-3}	ΔF_1	6.3	10	8.4
	ΔF_2	3	5.7	3.4
	ΔP_{12}	0.7	1.8	0.9
PT (s)	ΔF_1	0.16	0.28	0.37
	ΔF_2	0.84	0.69	1.27
	ΔP_{12}	0.36	0.61	1.03
Controller parameters of Area – 1	P	9.88	4.34	5.06
	I	9.78	3.46	4.26
	D	9.09	3.84	3.58
Controller parameters of Area – 2	P	7.18	4.99	1.86
	I	4.48	3.49	0.86
	D	1.32	5.40	1.59
% Improvement in ST	ΔF_1	24.15	23.8	
	ΔF_2	33.1	18.25	
	ΔP_{12}	10.55	22.81	

It is more evident in case-4 that dynamic response of power system is degraded as there is more participation of hydro source in regard to other sources in power system. This effect of degraded dynamic response can be improved by analyzing the proposed approach of varying participation of diverse source in Jaya based AGC of interconnected power system. PIv in case-4 is 0.000069 which is significantly improved in case-1 to 0.000026, case-2 to 0.0000084, case-3 to 0.0000059 and case-5 to 0.0000051.This is accomplished by decreasing the participation of hydro source and increasing the participation of other sources as in other cases. Further, by increasing the participation of thermal source in the power system, better dynamic performance and improvement in value of ST, FPu and PIv has been analyzed as depicted in case-2, case-3 and case-5. Inspection of dynamic responses reveals that the load disturbances have local dominance, FPu value of power system experienced more deviation in the area of disturbance as compared to other area.

In case-1, the value of FPu is (-0.0119) for frequency deviation in area-1 greater than (-0.0078) for frequency deviation in area-2 at 1% slp in area-1 and the value of FPu is (-0.0078) for frequency deviation in area-1 smaller than (-0.0120) for frequency deviation in area-2 at 1% slp in area-2. Similar trend can be seen for other cases. It has been observed that in case-2, the value of ST for frequency deviation in area-1 (7.21s) is smaller than frequency deviation in area-2 (12.95s) at 1% slp in area-1 and the value of ST for frequency deviation in area-1 (12.18s) is greater than frequency deviation in area-2 (6.28s) at 1% slp in area-2.
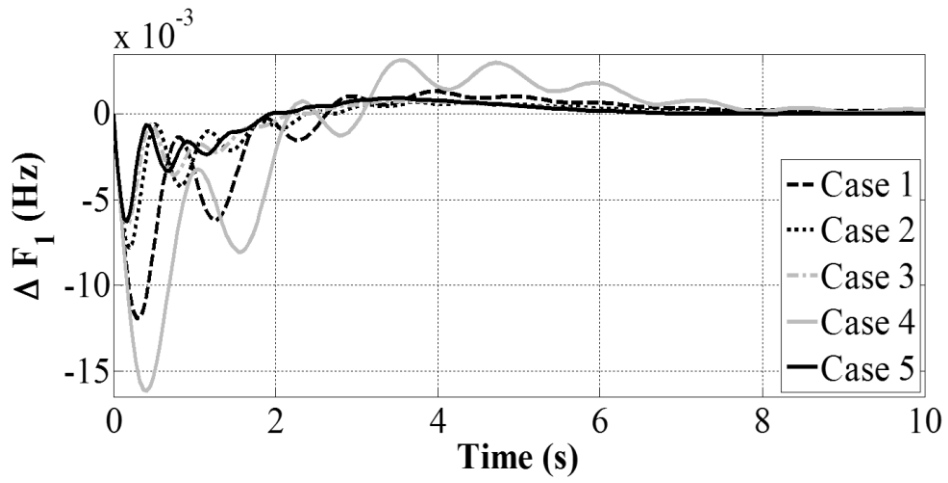
(a)
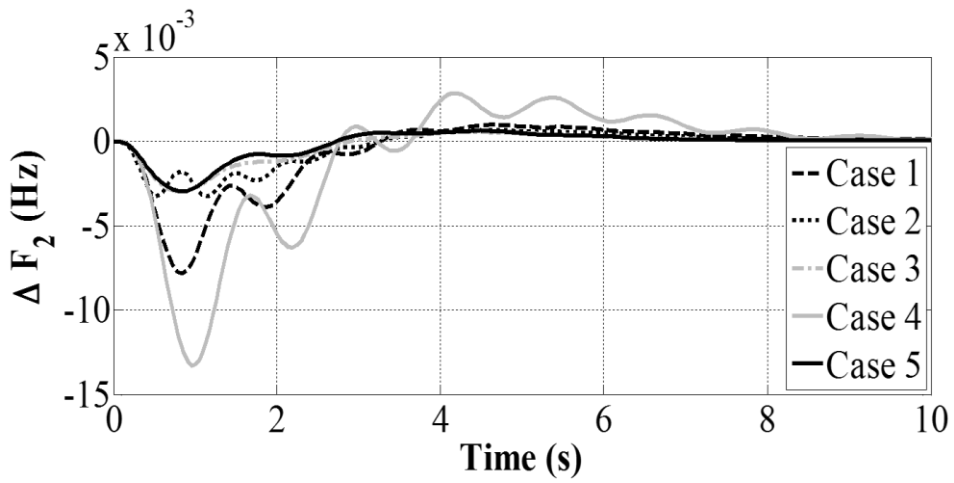
(b)
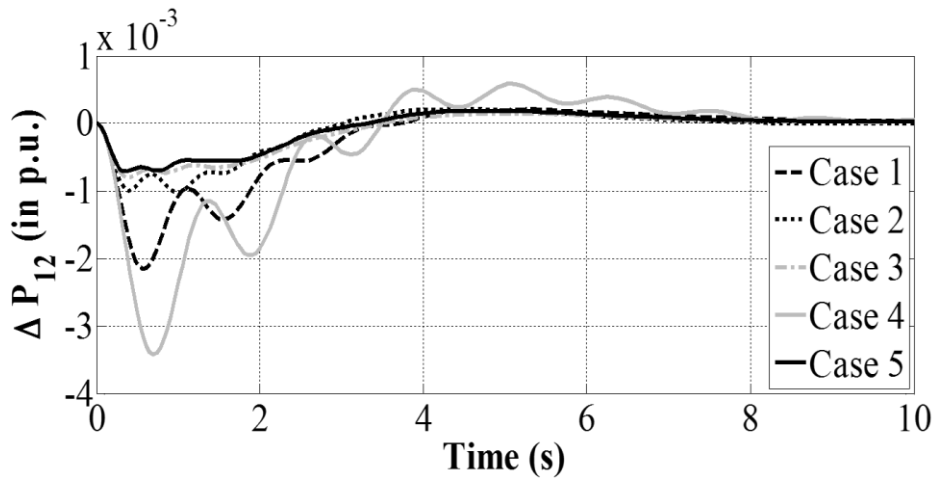
(c)

Fig. 4.4: Dynamic responses of power system with varying participation of diverse sources (a) ΔF_1 versus time (b) ΔF_2 versus time (c) ΔP_{12} versus time, at 1% slp in the control area-1.
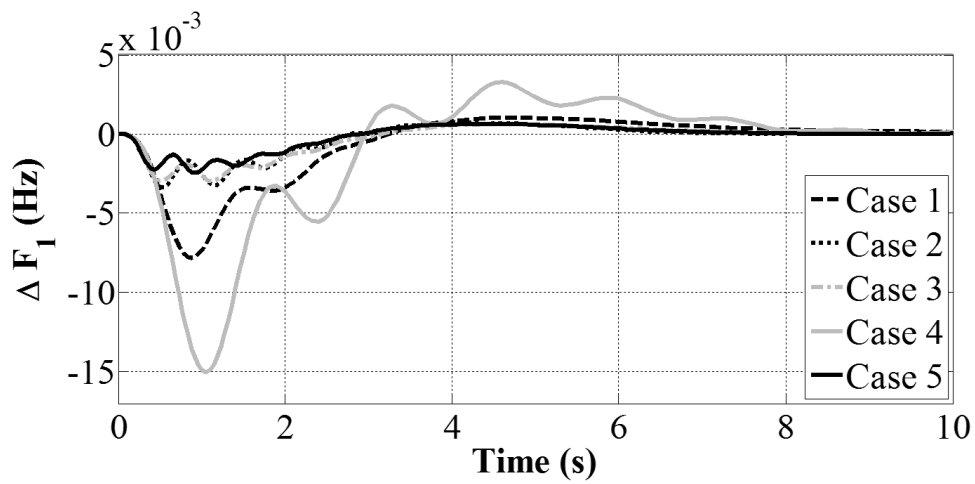
(a)
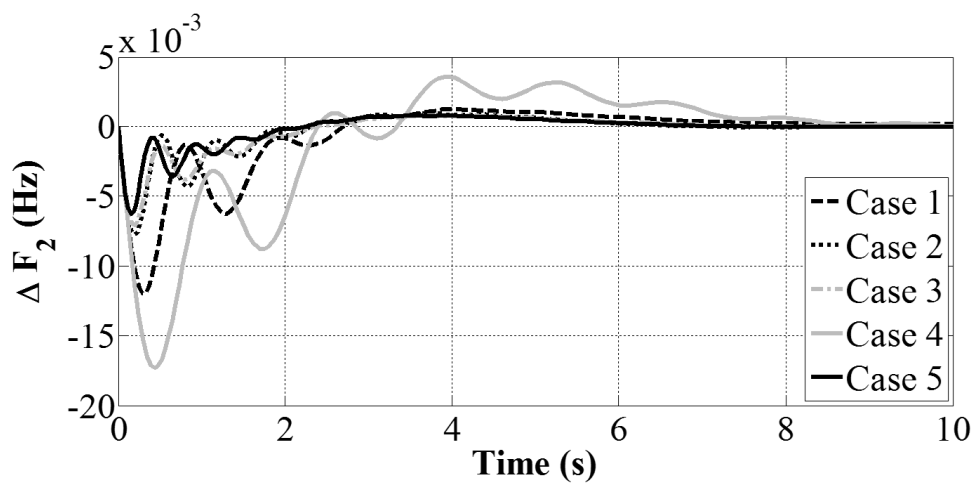
(b)
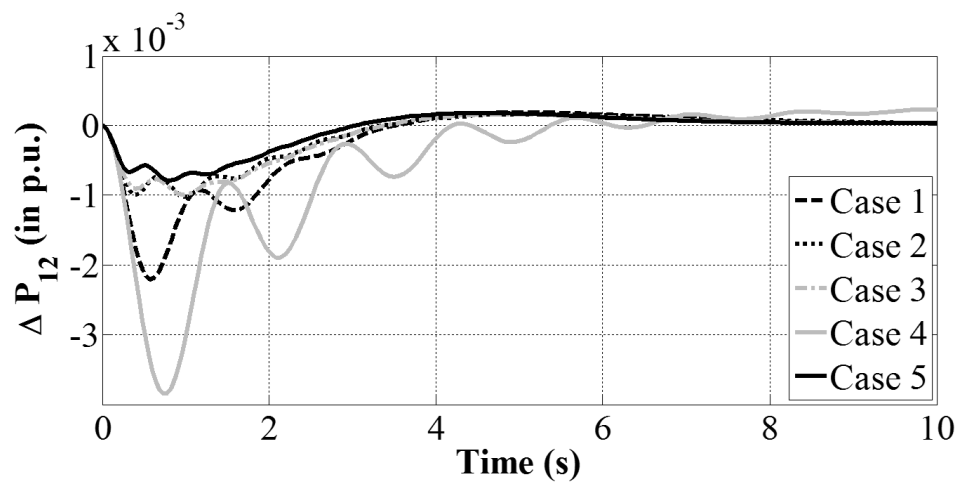
(c)

Fig. 4.5: Dynamic responses of power system with varying participation of diverse sources (a) ΔF_1 versus time (b) ΔF_2 versus time (c) ΔP_{12} versus time, at 1% slp in the control area-2.

Critical examination of dynamic responses reveals that the load disturbances have dominance on other area also. As, ST value of power system experienced more deviation in second area with respect to disturbance in first area.

TABLE 4. 3   Comparative performance parameters of different cases incorporating varying participation of diverse sources at 1% slp

	ST (s)						FPu $\times 10^{-2}$ (Hz) (-)					
	Area 1			Area 2			Area 1			Area 2		
Case	ΔF_1	ΔF_2	ΔP_{12}	ΔF_1	ΔF_2	ΔP_{12}	ΔF_1	ΔF_2	ΔP_{12}	ΔF_1	ΔF_2	ΔP_{12}
Case 1	7.43	9.05	8.60	9.23	7.63	8.36	1.19	0.78	0.22	0.78	1.20	0.22
Case 2	7.21	12.95	7.70	12.18	6.28	10.77	0.78	0.33	0.10	0.33	0.78	0.10
Case 3	6.43	7.85	13.73	8.13	6.87	13.69	0.64	0.30	0.07	0.30	0.71	0.09
Case 4	7.62	9.27	7.98	7.83	8.31	17.04	1.61	1.33	0.34	1.5	1.73	0.39
Case 5	6.25	7.70	13.13	7.71	6.58	13.12	0.63	0.30	0.07	0.25	0.63	0.07

TABLE 4. 4   Comparative PIv of different cases incorporating varying participation of diverse sources at 1% slp

ISE	PIv $\times 10^{-5}$				
	Case 1	Case 2	Case 3	Case 4	Case 5
Area 1	2.68	0.84	0.59	6.9	0.51
Area 2	2.73	0.84	0.81	8.3	0.51

4.5   Conclusion

This chapter demonstrates the effectiveness of novel Jaya based AGC of interconnected two area power system with diverse sources. The proposed human based nature-inspired Jaya based AGC approach is compared with other bio-inspired AI techniques like BAT and BFO techniques for the same system at 1% slp in control area-1. The beauty of this algorithm is that unlike other AI techniques, it requires only the common control parameters and does not require any algorithm specific control parameters which help in simulation to establish better dynamic response which further minimizes the frequency deviation and tie line power deviation in a shorter interval with lower values of first peak undershoot. The robustness analysis of Jaya based AGC of interconnected two area diverse source power system with random load disturbances in control area-1 also proves the supremacy of the proposed approach over other AI techniques.

Additionally, novel impact of varying participation of diverse power sources in Jaya based AGC strategy for interconnected two area power system has been implemented to design the PID controller of AGC strategy. The comparative analysis of varying participation of diverse source shows significant improvement in dynamic response in terms of frequency deviation and tie line power deviation, settling time, first peak undershoot and performance index value of the system in case of more participation of thermal source as compared to other two sources. Degraded values of performance index and peak absolute has been exhibited during more or equal participation of hydro power source as compared to combine participation of thermal and gas power sources. This effect of degraded dynamic response has been significantly improved by decreasing the participation of hydro power source as

67

compared to combine participation of thermal and gas power sources. Therefore, it may be concluded that the comparative study of implementation of varying participation of diverse sources may successfully be considered while designing AGC of interconnected diverse source power system.

<div align="right">

CHAPTER 5

</div>

JAYA BASED AGC OF TWO AREA INTERCONNECTED THERMAL-HYDRO-WIND AND THERMAL-HYDRO-DIESEL POWER SYSTEM WITH/ WITHOUT NONLINEARITIES

5.1   Introduction

The development and implementation of renewable sources has increased significantly during the last three decades. Among the renewable sources, wind source produces electricity economically. On the contrast, wind source is available in less populated area with a weak grid and it is unpredictable. Therefore, for secure operation of power system, wind sources require proper schemes for frequency control. However, undesirable behavior of renewable sources likes hydro and wind is regularly amended by researchers through incorporating different artificial techniques, energy sources, varying participation of sources etc. Regular increase in energy demand made the researchers to work towards the realistic hybrid interconnected multi source power system. To make the system realistic, researchers studied nonlinearities and participation factors incorporation in power system. A significant impact of varying participation of diverse source along with AI techniques has been seen in previous chapter. Nonlinearities namely boiler dynamics is due to turbine and boiler control act once after observing deviations in steam flow and pressure. Other nonlinearities like Speed Governor Dead Band (GDB) in other words as total magnitude of speed change while there is no change in valve position. GDB nonlinearity generally occurs for two

seconds oscillation occurs due to backlash non-linearity. Another nonlinearity Generation Rate Constraint (GRC) is defined as specified maximum rate for changed power generation. By proper selection of AI technique based controller for AGC of interconnected multi area multi source power system gives the opportunity to works well with nonlinearities also. So, a comparative analysis of AGC of interconnected power system with/without nonlinearities has been done between social human behavior based AI techniques with bio-inspired evolutionary based AI techniques incorporating varying participation of diverse sources. In power system with/without nonlinearities, participation of thermal sources is supposed to be more than hydro, wind and diesel sources. Equal participation of wind and diesel sources are supposed in power system with nonlinearities. The dynamic performances of power system is studied including the nonlinearities like Governor Dead Band (GDB), Generation Rate Constraint (GRC) and boiler dynamics at 1% slp and randomly varying load. The robustness of the proposed Jaya based AGC of two area interconnected power system with and without considering nonlinearities is presented under randomly varying load disturbance.

5.2   Power system under investigation

Investigations are performed on two models of power system consists of thermal-hydro-wind sources as first area, and thermal-hydro-diesel sources as second area as shown in Fig. 5.1. First power system model comprises of nonlinearities and different participation factors of each source and second power system model contain participation factors of each source but without nonlinearities. Social human behavior based new AI technique called Jaya technique is proposed to design PID controller for AGC of two area interconnected power systems including and excluding

70

nonlinearities. Nonlinearities namely boiler dynamics in thermal source, GRC in thermal and hydro sources, GDB in thermal and hydro sources are incorporated in power system and named as power system model-1 as shown in Fig.5.2. Turbine and boiler control act once after observing deviations in steam flow and pressure. Boiler dynamics description and nonlinearities values are well explained by some researchers [122,330]. GDB nonlinearity for two seconds oscillations occurs due to backlash non-linearity. Value of Backlash non-linearity as 0.02% (hydro sources) and 0.05% (thermal sources) is taken into account in the present work. For thermal units, a GRC for 3% per minute is considered in the present study. 270% per minute (raising) and 360% per minute (lowering) generation is the GRC value taken into account for hydro sources. Modeling for power system with nonlinearities are considered from [330]. Value of part (0.575) and parh (0.3) are supposed as the participation factor for reheat thermal and hydro sources. Participation factor of parw (0.125) is supposed for both wind and diesel sources. Specifications of power system without nonlinearities are acquired from [144] and are named as power system model-2, part (0.5747), parh (0.2873), parw (0.138) and parw (0.138) are supposed as the participation factor for reheat thermal, hydro, wind and diesel sources. Modeling of power system model-2 is given in [144]. Appendix B describes parameter values of power system including or excluding nonlinearities.

5.3   Optimization problem

PID controller with AGC is a popular and well accepted controller in literature. It helps in attaining faster response and stability for interconnected power system. In designing PID controller, frequency and tie-line power deviation are used as the base for the objective function. Amongst various performance criteria defined in AGC

studies [331], integral of time multiplied of absolute error (ITAE), integral of squared

error (ISE) and integral of absolute error (IAE), ITAE proves to be better performance

criteria. So, ITAE defined via. Eqn. (5.1) is used as the performance index to tune PID

controller.

$$\text{ITAE} = \int_0^T (|\Delta F_1| + |\Delta F_2| + |\Delta P_{12}|).\, t\, dt \qquad (5.1)$$

Where ΔF_1 and ΔF_2 is frequency deviation of area-1 and area-2, ΔP_{12} is tie line power

deviation of both areas, T is simulation time range.
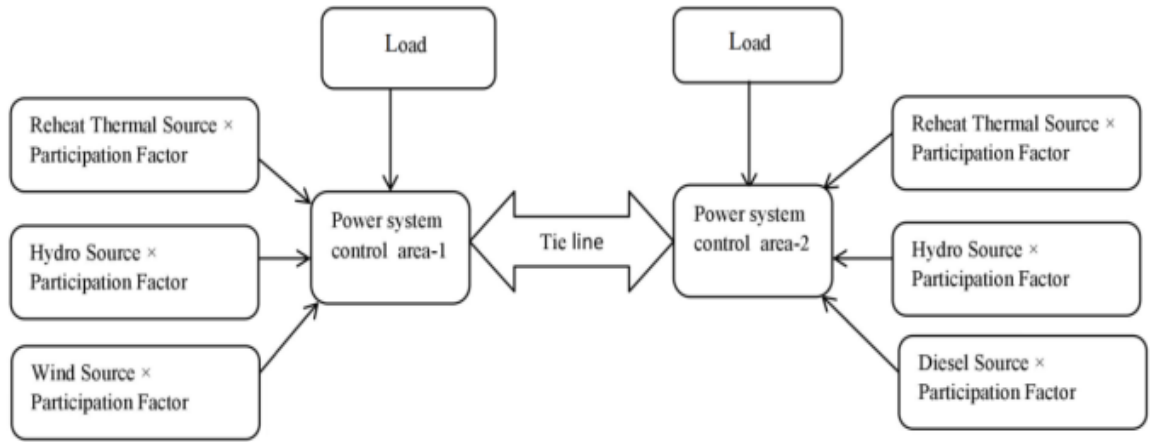
Fig.5.1: Two area interconnected power system with multi sources

Differential equation of PID controller of ith area is shown in Eqn. (5.2).

$$U_i = K_{Pi}ACE_i + K_{Ii} \int ACE_i dt + K_{Di} \frac{dACE_i}{dt} \qquad (5.2)$$

Where ACE_i is the area control error including frequency and tie line power deviation

for area-i. Value of i is 1 for area-1 and 2 for area-2. U_i is the control input for ith area.

Proportional (K_{Pi}), Integral (K_{Ii}) and Derivative (K_{Di}) are the PID controller parameter

for ith area in power system of both models.

PID controller for power system including or excluding nonlinearities is tuned by novel Jaya techniques. This procedure is repeated till the last iteration and designing of PID controller is accomplished with parameter values of PID controller. For novel Jaya tuned PID controller, parameters (k = 6), population (p = 25), termination criteria (i = 50) are considered. Controller provides six parameters each for two area power system with or without nonlinearities as given in Table 5.1.
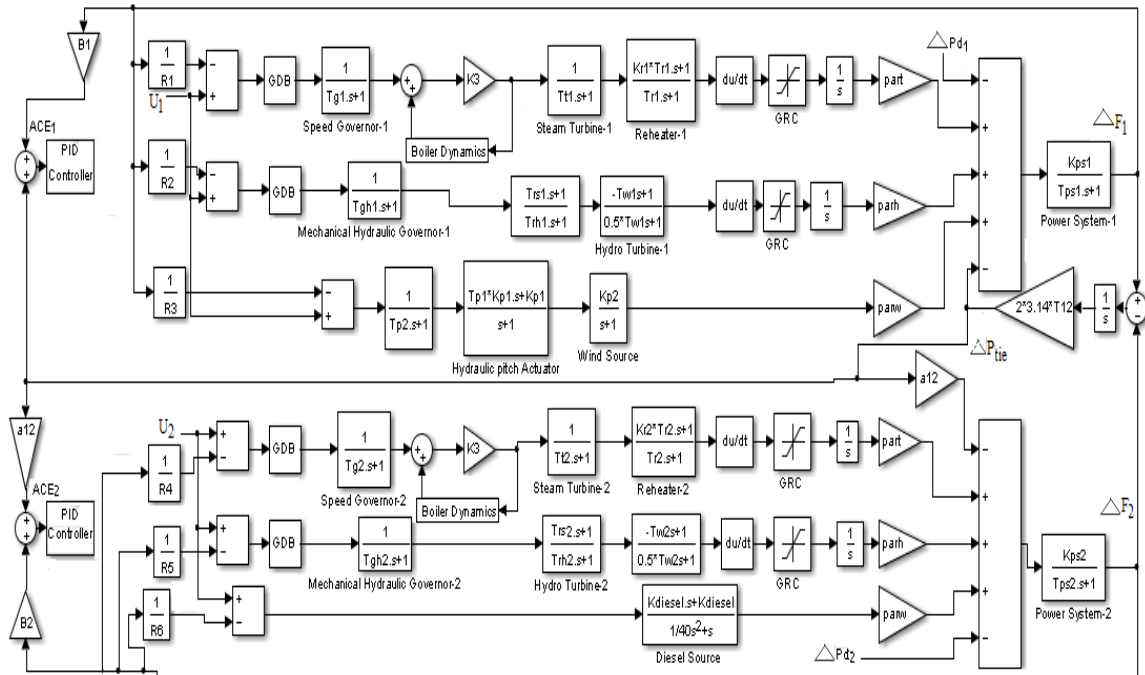
Fig.5.2: Transfer function block diagram of two-area interconnected power system with nonlinearities

5.4 Simulation results and discussions

5.4.1 Step load perturbation of 1% in control area-1 and control area-2 with nonlinearities

Two-Area interconnected power systems basically composed of four different sources namely reheat thermal, hydro, wind and diesel sources. Six parameters of proposed social human behavior based AI technique based PID controllers for power

system incorporating nonlinearities are shown in Table 5.1. Using novel Jaya based PID parameter values, the two power system models are simulated and set against other bio-inspired based AI techniques like DE, IPSO, BFA and social human behavior based TLBO algorithm. Comparative analysis in terms of performance values and percentage improvement in terms of ST is demonstrated in Table 5.2. Performance index (PIv) for Jaya-PID (0.06) is comparatively 95% better than DE-PID (1.32), 92.84% better than TLBO-PID (0.92) and 85.47% better than TLBO-PIDD (0.45) and hence proves that the proposed Jaya technique is far better than the other optimization techniques.

TABLE 5. 1   **Parameters for power system with and without nonlinearities**

PID Controller		power system model-1 (With nonlinearities)	power system model-2 (Without nonlinearities)
area - 1	K_{P1}	5	5
	K_{I1}	5	5
	K_{D1}	4.0946	2.06
area - 2	K_{P2}	3.6012	0.56
	K_{I2}	3.7251	3.39
	K_{D2}	5	0.01

Also, there is vast percentage improvement in settling time for Jaya in comparison of DE-PID as 67.68%, TLBO-PID as 65.09% and TLBO-PIDD as 60.59%. So, novel Jaya Algorithm is used as the formulation for the choice of PID controller for power system including or excluding nonlinearities. Dynamic performance of the power system model-1 under 1% slp in control area-1 and area-2 is depicted in Fig.5.3 (a-c) and Fig. 5.4 (a-c) respectively.

TABLE 5. 2   Comparative analysis of performance value and percentage improvement of power system including nonlinearities at 1% slp on area-1

Techniques	ST (s)				% Improvement in terms of ST			
	ΔF_1	ΔF_2	ΔP_{12}	ITAE	ΔF_1	ΔF_2	ΔP_{12}	ITAE
DE (PID)	19.68	21.93	25.89	1.32	67.68	47.33	63.07	95
TLBO (PID)	18.22	18.88	16.28	0.92	65.09	38.82	41.27	92.84
TLBO (PIDD)	16.14	16.79	12.77	0.45	60.59	31.20	25.13	85.47
JAYA (PID)	6.36	11.55	9.56	0.06				

TABLE 5. 3   Performance parameters values of Jaya based AGC of two area power system including nonlinearities

ST (s)						FPu $\times$ (-)0.01 (Hz)					
area-1			area-2			area-1			area-2		
ΔF_1	ΔF_2	ΔP_{12}	ΔF_1	ΔF_2	ΔP_{12}	ΔF_1	ΔF_2	ΔP_{12}	ΔF_1	ΔF_2	ΔP_{12}
6.36	11.55	9.56	3.55	2.83	6.23	1.74	0.95	0.43	0.09	0.22	0.02

Performance parameter values with respect to ST and FPu and PIv of Jaya based AGC of two area interconnected power system with nonlinearities are shown in Table 5.3. Frequency and tie line power deviation shows better results in terms of ST and FPu when load is applied in area-2 as comparison to the numerical evaluation of responses when load is applied in area-1. Similarly PIv for Jaya based AGC of two power system including nonlinearities gives better values in case of area-2 (ITAE – 0.0018) as compared to area-1 (ITAE – 0.066).

5.4.2 Random load in control area-1 and control area-2 with nonlinearities

Robustness of two area interconnected power system has been explored by applying randomly varying load in one of the control areas. Randomly varying load is applied for simulation time of 30 seconds as displayed in Fig.5.5. The dynamic response of power system with nonlinearities under randomly varying load in area-1 and area-2 is shown in Fig.5.6 (a-c) and Fig.5.7 (a-c).

It is evident that once again designed Jaya tuned PID controller gives satisfactory dynamic responses. It has been noticed that magnitude of frequency deviation of area-1 and area-2 and tie line power deviation of power system model-1 show reduced FPu value in case of random load applied in area-2 with respect to control area-1.

Moreover, the proposed Jaya based PID controller is capable to diminish the influence of perturbation and attain satisfactory dynamic responses of frequency and tie-line power deviation at randomly load in area-1 and area-2. Finally, it is understood that the offered approach is a robust for two area interconnected multi source power system including non-linearities.

Hence, proposed technique of Jaya Technique is used as the formulation for the choice of PID controller of power system model-2.
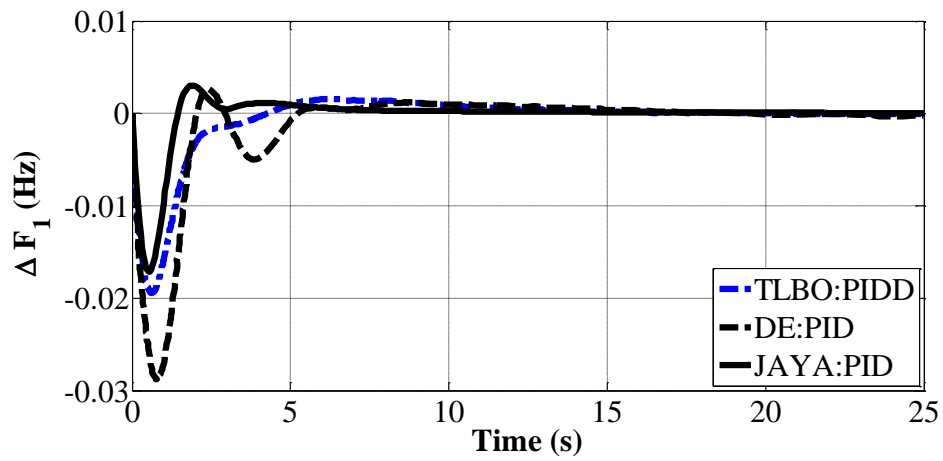
(a)
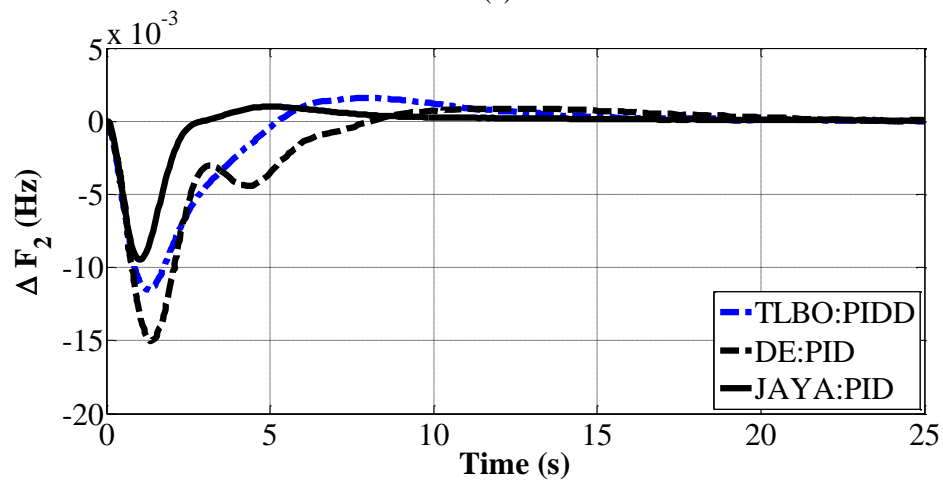
(b)
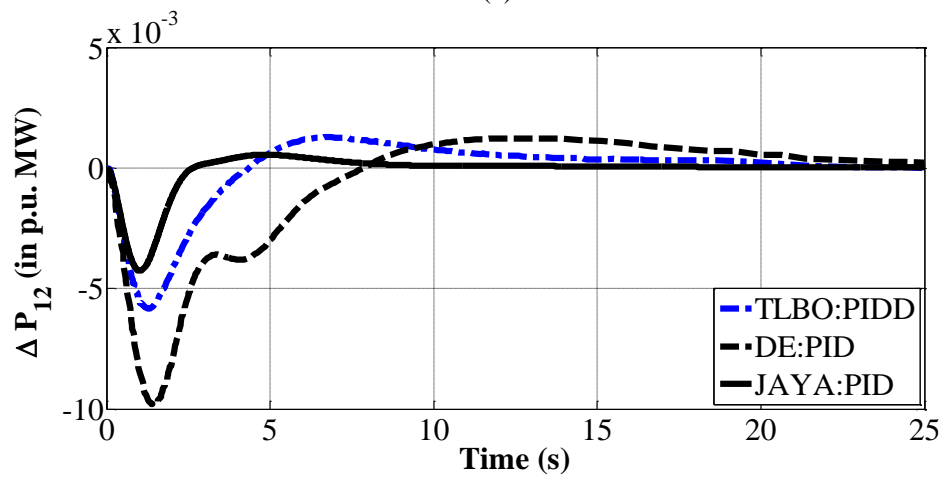
(c)

Fig.5.3: Dynamic response of two area interconnected power system with nonlinearities at 1% slp in control area-1 a) Frequency deviation of area-1 b) Frequency deviation of area-2 c) Tie line power deviation, Vs Time.
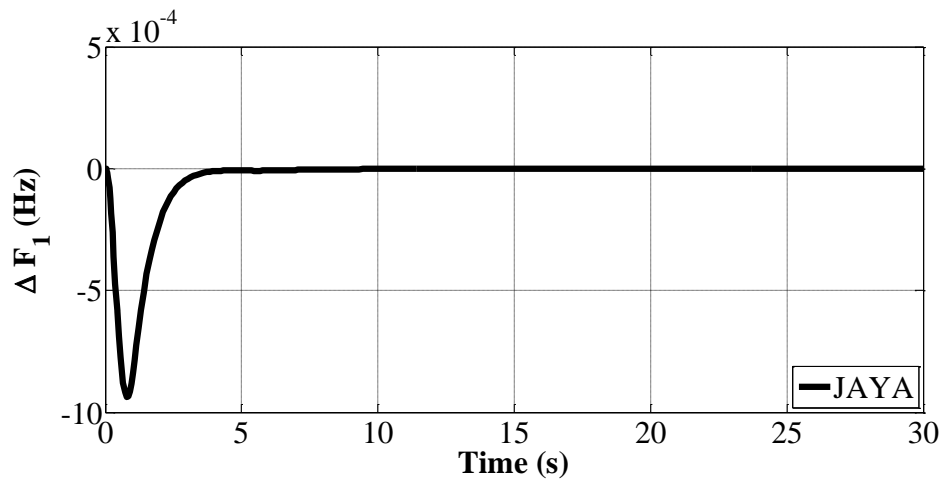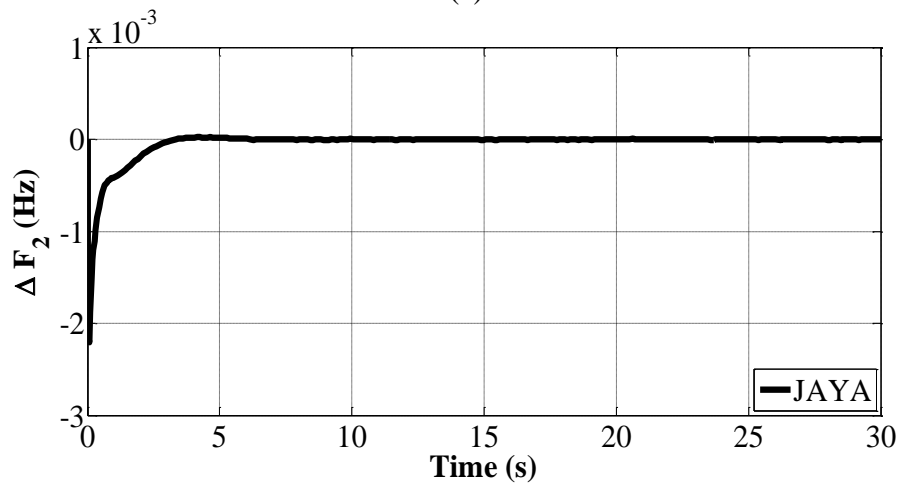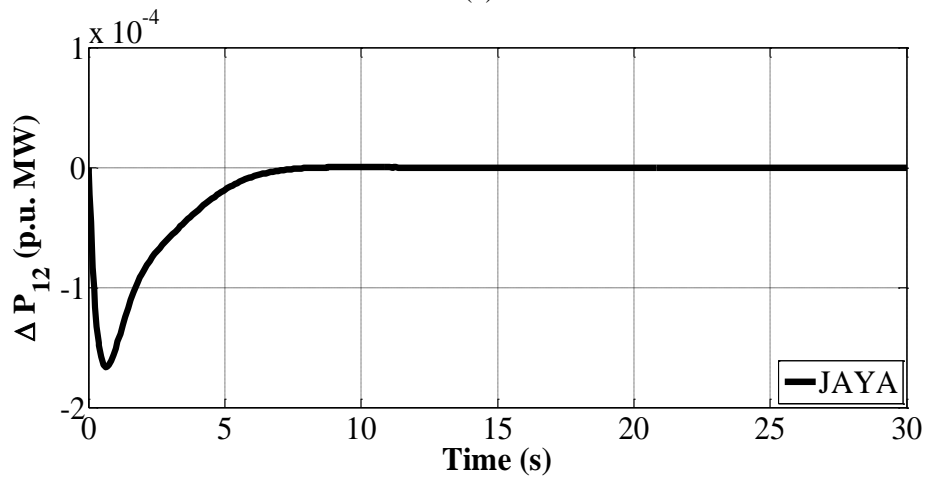
Fig.5.4: Dynamic Response of two area interconnected power system with nonlinearities at 1% slp in control area-2 a) Frequency deviation of area-1 b) Frequency deviation of area-2 c) Tie line power deviation, Vs Time.

5.4.3 Step load perturbation of 1% in control area-1 and control area-2 without nonlinearities

Six parameters of proposed social human behavior based AI technique based PID controllers for power system model-2 without nonlinearities are given in Table 5.1. Using novel Jaya based PID parameter values, two area interconnected multi source power system without nonlinearities are simulated and set against other bio-inspired based AI techniques like bio inspired IPSO, PSO and BFA and social human behavior based TLBO algorithm. Dynamic responses of power system model-2 under 1% slp in area-1 and area-2 are illustrated in Fig.5.8 (a-c) and Fig.5.9 (a-c). On comparing dynamic responses, it is affirmed that the performance of power system model-2 with novel Jaya Algorithm is far better than the considered IPSO, PSO and BFA optimization techniques with same PID controller.
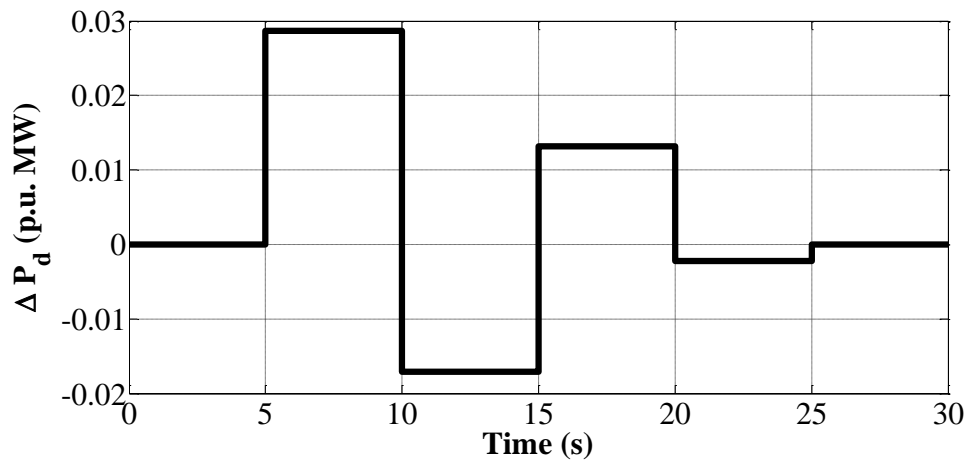
Fig.5.5:   Random load for power system model-1
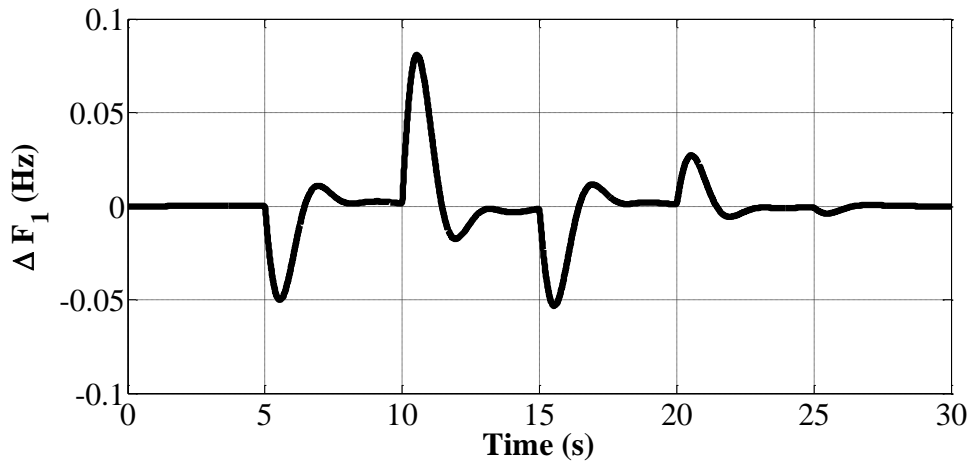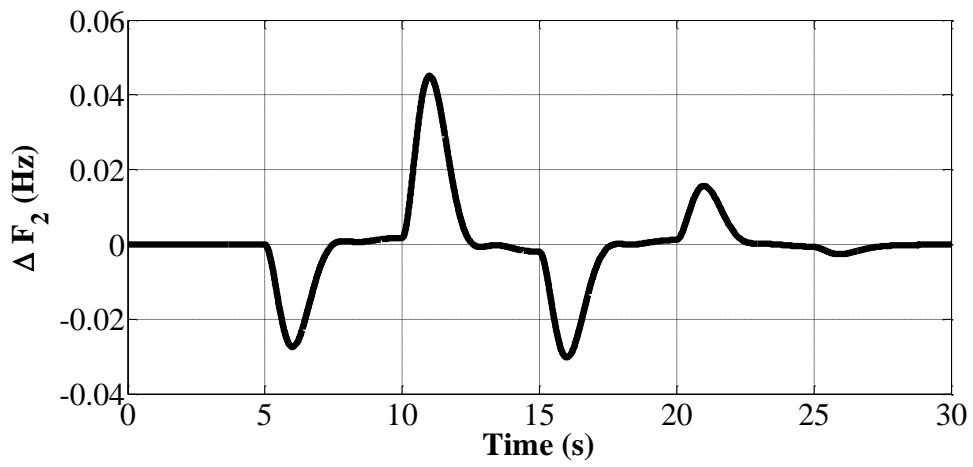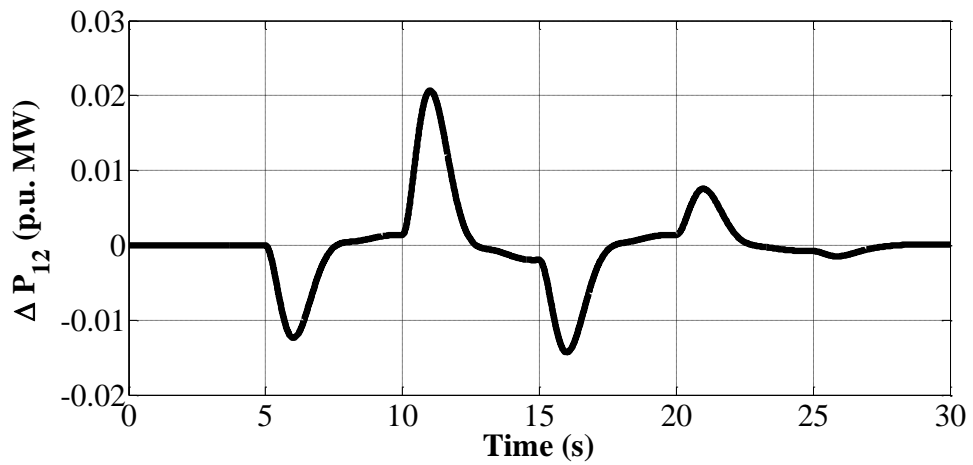
Fig.5.6: Dynamic Response of two area interconnected power system with nonlinearities at random load in control area-1 a) Frequency deviation of area-1 b) Frequency deviation of area-2 c) Tie line power deviation, Vs Time.

(a)

(b)

(c)
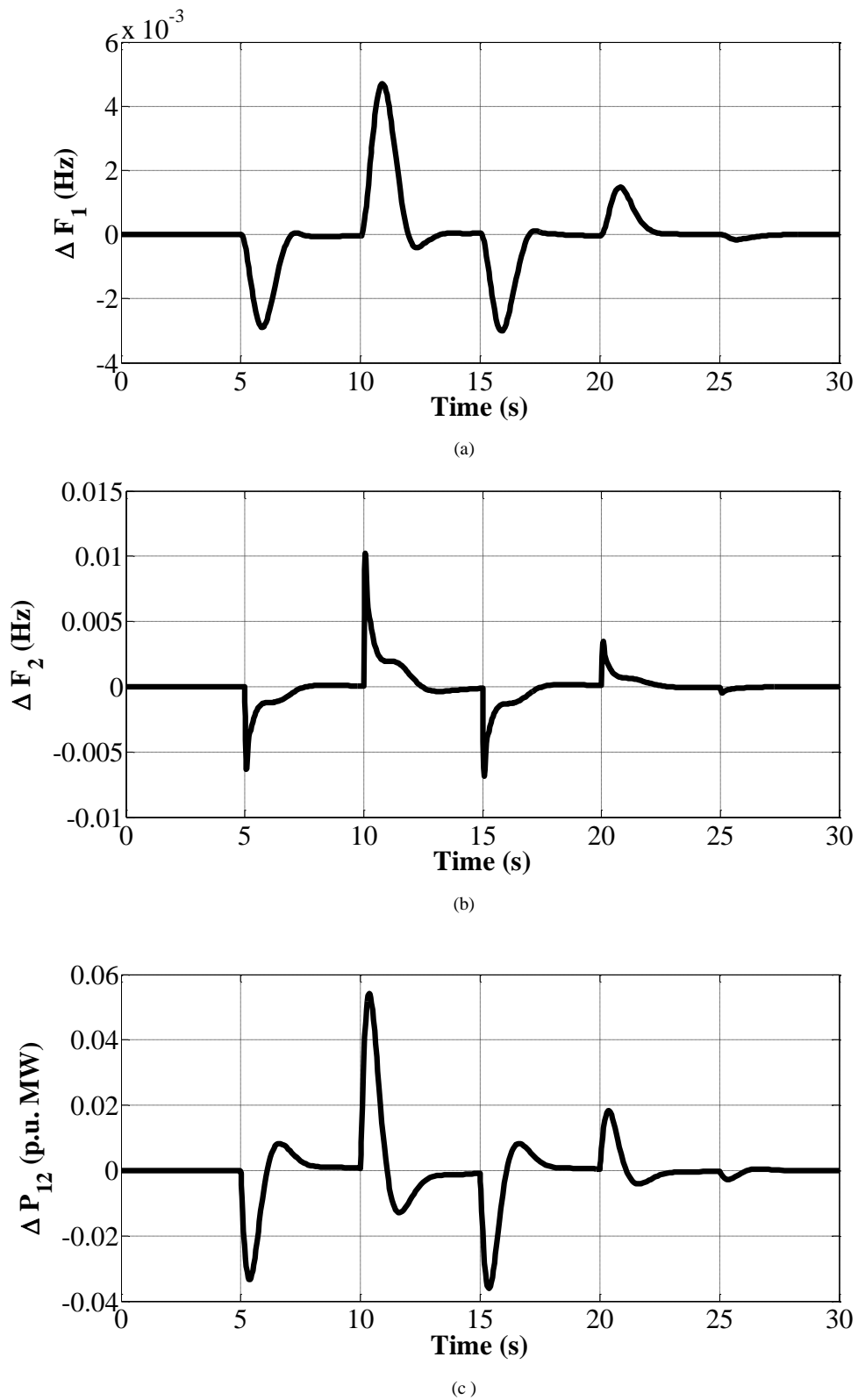
Fig.5.7: Dynamic Response of two area interconnected power system with nonlinearities at random load in control area-2 a) Frequency deviation of area-1 b) Frequency deviation of area-2 c) Tie line power deviation, Vs Time.

81

Moreover, performance parameters values of power system without nonlinearities at 1% slp in area-1 and area-2 are shown in Table 5.4. It shows improved performance parameter values in terms of ST and FPu when load is applied in area-2 as compared to area-1. Similarly reduced PIv is received for power system model at load in area-2 (thermal-hydro-wind) (ITAE – 0.003) as compared to area-1 (thermal-hydro-diesel) (ITAE – 0.0358). It shows that the dynamic responses of power system without nonlinearities develops more FPu and ST values when the load is considered in the area which has wind source as one of the multi-source. For proposed novel jaya based power system without nonlinearities under 1% slp in area-1, PIv for novel Jaya (ITAE – 0.0358) is compared with latest study [144] with IPSO (ITAE – 0.2036), BFA (ITAE – 0.2624) and PSO (ITAE - 0.2309) as different AI techniques. Hence, proves that novel Jaya technique gives better PIv and is used as the formulation for the choice of PID controller of power system without nonlinearities.

5.4.4 Random load in control area-1 and control area-2 without nonlinearities

Jaya based AGC two area interconnected multi source power system without nonlinearities is furthermore simulated at random load which is shown in Fig. 5.10.

TABLE 5. 4   Comparative performance analysis of power system without nonlinearities under 1% step load perturbation

ST (s)						FPu × (-)0.01 (Hz)					
area-1			area-2			area-1			area-2		
ΔF_1	ΔF_2	ΔP_{12}	ΔF_1	ΔF_2	ΔP_{12}	ΔF_1	ΔF_2	ΔP_{12}	ΔF_1	ΔF_2	ΔP_{12}
5.07	11.67	10.74	6.67	6.95	6.52	1.1	0.4	0.19	0.04	0.06	0.01
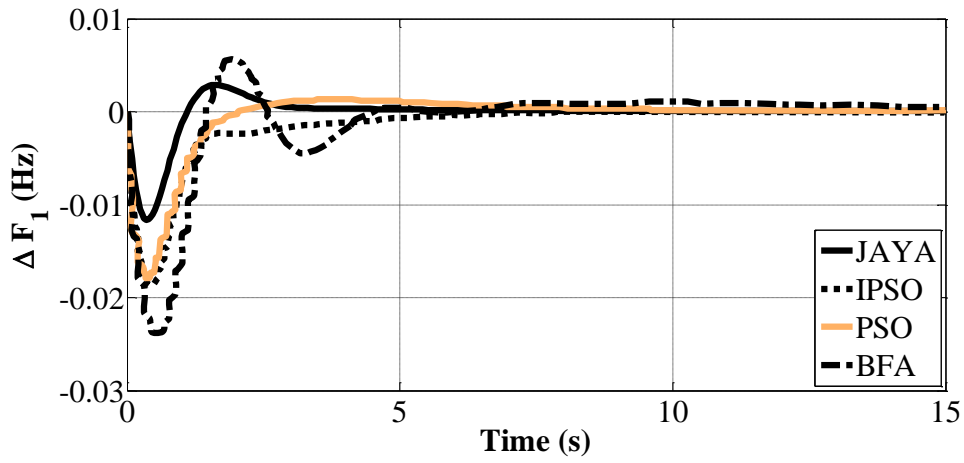
(a)
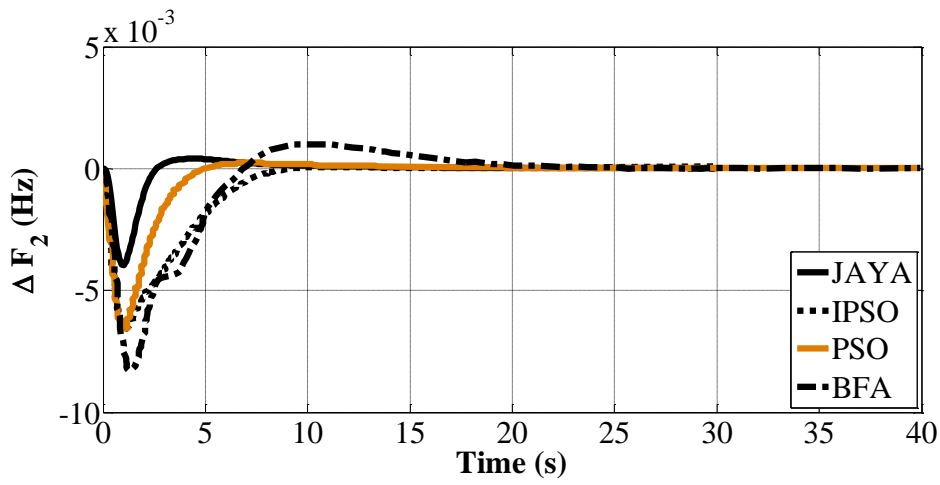
(b)
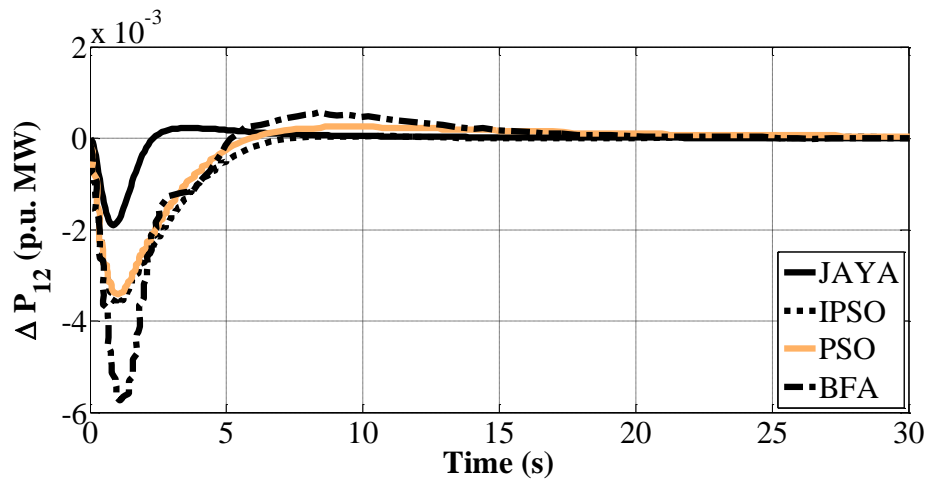
(c)

Fig.5.8: Dynamic Response of two area interconnected power system without nonlinearities at 1% slp in control area-1 a) Frequency deviation of Area-1 (ΔF_1) b) Frequency deviation of Area-2 (ΔF_2) c) Tie line power deviation (ΔP_{tie}), Vs Time.
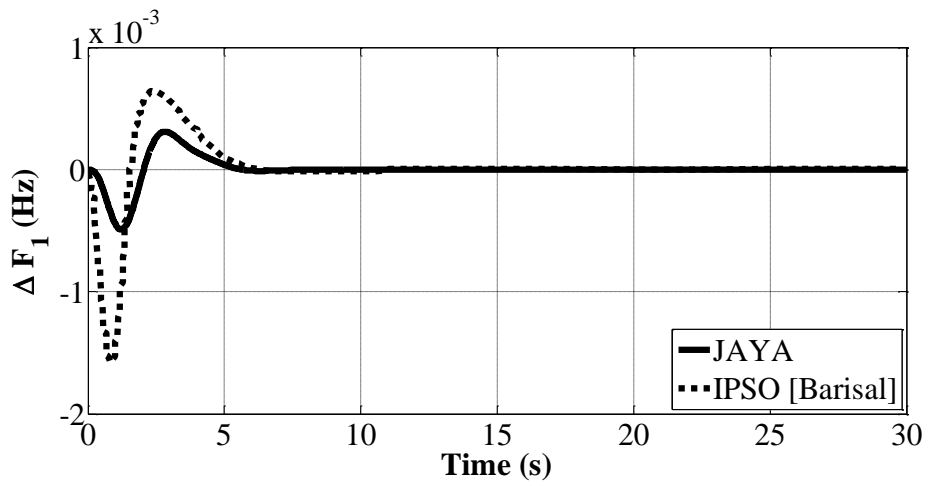
(a)
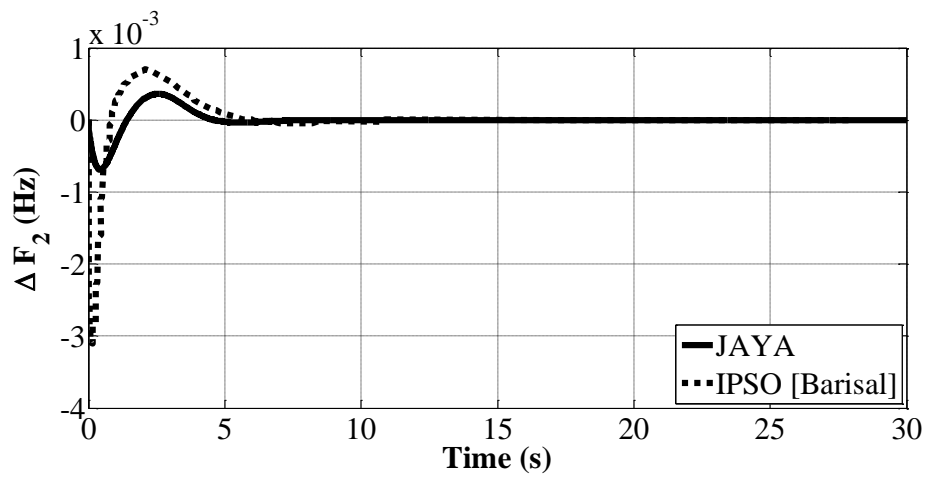
(b)
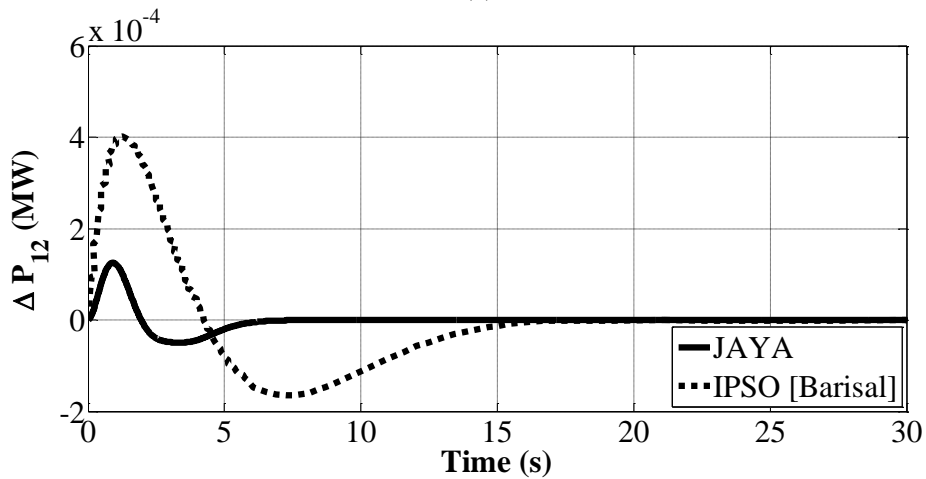
(c)

Fig.5.9: Dynamic Response of two area interconnected power system power system without nonlinearities at 1% slp in control area-2 a) Frequency deviation of area-1 b) Frequency deviation of area-2 c) Tie line power deviation, Vs Time

To check the robustness of power system without nonlinearities, random load is concerned for simulation time of 30 seconds as exhibited in Fig.5.10. The dynamic response of two area multi source power system without nonlinearities under random load in area-1 and area-2 is shown in Fig.5.11 (a-c) and Fig.5.12 (a-c). Critical inspection of dynamic response clearly indicates that Jaya based AGC of interconnected power system without nonlinearities gives satisfactory responses at random load in both areas. It has been noticed that magnitude of frequency deviation of both areas and tie line power deviation of power system model-1 show reduced magnitude of deviation in case of random load applied in area-2 with respect to area-1. Also, the novel Jaya based PID controller is able to minimize the effect of disturbances and achieve acceptable dynamic responses of frequency and tie-line power deviation in the presence of random load. Hence, it is understood that the offered approach is a robust for two area interconnected multi source power system without non-linearities.
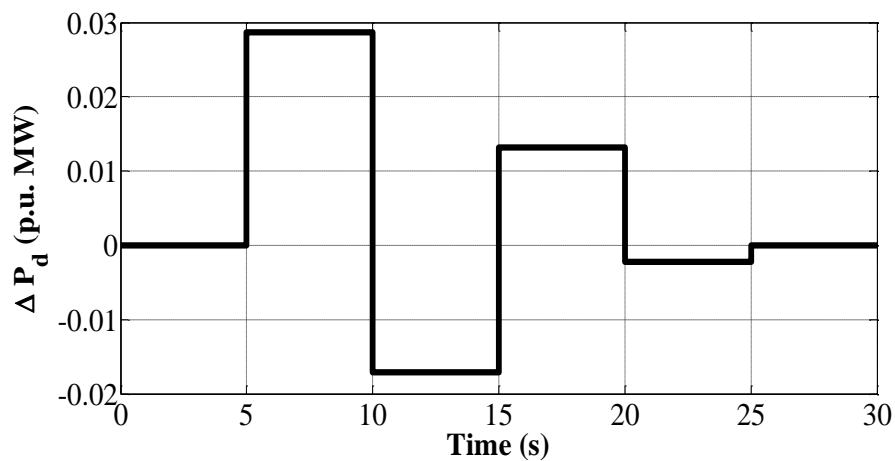
Fig.5.10:   Random load for power system model-2

85

(a)

(b)

(c)
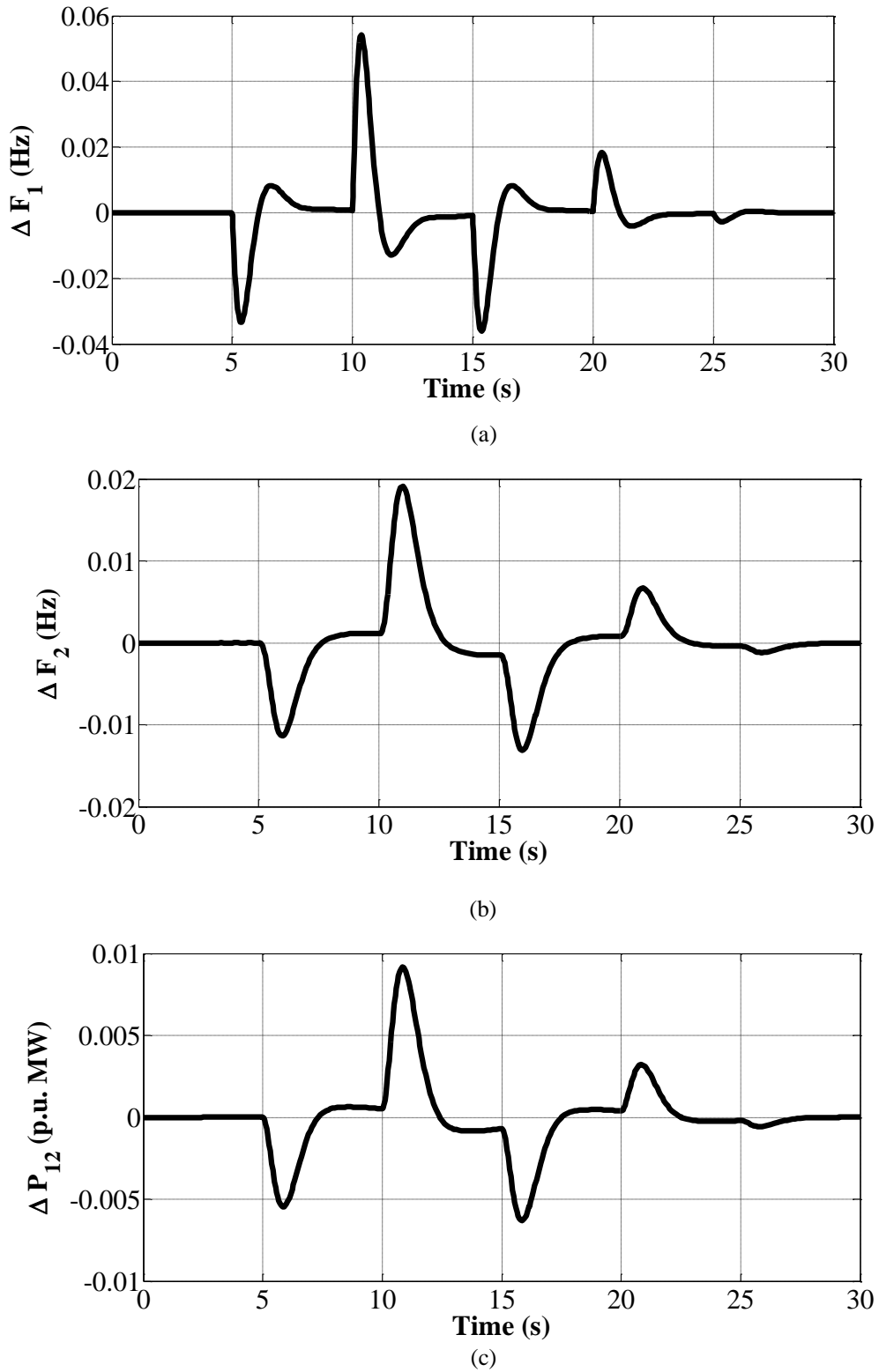
Fig.5.11:Dynamic Response of two area interconnected power system without nonlinearities at random load in control area-1 a) Frequency deviation of area-1 b) Frequency deviation of area-2 c) Tie line power deviation,Vs Time.
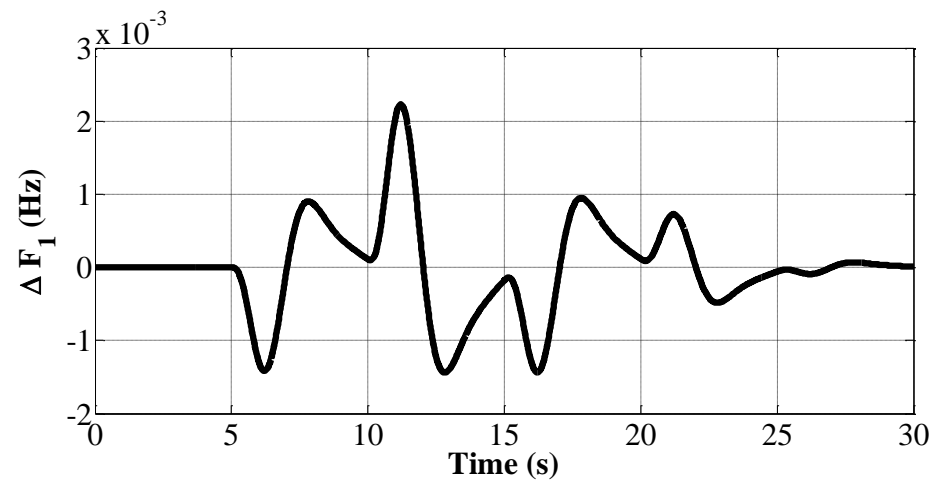
(a)
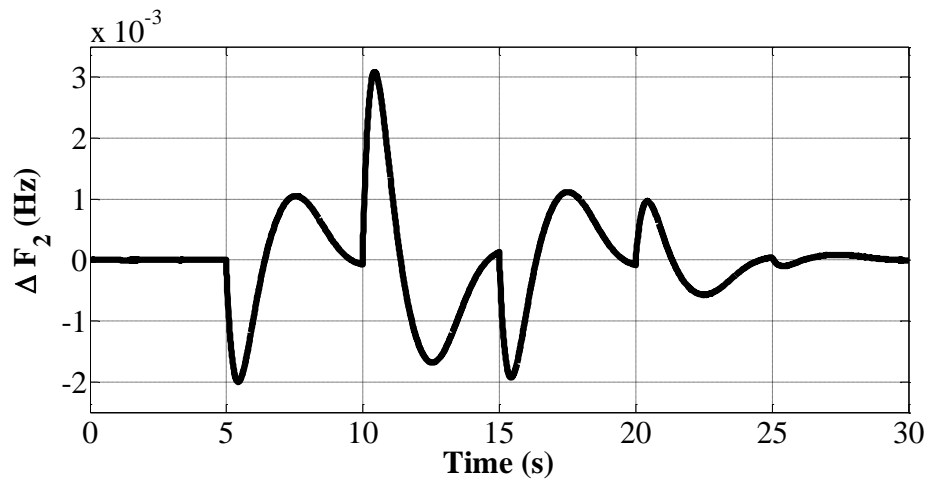
(b)
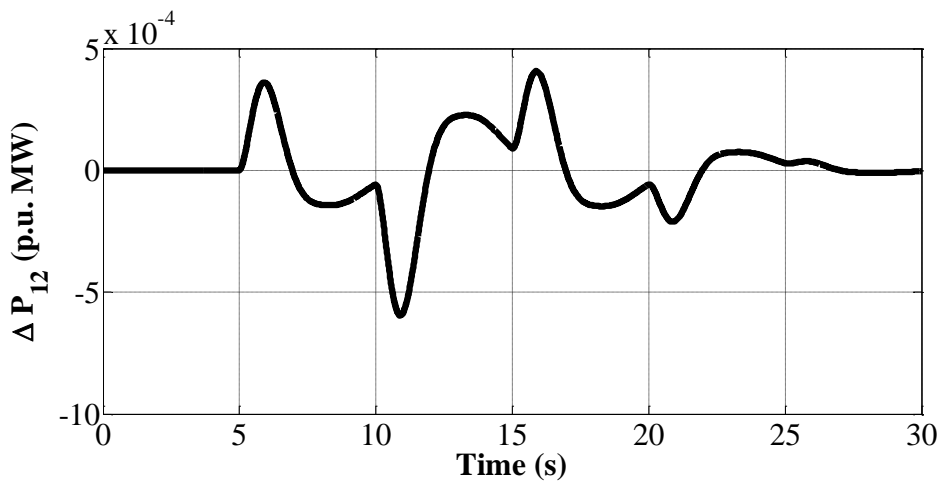
(c)

Fig.5.12:Dynamic Response of two area interconnected power system without nonlinearities at random load in control area-2 a) Frequency deviation of area-1 b) Frequency deviation of area-2 c) Tie line power deviation,Vs Time.

87

5.5   Conclusion

In this chapter, an attempt is made to design novel Jaya based PID controller for AGC of two area interconnected multi source power systems with/without nonlinearities. Effect of slp and random load in different areas of AGC of interconnected diverse sources power system with/without nonlinearities has been shown. Diverse sources have reheat-thermal, hydro, diesel and wind sources in control area. Nonlinearities that are GRC in thermal and hydro sources, GDB in thermal and hydro sources and boiler dynamics in thermal source are amalgamated in two area interconnected power system. The effectiveness of social human behavior based AI techniques with bio-inspired evolutionary based AI techniques incorporating varying participation of diverse sources is demonstrated by comparing the dynamic responses and performance parameter value in terms of settling time. Substantial enhancement in percentage illustrates the efficacy of novel Jaya based approach in two area interconnected power system with nonlinearities at 1% slp in area-1 and area-2. Also, proposed approach works well with two area interconnected power system without nonlinearities at 1% slp in area-1 and area-2. It is revealed that better dynamic responses is offered by social human behavior based AI techniques as compared to bio-inspired evolutionary based AI techniques like IPSO, PSO and BFA for power system without nonlinearities. Significant improvement in numerical values of dynamic responses of power system including and excluding nonlinearities has been witnessed when the load is considered in the area-2 (thermal-hydro-diesel) which has diesel source as one of the multi-source as compared to other area-1(thermal-hydro-wind) which has wind source as one of the multi-source. So, the effect of changing sources on system performances has also been inspected with proposed controller.

Moreover, robustness of the Jaya algorithm is validated at random load conditions in two area interconnected multi sources power system with/ without nonlinearities. Hence, the novelty of the proposed technique is legitimized.

OPTIMAL AGC OF THREE AREA INTERCONNECTED MULTI SOURCE POWER SYSTEMS

6.1   Introduction

The normal operation of an interconnected multi-area power system requires that each area maintains the load and generation balance. AGC tries to achieve this balance by maintaining the system frequency and the tie-line flows at their scheduled values. The AGC action is guided by the area control error (ACE), which is a function of system frequency and tie line flows. In AGC problem, frequency and tie line power should be kept as near scheduled value as possible which is difficult to achieve due to fluctuating nature of load. In a large interconnected power system, the generation usually comprises of a suitable mix of thermal, hydro, gas, wind and nuclear units. However these options are restricted by associated technical and operational features. A realistic situation may arise where area regulated by hydro generation is interconnected to another area regulated by thermal generation. Hydro units differ from thermal units in that the relatively large inertia of water used as a source of energy causes a considerable greater time lag in the response of changes of prime mover torque to changes in gate position, and also an initial tendency for the torque to change in a direction opposite to that finally produced. The speed governor characteristics of the hydro units are widely different from that of turbo governor due

to the effects of water inertia. A literature survey shows that most of the earlier works in the area of optimal AGC pertain to optimal and suboptimal AGC related to Linear quadratic regulator and there has been less attention on the designing of optimal AGC regulators by using structures of cost weighting matrices on interconnected thermal-hydro-gas power system. In the present chapter, optimal AGC of three area interconnected power system has been studied. Optimal AGC regulator has been designed to ascertain zero steady state frequency deviation under all operating conditions. For the same three areas an integral controller has been designed and the performance of the two types of controller has also been compared. The simulation results indicate that better control performance in terms of overshoot and settling time can be obtained by optimal AGC regulator.

6.2 Optimal control theory

Modern control theory helps in achieving the main objectives of AGC by effective design strategy. Design of optimal AGC regulator is explored for three area interconnected multi source power system with suitable structures of weighting matrices. Linear quadratic regulator (LQR) owns the top spot for Optimal AGC regulator design. The choice of weighting matrices propels the improvement in dynamic performance and stability of system. The linearized state space representation of power system can be given by following differential Eqn.(6.1,6.2)

$$\frac{dx}{dt} = Ax + BU + \Gamma P_d \qquad (6.1)$$

$$Y = Cx \qquad (6.2)$$

where x, U, P_d and Y are the state, control, disturbance and output vectors respectively. A, B, Γ and C are real constant matrices of compatible dimensions with respective vectors.

In matlab, optimal AGC regulators is obtained by using the approach of LQR by the following function

$$K = lqr\ (A,\ B,\ Q,\ R) \tag{6.3}$$

In the optimal control scheme the control inputs are generated by means of feedback from all the states with feedback constants to be determined in accordance with an optimal criterion. To design an optimal regulator for considering system, there is a need to unearth control vector as linear control law which can be given as:-

$$U\ =\ -\ K\ x \tag{6.4}$$

Where, optimal feedback matrix K is defined as

$$K = R^{-1}BP \tag{6.5}$$

In modern control terminology ΔP_{ci} is referred as control inputs U created by linear combinations of all states of the system. The state feedback law U minimizes the performance index J. By minimizing quadratic performance index, J as:-

$$J = \frac{1}{2}\int (x^{T}Qx + U^{T}RU]dt \tag{6.6}$$

Where, Q is real, symmetric and positive definite state cost weighting matrix and R is real, symmetric and positive definite control cost weighting matrix.

Different structures of Q and R are considered to explore the system stability as given in Table 6.2.

Where, P is the steady solutions of matrix riccati equation.

$$A^TP+PA-PBR^{-1}B^TP+Q = 0 \qquad (6.7)$$

Optimal feedback gains are obtained by solving the riccati equations. Stability of the system is assessed by eigenvalues of closed loop system which shows that system is more stable if it has higher values of negative real parts.

6.3   System investigated

The Optimal AGC strategy is investigated on three different three-area interconnected multi source power systems as defined in Table 6.1. First case of three-area interconnected power system comprises of non-reheat thermal, hydro and gas power sources as control areas. Second case of power system is non-reheat thermal interconnected power system. Third case of three-area interconnected power system consists of non-reheat thermal as first and third area and hydro as second control area.

TABLE 6. 1   Different cases of three area multi source power system

Cases	Types of Power system
1.	Non-reheat thermal, hydro and gas power system
2.	Non-reheat thermal power system only
3.	Non-reheat thermal, hydro and Non-reheat thermal power system
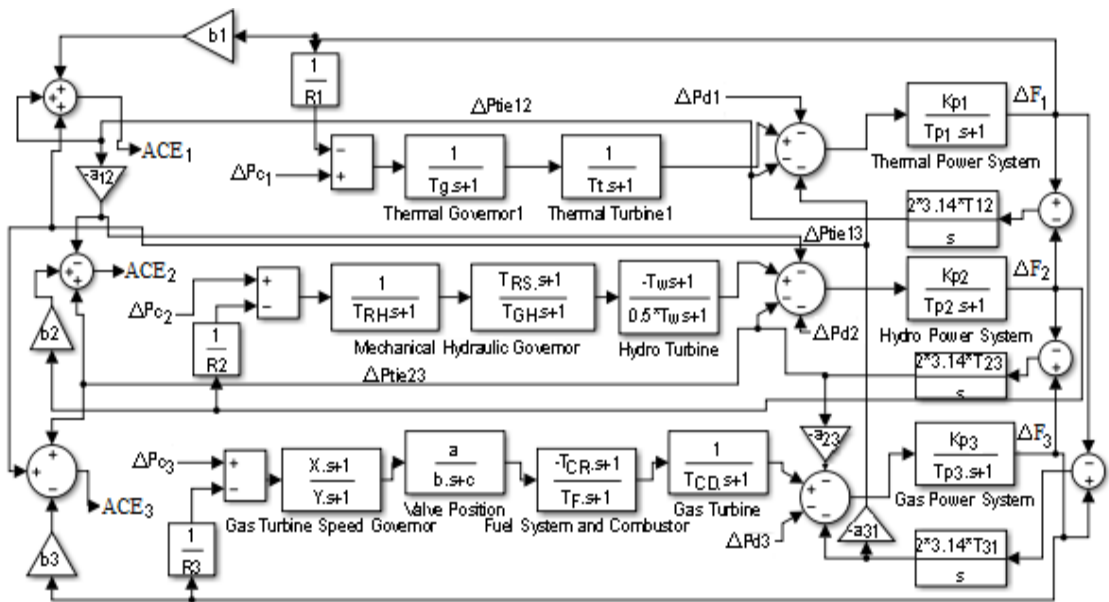
Fig. 6.1: Transfer function block diagram of three area non-reheat thermal-hydro-gas power system.
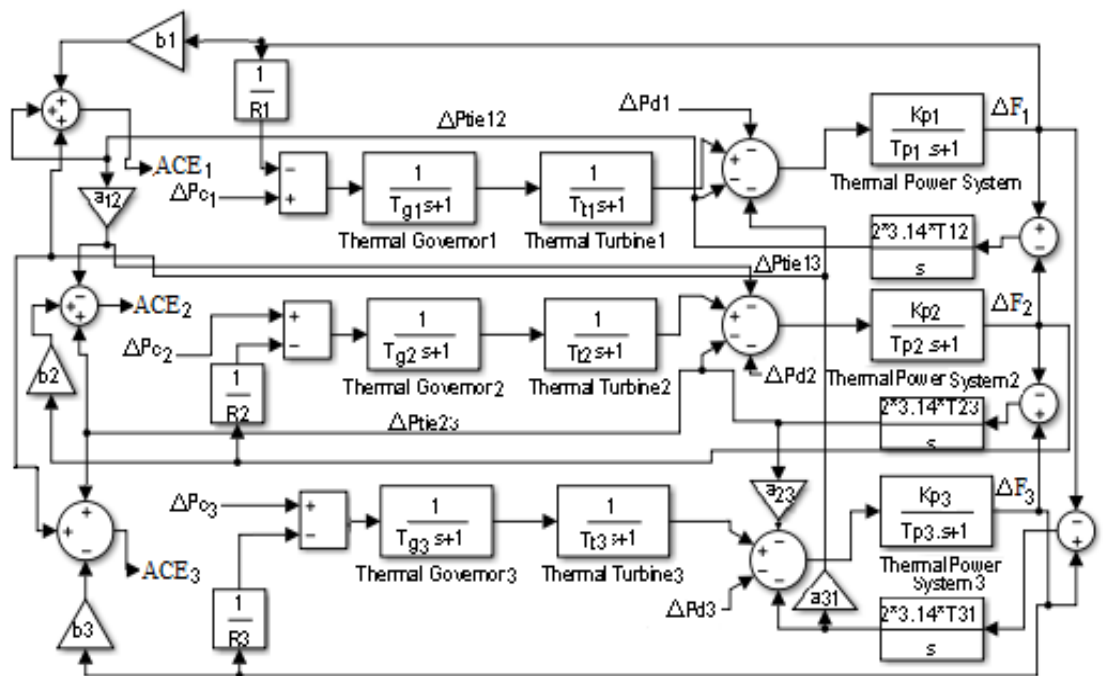
Fig. 6.2: Transfer function block diagram of three area non-reheat thermal power system.

94
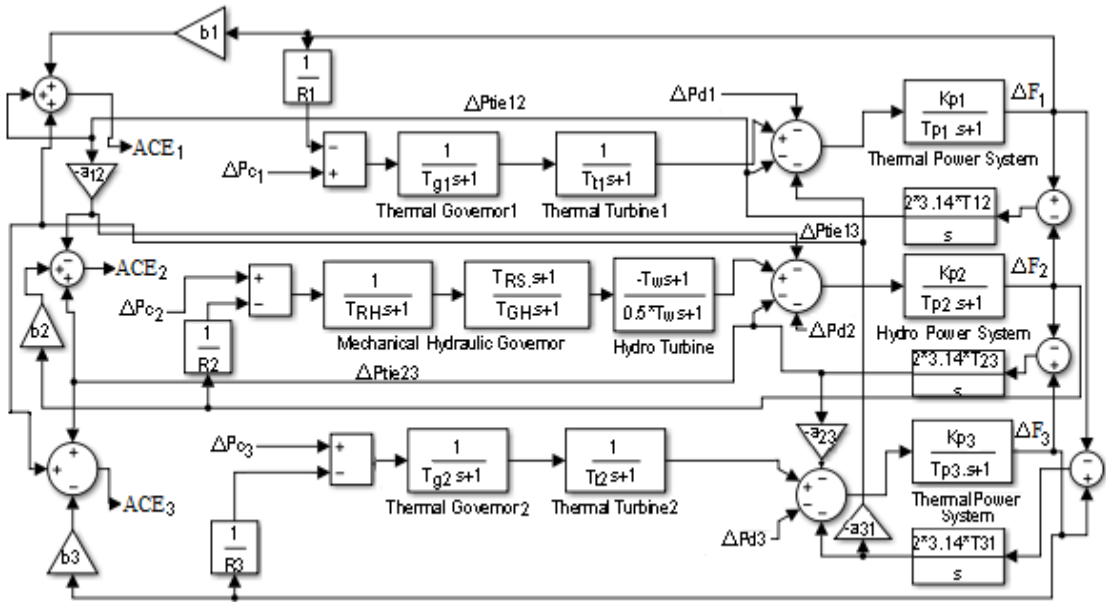
Fig. 6.3: Transfer function block diagram of three area non-reheat thermal hydro non-reheat thermal power system.

Each control area in optimal AGC of three-area interconnected power system is of equal capacity in each case. Parameter values of non reheat thermal, hydro and gas sources in interconnected power system are given in Appendix B. Fig.6.1 shows the Transfer Function block diagram of a three area non-reheat thermal-hydro-gas interconnected power system model. For the system analysis, 1% step load perturbation (slp) has been considered in each area. The system could undergo intolerable dynamic frequency changes with changes in load.

6.3.1 Dynamic model in state space model of system

Optimal AGC regulator is designed for three power systems by using Eqn. (6.1-6.7). Linear state space model for three power systems is obtained by defining the vectors x, U and P_d as follows:

For case-1 of non reheat thermal-hydro-gas power system

State vector

$$[x]^T = [\Delta F_1 \; \Delta P_{G1} \; \Delta X_{E1} \; \Delta F_2 \; \Delta P_{G2} \; \Delta X_h \; \Delta X_{RH} \; \Delta F_3 \; \Delta P_{G3} \; \Delta P_{FC} \; \Delta P_V \; \Delta X_g \; \Delta P_{tie12} \; \Delta P_{tie13}$$

$$\Delta P_{tie23} \; \int ACE_1 \; \int ACE_2 \; \int ACE_3] \qquad (6.8)$$

Control vector

$$[U]^T = [\Delta P_{c1} \; \Delta P_{c2} \; \Delta P_{c3}] \qquad (6.9)$$

Disturbance vector

$$[\Delta P_d]^T = [\Delta P_{d1} \; \Delta P_{d2} \; \Delta P_{d3}] \qquad (6.10)$$

In first case of power system, system state vector comprises of eighteen state variables. Order of A matrix is 18×18, B matrix is 18×3, Γ matrix is 18×3 and C matrix is 3×18. These matrices are further defined differently for different cases. System state matrix (A), control matrix (B) and disturbance matrix (Γ) of state space representation can be derived using differential equations by considering state vector as defined in Eqn. 6.8.

The differential equations for case-1 are defined as follows:

$$\dot{x_1} = -\frac{1}{T_{p1}}x_1 + \frac{K_{p1}}{T_{p1}}x_2 - \frac{K_{p1}}{T_{p1}}x_{13} - \frac{K_{p1}}{T_{p1}}x_{14} - \frac{K_{p1}}{T_{p1}}\Delta Pd_1 \qquad (6.11)$$

$$\dot{x_2} = -\frac{1}{T_t}x_2 + \frac{1}{T_t}x_3 \qquad (6.12)$$

$$\dot{x_3} = \frac{1}{T_g}U_1 - \frac{1}{R_1 T_g}x_1 - \frac{1}{T_g}x_3 \qquad (6.13)$$

$$\dot{x_4} = -\frac{1}{T_{p2}}x_4 + \frac{K_{p2}}{T_{p2}}x_5 + \frac{K_{p2}}{T_{p2}}x_{13} - \frac{K_{p2}}{T_{p2}}x_{15} - \frac{K_{p2}}{T_{p2}}\Delta Pd_2 \qquad (6.14)$$

$$\dot{x_5} = -\frac{2T_R}{R_2 T_{GH} T_{RH}} x_4 + \frac{2}{T_W} x_5 + \frac{2(T_{GH} + T_W)}{T_{GH} T_W} x_6 - \frac{2(T_{RH} - T_R)}{T_{GH} T_{RH}} x_7 - \frac{2T_R}{T_{GH} T_{RH}} U_2 \qquad (6.15)$$

$$\dot{x_6} = -\frac{T_R}{R_2 T_{GH} T_{RH}} x_4 - \frac{1}{T_{GH}} x_6 + \frac{(T_{RH} - T_R)}{T_{GH} T_{RH}} x_7 + \frac{T_R}{T_{GH} T_{RH}} U_2 \qquad (6.16)$$

$$\dot{x_7} = \frac{1}{T_{RH}} U_2 - \frac{1}{R_2 T_{RH}} x_4 - \frac{1}{T_{RH}} x_7 \qquad (6.17)$$

$$\dot{x_8} = -\frac{1}{T_{p3}} x_8 + \frac{K_{p3}}{T_{p3}} x_9 + \frac{K_{p3}}{T_{p3}} x_{14} + \frac{K_{p3}}{T_{p3}} x_{15} - \frac{K_{p3}}{T_{p3}} \Delta P_{d\,3} \qquad (6.18)$$

$$\dot{x_9} = -\frac{1}{T_{CD}} x_9 + \frac{1}{T_{CD}} x_{10} \qquad (6.19)$$

$$\dot{x_{10}} = -\frac{X T_{CR}}{bY R_3 T_F} x_8 - \frac{1}{T_F} x_{10} + \frac{Y + T_{CR}}{Y T_F} x_{11} - \frac{T_{CR}(b - cX)}{bY T_F} x_{12} + \frac{X}{bY} U_3 \qquad (6.20)$$

$$\dot{x_{11}} = -\frac{X}{bY R_3} x_8 - \frac{1}{Y} x_{11} + \frac{b - cX}{Yb} x_{12} + \frac{X}{bY} U_3 \qquad (6.21)$$

$$\dot{x_{12}} = -\frac{c}{b} x_{12} + \frac{1}{b} U_3 - \frac{1}{bR_3} x_8 \qquad (6.22)$$

$$\dot{x_{13}} = 0.15 x_1 - 0.15 x_4 \qquad (6.23)$$

$$\dot{x_{14}} = 0.15 x_1 - 0.15 x_8 \qquad (6.24)$$

$$\dot{x_{15}} = 0.15 x_4 - 0.15 x_8 \qquad (6.25)$$

$$\dot{x_{16}} = b_1 x_1 + x_{13} + x_{14} \qquad (6.26)$$

$$\dot{x_{17}} = b_2 x_4 - x_{13} + x_{15} \qquad (6.27)$$

$$\dot{x_{18}} = b_3 x_8 - x_{14} - x_{15} \qquad (6.28)$$

State space model for case-2 - non reheat thermal power system are:-

State vector

$$[x]^T = [\Delta F_1 \ \Delta P_{G1} \ \Delta X_{E1} \ \Delta F_2 \ \Delta P_{G2} \ \Delta X_{E2} \ \ \Delta F_3 \ \Delta P_{G3} \ \Delta X_{E3} \ \Delta P_{tie12} \ \Delta P_{tie13} \ \Delta P_{tie23} \ \int ACE_1$$

$$\int ACE_2 \ \int ACE_3] \tag{6.29}$$

Control vector

$$[U]^T = [\Delta P_{c1} \ \Delta P_{c2} \ \Delta P_{c3}] \tag{6.30}$$

Disturbance vector

$$[\Delta P_d]^T = [\Delta P_{d1} \ \Delta P_{d2} \ \Delta P_{d3}] \tag{6.31}$$

In second case of power system, system state vector are equipped with fifteen state variables. Order of A matrix is 15×15, B matrix is 15×3, Γ matrix is 15×3 and C matrix is 3×15. System state matrix (A), control matrix (B) and disturbance matrix (Γ) of state space representation of case-2 can be derived using differential equations by considering state vector as defined in Eqn. 6.29.

The differential equations are defined as follows:

$$\dot{x_1} = -\frac{1}{T_{p1}}x_1 + \frac{K_{p1}}{T_{p1}}x_2 - \frac{K_{p1}}{T_{p1}}x_{10} - \frac{K_{p1}}{T_{p1}}x_{11} - \frac{K_{p1}}{T_{p1}}\Delta Pd_1 \tag{6.32}$$

$$\dot{x_2} = -\frac{1}{T_{t1}}x_2 + \frac{1}{T_{t1}}x_3 \tag{6.33}$$

$$\dot{x_3} = \frac{1}{T_{g1}}U_1 - \frac{1}{R_1 T_{g1}}x_1 - \frac{1}{T_{g1}}x_3 \tag{6.34}$$

$$\dot{x_4} = -\frac{1}{T_{p2}}x_4 + \frac{K_{p2}}{T_{p2}}x_5 + \frac{K_{p2}}{T_{p2}}x_{10} - \frac{K_{p2}}{T_{p2}}x_{12} - \frac{K_{p2}}{T_{p2}}\Delta Pd_2 \tag{6.35}$$

$$\dot{x_5} = -\frac{1}{T_{t2}}x_5 + \frac{1}{T_{t2}}x_6 \tag{6.36}$$

$$\dot{x_6} = \frac{1}{T_{g2}}U_2 - \frac{1}{R_2 T_{g2}}x_4 - \frac{1}{T_{g2}}x_6 \tag{6.37}$$

$$\dot{x_7} = -\frac{1}{T_{p3}}x_8 + \frac{K_{p3}}{T_{p3}}x_9 + \frac{K_{p3}}{T_{p3}}x_{11} - \frac{K_{p2}}{T_{p2}}x_{12} - \frac{K_{p2}}{T_{p2}}\Delta Pd_3 \qquad (6.38)$$

$$\dot{x_8} = -\frac{1}{T_{t3}}x_8 + \frac{1}{T_{t3}}x_9 \qquad (6.39)$$

$$\dot{x_9} = \frac{1}{T_{g3}}U_3 - \frac{1}{R_3 T_{g3}}x_7 - \frac{1}{T_{g3}}x_9 \qquad (6.40)$$

$$\dot{x_{10}} = 0.15x_1 - 0.15x_4 \qquad (6.41)$$

$$\dot{x_{11}} = 0.15x_1 - 0.15x_7 \qquad (6.42)$$

$$\dot{x_{12}} = 0.15x_4 - 0.15x_7 \qquad (6.43)$$

$$\dot{x_{13}} = b_1 x_1 + x_{10} + x_{11} \qquad (6.44)$$

$$\dot{x_{14}} = b_2 x_4 - x_{10} + x_{12} \qquad (6.45)$$

$$\dot{x_{15}} = b_3 x_8 - x_{11} - x_{12} \qquad (6.46)$$

State space model for case-3 of non reheat thermal hydro – non reheat thermal power system are:-

State vector

$$[x]^T = [\Delta F_1 \ \Delta P_{G1} \ \Delta X_E \ \Delta F_2 \ \Delta P_{G2} \ \Delta X_h \ \Delta X_{RH} \ \Delta F_3 \ \Delta P_{G3} \ \Delta X_{E3} \ \Delta P_{tie12} \ \Delta P_{tie13} \ \Delta P_{tie23}$$
$$\int ACE_1 \ \int ACE_2 \ \int ACE_3] \qquad (6.47)$$

Control vector

$$[U]^T = [\Delta P_{c1} \ \Delta P_{c2} \ \Delta P_{c3}] \qquad (6.48)$$

Disturbance vector

$$[\Delta P_d]^T = [\Delta P_{d1} \ \Delta P_{d2} \ \Delta P_{d3}]$$ (6.49)

In third case of power system, system state vector comprises of sixteen state variables. Order of A matrix is 16×16, B matrix is 16×3, Γ matrix is 16×3 and C matrix is 3×16.

System state matrix (A), control matrix (B) and disturbance matrix (Γ) of state space representation of case-3 can be derived using differential equations by considering state vector as defined in Eqn. (6.47).

The differential equations are defined as follows:

$$\dot{x_1} = -\frac{1}{T_{p1}}x_1 + \frac{K_{p1}}{T_{p1}}x_2 - \frac{K_{p1}}{T_{p1}}x_{11} - \frac{K_{p1}}{T_{p1}}x_{12} - \frac{K_{p1}}{T_{p1}}\Delta Pd_1$$ (6.50)

$$\dot{x_2} = -\frac{1}{T_{t1}}x_2 + \frac{1}{T_{t1}}x_3$$ (6.51)

$$\dot{x_3} = \frac{1}{T_{g1}}U_1 - \frac{1}{R_1 T_{g1}}x_1 - \frac{1}{T_{g1}}x_3$$ (6.52)

$$\dot{x_4} = -\frac{1}{T_{p2}}x_4 + \frac{K_{p2}}{T_{p2}}x_5 + \frac{K_{p2}}{T_{p2}}x_{11} - \frac{K_{p2}}{T_{p2}}x_{12} - \frac{K_{p2}}{T_{p2}}\Delta Pd_2$$ (6.53)

$$\dot{x_5} = -\frac{2T_R}{R_2 T_{GH} T_{RH}}x_4 + \frac{2}{T_W}x_5 + \frac{2(T_{GH}+T_W)}{T_{GH} T_W}x_6 - \frac{2(T_{RH}-T_R)}{T_{GH} T_{RH}}x_7 - \frac{2T_R}{T_{GH} T_{RH}}U_2$$ (6.54)

$$\dot{x_6} = -\frac{T_R}{R_2 T_{GH} T_{RH}}x_4 - \frac{1}{T_{GH}}x_6 + \frac{(T_{RH}-T_R)}{T_{GH} T_{RH}}x_7 + \frac{T_R}{T_{GH} T_{RH}}U_2$$ (6.55)

$$\dot{x_7} = \frac{1}{T_{RH}}U_2 - \frac{1}{R_2 T_{RH}}x_4 - \frac{1}{T_{RH}}x_7$$ (6.56)

$$\dot{x_8} = -\frac{1}{T_{p3}}x_8 + \frac{K_{p3}}{T_{p3}}x_9 + \frac{K_{p3}}{T_{p3}}x_{12} + \frac{K_{p3}}{T_{p3}}x_{13} - \frac{K_{p3}}{T_{p3}}\Delta Pd_3$$ (6.57)

$$\dot{x}_9 = -\frac{1}{T_{t3}}x_9 + \frac{1}{T_{t3}}x_{10} \tag{6.58}$$

$$\dot{x}_{10} = \frac{1}{T_{g3}}U_3 - \frac{1}{R_3 T_{g3}}x_8 - \frac{1}{T_{g3}}x_{10} \tag{6.59}$$

$$\dot{x}_{11} = 0.15x_1 - 0.15x_4 \tag{6.60}$$

$$\dot{x}_{12} = 0.15x_1 - 0.15x_8 \tag{6.61}$$

$$\dot{x}_{13} = 0.15x_4 - 0.15x_8 \tag{6.62}$$

$$\dot{x}_{14} = b_1 x_1 + x_{11} + x_{12} \tag{6.63}$$

$$\dot{x}_{15} = b_2 x_4 - x_{11} + x_{13} \tag{6.64}$$

$$\dot{x}_{16} = b_3 x_8 - x_{12} - x_{13} \tag{6.65}$$

Different approaches are applied to develop different structures of control cost weighting matrix (R) and state cost weighting matrix (Q) in the next section. Eventually, these structures of cost weighting matrices are used to design optimal AGC regulator and help us to explore the dynamic performance and stability of three area interconnected multi source power system at 1% slp in each area.

6.4   Optimal AGC regulator design by considering various case study of developing cost weighting matrices.

The control inputs underlying the optimal scheme are formed by means of full state feedback from all the states in the considered power systems. Designing of optimal AGC regulator for three-area interconnected multi source power systems is accomplished by considering various case study of developing structures of weighting

matrices Q and R as defined in Table 6.2. Formation and selection of various structures of cost weighting matrices requires organize and sagacious way for designing optimal AGC regulator which influence dynamic performance of interconnected multi source power systems. In this chapter, various methods are developed for weighting matrices selection, which would result in suitable cost function for the considered power systems.

TABLE 6. 2   Optimal AGC regulators design using different structures of weighting matrices

Case study	Various structures of cost weighting matrices
1	Cost weighting matrices based on the minimum performance index of system - Qm, R1
2	Cost weighting matrices by giving equal importance to each state variable - Q1, R1
3	Cost weighting matrices based on scaling method - Qs, Rs

The structure of cost weighting matrices and formulation of performance index for the power system under consideration for various cases are as follows:

Case study 1 – Cost weighting matrices based on the minimum performance index of system - Qm, R1- Matrix of control cost weighting matrix (R) is an identity matrix of order 3×3. State cost weighting matrix for optimal AGC of interconnected three area multi source power system are based on the minimum performance index of system assumed by Fosha [90]. This performance index is designed on the basis of the

excursion of ACE, ∫ACE and control vectors about the steady values minimization and can be specified as:-

$$J = \frac{1}{2} \int [ACE_1^2 + ACE_2^2 + ACE_3^2 + \int ACE_1^2 \, dt + \int ACE_2^2 \, dt + \int ACE_3^2 \, dt +$$

$$k(U_1^2 + U_2^2 + U_3^2)] \, dt \tag{6.66}$$

For case-1 of power system (non reheat thermal-hydro-gas)

The state cost weighting matrix and control cost weighting matrix are of order 18×18 and 3×3 respectively. Matrix of state cost weighting matrix is given in Appendix A.

For case-2 of power system (non reheat thermal)

The control cost weighting matrix is a unit matrix of order 3×3. The state cost weighting matrix is of order 15×15 and given in Appendix A.

For case-3 of power system (non reheat thermal-hydro- non reheat thermal)

The control cost weighting matrix is a unit matrix of order 3×3. The state cost weighting matrix is of order 16×16 and given in Appendix A.

Dynamic performances of the system by considering cost weighting matrices based on the minimum performance index of system are simulated and compared in the next section.

Case study 2 – Cost weighting matrices by giving equal importance to each variable as one- Q1, R1- Optimal AGC regulator of three areas interconnected power systems is designed by considering cost weighting matrices by giving equal importance to each variable as one at 1% slp in each area. Control cost weighting matrix is of unit

matrix of order 3×3 for all the three cases. For case-1, case-2 and case-3, structures of state cost weighting matrix are of unit matrix of order 18×18, 15×15 and 16×16 respectively.

Case study 3 – Cost weighting matrices based on scaling method - Qs, Rs. Optimal AGC regulator of three areas interconnected power systems is designed by considering the scaling method on cost weighting matrices at 1% slp in each area. Initially, control cost weighting matrix is of unit matrix of order 3×3 for all the three cases. New weighting matrices after scaling [190,191] are given as:-

$$Rs = 0.05 \times R1 \tag{6.67}$$

$$Qs(i,i) = Q(i,i)\, 0.05^{(n-i)/n}$$
(6.68)

Where i = 1 to n

In this case study, new control cost weighting matrix for all the three cases is procured by multiplying unit matrix of order 3×3 with the weight as 0.05 by using equation no. 6.67.

For case-1, case-2 and case-3, order of state cost weighting matrix are of 18×18, 15×15 and 16×16 respectively. Structure of state cost weighting matrix is developed by considering value of n is 18, 15 and 16 in equation no. 6.68 for case-1, case-2 and case-3 respectively as shown in Appendix A.

Optimal AGC regulator for three area interconnected power systems at 1% slp in each area with scaled structured as Qs and Rs matrices is designed and its dynamic performances and stability are analysed and compared in next section.

6.5   Simulation results and discussions

6.5.1   Non reheat thermal hydro-gas power system at 1% step load perturbation

Optimal AGC of three areas interconnected non-reheat thermal-hydro-gas power system under the wake of 1% slp in each area is simulated. It is assumed that three areas are of identical capacity. Design of optimal AGC regulators is accomplished by using various structures of cost weighting matrices as defined in Table 6.2. Optimal feedback gain matrix, eigen values and dynamic response characteristics of considered system with various case studies are computed to examine the stability of power system. To validate the effectiveness of optimal AGC regulator with structures of control and state cost weighting matrices, dynamic response of system for frequency and tie line power deviation is procured with 1% slp in each area as shown in Fig. 6.4 (a-f). From inspection of response plots, it is palpable that dynamic responses of frequency and tie-line deviation for all the three case study tend to settle down at zero steady state value for 1% slp in each area. The comparison of plots shows that system response offered by optimal AGC regulators which are designed with structures of cost weighting matrices based on scaling method in case study 3 are less affected by 1% slp in each area as compared to optimal AGC regulators which are designed by using structures of cost weighting matrices described in case study 1 and case study 2. An analysis of optimal feedback gain matrix in Table 6.3 reveals that the design of weighting matrices in case study 1 shows a decrease in feedback gains as compared to other case studies of optimal AGC of three area interconnected non-reheat thermal-hydro-gas power system. Eigenvalues of closed loop system in Table 6.4 show that none of the eigenvalues lie in the right half of s plane for all the three case studies. So, the system is said to be stable for all the three case studies. It is observed that the

Optimal AGC of case study 1 has five complex eigenvalues in comparison to four in case study 2 and three in case study 3. Also, considerable improvement has been seen in negative real parts of eigen value for case study 3 (-65.1302) as compared to case study 2 (-30.6810) and case study 1 (-19.8883). Critical inspection of eigen values reveals that the optimal AGC in case study 3 has better stability, hence better stability margin as compared with other cases considered. Numerical values of dynamic responses in terms of system characterstics are depicted in Table 6.5.

System characteristics reveals the magnitudes of settling time (ST), first peak undershoot (FPu), peak time (PT) and rise time (RT) for optimal AGC for three area non-reheat thermal-hydro-gas interconnected power system. These system characterstics values are attained for frequency deviation in each area.
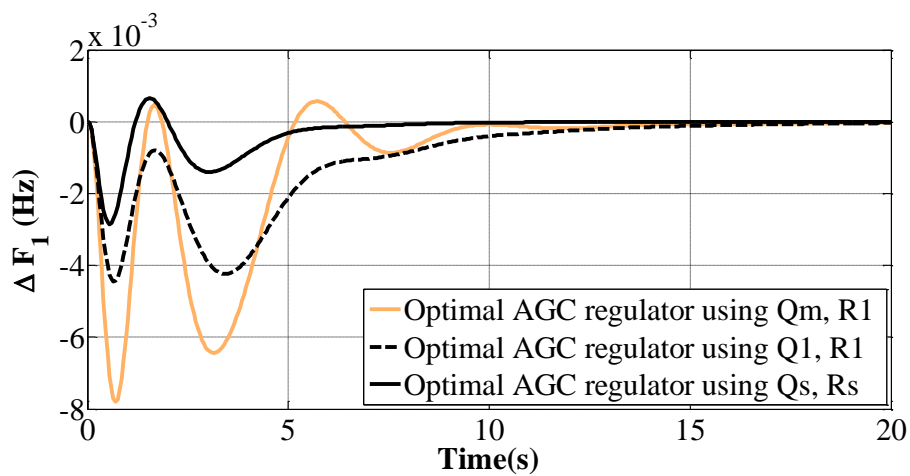
(a)
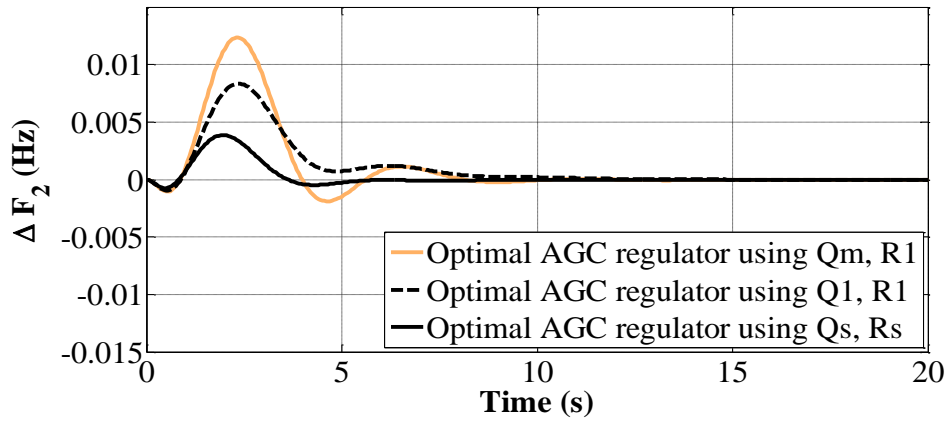
(b)
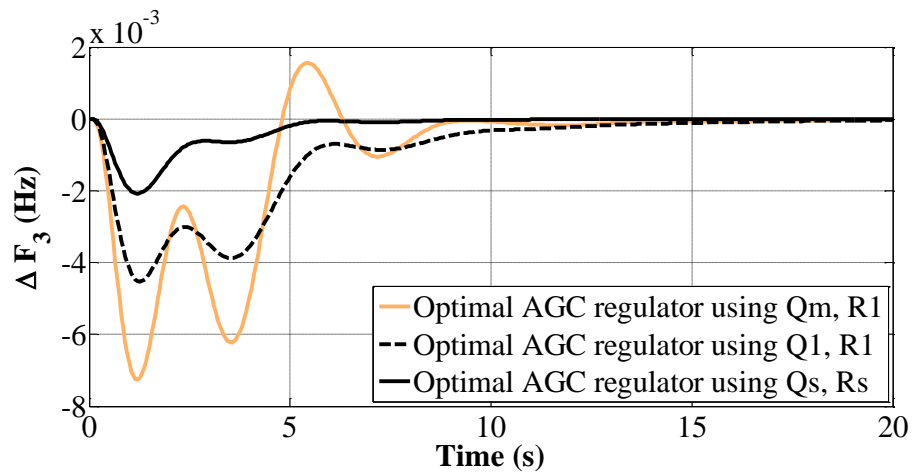
(c)
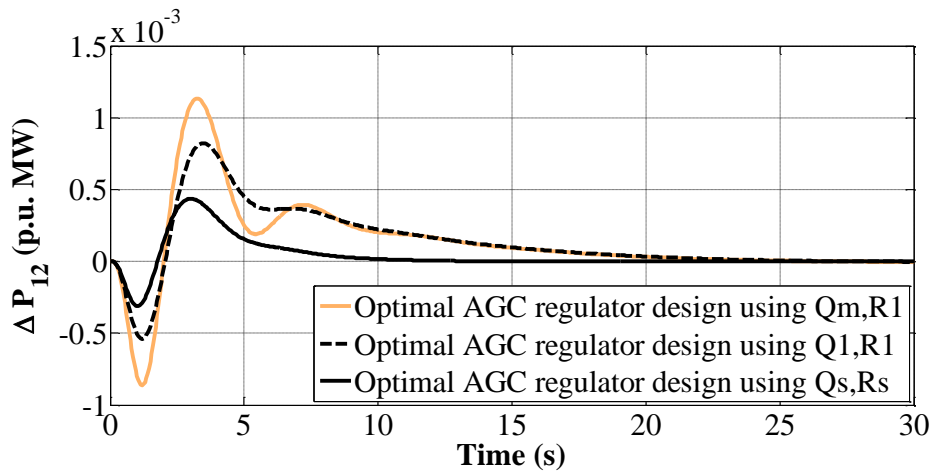
(d)

(e)

(f)

Fig. 6.4: Dynamic response of non-reheat thermal-hydro-gas interconnected power system at 1% slp in each area (a) Frequency deviation of area-1 (b) Frequency deviation of area-2 (c) Frequency deviation of area-3 (d) Tie line Power deviation between area-1 and area-2 (e) Tie line power deviation between area-2 and area-3 (f) Tie line power deviation between area-1 and area-3, Vs Time.

Critical examination of Table 6.5 reveals that ST, FPu, PT and RT values for frequency deviation of each control area for optimal AGC regulators with the structure of cost weighting matrices in case study 3 are reduced appreciably as compared to optimal AGC regulators with the structure of cost weighting matrices in other two case studies.

TABLE 6. 3   Optimal feedback gain matrix K for non reheat thermal-hydro-gas power system

Case study 1	[0.4949 0.7363 0.1781 0.1352 0.8044 2.6257 -0.2163 0.1255 0.1325 0.1292 0.1908 -0.0977 1.6937 0.1640 -1.5297 0.9141 0.4055 -0.0062 0.0614 0.0797 0.0187 0.0588 0.7323 3.1035 4.7940 0.1466 0.1533 0.1321 0.1266 -0.0607 1.8618 0.1021 -1.7597 -0.3889 0.8720 -0.2972 0.0999 0.1010 0.0215 0.0120 0.3769 1.7589 0.0294 0.5843 0.7370 0.7806 1.3270 -0.6898 1.1647 1.1084 -0.0564 -0.1151 0.2741 0.9548]
Case study 2	[1.0213 1.6314 0.6935 0.1749 1.1441 3.8094 -0.2344 0.2175 0.2105 0.1904 0.3100 -0.1676 1.8648 -0.3462 -2.2110 0.8987 0.4385 -0.0020 0.1823 0.1765 0.0281 -0.2521 0.8028 5.0693 4.9430 0.3730 0.3502 0.2589 0.1383 -0.0627 3.4862 0.1694 -3.3168 -0.4231 0.8661 -0.2661 0.1806 0.1439 0.0214 0.0317 0.4140 1.9733 0.1180 0.9444 1.3672 1.5091 2.3999 -0.7568 1.4076 2.7906 1.3829 -0.1150 0.2400 0.9639]
Case study 3	[1.8293 2.4464 0.9854 1.0795 3.4166 8.6215 -0.1519 0.3425 0.3998 0.4289 0.7479 -0.4224 5.2087 1.4202 -3.7885 3.2203 2.1465 -0.3220 0.2844 0.2444 0.0333 0.5702 4.5728 16.7538 6.4459 0.8338 0.6773 0.4020 0.0050 0.0161 10.6738 -0.4229 -11.0967 -1.9849 3.4067 -0.9051 0.2925 0.1952 0.0242 0.4388 1.0091 2.7507 0.0759 2.7450 3.4895 3.6196 5.7300 -0.9634 1.7152 6.3571 4.6419 -0.1739 0.8642 4.3677]

TABLE 6. 4   Eigen values for non reheat thermal-hydro-gas power system

Case study 1	Case study 2	Case study 3
-19.8883	-30.6810	-65.1302
-13.2852	-17.8405	-20.3748
-6.7344	-6.0398	-5.3812
$-1.5207 \pm 3.0644i$	$-2.6881 \pm 2.5485i$	$-2.5529 \pm 2.3556i$
$-0.6595 \pm 2.1500i$	$-1.0595 \pm 1.6369i$	$-0.7748 \pm 1.7673i$
$-0.5221 \pm 1.4361i$	$-0.6451 \pm 1.6033i$	$-1.2632 \pm 1.4262i$
$-0.6724 + 0.1622i$	-3.2395	-3.9696
$-0.6724 -0.1622i$	-0.3975	-3.0262
$-0.1400 + 0.0910i$	-0.4469	-1.5070
$-0.1400 - 0.0910i$	-0.8467	-0.2151
-3.0686	-1.1717	-0.4151
-2.8172	-3.0474	-0.7356
-1.1474	$-0.1401 +0.0881i$	-1.1392
-0.7474	$-0.1401 -0.0881i$	-1.0856

Moreover, system response characteristics offered by the design of weighting matrices based on scaling method are appreciable better when compared to other case studies.

Therefore, it is concluded that the design of cost weighting matrices in case study 3, optimal AGC regulator design using scaling method for cost weighting matrices proposes improvement in system stability and dynamic performances as compared to other considered structures in case study 1 and case study 2. However, dynamic stability of system achieved by designing optimal AGC regulators with structures in case study 2 is comparatively better than offered by designing optimal AGC regulators with structures in case study 1

TABLE 6. 5   **System response characteristics for non reheat thermal-hydro-gas power system**

S. No.	System state variable	Case study	FPu (Hz) (-)	PT (s)	RT (s)×10^{-4}	ST (s)
1	ΔF_1 (Hz)	1	0.0078	0.70	2.809	12.65
		2	0.0045	0.65	8023	16.23
		3	0.0029	0.55	0.165	8.49
2	ΔF_2 (Hz)	1	0.0124	2.35	79	7.77
		2	0.0084	2.35	78	10.64
		3	0.0039	1.95	0.0692	8.21
3	ΔF_3 (Hz)	1	0.0073	1.20	47722	12.68
		2	0.0045	1.25	299398	15.97
		3	0.0021	1.20	299	8.73

6.5.2   Non reheat thermal power system at 1% step load perturbation

With various design of optimal AGC regulator as given in previous section, comparative analysis is now made to explore the optimal AGC of three area interconnected thermal power system performance under a 1% slp in each area. Design of optimal AGC regulators for three areas interconnected non-reheat thermal power system is accomplished by using various structures of cost weighting matrices as defined in Table 6.2. Performance of optimal AGC of three area interconnected thermal power system has been schematized in-terms of optimal feedback gain, dynamic responses, eigen values, dynamic response and system response characteristics. To validate the effectiveness of optimal AGC regulator with structures of control and state

cost weighting matrices, dynamic response of system for frequency and tie line power deviation is procured with 1% slp in each area as shown in Fig. 6.5(a-f). Critical examination of dynamic response plots reveals that dynamic responses of frequency and tie-line deviation for all the three case studies tend to settle down at zero steady state value for 1% slp in each area with less than 15 seconds of settling time. Comparison of magnitude of frequency deviation and tie-line deviation for all the three case studies clearly reveal that less time is taken to damp out oscillations with the optimal AGC regulator which are designed using case study 3 over the optimal AGC regulator which are designed using case study 1 and case study 2. The comparison of plots shows that system response offered by optimal AGC regulators which are designed with structures of cost weighting matrices based on scaling method in case study 3 are less affected by 1% slp in each area as compared to optimal AGC regulators which are designed by using structures of cost weighting matrices described in case study 1 and case study 2. An analysis of optimal feedback gain matrix in Table 6.6 reveals that the design of weighting matrices in case study 3 shows an increase in feedback gains as compared to other case studies of optimal AGC of three area interconnected non-reheat thermal power system. Eigenvalues of closed loop system in Table 6.7 show that none of the eigenvalues lie in the right half of s plane for all the three case studies. So, the system is said to be stable for all the three case studies. It is observed that the Optimal AGC of case study 1 and case study 2 have five complex eigenvalues in comparison to three in case study 3. Also, considerable improvement has been seen in negative real parts of eigen value for case study 3 (-28.2831) as compared to case study 2 (-17.8415) and case study 1 (-13.2923). Critical inspection of eigen values reveals that the optimal AGC in case study 3 has better stability, hence

better stability margin as compared with other cases considered. Numerical values of dynamic responses in terms of system characterstics are depicted in Table 6.8. System characteristics reveals the magnitudes of settling time (ST), first peak undershoot (FPu), peak time (PT) and rise time (RT) for optimal AGC for three area non-reheat thermal interconnected power system. These system characterstics values are attained for frequency deviation in each area. For the 1% step load perturbation in three areas, Table 4.8 shows that the system characteristics settling time value for case study 1 is 6.48 seconds, 6.10 seconds and 6.31 seconds and for case study 2 is 10.98 seconds, 10.98 seconds and 10.98 seconds in the area1, area2 and area3 respectively is diminished to 2.81 seconds, 3.13 seconds and 3.63 seconds in the area1, area2 and area3 respectively when optimal AGC regulators are designed using the scaling method for the structures of cost weighting matrices

(a)

(b)

(c)

(d)

113
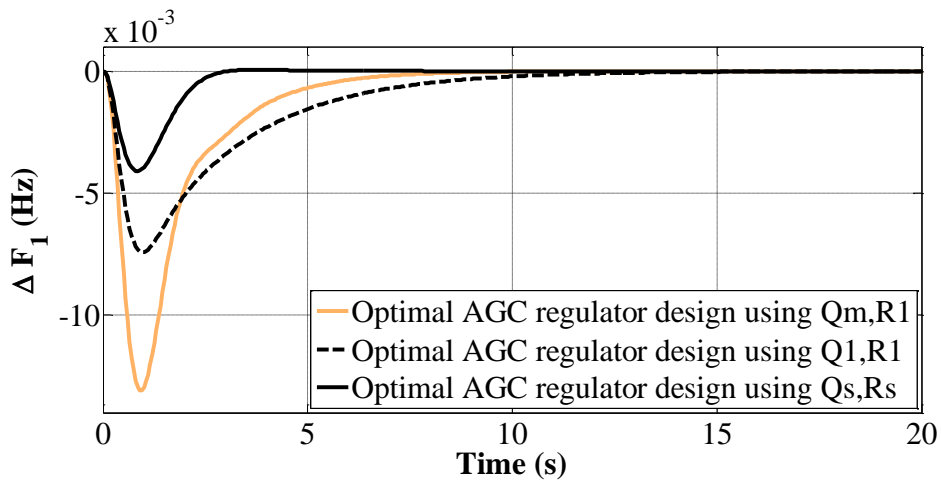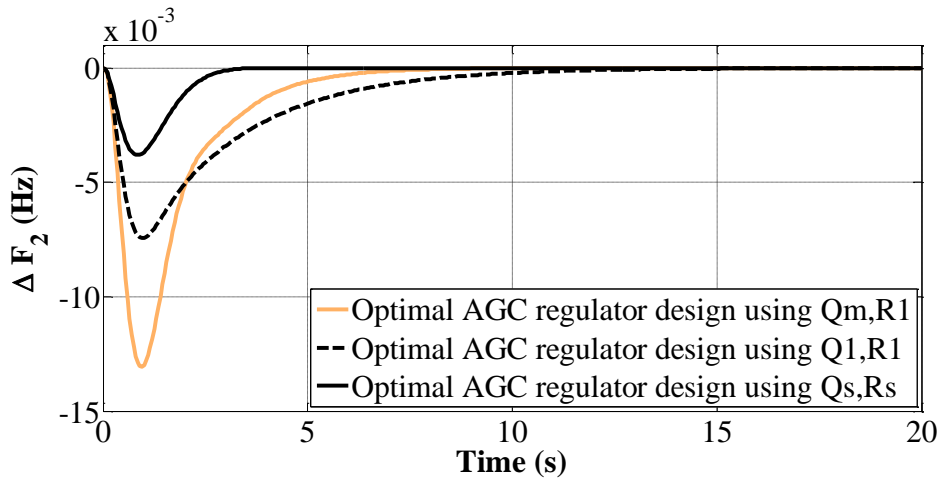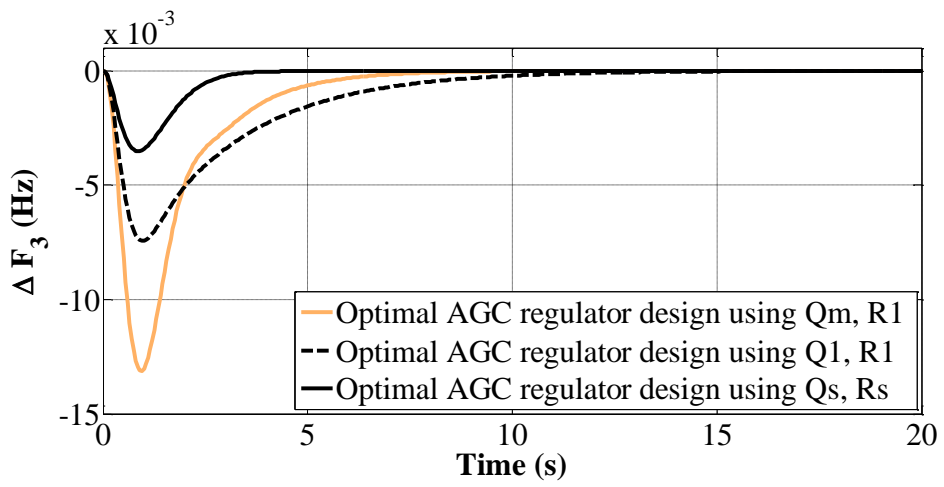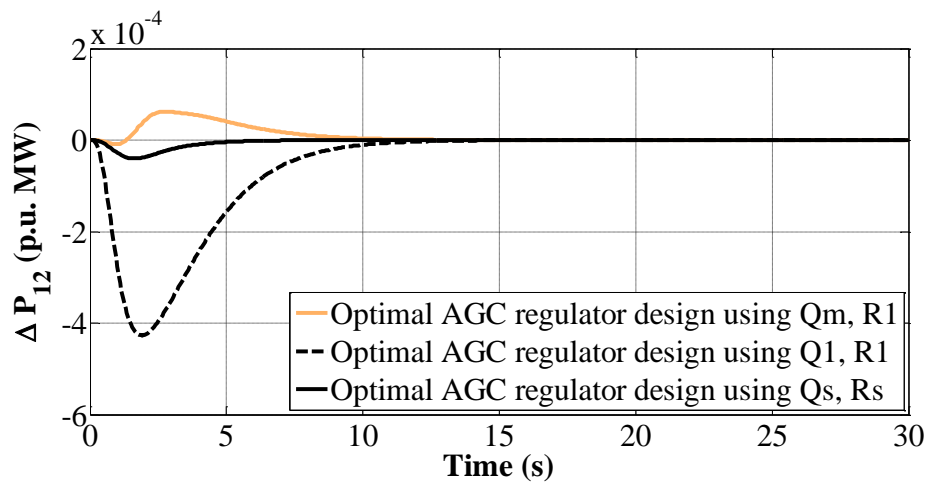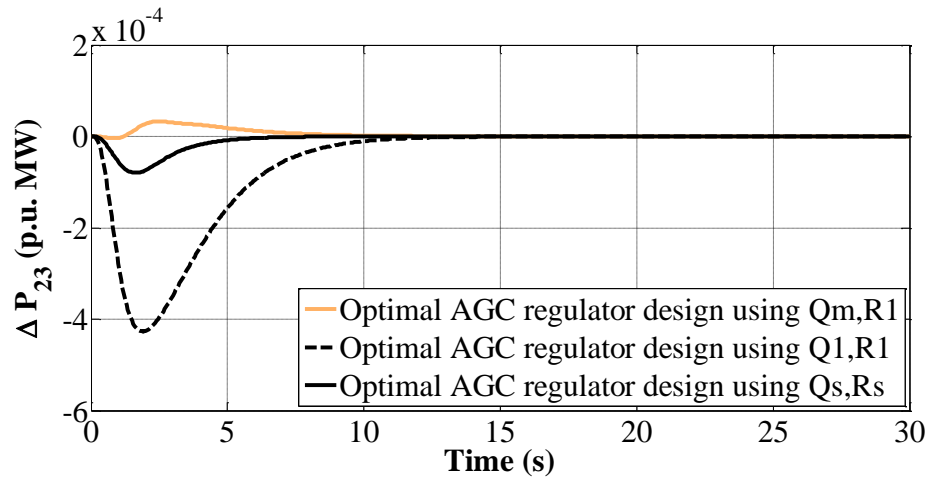
(e)
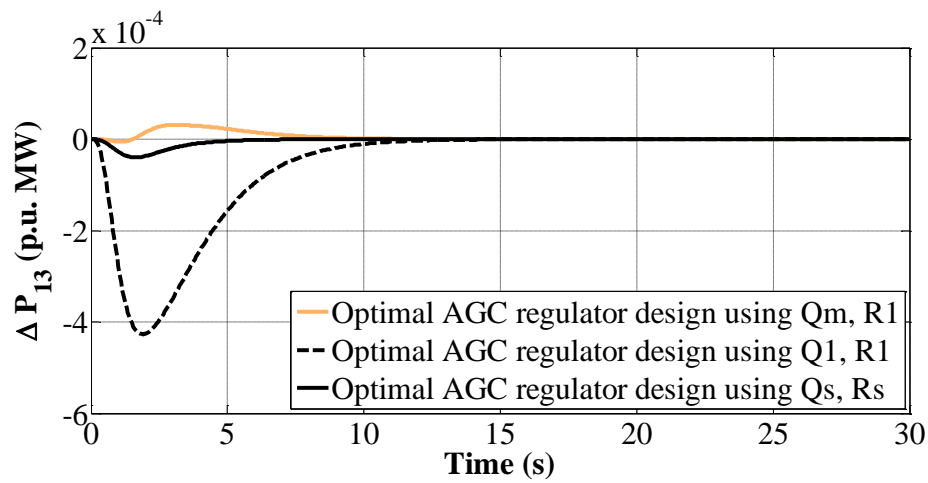
(f)

Fig. 6.5: Dynamic response of non-reheat thermal power system at 1% slp in each area (a) Frequency deviation of area-1 (b) Frequency deviation of area-2 (c) Frequency deviation of area-3 (d) Tie line power deviation between area-1 and area-2 (e) Tie line power deviation between area-2 and area-3 (f) Tie line power deviation between area-1 and area-3, Vs Time.

Critical examination of Table 6.8 reveals that ST, FPu, PT and RT values for frequency deviation of each control area for optimal AGC regulators with the structure of cost weighting matrices in case study 3 are reduced appreciably as compared to optimal AGC regulators with the structure of cost weighting matrices in other two case studies. Therefore, it is concluded that the design of cost weighting matrices in case

study 3, optimal AGC regulator design using scaling method for cost weighting matrices proposes improvement in system stability and dynamic performances as compared to other considered structures in case study 1 and case study 2. However, the magnitudes of settling time, rise time and peak time for Optimal AGC in case study 1 are reduced appreciably as compared to case study 2.

6.5.3 Non reheat thermal-hydro-non reheat thermal power system at 1% step load perturbation

Optimal AGC regulators of three areas interconnected thermal hydro thermal power system under the wake of 1% slp in each area are designed by considering various structures of cost weighting matrices which are defined in Table 6.2.

TABLE 6. 6   Optimal feedback gain matrix K for non-reheat thermal power system

Case study 1	[-0.3820 -0.6005 -0.1488 0.0380 0.0371 0.0073 -0.0012 0.0291 0.0089 -0.0142 0.1880 0.2022 -0.9951 0.0427 -0.0891 0.0062 0.0262 0.0073 -0.4004 -0.6282 -0.1539 0.0469 0.0370 0.0063 -0.0736 -0.2050 -0.1314 -0.0500 -0.9954 0.0818 0.0562 0.0482 0.0089 -0.0098 0.0178 0.0063 -0.3909 -0.6161 -0.1512 0.3221 0.1319 -0.1902 0.0851 -0.0858 -0.9927]
Case study 2	[-0.8538 -1.4884 -0.6691 0.0102 0.0161 0.0026 0.0102 0.0161 0.0026 0.7732 0.7732 0.0000 -1.0000 0.0000 0.0000 0.0102 0.0161 0.0026 -0.8538 -1.4884 -0.6691 0.0102 0.0161 0.0026 -0.7732 0.0000 0.7732 0.0000 -1.0000 0.0000 0.0102 0.0161 0.0026 0.0102 0.0161 0.0026 -0.8538 -1.4884 -0.6691 0.0000 -0.7732 -0.7732 0.0000 -0.0000 -1.0000]
Case study 3	[0.9339 1.4354 1.2376 -0.0222 -0.0122 0.0012 -0.0375 -0.0102 0.0047 -0.6291 -0.5332 0.0959 -3.6596 0.0410 0.0924 -0.0202 -0.0336 -0.0056 1.0354 1.5719 1.4042 -0.0476 -0.0323 0.0000 0.8355 0.1651 -0.6704 -0.0363 -4.0493 0.0479 -0.0320 -0.0559 -0.0101 -0.0441 -0.0563 -0.0079 1.1541 1.7250 1.5878 0.0703 0.9785 0.9082 -0.0760 -0.0425 -4.4709]

It is assumed that three areas in optimal AGC of three area interconnected

thermal hydro thermal power system are of identical capacity. Optimal feedback gain matrices, eigen values, dynamic responses and system response characteristics for various case studies are computed to examine performance and dynamic stability of system.

TABLE 6. 7   Eigen values for non-reheat thermal power system

Case study 1	Case study 2	Case study 3
-13.2923	-17.8415	-28.2831
-13.2853	-17.8387	-33.4356
-13.2818	-17.8387	-30.7102
$-1.5374 \pm 3.2723i$	$-2.9581 \pm 2.5082i$	$-1.9172 \pm 1.0322i$
$-1.3663 \pm 3.0858i$	$-2.5181 \pm 2.6312i$	$-1.3821 \pm 1.9345i$
$-1.7840 \pm 2.8660i$	$-2.5181 \pm 2.6312i$	$-1.3677 +1.9192i$
$-1.0259 + 0.3080i$	-0.3920	$-1.3677 -1.9192i$
$-1.0259 - 0.3080i$	$-0.6853 + 0.0333i$	-3.7437
$-0.6354 + 0.1122i$	$-0.6853 - 0.0333i$	-3.2220
$-0.6354 - 0.1124i$	$-0.6853 + 0.0333i$	-0.7914
-0.6924	$-0.6853 - 0.0333i$	-0.7959

TABLE 6. 8 System response characteristics for non-reheat thermal power system

S. No.	System state variable	Case Study	FPu (Hz) (-)	PT (s)	RT (s)$\times 10^{-4}$	ST (s)
1	ΔF_1 (Hz)	1	0.0131	0.90	0.0006	6.48
		2	0.0074	0.95	0.8942	10.98
		3	0.0041	0.85	0.0194×10^{-4}	2.81
2	ΔF_2 (Hz)	1	0.0131	0.95	0.0004	6.10
		2	0.0074	0.95	0.8942	10.98
		3	0.0038	0.85	0.0006×10^{-4}	3.13
3	ΔF_3 (Hz)	1	0.0131	0.95	3148	6.31
		2	0.0074	0.95	0.8942	10.98
		3	0.0035	0.85	0.0070	3.63

For various case study, comparison of dynamic responses of optimal AGC of power system which are obtained by using different structures of cost weighting

matrices is shown in Fig. 6.6 (a-f). Inspection of plots reveals that dynamic responses of frequency and tie-line deviation for all the three case studies tend to settle down at zero steady state value for 1% slp in each area. Comparison of magnitude of frequency deviation and tie-line deviation for all the three case studies clearly reveal that less time is taken to damp out oscillations with the optimal AGC regulator which are designed using case study 3 over the optimal AGC regulator which are designed using case study 1 and case study 2. Even if second area of power system is hydro power system, better system response is offered by optimal AGC regulators which are designed with structures of cost weighting matrices based on scaling method in case study 3 as compared to optimal AGC regulators which are designed by using structures of cost weighting matrices described in case study 1 and case study 2. An analysis of optimal feedback gain matrix in Table 6.9 reveals that the design of weighting matrices in case-1 shows a decrease in feedback gains as compared to case study 2 and case study 3. System is stable for all the three case studies as none of the eigenvalues have positive real parts as shown in Table 6.10. It is apparent that Optimal AGC has negative real parts of eigen value for case study 3 (-34.1656) as compared to case study 2 (-17.8384) and case study 1 (-13.2886). It reveals that Optimal AGC regulator for thermal-hydro-thermal power system gives better stability in case study 1, hence better stability margin as compared with other case studies. It is evident from the Table 6.11 that system response characteristics value in terms of magnitudes of ST, FPu, PT and RT for Optimal AGC in case study 3 is reduced appreciably as compared to other cases. With the design of optimal AGC regulator based on scaling method of cost weighting matrices, settling time value of frequency deviation in each area is of 8.27 seconds, 7.8 seconds and 8.73 seconds in case study 1 and 10.29 seconds, 8.79 seconds and 8.92

117

seconds in case study 2 of area1, area2 and area3 respectively is diminished to 6.6 seconds, 4.98 seconds and 5.67 seconds in the area1, area2 and area3 respectively. Though, system response characteristics offered by the design of weighting matrices based on case study 1 are appreciable better when compared to case study 2. Therefore, it is concluded that the design of optimal AGC regulators based on cost weighting matrices in case study 3 proposes improvement in system stability and dynamic performances as compared to other considered designs.

(a)

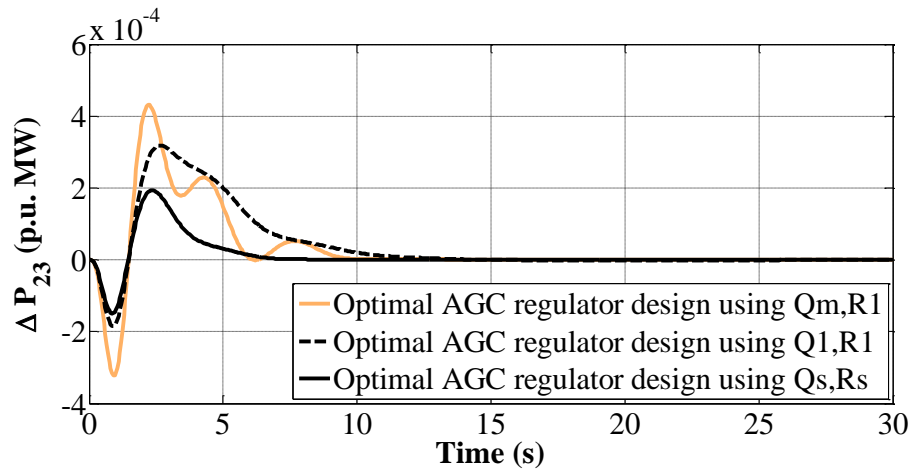(b)
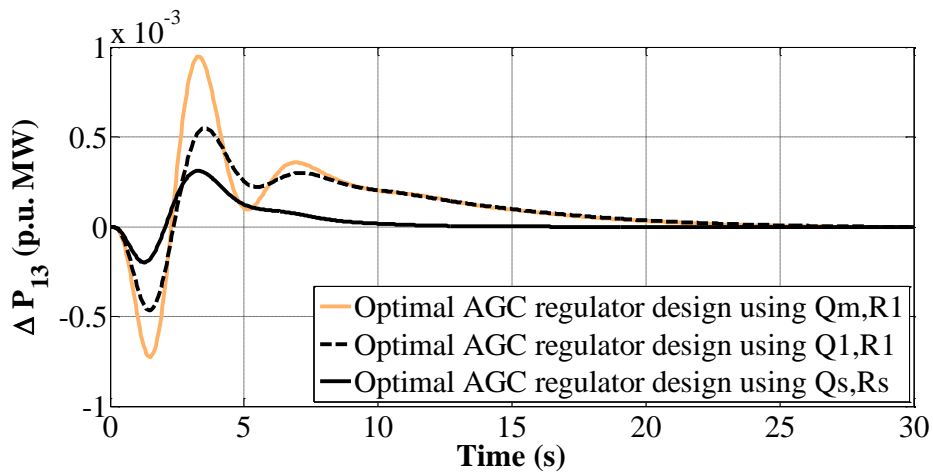

(c)

(d)

119
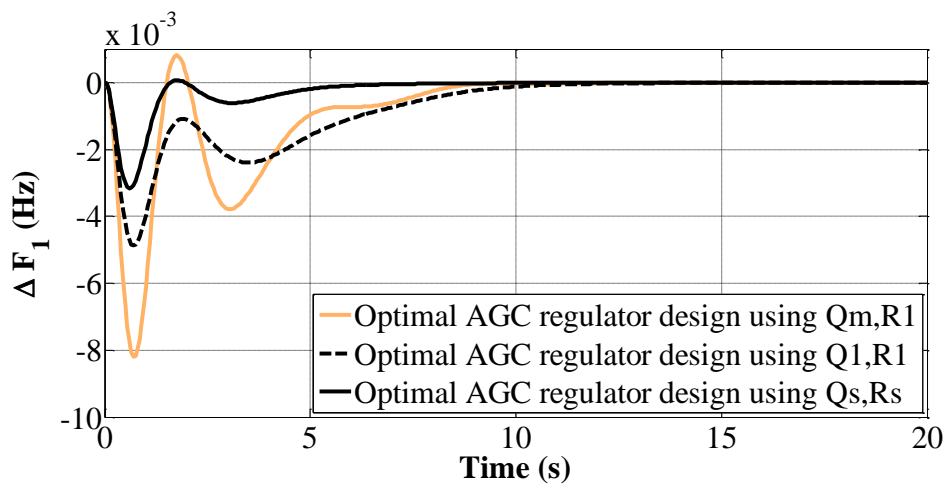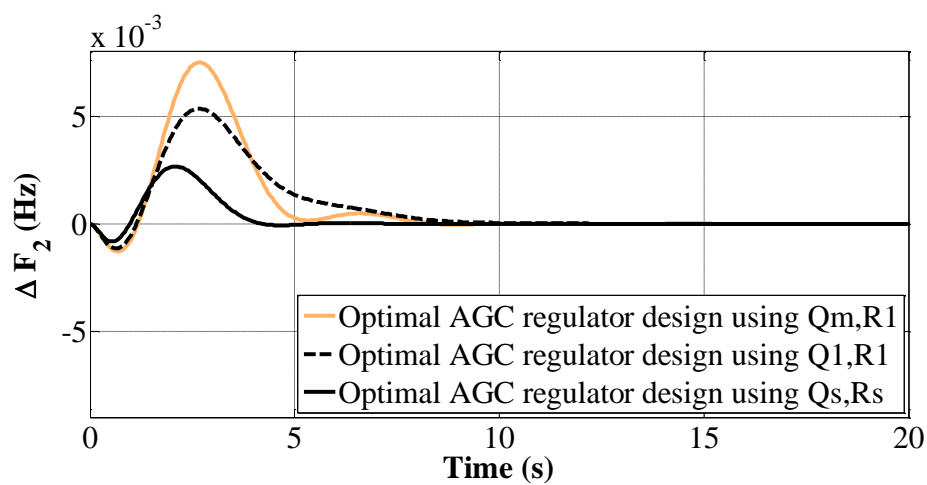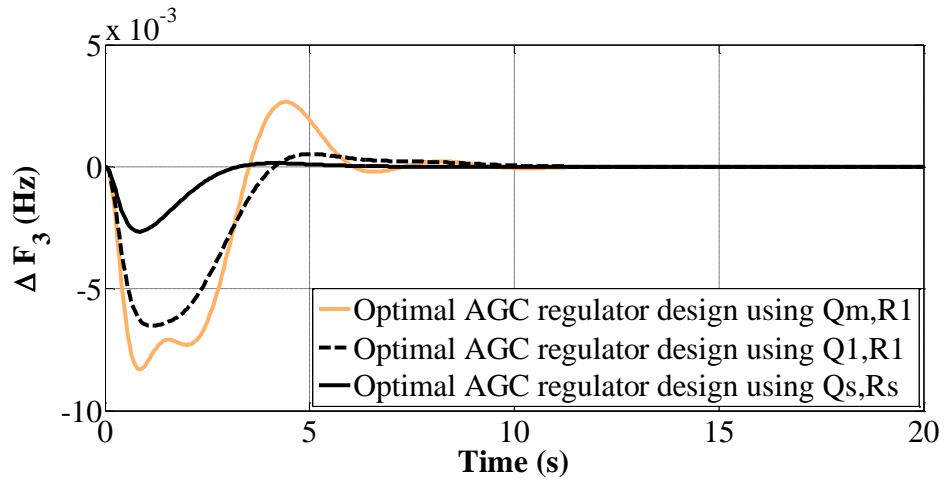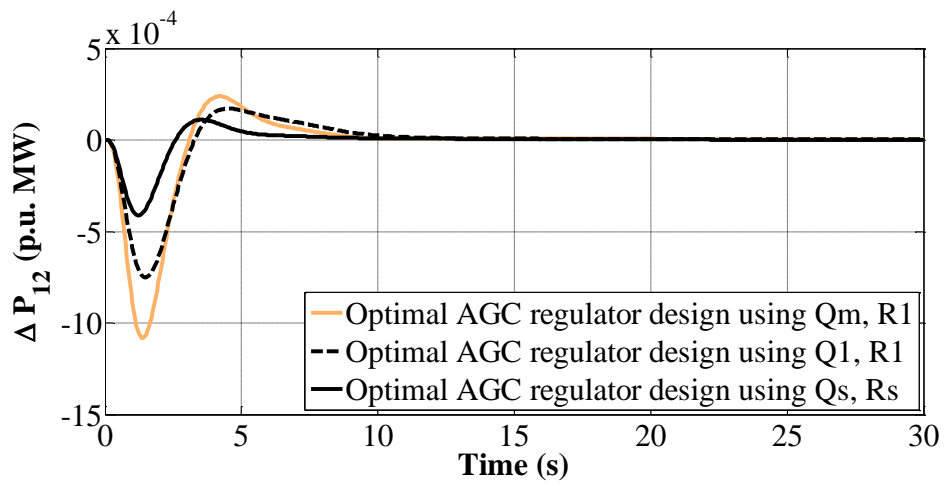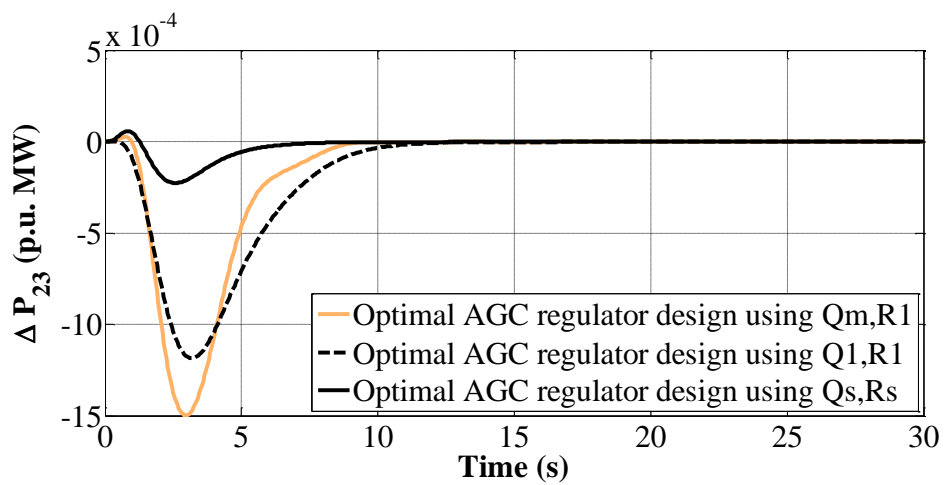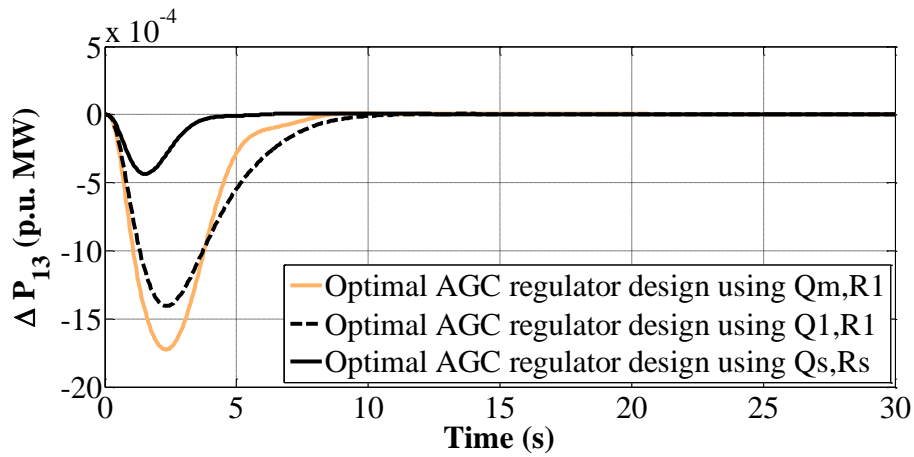
(f)

Fig. 6.6: Dynamic response of non-reheat thermal power system at 1% slp in each area (a) Frequency deviation of area-1 (b) Frequency deviation of area-2 (c) Frequency deviation of area-3 (d) Tie line power deviation between area-1 and area-2 (e) Tie line power deviation between area-2 and area-3 (f) Tie line power deviation between area-1 and area-3, Vs Time.

TABLE 6. 9   Optimal feedback gain matrix K for non-reheat thermal hydro non-reheat thermal power system

Case study 1	[0.4348	0.6693	0.1641	-0.5792	-0.6520	0.0983	0.9467	0.1002
	0.1045	0.0242	2.3458	0.4507	-2.6800	-0.0695	0.0600	0.3005
	0.1250	0.1289	0.0281	-1.3509	-1.1069	1.8170	2.0699	0.1845
	0.0928	0.0106	4.1607	-1.1989	-2.4405	-0.1682	-2.3830	0.5747
	0.1337	0.1162	0.0242	-1.0716	-3.1894	-6.1724	3.5365	0.8291
	1.0822	0.2554	0.4404	-1.2437	-7.3772	1.6382	7.0585	0.7612]
Case study 2	[1.0304	1.6635	0.6963	-0.4097	-0.1383	1.0796	0.5563	0.0282
	0.0466	0.0093	3.2125	1.3324	-2.4854	-0.7830	-0.5856	0.2910
	0.1937	0.1725	0.0265	-1.9119	-1.1350	4.0637	2.8906	0.0668
	-0.0605	-0.0160	6.1905	-1.1881	-2.5193	-0.5537	-4.9295	0.5838
	0.1359	0.0732	0.0093	-0.7907	-3.4658	-8.0987	3.0961	1.4396
	2.0143	0.7502	-0.9810	-1.5155	-8.2119	2.9286	10.3901	0.7580]
Case study 3	[1.7780	2.4501	1.0111	-0.0594	0.9580	3.4942	-0.0293	0.0197
	0.1776	0.0185	5.0670	3.2241	-1.1908	1.2790	-1.7227	0.2338
	0.2749	0.2254	0.0295	-2.3077	0.4589	11.1756	4.1802	0.0151
	-0.1721	-0.0181	10.6443	-3.2145	0.8392	-0.7371	-11.9377	2.0709
	0.3807	0.1801	0.0185	-0.5841	-3.0833	-7.2920	1.6197	3.3265
	4.3556	2.1307	-0.8717	-3.5931	-10.7418	7.1129	13.4417	3.9569]

TABLE 6. 10 Eigen values for non-reheat thermal hydro non-reheat thermal power system

Case study 1	Case study 2	Case study 3
-13.2886	-17.8384	-34.1656
-13.3049	-17.8427	-20.7915
$-1.4032 \pm 3.2289i$	$-3.0827 \pm 2.4988i$	$-3.4864 \pm 2.0318i$
$-1.9230 \pm 2.8161i$	$-2.4136 \pm 2.6859i$	$-2.2050 \pm 2.5787i$
-3.1169	-3.0828	-3.0913
$-0.5832 \pm 1.6114i$	$-0.6928 \pm 1.5469i$	$-0.9183 \pm 1.5895i$
$-0.8158 \pm 0.5580i$	$-0.9891 \pm 0.4712i$	-2.2502
$-1.0200 \pm 0.4503i$	$-0.7158 \pm 0.3764i$	$-1.0001 \pm 0.3472i$
-0.7808	-0.7455	$-0.9313 \pm 0.4322i$
-0.0385	-0.0599	-0.1170

TABLE 6. 11 System response characteristics for non-reheat thermal hydro non-reheat thermal power system

S. No.	System state variable	Case study	FPu (Hz) (-)	PT (s)	RT (s)×10⁻⁴	ST (s)
1	ΔF_1 (Hz)	1	0.0082	0.70	57	8.27
		2	0.0049	0.70	36	10.29
		3	0.0032	0.60	13	6.6
2	ΔF_2 (Hz)	1	0.0075	2.65	7.63	7.80
		2	0.0054	2.65	4.53	8.79
		3	0.0027	2.10	1.16	4.98
3	ΔF_3 (Hz)	1	0.0083	0.85	55	8.73
		2	0.0065	1.15	32	8.92
		3	0.0027	0.85	12	5.67

6.6   Conclusion

Designing and implementation of optimal AGC regulators has been carried out for three optimal AGC of interconnected multi source power systems with various structures of cost weighting matrices. First power system consists of non-reheat thermal-hydro-gas interconnected power system, second power system consists of non-reheat thermal interconnected power system and third power system consists of non-reheat thermal-hydro- non-reheat thermal interconnected power system. Three different structures of cost weighting matrices have been inspected for the design of optimal AGC regulators. One of the novel approaches for design of cost weighting matrices is based on the scaling method. To validate the effectiveness of optimal AGC regulator with structures of control and state cost weighting matrices, dynamic response of system for frequency and tie line power deviation is procured with 1% slp in each area. Optimal feedback gain matrix, eigen values, dynamic response characteristics and dynamic responses are the assessment to examine the stability of power system. The investigation carried out reveal that optimal AGC regulator based on structures of control and state cost weighting matrices with scaling method offer remarkable improvement in dynamic stability as compared to other designed regulators. For all the three power system with different sources, appreciable favourable dynamic responses are accomplished with optimal AGC regulators based on structures of control and state cost weighting matrices by way of scaling method. Investigation of eigen values ensures the stability of power system with various structures of cost weighting matrices. From the dynamic responses of optimal AGC of three area interconnected multi source power systems, it is concluded that that there is appreciable reduction in

settling time, peak time, rise time and first peak undershoot magnitude with implementation of optimal AGC regulators based on scaling method.

AGC OF THREE AREA INTERCONNECTED MULTI SOURCE POWER SYSTEMS WITH SUPERCONDUCTING MAGNETIC ENERGY STORAGE

7.1 Introduction

The uncertainty of available resources and desire to achieve minimal frequency and tie line power deviation with renewable sources in an interconnected power system developed the need of energy storage system. Energy storage system has the feature to provide and absorb power at the time of load disturbances. The ability of charging and discharging batteries depends on the type of energy storage system. Short comings of battery energy storage system like low discharge rate and high maintenance leads to the popularity of Super Conducting Magnetic Energy Storage System (SMES) as one of the efficient energy storage system. SMES has the capability of rapid response with high energy efficiency. It convert directly from one form to another and take less time for discharging and charging. Since the evolution of SMES in 1970, it attains considerable attention for application in power system to achieve effective system performance and response at load disturbances. Its application includes stability improvement, fast spinning reserve, sub synchronous damping, load leveling, active and reactive power control. SMES unit converts ac to dc power conversion for superconducting coil. SMES unit consists of a coil under cryogenic temperature, star-delta 3 phase transformer and power conditioning system.

The detail SMES unit configuration is shown in Fig.7.1.
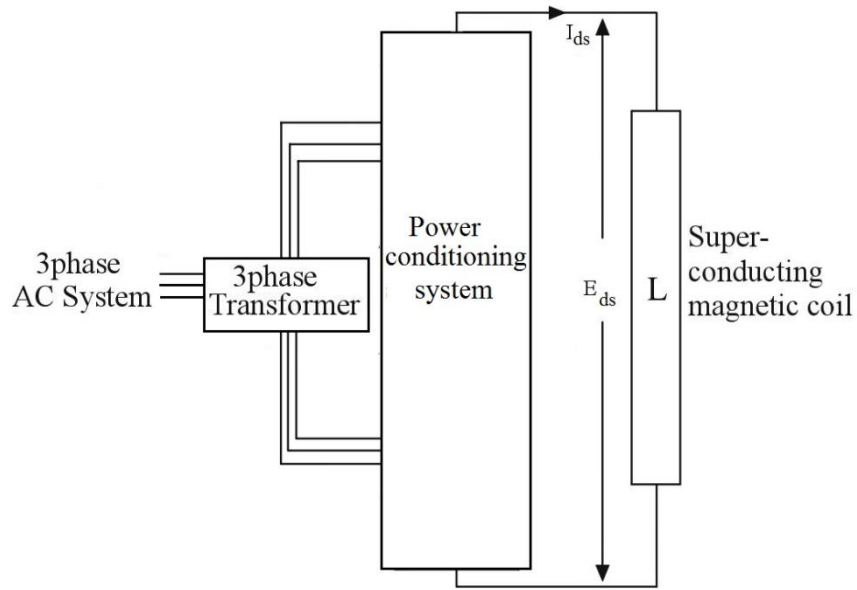
Fig.7. 1: SMES unit configuration

Advancement in power electronics and superconducting technologies have pushed SMES to be used as one of the promising energy storage system to be power system.

7.2   Modeling of superconducting magnetic energy storage system

SMES has high power density, smaller size and reduced weight. Superconducting coil is the heart of SMES unit. Designing of coil depends on many factors such as energy/mass ratio parameter, forces, fields etc. and these coils are in the form of solenoid which is simple and cost effective as compared to toroid. Coil inductance, maximum voltage and maximum current value play major role in deciding the rating of maximum energy drawn by SMES. Losses in SMES are mainly due to the refrigeration required for its maintenance below critical temperature. Low temperature superconducting coil are placed in helium vessel and stores dc magnetic field. Power conditioning system in SMES unit consists of 12 pulse bridge converter. In SMES unit

125

operation, charging, discharging or dynamic stability at disturbances is stabilized by inductor voltage. During normal operation, power conditioning system provides dc voltage as E_{ds} across the inductor. After the inductor current (I_{ds}) reached its rated value, the superconducting coil maintains its value by adjusting the inductor voltage and unit is ready to connect in power system. The coil gets charge to normal current during charging mode and provides high current. Transformer and converter losses are neglected. By controlling firing angles (αs) of converter, dc voltage across inductor (E_{ds}) can be varied in wide range. The relation of firing angle of converter and inductor voltage can be given as follows:-

$$E_{ds} = 2E_{ds0}\cos_{\alpha s} - 2I_{ds}R_{Ds} \tag{7.1}$$

Where R_{Ds} is equivalent commutating resistance (kΩ).

Stored energy of inductor (W_{sm}) at any instant is given as:-

$$W_{sm} = LI_{ds}^2/2 \tag{7.2}$$

Area Control Error (ACE) is considered as a control signal in each area of interconnected power system. With deviation in control signal, dynamic stability of AGC of interconnected power system is more stabilized with SMES unit at load disturbances. This deviation in dc voltage is repeatedly controlled by converter. Also, value of inductor current deviation is applied as negative feedback signal in SMES unit to restore its value after disturbances. The block diagram of SMES unit with negative current feedback is displayed in Fig.7.2 .

So, voltage deviation across inductor can be given as:-

$$\Delta E_{ds}(s) = (1/(1 + sT_{dcs}))(K_{s0}ACE(s) - K_{Ids}\Delta I_{ds}(s)) \tag{7.3}$$
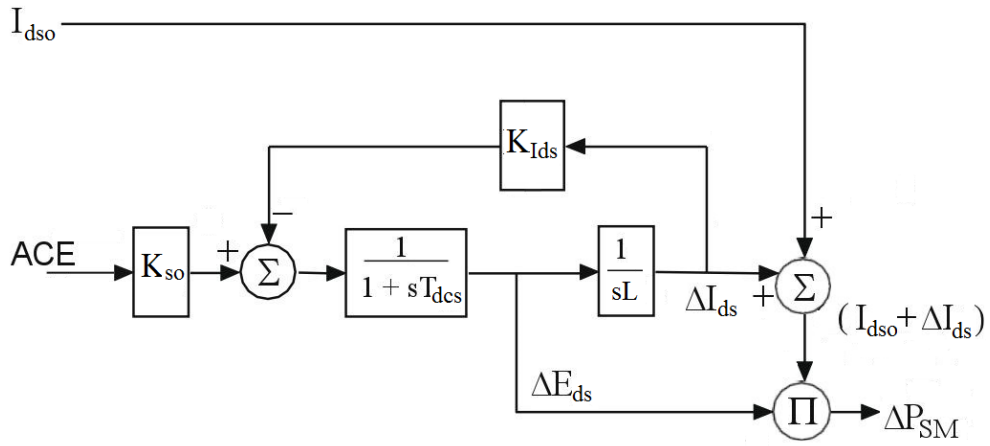
Fig.7. 2:   Block diagram representation of SMES unit

Also, the general equation of current deviation across inductor can be given as :-

$$\Delta I_{ds}(s) = \Delta E_{ds}(s)/sL \tag{7.4}$$

Where ΔE_{ds} and ΔI_{ds} are incremental change in converter voltage (kV) and inductor current (kA), T_{dcs} is converter time delay (s), K_{so} is the gain of the control loop (kV/unit ACE), L is the coil inductance (H), I_{dso} (kA) and E_{dso} (kV) are inductor current and voltage value before disturbances, K_{Ids} is the gain corresponding to negative current feedback (kV/kA).

Power flow in the superconducting coil at any instant can be given as:-

$$PSM = E_{ds}I_{ds} \tag{7.5}$$

Initial power flow (PSM) into the inductor coil without disturbance is expressed as:

$$PSM_0 = E_{ds0}I_{ds0} \tag{7.6}$$

Power flow deviation in the superconducting coil after disturbances can be given as:-

127

$$\Delta PSM = (E_{ds0} + \Delta E_{ds})(I_{ds0+}\Delta I_{ds}) \qquad (7.7)$$

So, power flow deviation is expressed as:-

$$\Delta PSM = \left(\Delta E_{ds}(I_{ds0} + \Delta I_{ds})\right) + E_{ds0} * (I_{ds0} + \Delta I_{ds}) \qquad (7.8)$$

As in the storage mode $E_{ds0} = 0$, so it's neglected and power flow deviation is stated in per unit of rated power as:-

$$\Delta PSM = \Delta E_{ds} * (I_{ds0+}\Delta I_{ds})/P_{rated} \qquad (7.9)$$

In superconducting coil, inductor value is assumed as 2.65H & inductor current is assumed as 4.5kA [122, 242, 256]. So, energy stored of inductor is calculated by applying equation no. 7.2 and can be given as:-

$$W_{sm} = 2.65 \times 4.5^2/2 \qquad (7.10)$$

The considered value of stored energy in inductor is 30MJ or its equivalent to 8.4 kWh. A small size of SMES (10MW/30 MJ) with high rate of repetitive field changes are connected in each area of power system under investigation.

7.3   Power system under investigation

The role of AGC is to operate the successful operation of power system. AGC control active power by using governor system. At sudden load changes, AGC of interconnected power system with artificial intelligent based controllers reduces its effect. But this approach does not give satisfactory result for multi area multi source power system. Especially in case of renewable sources likes hydro power system which took comparable more time to settle stability in dynamic responses at load disturbances in multi area. Different cases of three area multi source power system are

categorized in Table 7.1. Each control area of equal rating of 2000MW is considered in AGC of interconnected three area multi source power system. Transfer function model of three area multi source power system which are studied as given in Fig. (7.3-7.5). Modeling of individual control area of power system is already explained in chapter 3.

State space representation of three area of multi source power system is given as:

State space model:

$$X^{\cdot} = A\,x + B\,U + \Gamma P_D \tag{7.11}$$

$$Y = Cx \tag{7.12}$$

Where $X^{\cdot}$, U, P_D and Y are the state, control, disturbance and system output vectors, respectively. A, B, C and Γ are real constant matrices of compatible dimensions. Specific parameters for each control area of multi source power system is given in Appendix B.

Linear state space model for three cases of power system is obtained by defining the vectors x, u and p for each and can be given as:

For case-1 of power system (Non-reheat thermal, hydro and gas power system)

State vector

$[x]^{T} = [\Delta F_1\ \Delta P_{G1}\ \Delta X_{E1}\ \Delta F_2\ \Delta P_{G2}\ \Delta X_h\ \Delta X_{RH}\ \Delta F_3\ \Delta P_{G3}\ \Delta P_{FC}\ \Delta V_P\ \Delta X_g\ \Delta P_{tie12}\ \Delta P_{tie13}$

$\Delta P_{tie23}\ \int ACE_1\ \int ACE_2\ \int ACE_3]$ \hfill (7.13)

Control vector

$[U]^{T} = [\Delta P_{c1}\ \Delta P_{c2}\ \Delta P_{c3}\,]$ \hfill (7.14)

Disturbance vector

$$[\Delta P_d]^T = [\Delta P_{d1} \ \Delta P_{d2} \ \Delta P_{d3}] \tag{7.15}$$

The control signal will be of the form:

$$\Delta Pc_i(t) = - IC_i \int (ACE_i) \, dt \tag{7.16}$$

$$ACE_i = b_i \, \Delta F_i(t) + \sum \Delta P_{tie \, ij}(t) \tag{7.17}$$

$$\Delta P_{tie \, ij}(t) = T_{ij} [\Delta F_i(t) - \Delta F_j(t)] \tag{7.18}$$

Where j =1 to 3, j ≠ i   (7.19)

TABLE 7. 1 Different cases of three area multi source power system with SMES

Cases	Types of Power system
1.	Non-reheat thermal, hydro and gas power system
2.	Non-reheat thermal power system only
3.	Non-reheat thermal, hydro and Non-reheat thermal power system
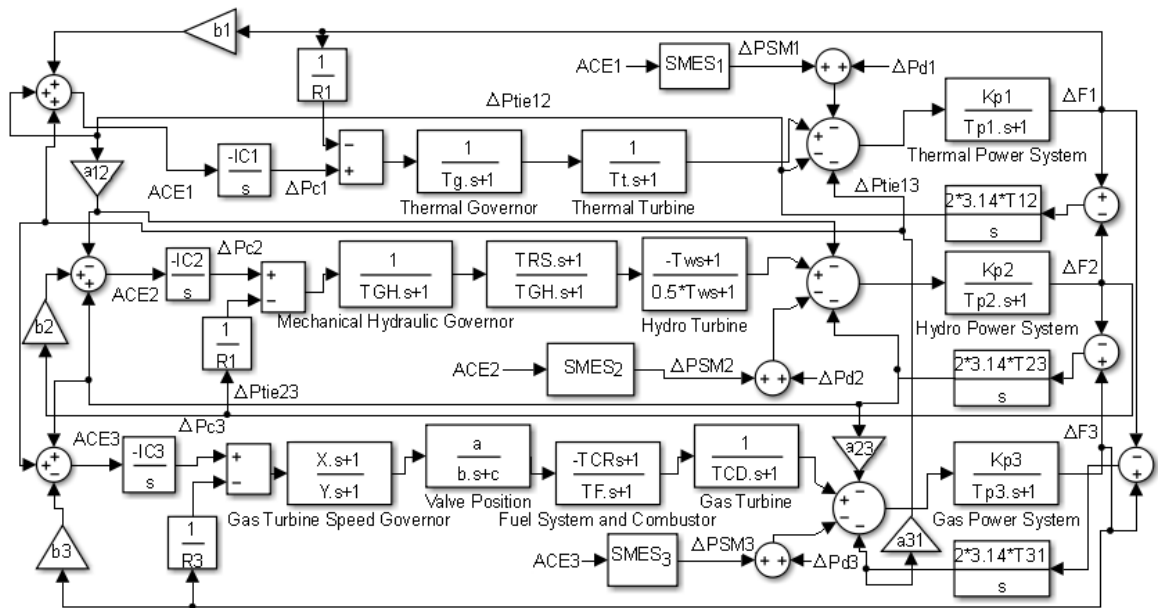
Fig.7. 3:   Transfer function block diagram of three area non-reheat thermal-hydro-gas power system model with SMES

130
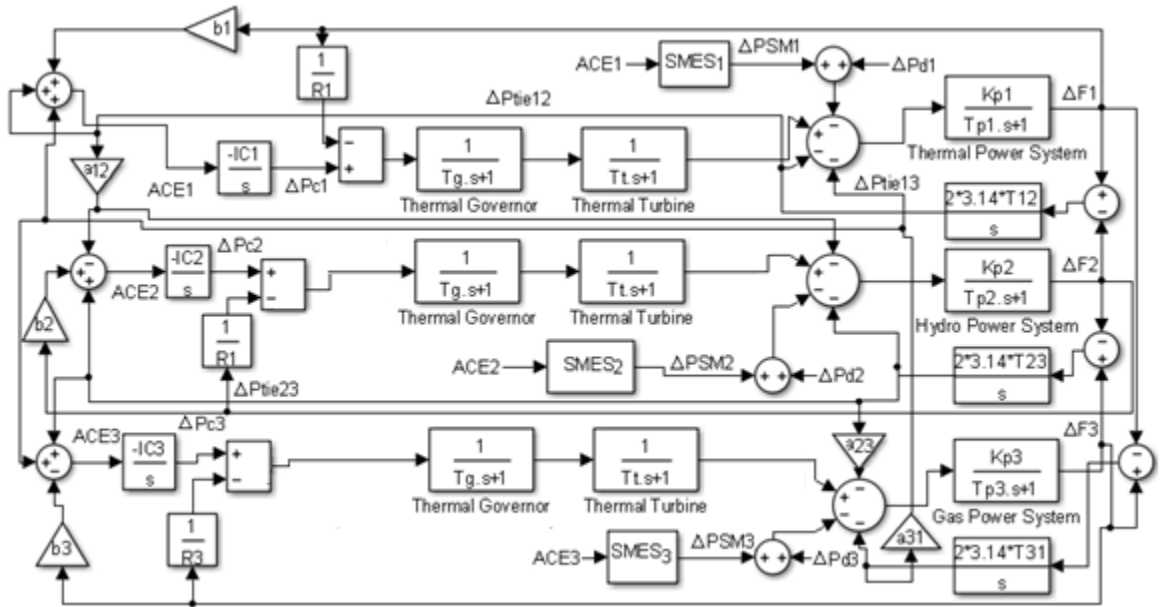
Fig.7. 4: Transfer function block diagram of three area non-reheat thermal power system model
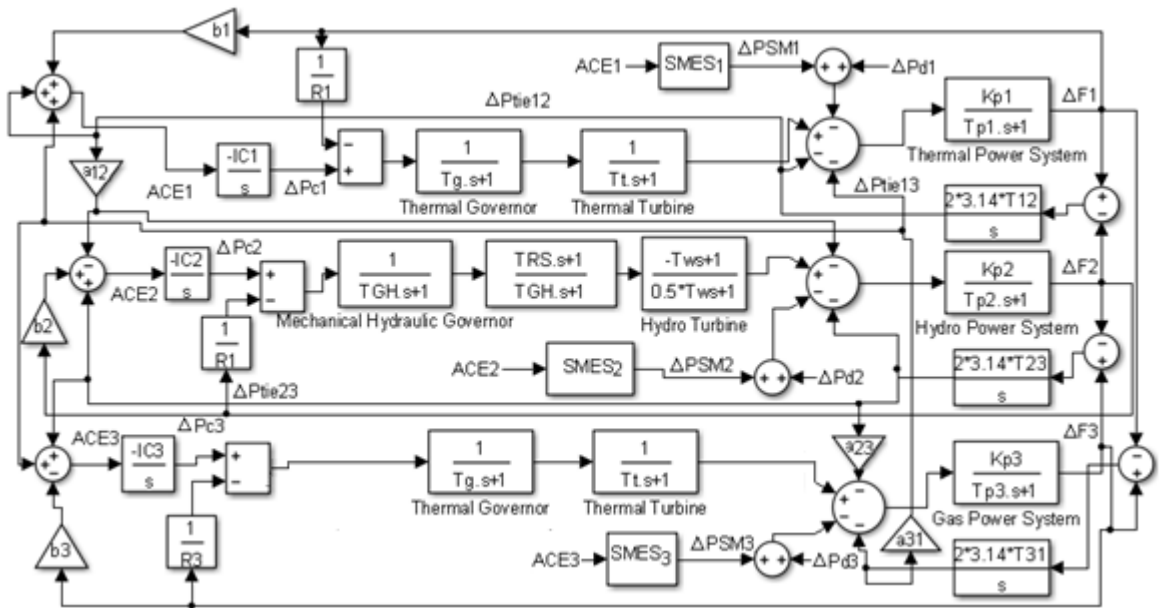
Fig.7. 5: Transfer function block diagram of three area non-reheat thermal-hydro- non-reheat thermal power system model

131

7.4   Optimization problem

Various bio-inspired optimization techniques like PSO and GA is applied to optimize IC of AGC of interconnected three area multi source power with or without SMES. Integral Controller (IC) is applied in each area of interconnected multi source power system with or without SMES. ACE is considered as the control signal and is used to formulate objective function of power system. ISE reduces large error and therefore, it is considered as the performance index of power system. Performance index value (PIv) of three area power system is expresses in equation no. .

$$(PIv) = \sum_{i=1}^{3} \int ACE_i^2 \, dt \qquad\qquad (7.20)$$

The simulation time of 50s is considered for PIv of all the IC.

7.5   Simulation results and discussions

7.5.1   Non-reheat thermal-hydro-gas power system at 1% step load perturbation

Three area non-reheat thermal, hydro and gas interconnected power system is simulated by including and excluding SMES unit at 1% step load perturbation (slp) in each area. Parameters of various bio inspired tuned IC for power system with or without SMES which are designed to minimize objective function by using Eqn. 7.20 is given in Table 7.2. It is apparent from Table 7.2 that PSO tuned IC power system with SMES (PIv=0.39×10^{-3}) is superior in terms of PIv to GA tuned IC power system with SMES (PIv=0.57×10^{-3}) and PSO tuned IC power system without SMES (PIv=54×10^{-3}). The enhancement in dynamic responses of non-reheat thermal, hydro and gas interconnected power system with SMES as compared to power system without SMES is evident from Fig. 7.3 (a-f) in terms of modes as settling time (ST), first peak

undershoot (FPu), first peak time (FPt). This clearly reveals that application of SMES in power system certainly helps the power system to achieve AGC objectives. Comparative analysis of usage of different bio-inspired artificial techniques like PSO and GA for designing of IC for AGC of interconnected multi area multi source power system has been done in Table 7.2. Critical examination of analysis shows that PSO tuned IC power system with SMES intervene better results in terms of PIv, dynamic responses and its performance measures with respect to different modes as ST, FPu and FPt.

TABLE 7. 2   **Comparative analysis of different bio-inspired artificial technique for tuning AGC of interconnected thermal-hydro-gas power system including and excluding SMES**

Modes		PSO Tuned AGC with SMES	GA Tuned AGC with SMES	PSO Tuned AGC without SMES
ST (s)	ΔF_1	30	46	71
	ΔF_2	41.7	44	62
	ΔF_3	30	46	60
	ΔP_{12}	46	46	73
	ΔP_{23}	46	58	74
	ΔP_{13}	5.9	27	37
FPu $\times 10^{-3}$ (Hz)	ΔF_1	5	5.1	37
	ΔF_2	5.6	5.7	78
	ΔF_3	5.3	5.3	42
	ΔP_{12}	0.7	0.7	10.2
	ΔP_{23}	0.7	0.8	9
	ΔP_{13}	0.2	0.5	1.9
FPt (s)	ΔF_1	0.2	0.2	2.6
	ΔF_2	0.5	0.6	1.6
	ΔF_3	0.2	0.2	1.1
	ΔP_{12}	1.8	10.3	2.6
	ΔP_{23}	2.5	2.5	2.7
	ΔP_{13}	1.2	2.7	1.9
PIv $\times$ 0.0001		0.39	0.57	54
IC	IC1	17	0.9	0.4
	IC2	15.5	12	0.3
	IC3	8.8	11	0.1

Comparative performance evaluation shows that PIv for PSO tuned IC power system with SMES as 31.5% and 99.2% times better than GA tuned IC power system with SMES and PSO tuned IC power system without SMES as shown in Table 7.3. Therefore, comparison of percentage improvement of frequency and tie-line deviation assists the criterion for judgment of betterment of proposed approach of PSO tuned IC power system with SMES than other considered bio-inspired artificial technique.

(a)

(b)

(c)

(d)

(e)

135
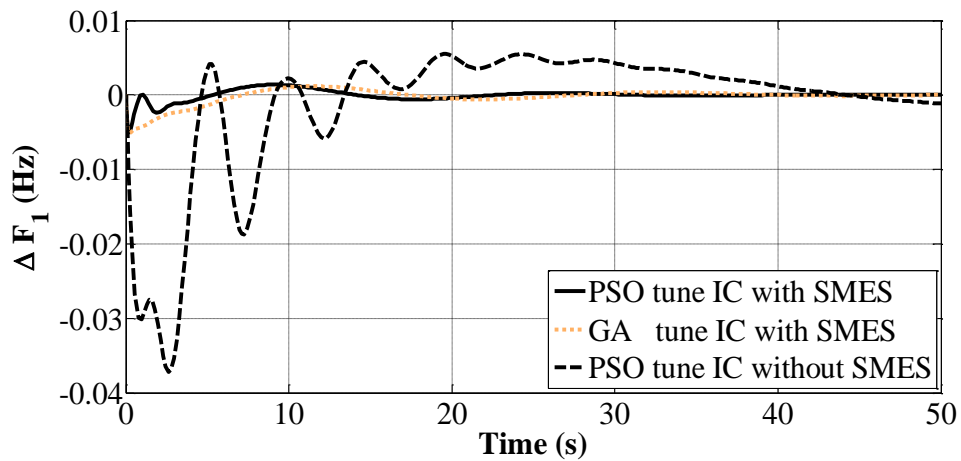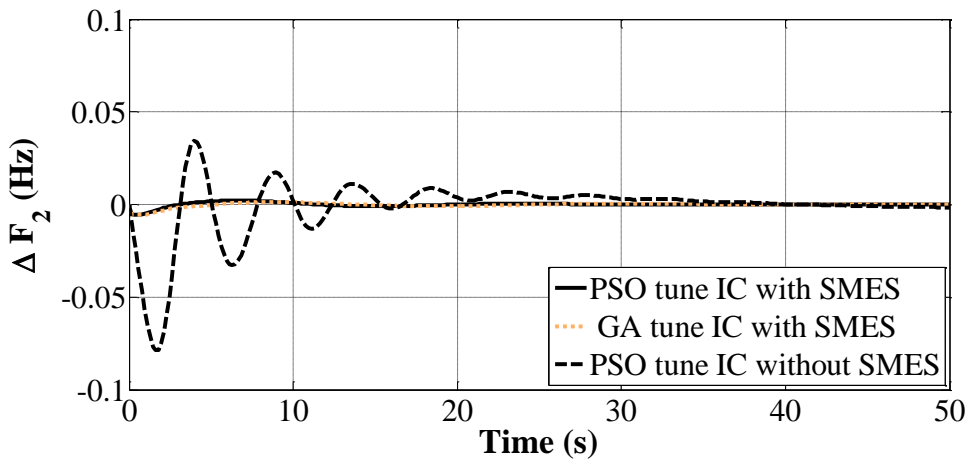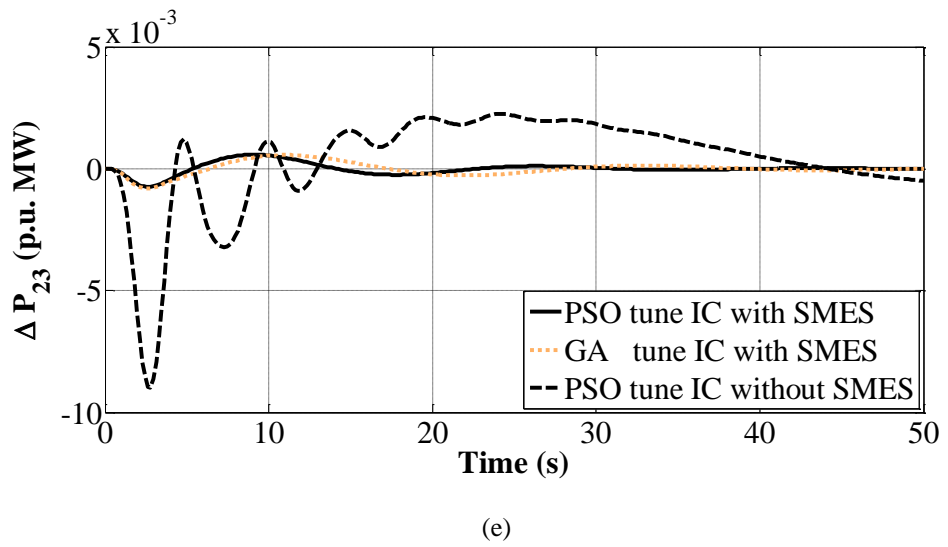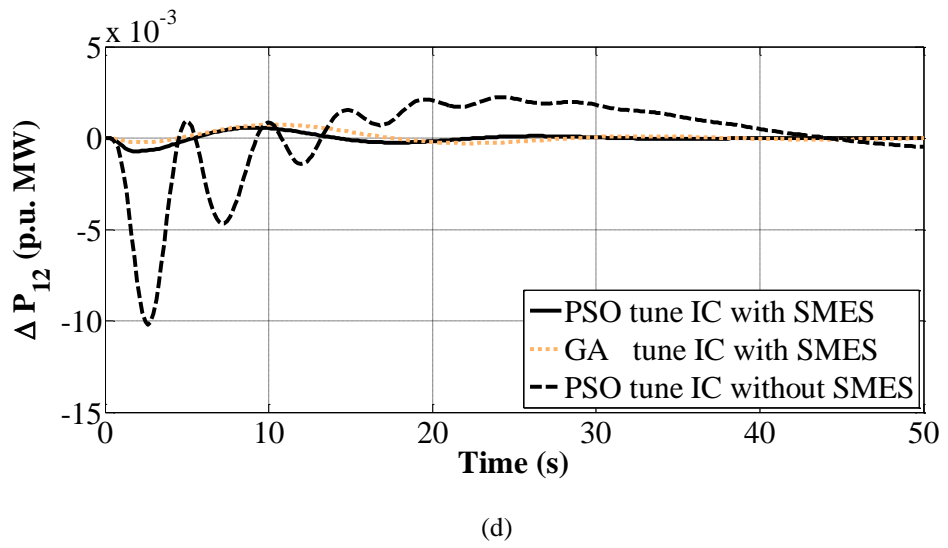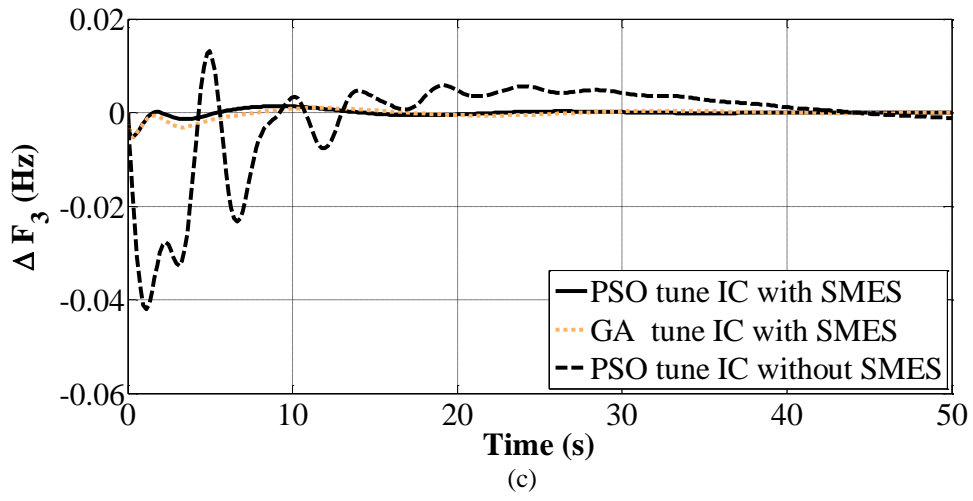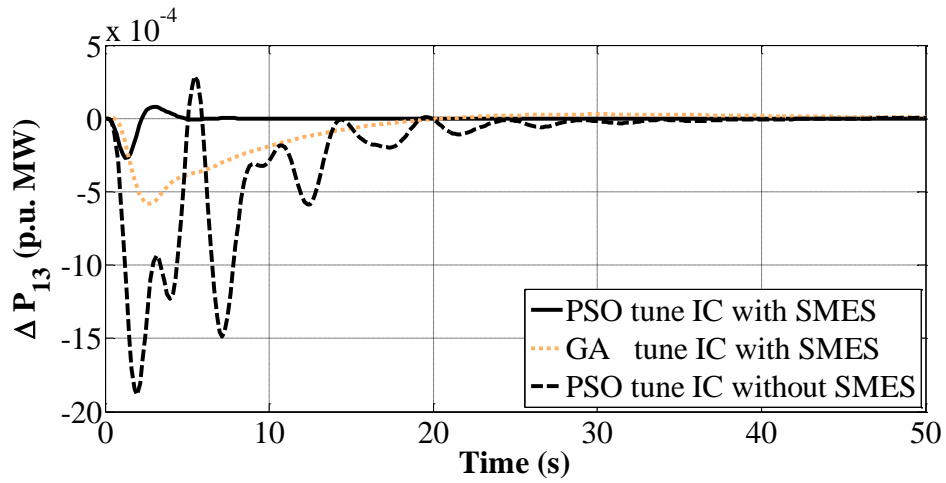
(f)

Fig.7. 6: Dynamic response of non-reheat thermal, hydro and gas power system with and without SMES at 1% slp in each area (a) Frequency deviation of area-1 (b) Frequency deviation of area-2 (c) Frequency deviation of area-3 (d) Tie line power deviation between area-1 and area-2 (e) Tie line power deviation between area-2 and area-3 (f) Tie line power deviation between area-1 and area-3 , Vs Time.

TABLE 7. 3 **Comparative performance evaluation of thermal-hydro-gas power system at 1% slp in each area**

	Modes	PSO Tune AGC without SMES	GA Tune AGC with SMES	PSO Tune AGC with SMES
ST (s)	ΔF_1	71	46	30
	ΔF_2	62	44	41.7
	ΔF_3	60	46	30
	ΔP_{12}	73	46	46
	ΔP_{23}	74	58	46
	ΔP_{13}	37	27	5.9
% Improvement in terms of ST	ΔF_1	57.7	35	
	ΔF_2	33.8	7	
	ΔF_3	50	35	
	ΔP_{12}	37	0	
	ΔP_{23}	38	21	
	ΔP_{13}	84	78	
PIv	ISE	99.2	31.5	

136

Percentage improvement frequency deviation of control area-1 and area-3 for PSO tuned IC power system with SMES is 35% and more than 50% better than GA tuned IC power system with SMES and PSO tuned IC power system without SMES. To manifest the potential of PSO tuned IC of AGC of interconnected multi area multi source power system with SMES, the study is further extended to analyze the effect of 1% slp in different areas of interconnected multi source power system as shown in Fig. 7.7 (a-f) and Table 7.4.

TABLE 7. 4   Comparative Study of AGC strategy of multi area non-reheat thermal-hydro-gas power system incorporating SMES at 1% step load perturbation at different control areas

1% slp at		Area1	Area2	Area3	Area all
ST (s)	ΔF_1	3.42	47	4.78	30
	ΔF_2	3.24	42.73	4.72	41.7
	ΔF_3	3.36	47.1	5.13	30
	ΔP_{12}	3.24	47.07	48.1	46
	ΔP_{23}	48	47.09	6.43	46
	ΔP_{13}	3.3	37	5.87	5.9
FPu ×10⁻³ (Hz) (-)	ΔF_1	4.8	1.7	0.89	5
	ΔF_2	0.68	5	0.99	5.6
	ΔF_3	0.65	1.6	4.9	5.3
	ΔP_{12}	0.23	0.7	0.01	0.72
	ΔP_{23}	0.006	0.69	0.34	0.35
	ΔP_{13}	0.23	0.005	0.35	0.27
FPt (s)	ΔF_1	0.15	2.09	0.88	0.21
	ΔF_2	0.65	0.22	0.88	0.51
	ΔF_3	0.65	1.87	0.21	0.21
	ΔP_{12}	0.51	2.23	1.9	1.87
	ΔP_{23}	1.69	2.23	0.88	2.55
	ΔP_{13}	0.51	3.93	0.88	1.24
PIv × 0.0001	**ISE**	0.18	3.3	0.34	3.9

Dynamic responses in terms of frequency and tie-line deviation for PSO tuned IC power system with SMES at 1% slp in different control areas are shown in Fig. 7.7(a-f). Critical examination of Table 7.4 reveals that performance measures with respect to ST, FPu and FPt and PIv is remarkably better when 1% slp in area 1 (thermal) or area 3 (gas) as compared to disturbance in area 2 (hydro) and area-all. This is due to the participation of hydro sources in multi-source power system which destroys the system response as compared to thermal and gas sources. The sluggishness effect of hydro is highly suppressed by the application of SMES in AGC strategy as compared to without SMES system. During disturbance in hydro sources for case2 and case4, numerical values of frequency and tie-line deviation in terms of ST are better in case of slp in all area as compared to slp in only hydro source.

(a)

(b)

(c)

(d)

139
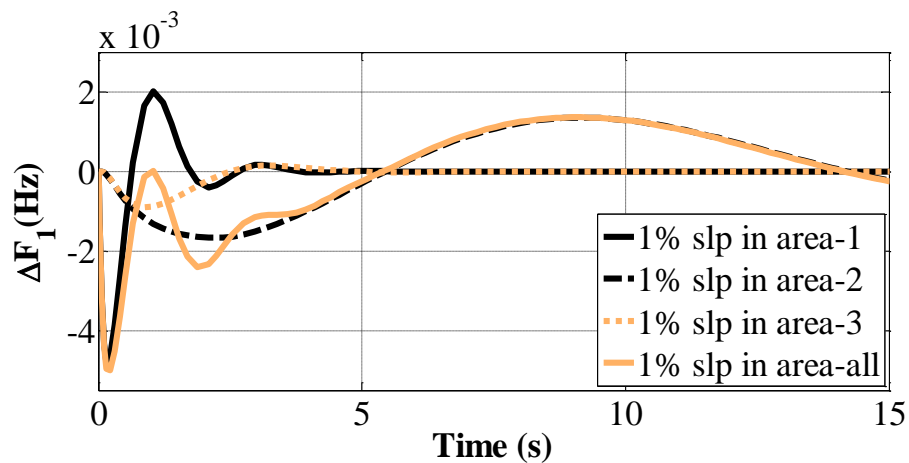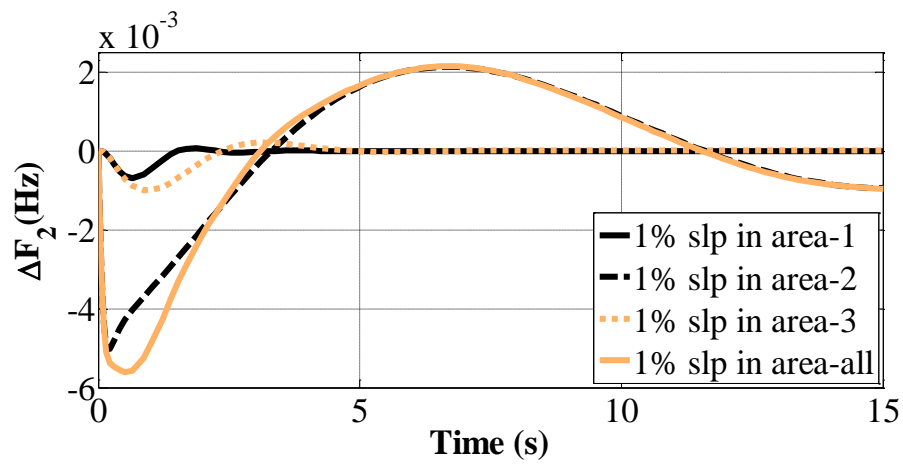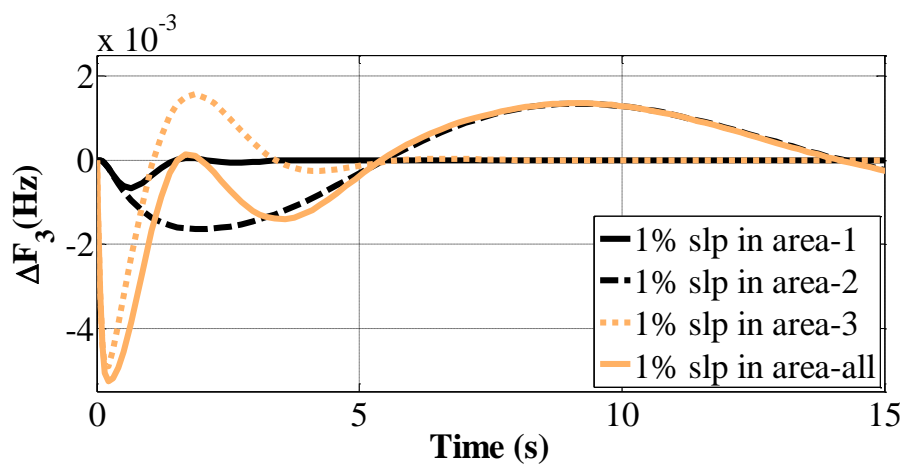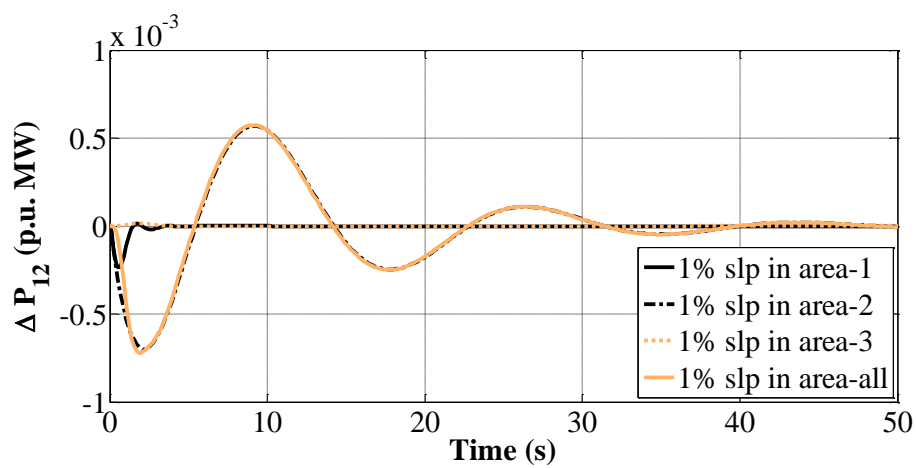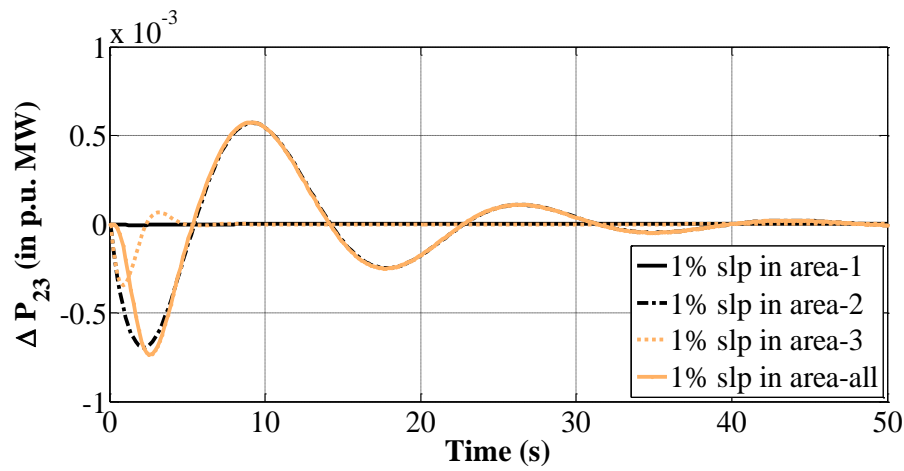
(e)
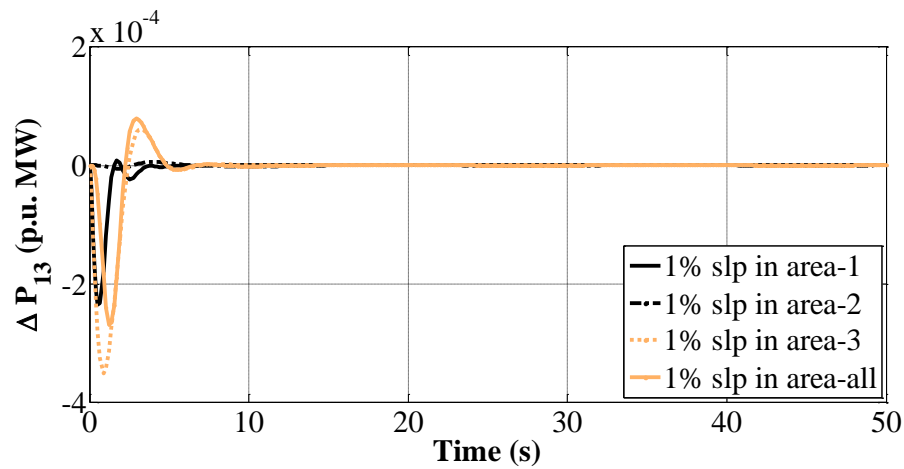
(f)

Fig.7. 7: Dynamic response of non-reheat thermal, hydro and gas power system with SMES at 1% slp in different areas (a) Frequency deviation of area-1 (b) Frequency deviation of area-2 (c) Frequency deviation of area-3 (d) Tie line power deviation between area-1 and area-2 (e) Tie line power deviation between area-2 and area-3 (f) Tie line power deviation between area-1 and area-3 , Vs Time.

7.5.2 Non-reheat thermal power system at 1% step load perturbation

Dynamic response of PSO tuned IC of AGC of three area non-reheat thermal interconnected power system with SMES is simulated at 1% slp in different area is demonstrated in Fig. 7.8(a-f). Three parameters of IC for power system with SMES are designed to minimize objective function as given in Table 7.7. Critical examination of

Fig.7.8(d) reveals that tie-line power deviation of area 1 and area 2 exhibits less oscillation, less FPu and more FPt when 1% slp is considered in area 3.

TABLE 7. 5   **Comparative study of AGC strategy of multi area non-reheat thermal power system incorporating SMES at 1% step load perturbation at different control areas**

1% slp at		Area1	Area2	Area3	Area all
ST (s)	ΔF_1	3.43	4.3	3.5	3.89
	ΔF_2	3.33	3.47	3.66	3.37
	ΔF_3	3.33	3.41	2.81	2.43
	ΔP_{12}	3.33	3.51	6.09	5.06
	ΔP_{23}	5.69	3.45	4.08	4.49
	ΔP_{13}	3.33	5.91	4.11	3.8
FPu $\times 10^{-3}$ (Hz) (-)	ΔF_1	4.8	0.68	0.74	5
	ΔF_2	0.63	4.8	0.74	5
	ΔF_3	0.63	0.65	4.8	5
	ΔP_{12}	0.23	0.23	0.0007	0.1
	ΔP_{23}	0.0001	0.23	0.27	0.1
	ΔP_{13}	0.23	0.002	0.27	0.2
FPt (s)	ΔF_1	0.15	0.66	0.66	0.21
	ΔF_2	0.66	0.15	0.66	0.21
	ΔF_3	0.66	0.66	0.15	0.21
	ΔP_{12}	0.51	0.51	1.81	1.22
	ΔP_{23}	2.03	0.66	0.66	1.34
	ΔP_{13}	0.51	1.81	0.66	1.22
PIv $\times$ 0.0001	**ISE**	0.18	0.18	0.2	0.5

Similar behavior can be seen in case of tie-line power deviation of area 2 and area 3 and tie-line power deviation of area 1 and area 3 in Fig. 7.8(e-f). It is apparent from Table 7.5 that PIv of power system at 1% slp in all area (PIv=0.5×10^{-5}) is inferior to1% slp in any of the control area. It is observed from Fig. 7.8 (a) that value of FPu is more and FPt is less in case of frequency deviation of area 1 when 1 % slp in area 1 as

compared to other areas. Corresponding trends of frequency deviation of area 2 and frequency deviation of area 3 can be seen in Fig. 7.8 (b-c).
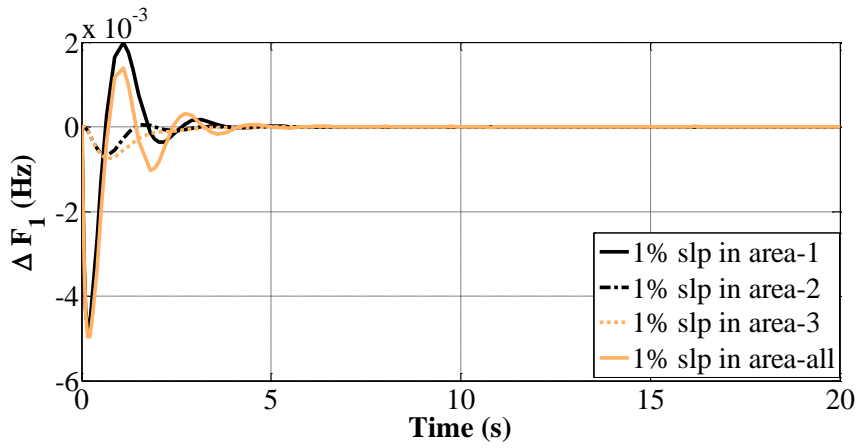
(a)
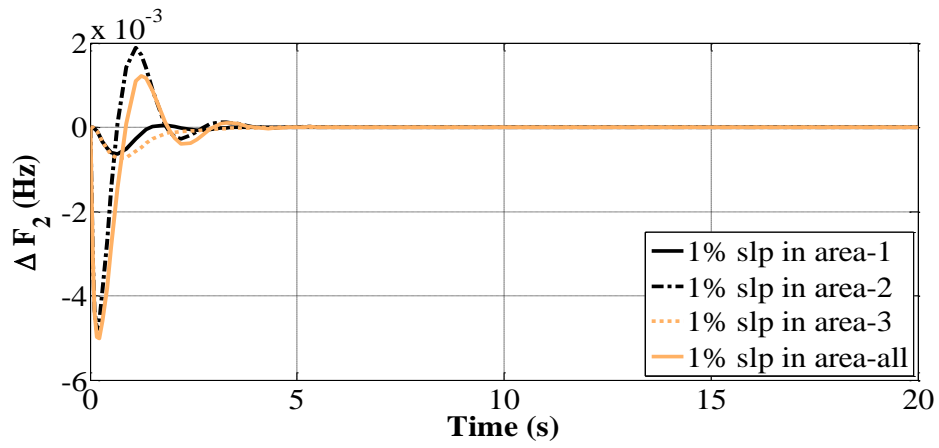
(b)
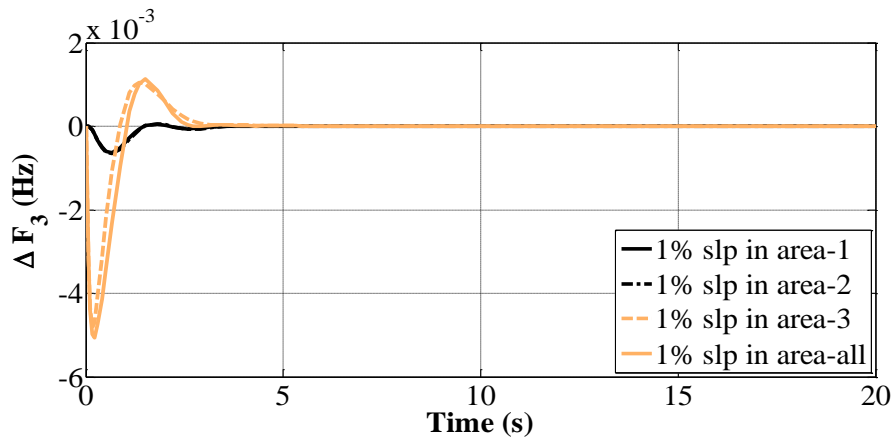
(c)
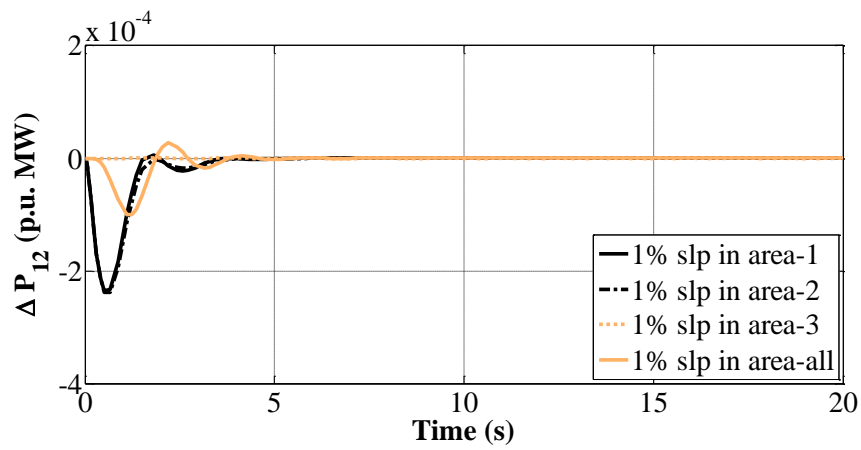
(d)
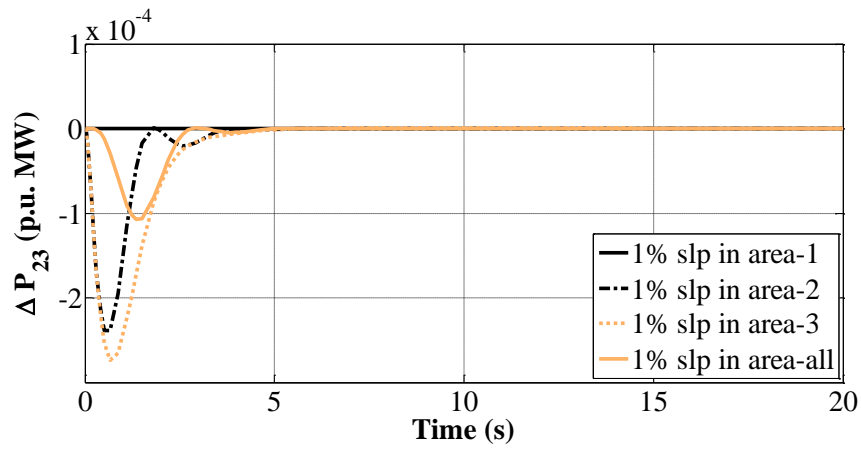
(e)
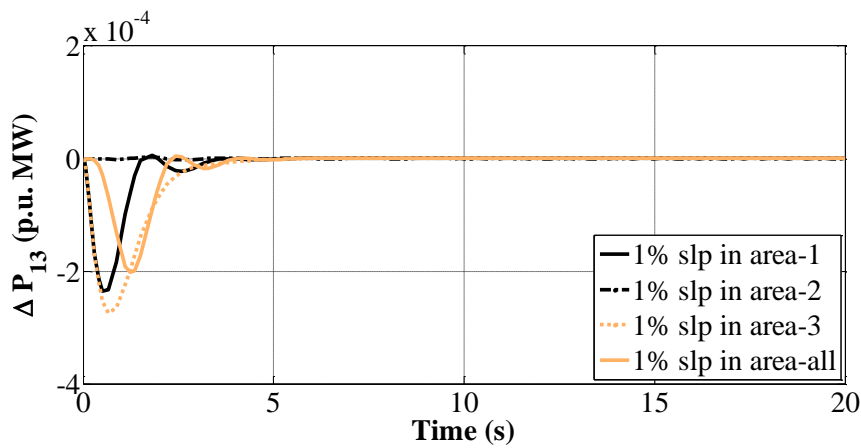
(f)

Fig.7. 8: Dynamic responses of non-reheat thermal power system with SMES at 1% slp in different control areas (a) Frequency deviation of area-1 (b) Frequency deviation of area-2 (c) Frequency deviation of area-3 (d) Tie line power deviation between area-1 and area-2 (e) Tie line power deviation between area-2 and area-3 (f) Tie line power deviation between area-1 and area-3, Vs Time.

143

7.5.3 Non-reheat thermal -hydro-non-reheat thermal power system at 1% step load perturbation

Three area non-reheat thermal, hydro and non-reheat thermal interconnected power system including SMES is simulated at 1% slp in different areas. Three parameters of IC for power system with SMES are designed to minimize objective function is given in Table 7.7.

TABLE 7. 6   **Compartive study of AGC strategy of multi area non-reheat thermal hydro non-reheat thermal power system incorporating SMES at 1% step load perturbation at different control areas**

1% slp at		Area1	Area2	Area3	Area all
ST (s)	ΔF_1	3.41	47.08	5.76	32.93
	ΔF_2	3.33	42.83	5.13	32.16
	ΔF_3	3.38	47.09	4.34	32.87
	ΔP_{12}	3.22	47.07	41.41	42.78
	ΔP_{23}	39.06	47.07	4.73	42.9
	ΔP_{13}	3.31	17.35	5.23	3.95
FPu ×10⁻³ (Hz) (-)	ΔF_1	4.8	1.7	0.84	5
	ΔF_2	0.68	5	0.91	5.6
	ΔF_3	0.64	1.7	4.8	5.1
	ΔP_{12}	0.23	0.7	0.018	0.72
	ΔP_{23}	0.008	0.69	0.31	0.67
	ΔP_{13}	0.23	0.002	0.31	0.17
FPt (s)	ΔF_1	0.15	2.24	0.86	0.21
	ΔF_2	0.65	0.21	1.04	0.5
	ΔF_3	0.65	2.11	0.15	0.21
	ΔP_{12}	0.5	2.11	2.11	1.86
	ΔP_{23}	1.68	2.24	0.86	2.36
	ΔP_{13}	0.5	2.11	0.86	1.23
PIv × 0.0001	ISE	0.18	3.31	0.28	3.81

(a)

(b)

(c)

145
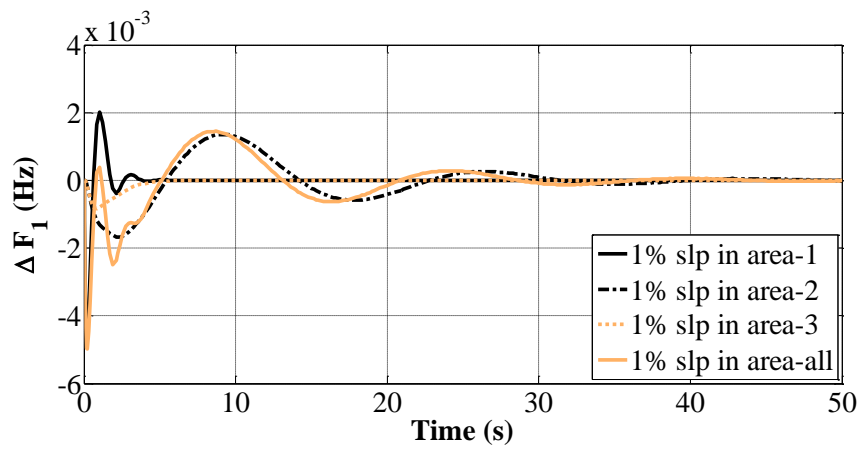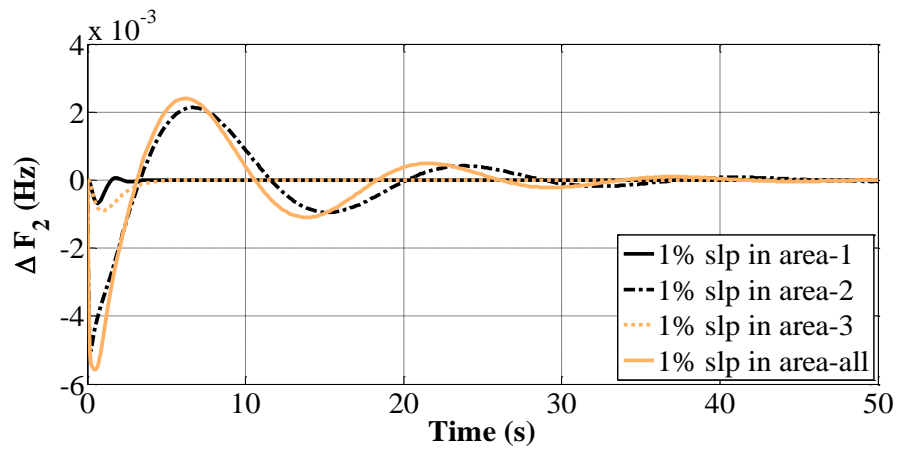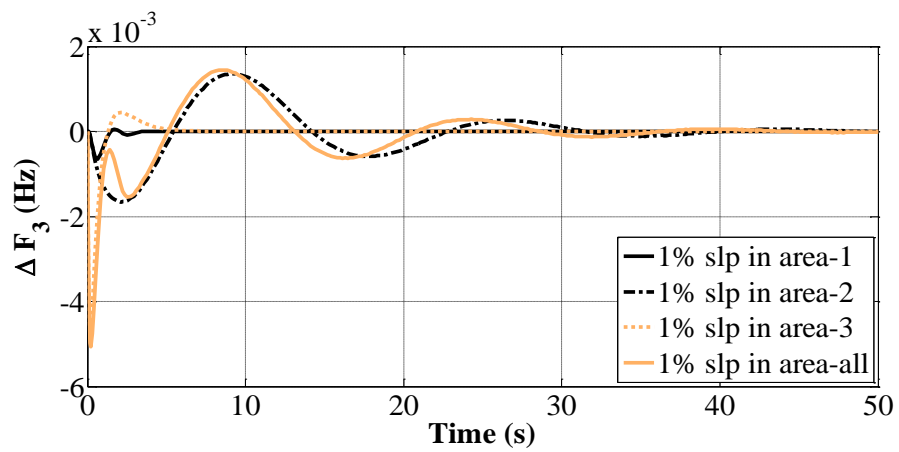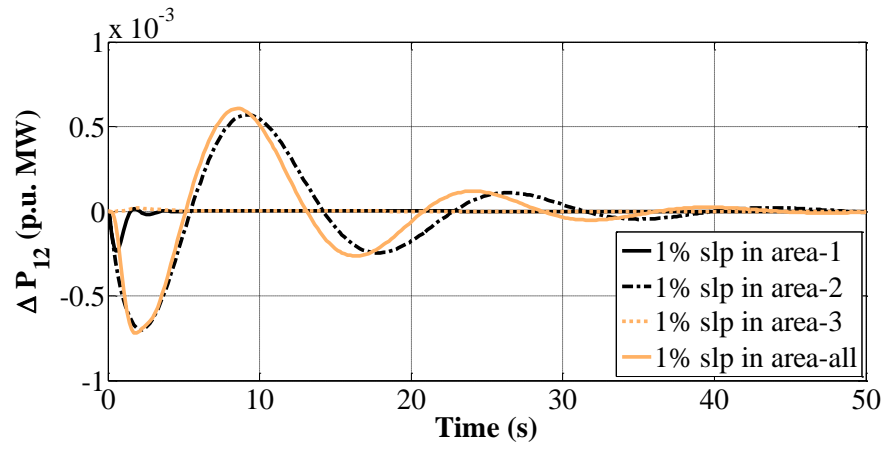
(d)
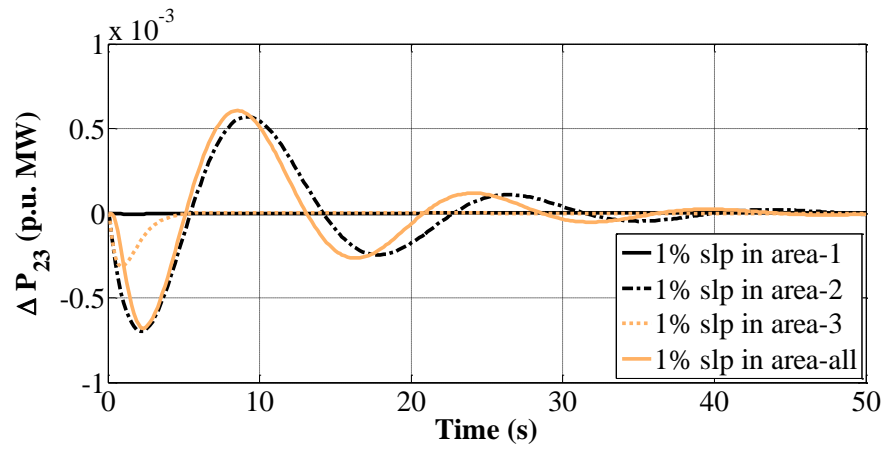
(e)
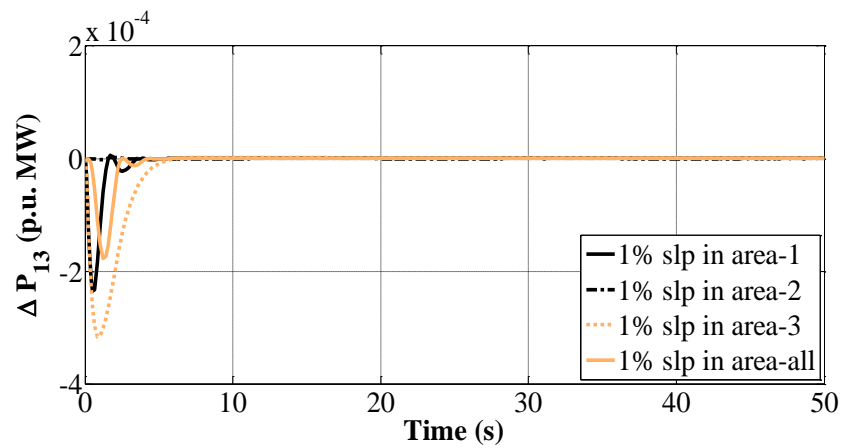
(f)

Fig.7. 9: Dynamic responses of non-reheat thermal, hydro and non-reheat thermal power system with SMES at 1% slp in different control areas (a) Frequency deviation of area-1 (b) Frequency deviation of area-2 (c) Frequency deviation of area-3 (d) Tie line power deviation between area-1 and area-2 (e) Tie line power deviation between area-2 and area-3 (f) Tie line power deviation between area-1 and area-3, Vs Time.

Dynamic responses in terms of frequency and tie-line deviation for PSO tuned IC power system with SMES at 1% slp in different control areas are shown in Fig. 7.9(a-f). Critical examination of Table 7.6 reveals that performance measures with respect to ST, FPu and FPt and PIv is remarkably better when 1% slp in area 1 or area 3 (thermal) as compared to disturbance in area 2 (hydro) and area all. This is due to the participation of hydro sources in multi-source power system which has the characteristics of non-minimum phase.

The sluggishness effect of hydro is considerably suppressed when 1% slp is applied in all area. Critical examination of Fig.7.9 (d) reveals that tie-line power deviation of area 1 and area 2 exhibits less oscillation, less FPu and more FPt and ST when 1% slp is considered in area 3. Similar conduct can be seen in case of tie-line power deviation of area 2 and area 3 and tie-line power deviation of area 1 and area 3 in Fig. 7.9(e-f). It is evident from Table 7.6 that PIv of power system at 1% slp in all area (PIv=3.81×10^{-5}) is inferior to1% slp in any of the control area. It is observed from Fig. 7.9 (a) that value of FPu is comparatively more and FPt and ST are comparatively less in case of frequency deviation of area 1 when 1 % slp in area 1 as compared to other areas. Corresponding trends of frequency deviation of area 2 and frequency deviation of area 3 with respect to area2 and area3 can be seen in Fig. 7.9 (b-c). In interconnected power system, it has been notice that effect of 1% slp in all area gives better system response in terms of ST and FPu as compared to 1% slp in area 2 (hydro).

7.5.4 Comparison of AGC of three area interconnected multi source power system with SMES

Comparison of dynamic responses in terms of frequency deviation for three cases of interconnected multi area multi source power system including SMES at 1% slp in all control areas is shown in Fig. 7.10. Three parameters of IC for each power system with SMES are designed to minimize objective function are given in Table 7.7. It has been detected that FPu and ST of dynamic responses for case 2 is quite less as compared to other two cases. the sluggishness of responses is due to the effect of hydro sources.

TABLE 7. 7   Parameter values for power system at 1% slp

IC		K_{IC1}	K_{IC2}	K_{IC3}
Case-1	Area-1	15.5	0.75	1
	Area-2	12	15.5	8.8
	Area-3	12	1.6	8.3
	Area all	17	15.5	8.8
Case-2	Area-1	15.5	5.5	5
	Area-2	20	14.5	8.8
	Area-3	18.15	15.12	8.8
	Area all	20	13.5	8.8
Case-3	Area-1	15.51	0.12	8.8
	Area-2	20	15.5	8.8
	Area-3	20	0.16	5
	Area all	18.15	18	8.8
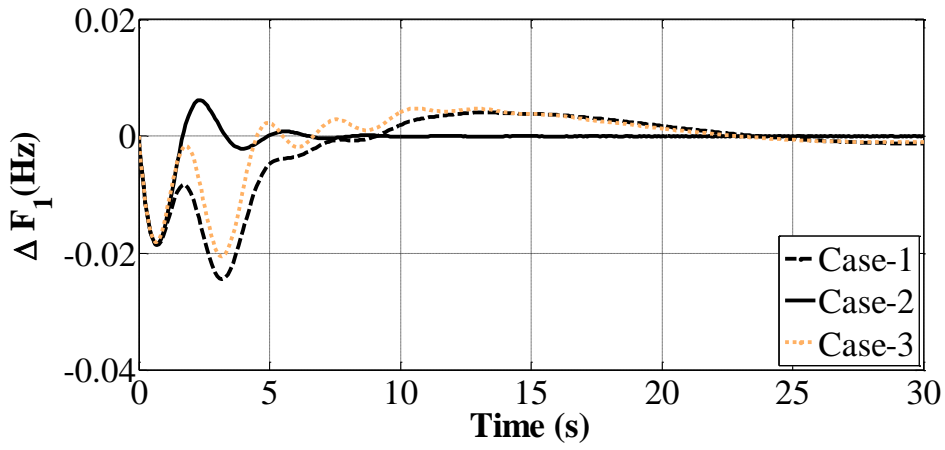
(a)
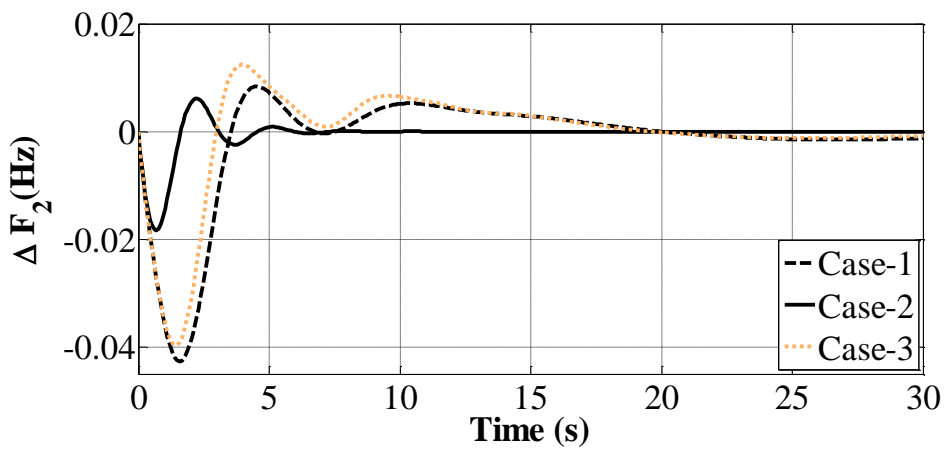
(b)
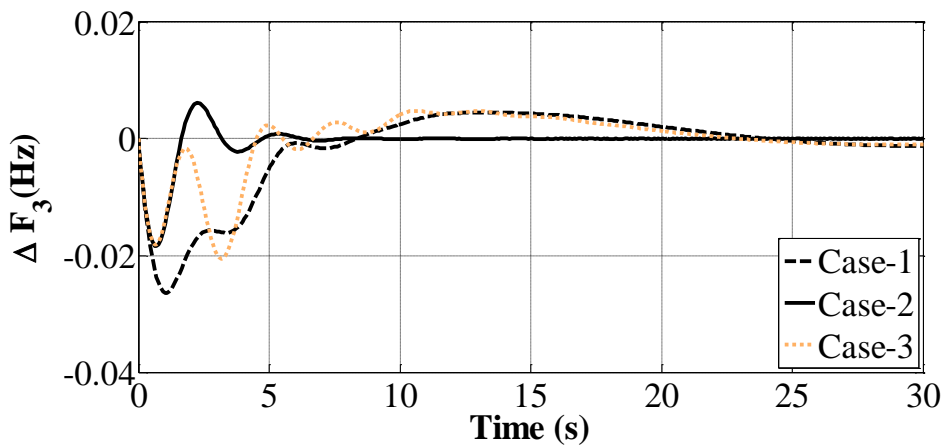
(c)

Fig.7. 10: Comparison of dynamic responses of power systems with SMES under investigation at 1% slp in each control area (a) Frequency deviation of area-1 (b) Frequency deviation of area-2 (c) Frequency deviation of area-3, Vs Time.

149

7.6   Conclusion

In this Chapter, PSO tuned IC is proposed for AGC of interconnected multi area multi source power system with SMES. To portray potential benefits of proposed approach to non-reheat thermal, hydro and gas interconnected multi area power system, comparative performance of different bio-inspired artificial technique has been done. Percentage improvement of frequency and tie-line deviation responses in terms of ST and PIv assists the criterion for judgment of betterment of proposed approach of PSO tuned IC power system with SMES than PSO tuned IC without SMES and GA tuned IC power system with SMES. This clearly reveals that application of SMES in power system certainly helps the power system to achieve AGC objectives. The proposed approach is extended to three area non-reheat thermal interconnected power system with SMES and three area non-reheat thermal, hydro and non-reheat thermal interconnected power system with SMES. Moreover, effect of 1% slp in different control areas is studied in three cases of power systems. Significant improvement in the dynamic responses of power system has been observed in case of thermal and gas power sources. Degradation of system due to the presence of hydro sources in interconnected multi source power system is noticeably reduced by considering 1% slp in all area as compared to 1% slp in individually areas.

CHAPTER 8

AGC OF THREE AREA INTERCONNECTED MULTI SOURCE POWER SYSTEMS WITH BATTERY ENERGY STORAGE SYSTEM

8.1   Introduction

The uncertainty of available resources and desire to achieve minimal frequency and tie line power deviation developed the need of energy storage system in power system. Features of good energy storage system are to provide and absorb power at the time of load disturbances and have ability to charge and discharge in short span. The power system comprises of large number of generators interconnected by network of transmission lines which provide power to the consumers at rated voltage and frequency. Generally, the interconnected power system contains thermal and hydro power generation as a research. Deviation in frequency occurs due to real power dispatch among generator and load, while the cause of voltage variations is reactive power imbalance in the power system. According to the definition of AGC, active power balance is achieved by controlling power generation. The characteristics of governors, and its effect on tie line power and frequency are considered for electric power system. Further, AGC of two area hydro thermal interconnected power system incorporating various controllers were elucidated. If a real power mismatch, frequency and tie line power exchanges between interconnected power systems are significant

variables. A single variable called Area control Error (ACE) weighs these variables together. Additionally, the impact of including load generation participation factors for AGC of two area multi source power system was analyzed. Some important aspects of multi source as thermal, hydro and gas interconnected power system were considered for single or maximum two areas. Due to shortage of resources, it is difficult to combine multi source in one area. So, in a realistic power system there is a need to consider different sources as an individual area which is further interconnected to make a power system. BESS creates interest in utilities and transmission system operators. Incremental block diagram of a BESS was operated to the two area thermal power system . Previous study shows that few studies has been devoted to the AGC of interconnected three area thermal- gas-hydro power system with BESS.

In this chapter effect of BESS on AGC of multi source interconnected power generation is analyzed. Hence, it is seen that BESS in multi source generation system improves performance of the system and reduces overshoots of dynamic frequency deviation under load disturbances.

8.2   Modelling of battery energy storage system

BESS is composed of three phase supply, converter, battery and control scheme as shown in Fig. 8.1. Role of 12-pulse bridge converter is to convert ac to dc during charging mode and dc to ac during discharging mode. The ideal no-load maximum dc voltage (E_{d0}) of the converter is considered as Eqn. (8.1).

$$E_{d0} = \frac{6\sqrt{6}}{\pi} E_{tn} \tag{8.1}$$
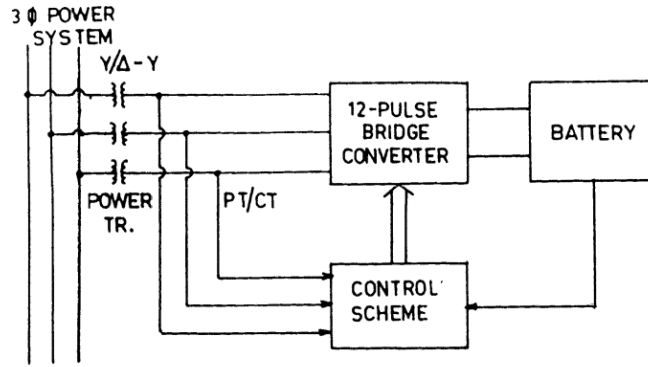
Fig.8. 1: A schematic description of a BESS plant

Where, E_{tn} is the line to neutral r.m.s voltage. The terminal voltage of battery (E_{bt}) is attained from,

$$E_{bt} = E_{d0} \cos \propto^0 - R_c I_{BESS} \tag{8.2}$$

$$E_{bt} = \frac{3\sqrt{6}}{\pi} E_{tn}(\cos \propto^{1^0} + \cos \propto^{2^0}) - \frac{6}{\pi} X_{c0} I_{BESS} \tag{8.3}$$

Where, $\propto^{k^0}$ is firing angle of k converter, I_{BESS} is the dc current flowing into battery, X_{c0} is commutating resistance.

The equivalent circuit of BESS consisting of converter and battery is shown in Fig.8.2. The expression for d.c. current flowing into the battery can be specified as follows:-

$$I_{BESS} = \frac{E_{bt} - E_{b0c} - E_{bl}}{r_{bt} + r_{bs}} \tag{8.4}$$

$$E_{b0c} = \frac{r_{bp}}{1 + sr_{bp}c_{bp}} \quad I_{BESS} \tag{8.5}$$

$$E_{bl} = \frac{r_{bl}}{1+sr_{bl}c_{bl}} \qquad I_{BESS} \tag{8.6}$$

Suppose $T_{bp} = r_{bp}\,c_{bp}$ and $T_{bl} = r_{bl}\,c_{bl}$ and used in incremental BESS model.

Where, E_{bl} and E_{b0c} is overvoltage and open-circuit value of battery, r_{bt} , r_{bs} , r_{bp} and r_{bl} are connecting, standard internal, self-discharge and overvoltage resistance and c_{bc} , c_{bp} and c_{bl} are overvoltage, battery and overvoltage capacitance.

Power engaged by BESS with respect to converter circuit analysis is written as,

$$P_{BESS} = \frac{3}{\pi}\sqrt{6}\,E_{tn}I_{BESS}(\cos \propto^{1^0} + \cos \propto^{2^0}) \tag{8.7}$$

$$Q_{BESS} = \frac{3}{\pi}\sqrt{6}\,E_{tn}I_{BESS}(\sin \propto^{1^0} + \sin \propto^{2^0}) \tag{8.8}$$

In present study of AGC only active power modulation control strategy is represented as:-

$$\propto^{1^0} = -\propto^{2^0} = \propto^0 \tag{8.9}$$

Then,

$$P_{BESS} = \frac{6}{\pi}\sqrt{6}\,E_{tn}I_{BESS}\cos \propto^0 \tag{8.10}$$

By substituting no load dc voltage in equation no. , active power can be written as:-

$$P_{BESS} = E_{d0}I_{BESS}\cos \propto^0 \tag{8.11}$$

$$Q_{BESS} = 0 \tag{8.12}$$

Let us assume d.c. voltage without overlap as E_{c0} and expression can be given as:-

$$E_{c0} = E_{d0}\cos \propto^0 \tag{8.13}$$

154

So, active power in AGC is written as:-

$$P_{BESS} = E_{c0}I_{BESS} \qquad (8.14)$$

Linearizing the above equation, we get the incremental BESS power as,

$$\Delta P_{BESS} = E_{c0}{}^{\circ}\Delta I_{BESS} + I_{BESS}{}^{\circ}\Delta E_{c0} \qquad (8.15)$$

The incremental block diagram of BESS is represented as Fig. 8.3.
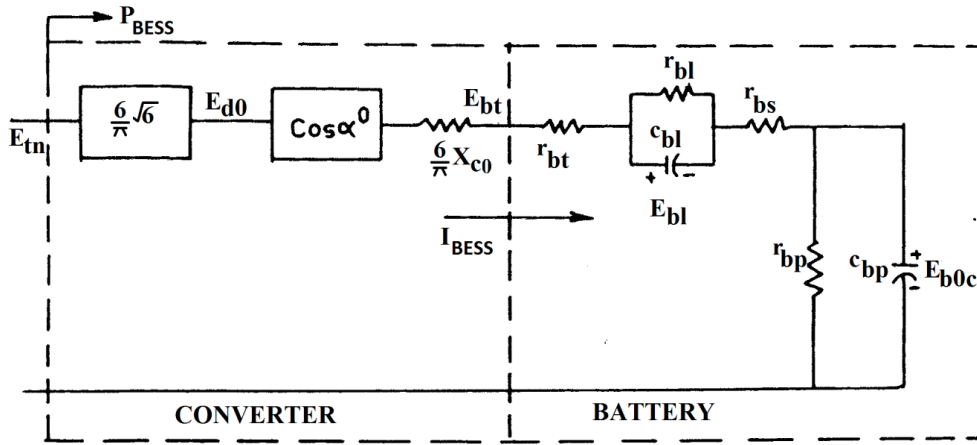
Fig.8. 2: Equivalent circuit diagram of BESS

By adjusting the firing angle for AGC with BESS, d.c. voltage without overlap works in constant power mode, which are further separated into voltage deviation and responded voltage after system disturbances as follows:-

$$\Delta E_{c0}=\Delta E_p + \Delta E_d \qquad (8.16)$$

Now,

$$\Delta P_{BESS} = E_{c0}{}^{\circ}\Delta I_{BESS} + I_{BESS}{}^{\circ}\Delta E_p + I_{BESS}{}^{\circ}\Delta E_d \qquad (8.17)$$

For smooth functioning of AGC with BESS we assume

$$E_{c0}{}^{\circ}\Delta I_{BESS} + I_{BESS}{}^{\circ}\Delta E_p = 0 \qquad (8.18)$$

155

So,

$$\Delta E_p = -E_{c0}{}^\circ(\Delta I_{BESS}/I_{BESS}{}^\circ) \tag{8.19}$$

By substituting the value of dc voltage without overlap in above equation, we get voltage deviation as follows:-

$$\Delta E_p = -E_{d0}\cos \propto {}^\circ(\Delta I_{BESS}/I_{BESS}{}^\circ) \tag{8.20}$$

Therefore, we get power deviation as:-

$$\Delta P_{BESS} = I_{BESS}{}^\circ\Delta E_d \tag{8.21}$$

Thus to provide a damping effect in AGC of interconnected power systems incorporating BESS with input signal to BESS is the deviation of ACE in each area. Thus, voltage deviation in each control area of interconnected power system with BESS can be given as:-

$$\Delta E_d = (K_{BESS}/(1 + s\ T_{BESS}))\ \Delta ACE \tag{8.22}$$
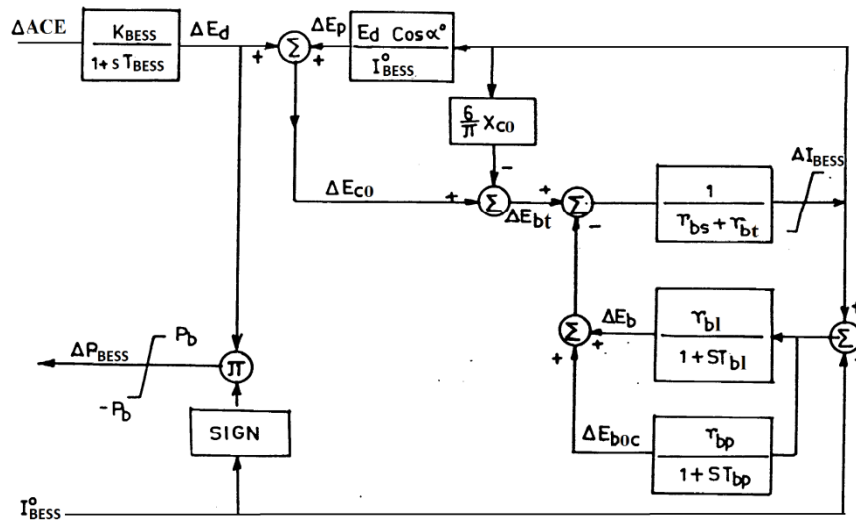
Fig.8. 3: The incremental block diagram of BESS

156

During peak load period, energy is provided by BESS during discharging mode. At discharging mode, BESS operates at $(\beta^{\circ}=\pi - \alpha^0)$ as an ignition angle for the converter.

8.3   Power system under investigation

BESS provides fast active power compensation and manage sudden demand of power requirement in load, thus effectively dampening the frequency oscillations due to large disturbances in load. In this chapter effect of BESS in AGC of interconnected multi area multi source power system is explored at load disturbances in different areas. Its dynamic responses in terms of deviation of frequency and tie-lie power are considered for comparative analysis of AGC strategy. In this chapter, effect of load disturbances in different areas has been studied for four different cases of power system incorporating BESS. These four cases have various sources in three area interconnected power system as defined in Table 8.1. Parameter values considered in interconnected power system are given in Appendix B.

TABLE 8. 1   Different cases of three area interconnected multi source power system with BESS

Cases	Types of Power system
1.	Reheat thermal, gas and hydro power system
2.	Non-reheat thermal, hydro and gas power system
3.	Non-reheat thermal interconnected power system
4.	Non-reheat thermal, hydro and non-reheat thermal power system
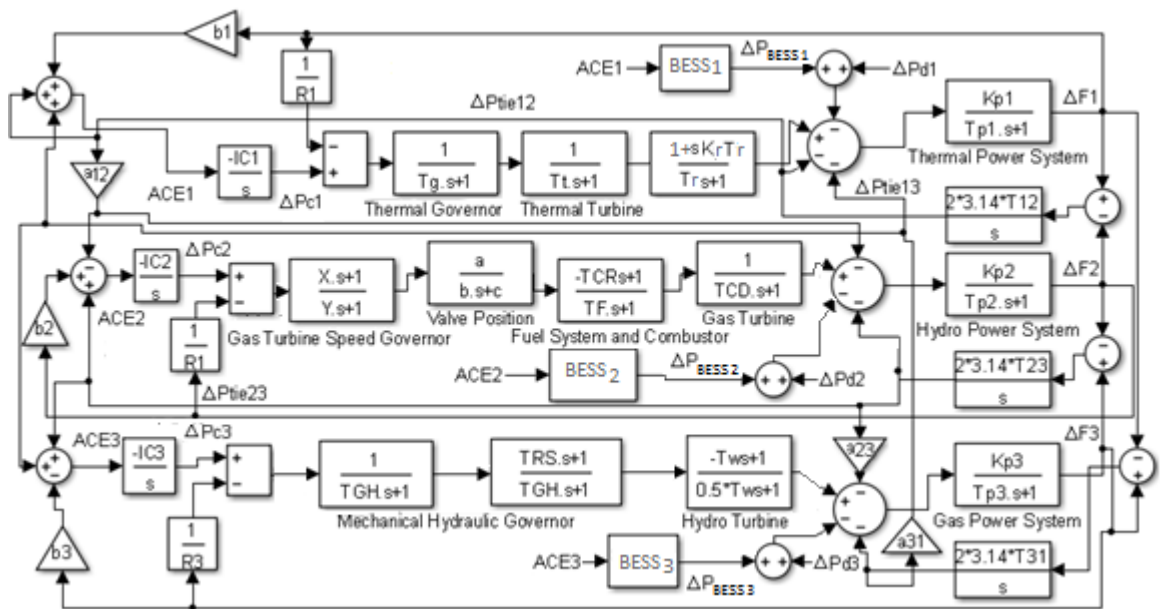
Fig.8. 4: Transfer fuction block diagram of three area reheat thermal-gas-hydro power system with BESS.
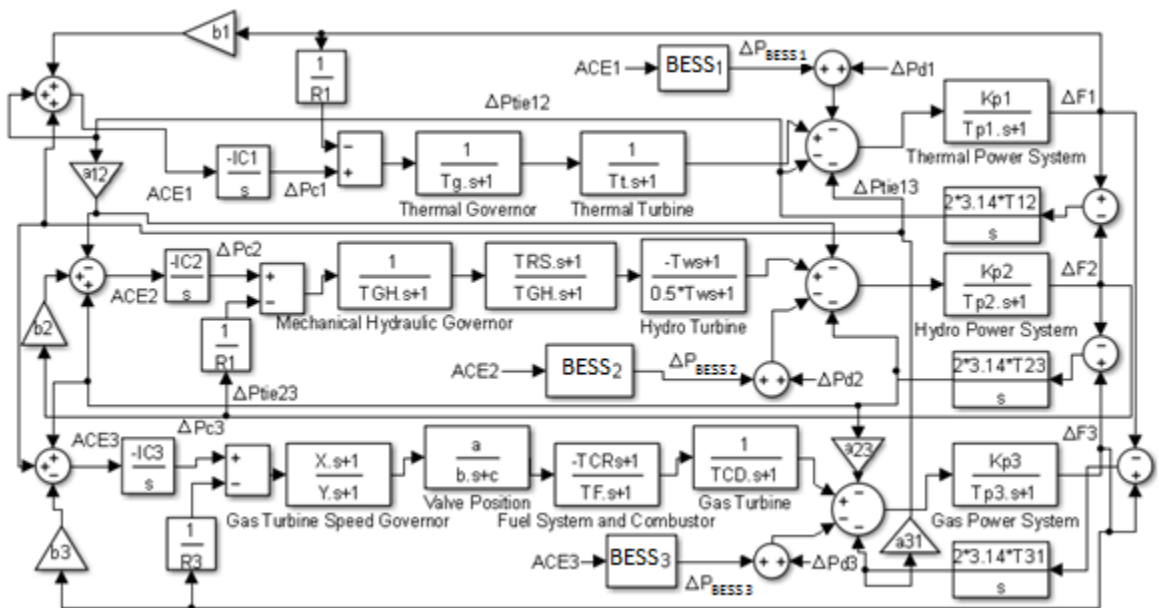
Fig.8. 5: Transfer fuction block diagram of three area non-reheat thermal-hydro-gas power system with BESS.
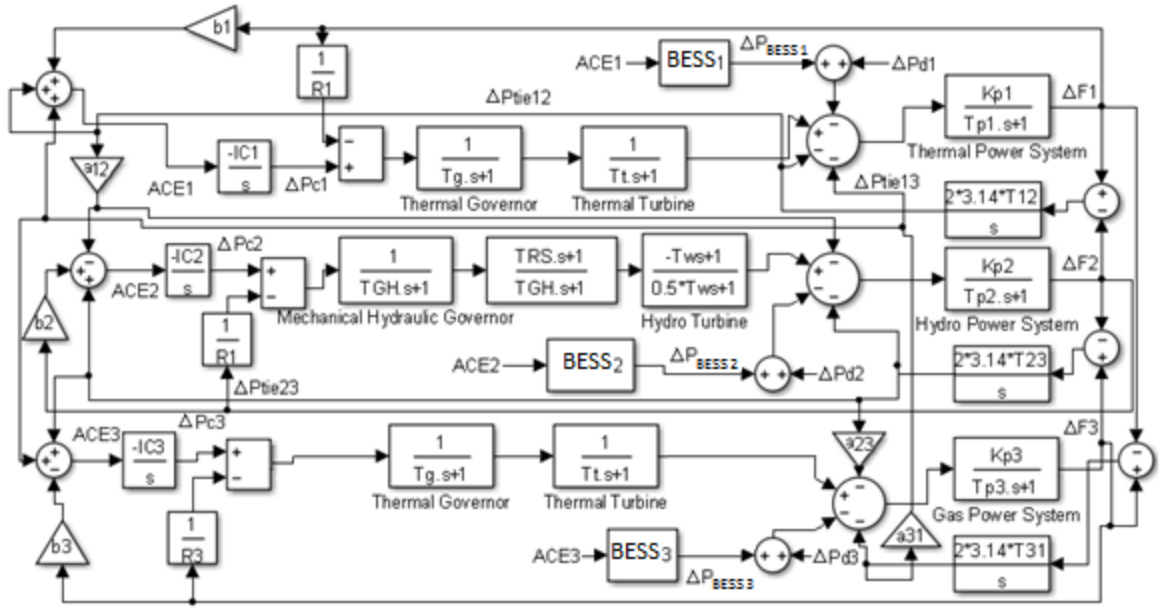
Fig.8. 6:   Transfer fuction block diagram of three area non-reheat thermal power system with BESS.

8.4   Optimization problem

Integral controller is applied in each area of interconnected multi source power system with or without BESS. ACE is considered as the control signal and is used to formulate objective function of power system. ISE reduces large error and therefore, it is considered as the performance index of power system. Performance index value of three area power system is expressed in equation no.8.23 .

$$PIV = \sum_{i=1}^{3} \int ACE_i^2 \, dt \tag{8.23}$$

The simulation time of 50s is considered for PIv of all the IC. Bio-inspired optimization technique PSO is applied to optimize IC of AGC of interconnected three area multi source power with or without BESS.
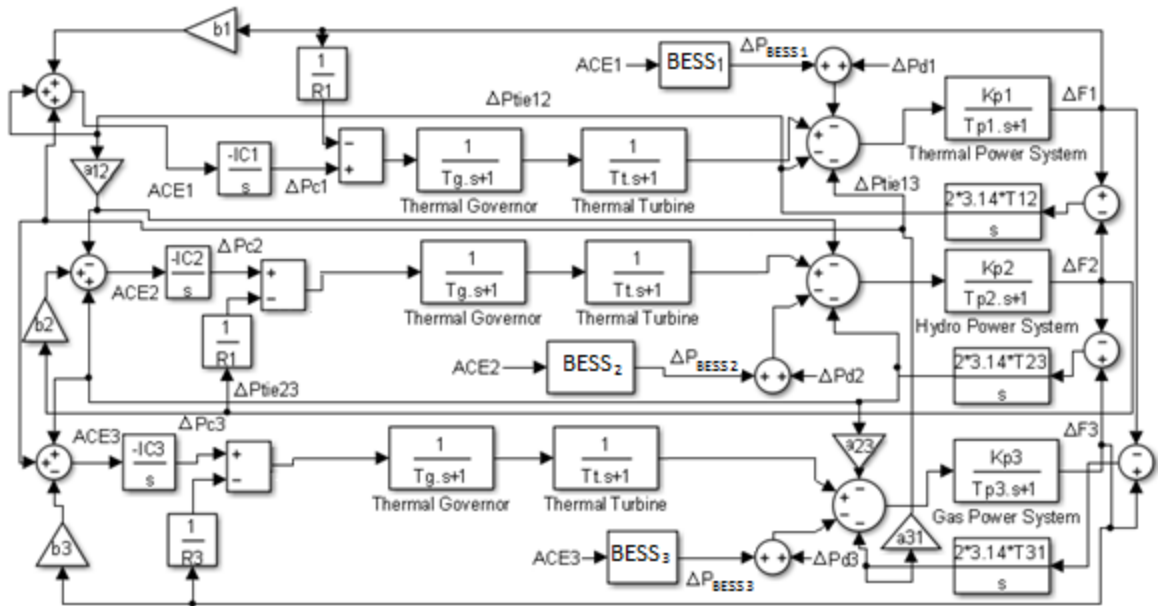
159

Fig.8. 7: Transfer fuction block diagram of three area non-reheat thermal-hydro-non-reheat thermal power system with BESS

8.5   Simulation results and discussions

8.5.1   Reheat thermal-hydro-gas power system at 1% step load perturbation

AGC of three area interconnected reheat thermal, gas and hydro power system is simulated by including and excluding BESS at 1% slp in each area. PSO tuned IC for power system with or without BESS are aimed to minimize objective function. Comparison of frequency deviation of each area in power system including or excluding BESS at 1% slp in each area is shown in Fig. 8.4(a-c). It is clear from Fig. 8.4 (a-c) that dynamic responses of PSO tuned IC of AGC of interconnected thermal, gas and hydro power system with BESS is significantly superior than PSO tuned IC power system without BESS.
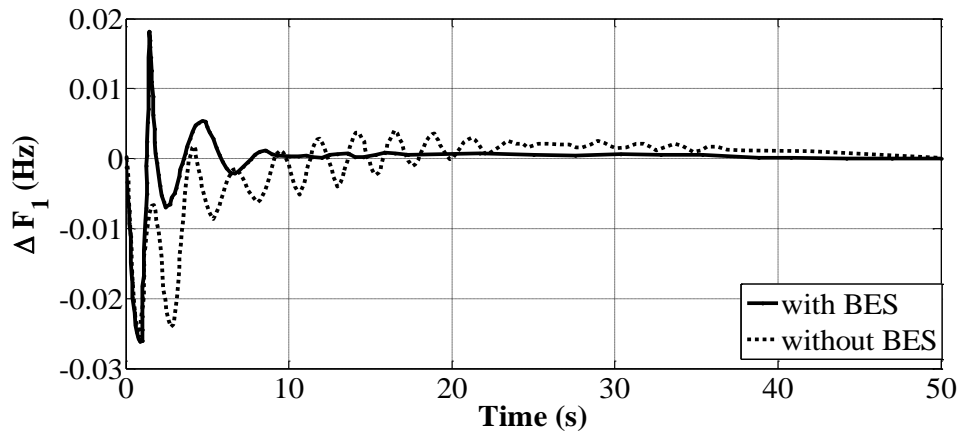
(a)
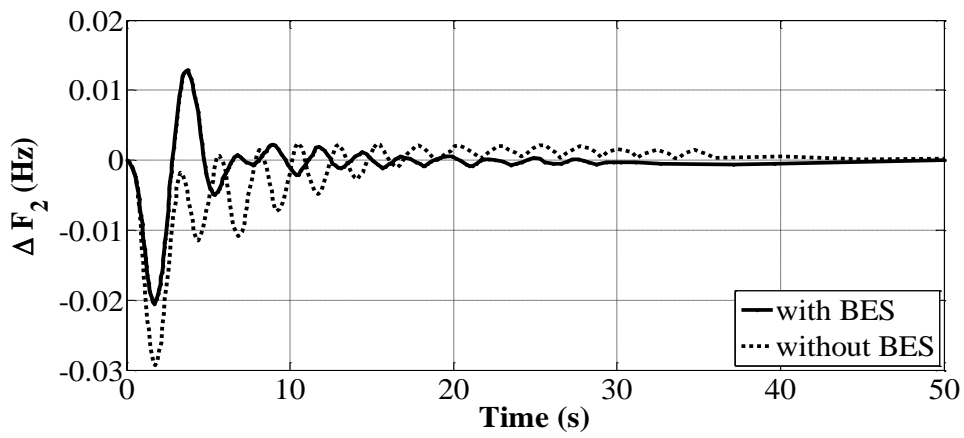
(b)
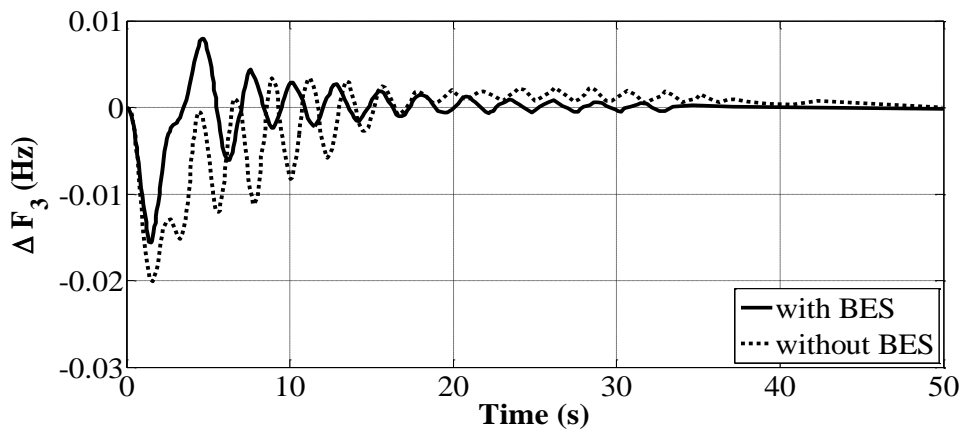
(c)

Fig.8. 8:   Dynamic response of reheat thermal, hydro and gas power system with BESS at 1% slp in each area (a) Frequency deviation of area-1 (b) Frequency deviation of area-2 (c) Frequency deviation of area-3, Vs Time.

Performance of dynamic responses are numerically evaluated in terms of five modes as settling time (ST), first peak undershoot (FPu), first peak time (FPt), performance index value (PIv) and percentage improvement of ST as indicated in Table 8.2. Critical examination of Table 8.2 unveils that PIv which specifies the cost of objective function of power system with BESS (PIv = 0.000457) is comparatively better than power system without BESS (PIv = 0.001157). The proposed controller - PSO tuned IC for power system with BESS is able to minimize the ST. This is supported by the value of percentage improvement in ST as 67% in area-1, 31.02% in area-2 and 27.31% in area-3.

TABLE 8. 2 **Comparative analysis of AGC of interconnected thermal-hydro-gas power system including and excluding BESS**

System Modes	Without BESS			With BESS+ACE		
	ΔF_1	ΔF_2	ΔF_3	ΔF_1	ΔF_2	ΔF_3
ST (s)	41.44	40.32	43.68	13.59	27.81	31.75
FPu (Hz) (-)	0.02	0.03	0.02	0.02	0.02	0.01
FPt (s)	0.62	1.848	1.67	0.59	1.76	1.58
PIv	0.001157			0.000457		
IC	7.9	-8	15.9	0.41	0.96	0.52
% Improvement in terms of ST				67	31.02	27.31

A similar drift can be seen with FPt of power system with BESS. It has been noticed that ST of dynamic responses in control area-3 (hydro-31.75s) is more than the control area-2 (gas-27.81s) and control area-1 (thermal-13.59s). This is due to the effect of non-minimum phase characteristics of hydro source in interconnected power system with BESS.

		Area1	Area2	Area3	Area all
ST (s)	ΔF_1	2.5	29.76	7.16	17.91
	ΔF_2	3.73	17.57	7.17	23.51
	ΔF_3	3.74	29.76	4.93	17.91
	ΔP_{12}	3.73	29.76	34.87	44.89
	ΔP_{23}	6.48	29.76	7.21	44.46
	ΔP_{13}	3.74	33.89	7.18	7.16
FPu × (-)10^{-5} (Hz)	ΔF_1	66	7.3	3.29	66
	ΔF_2	1.9	66	3.3	66
	ΔF_3	1.9	7.3	66	66
	ΔP_{12}	0.8	3.1	0.002	3.14
	ΔP_{23}	0.0006	3.09	1.39	3.5
	ΔP_{13}	0.82	0.0015	1.39	1.49
FPt (s)	ΔF_1	0.017	2.08	0.7	0.017
	ΔF_2	0.37	0.017	0.7	0.017
	ΔF_3	0.37	2.08	0.017	0.017
	ΔP_{12}	0.37	2.08	1.56	2.19
	ΔP_{23}	1.22	2.08	0.7	2.28
	ΔP_{13}	0.37	6.88	0.7	0.86
PIv × 10^{-6}	**ISE**	0.0042	0.052	0.008	0.068

8.5.2 Non-reheat thermal-hydro-gas power system at 1% step load perturbation

AGC of three area interconnected non-reheat thermal, hydro and gas power system is simulated by including BESS at 1% slp in different control areas. PSO tuned IC for power system with BESS is proposed to minimize objective function by using Eqn. 8.23. Comparison of frequency deviation and tie-line power deviation of power system including BESS at 1% slp in different area is shown in Fig 8.5 (a-f).

Performance measures of dynamic responses are numerically evaluated in terms of settling time (ST), first peak undershoot (FPu), first peak time (FPt) and performance index value (PIv) as indicated in Table 8.3 . Critical examination of Table 8.3 reveals that performance measures with respect to ST, FPu and FPt and PIv is remarkably better when 1% slp in area 1 (thermal) or area 3 (gas) as compared to disturbance in area 2 (hydro) and area all. This is due to the participation of hydro sources in multi-source power system which turns down the system response as confronted to thermal and gas sources. The unsteady effect of hydro is highly damped by the use of BESS in AGC concepts.

During perturbation in area-2 and area-all of non-reheat thermal-hydro-gas power system with BESS, the numerical values of frequency and tie-line deviation in terms of ST are better in case of slp in area-all as compared to slp in only hydro source i.e. area-2. It has been observed that PIv of power system at 1% slp in all area (PIv=6.8×10^{-8}) is higher than 1% slp in any of the control area. Critical inspection discloses that for frequency deviation of area-1 in power system under 1 % slp in area-1 gives FPu value greatest, ST value smallest and FPt value smallest in area-1 among the considered cases of slp in area-2 and area-3. A similar analysis has been discovered for frequency deviation of area-2 and area-3 when power system is under 1 % slp in area-2 and area-3 respectively. It has been analyzed that when power system is under 1 % slp in area-1, tie-line power deviation between area-2 and area-3 are drive to transients although there is no contribution from area-2 and area-3 and it gives FPu value less, ST value more and FPt value more in area-1 among other tie-line power deviation of the same case. Similar trend can be seen for other two cases of power system with BESS at 1 % slp in area-2 and area-3.

(a)

(b)

(c)
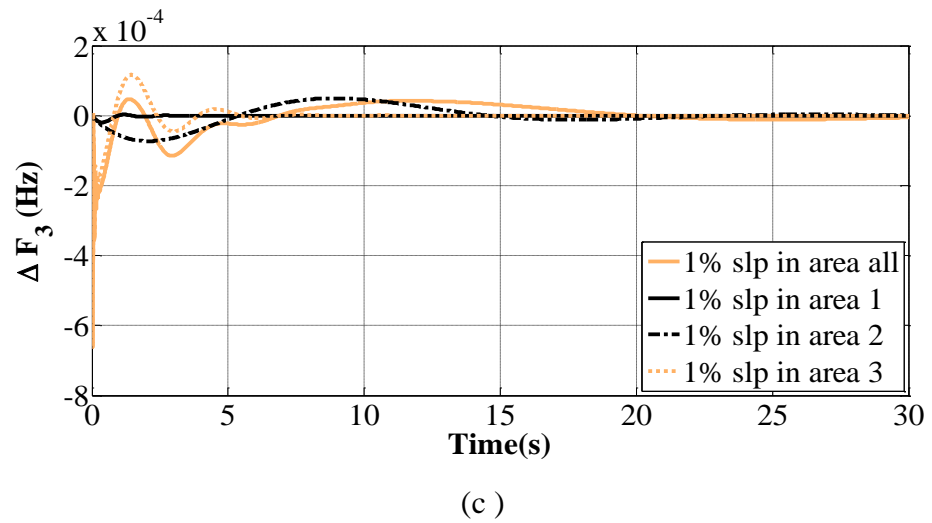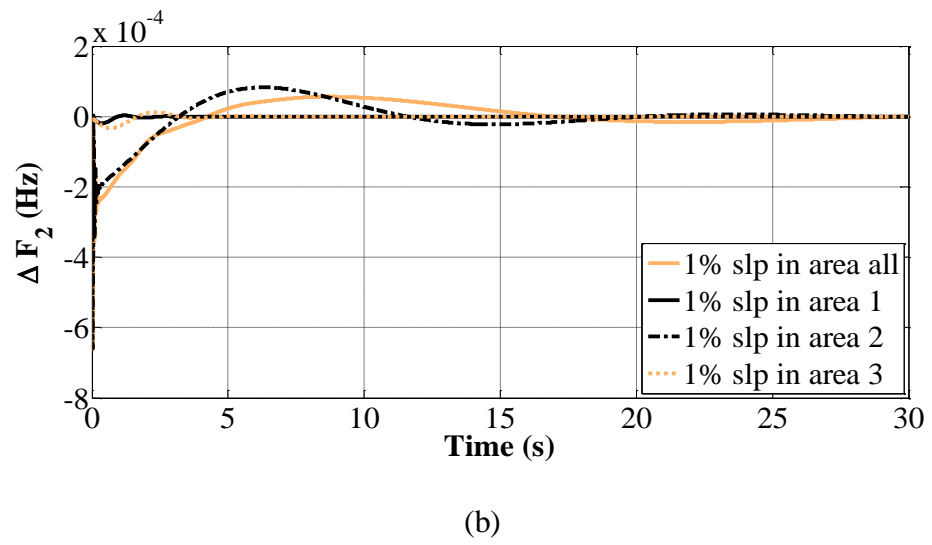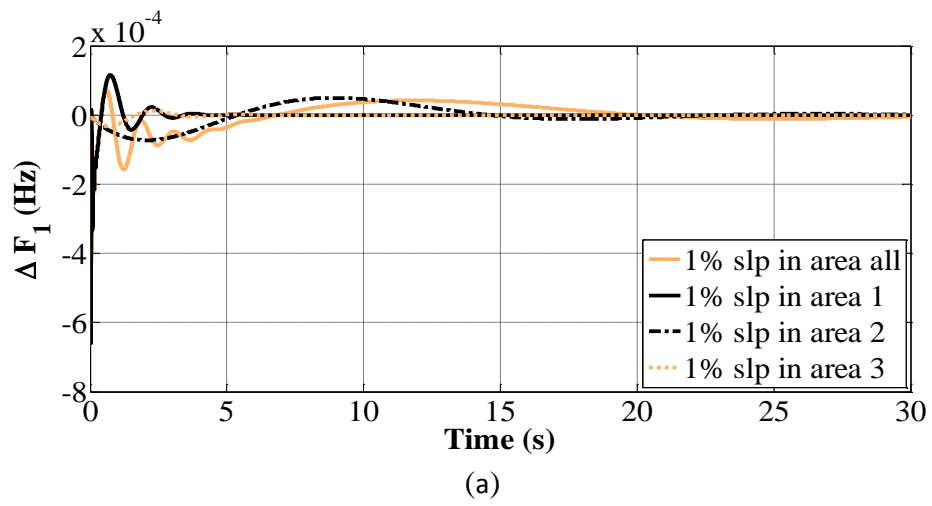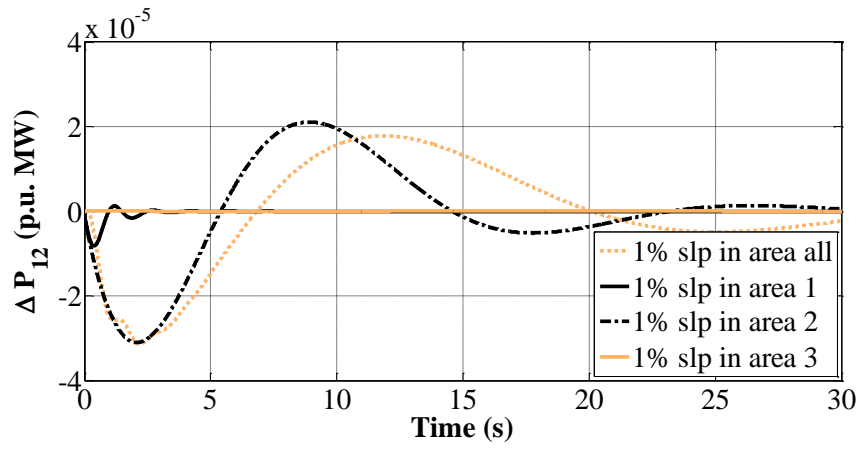
(d)
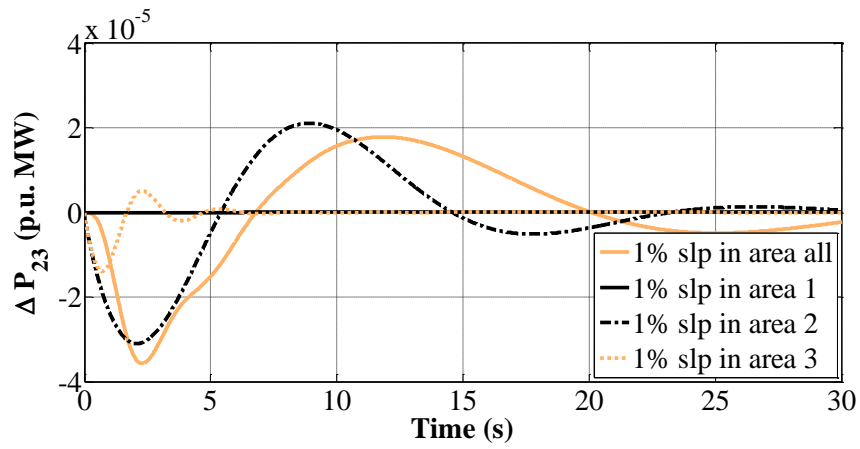
(e)
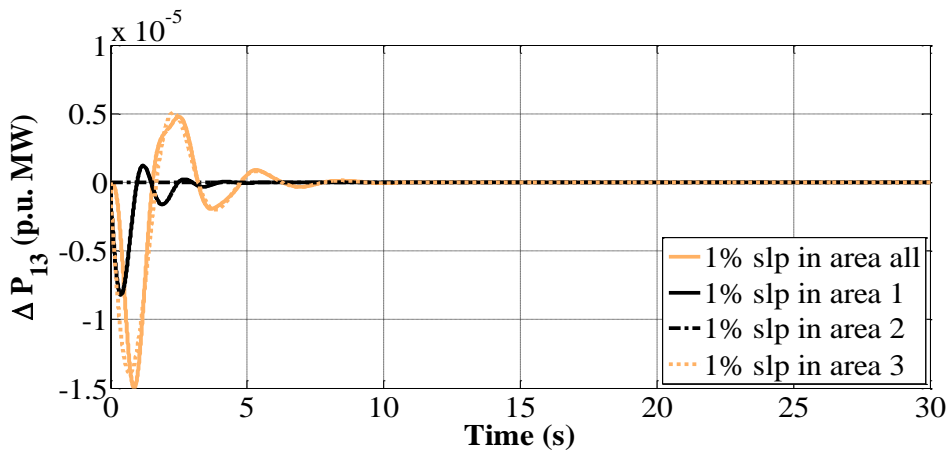
(f)

Fig.8. 9: Dynamic response of non-reheat thermal, hydro and gas interconnected power system with BESS at 1% slp in different areas (a) Frequency deviation of area-1 (b) Frequency deviation of area-2 (c) Frequency deviation of area-3 (d) Tie line power deviation between area-1 and area-2 (e) Tie line power deviation between area-2 and area-3 (f) Tie line power deviation between area-1 and area-3 , Vs Time.

166

TABLE 8. 4   **Comparative Study of AGC strategy of multi area non-reheat thermal power system incorporating BESS at 1% slp at different control areas**

		Area1	Area2	Area3	Area all
ST (s)	ΔF_1	1.72	4.24	3.6	1.66
	ΔF_2	3.6	3.22	3.61	3.2
	ΔF_3	3.6	4.24	1.72	2.5
	ΔP_{12}	3.6	4.23	8	3.69
	ΔP_{23}	12.7	4.23	3.61	4.15
	ΔP_{13}	3.6	6.72	3.61	3.52
FPu × (-)10⁻⁵ (Hz)	ΔF_1	66	1.69	2.5	66
	ΔF_2	2.5	66	2.5	66
	ΔF_3	2.5	1.69	66	66
	ΔP_{12}	1.06	0.7	0.00011	1
	ΔP_{23}	0.00004	0.7	1.06	0.54
	ΔP_{13}	1.06	0.00003	1.06	0.52
FPt (s)	ΔF_1	0.017	0.31	0.53	0.017
	ΔF_2	0.53	0.017	0.53	0.017
	ΔF_3	0.53	0.31	0.017	0.017
	ΔP_{12}	0.53	0.3	0.9	0.82
	ΔP_{23}	0.93	0.3	0.53	0.74
	ΔP_{13}	0.53	1.54	0.53	0.98
PIv × 10⁻⁶	**ISE**	0.0047	0.0045	0.0047	0.0134

8.5.3   Non-reheat thermal power system at 1% step load perturbation

AGC of three area interconnected non-reheat thermal interconnected power system is simulated by including BESS at 1% slp in different control areas. PSO tuned IC for power system with BESS is proposed to minimize objective function.

Comparison of frequency deviation and tie-line power deviation of power system including BESS at 1% slp in different areas is shown in Fig 8.6 (a-f). Performance measures of dynamic responses are numerically evaluated in terms of settling time (ST), first peak undershoot (FPu), first peak time (FPt) and performance index value (PIv) as indicated in Table 8.4. Critical examination of Table 8.4 reveals that value of ST is remarkably better for the case of 1% slp in area-all as juxtaposed with other three cases of 1% slp in individual area. It has been observed that PIv of power system at 1% slp in all area (PIv=1.3×10^{-8}) is higher than 1% slp in any of the control areas. Acute study discloses that for frequency deviation of area-1 in power system under 1 % slp in area-1 gives FPu value greatest, ST value smallest and FPt value smallest in area-1 among the considered cases of slp in area-2 and area-3. A similar trend has been learnt for frequency deviation of area-2 and area-3 when power system is under 1 % slp in area-2 and area-3 respectively. It has been explored that when power system is under 1 % slp in area-1, tie-line power deviation between area-2 and area-3 are drive to transients although there is no contribution from area-2 and area-3 and it gives FPu value less, ST value more and FPt value more in area-1 among other tie-line power deviation of the same case.

Similar trend can be seen for other two considered cases of power system with BESS at 1 % slp in area-2 and area-3.
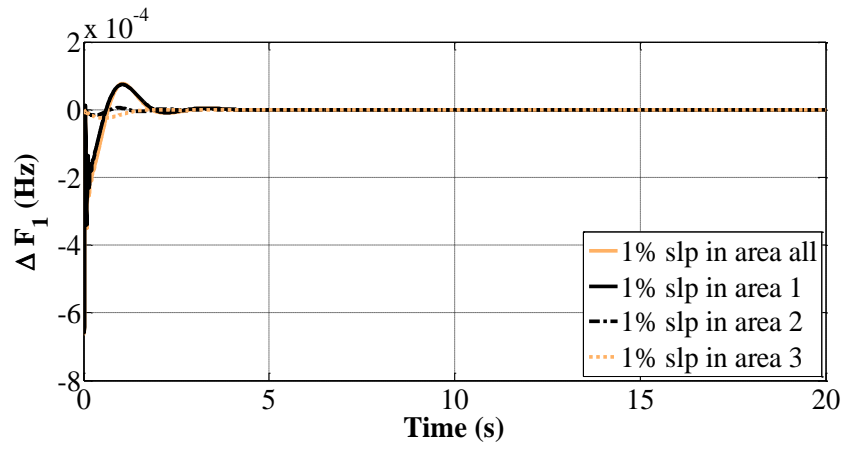
(a)
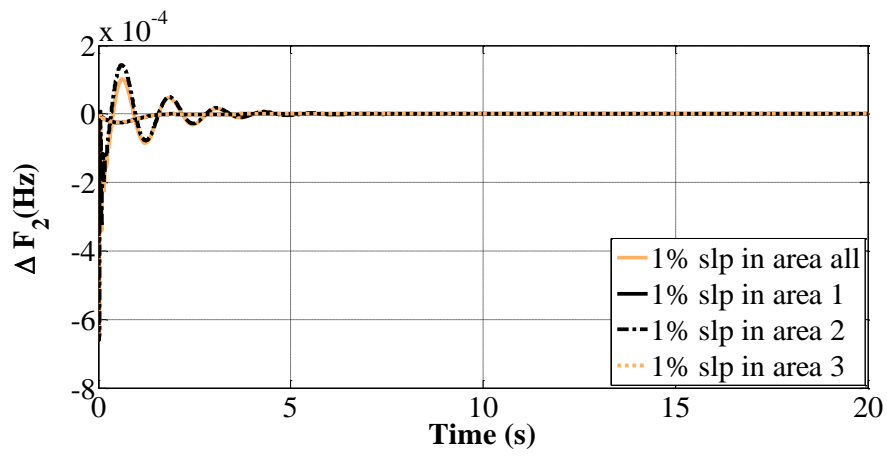
(b)
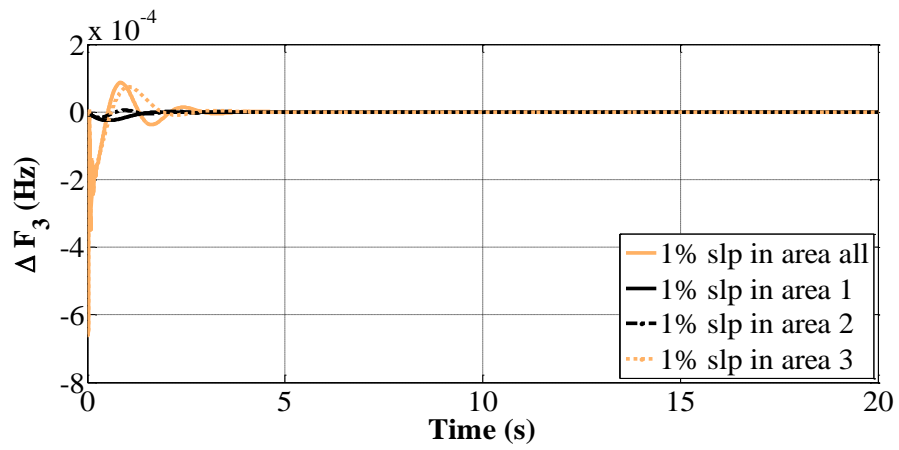
(c)
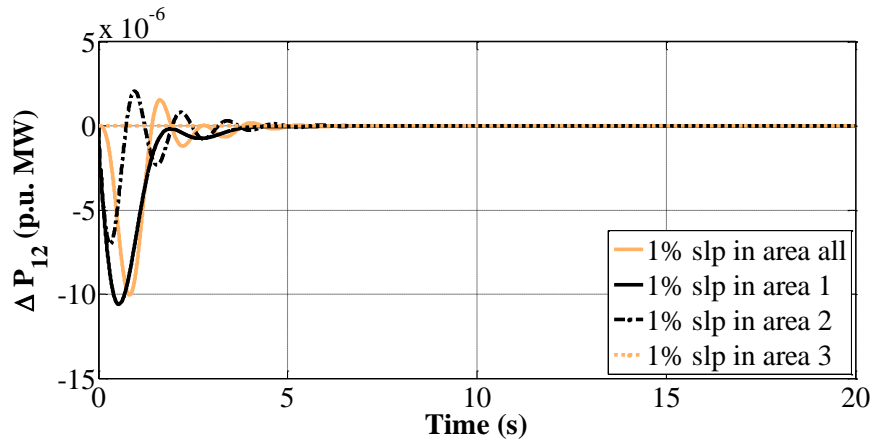
(d)
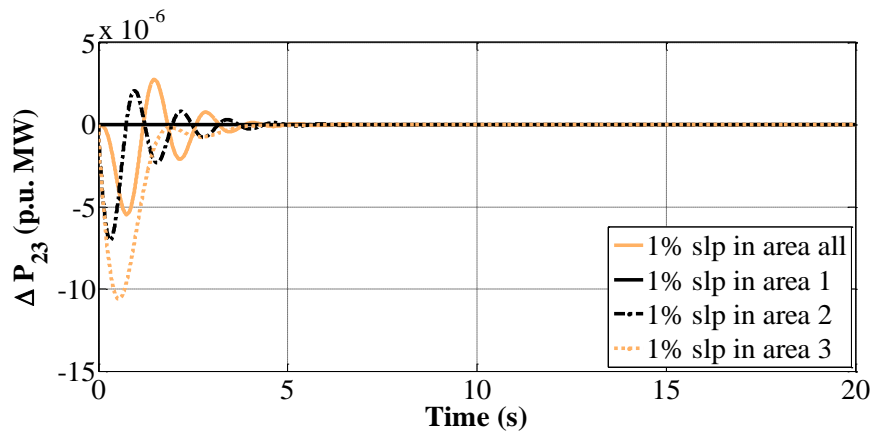
(e)
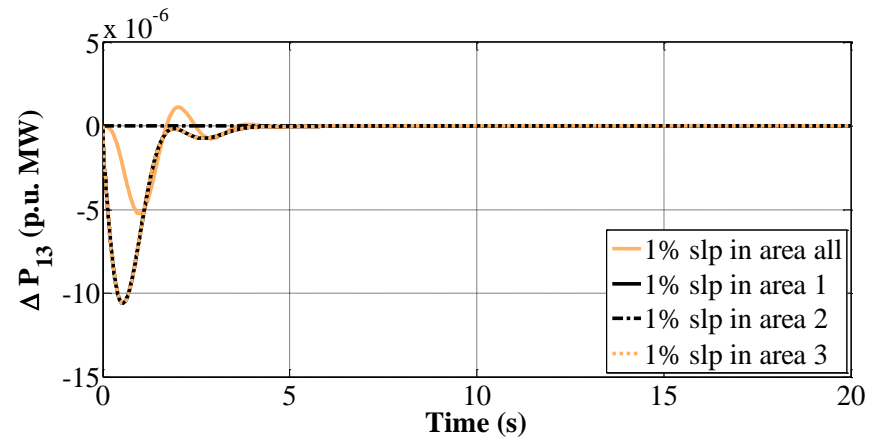
(f)

Fig.8. 10: Dynamic response of non-reheat thermal interconnected power system with BESS at 1% slp (a)Frequency deviation of area-1(b)Frequency deviation of area-2(c)Frequency deviation of area-3(d)Tie line power deviation between area-1 and area-2(e)Tie line power deviation between area-2 and area-3 (f) Tie line power deviation between area-1 and area-3 , Vs Time.

8.5.4 Non-reheat thermal -hydro- non-reheat thermal power system at 1% step load perturbation

AGC of three area interconnected non-reheat thermal, hydro and non-reheat thermal power system is simulated by including BESS at 1% slp in different control areas. PSO tuned IC for power system with BESS is proposed to minimize objective function. Comparison of frequency deviation and tie-line power deviation of power system including BESS at 1% slp in different area is shown in Fig 8.7 (a-f). Performance measures of dynamic responses are numerically evaluated in terms of settling time (ST), first peak undershoot (FPu), first peak time (FPt) and performance index value (PIv) as indicated in Table 8.5. Critical examination of Table 8.5 reveals that performance measures with respect to ST, FPu and FPt and PIv is remarkably better when 1% slp in area 1 or area 3 (thermal) as assessed with the case of disturbance in area 2 (hydro) and area all. Participation of hydro sources in multi-source power system hindered system response due to its self-induced instabilities. This unsteady effect of hydro is highly improved by the use of BESS in power system. During perturbation in area-2 and area-all of non-reheat thermal-hydro-non-reheat thermal power system with BESS, the numerical values of frequency and tie-line deviation in terms of ST are better in case of slp in area-all as compared to slp in only hydro source i.e. area-2. It has been observed that PIv of power system at 1% slp in all area (PIv=6.1×10^{-8}) is higher than 1% slp in any of the control area. Critical inspection discloses that for frequency deviation of area-1 in power system under 1 % slp in area-1 gives FPu value

171

greatest, ST value smallest and FPt value smallest among the considered cases of slp in area-2 and area-3.

TABLE 8. 5   **Comparative Study of AGC strategy of multi area non-reheat thermal-hydro- non-reheat thermal power system incorporating BESS at 1% slp at different control areas**

		Area1	Area2	Area3	Area all
ST (s)	ΔF_1	2.5	35.38	3.58	15.13
	ΔF_2	3.72	20.34	3.56	20.33
	ΔF_3	3.74	35.38	1.72	15.13
	ΔP_{12}	3.74	35.38	29.04	35.42
	ΔP_{23}	35.34	35.38	3.61	35.41
	ΔP_{13}	3.74	8.26	3.61	3.29
FPu × (-)10^{-5} (Hz)	ΔF_1	66	7.23	2.51	66
	ΔF_2	1.95	66	2.52	66
	ΔF_3	1.95	7.24	66	66
	ΔP_{12}	0.81	3.07	0.0027	3.03
	ΔP_{23}	0.001	3.07	1.06	3.05
	ΔP_{13}	0.81	0.0006	1.06	0.69
FPt (s)	ΔF_1	0.017	2.15	0.53	0.017
	ΔF_2	0.37	0.017	0.54	0.017
	ΔF_3	0.37	2.16	0.017	0.017
	ΔP_{12}	0.37	2.15	1.35	2.45
	ΔP_{23}	1.34	2.15	0.53	2.06
	ΔP_{13}	0.37	1.34	0.53	0.92
PIv × 10^{-6}	**ISE**	0.004	0.052	0.004	0.061

(a)

(b)

(c)

173
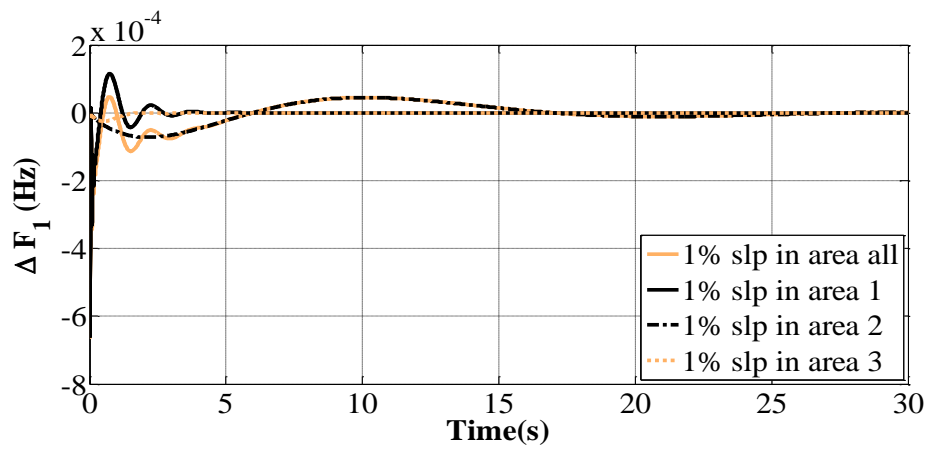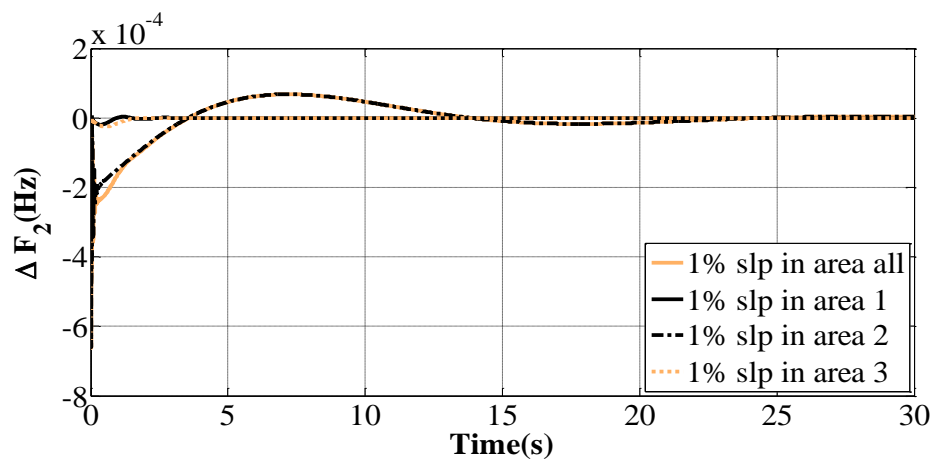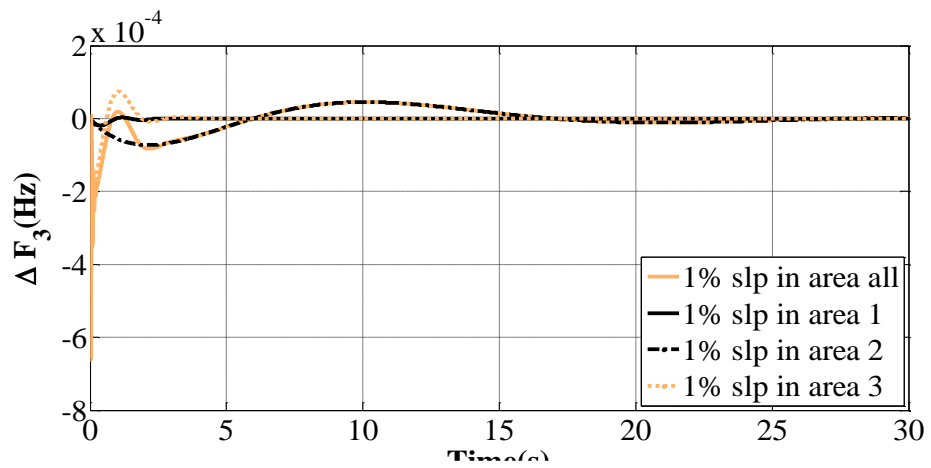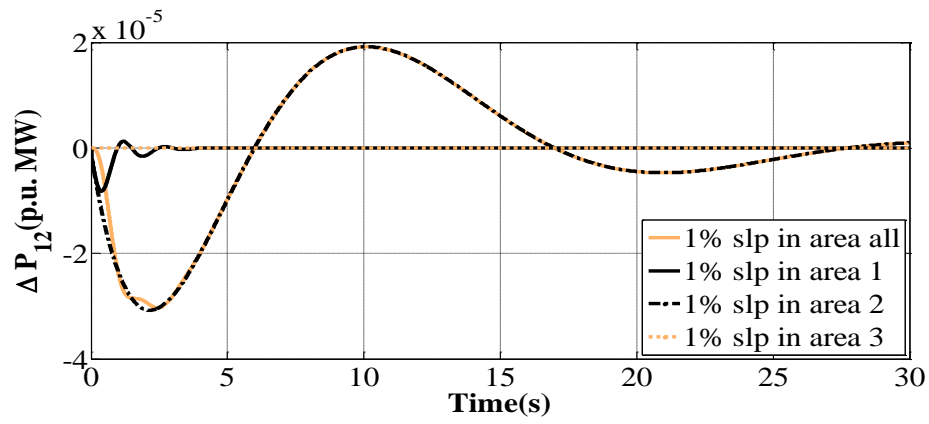
(d)
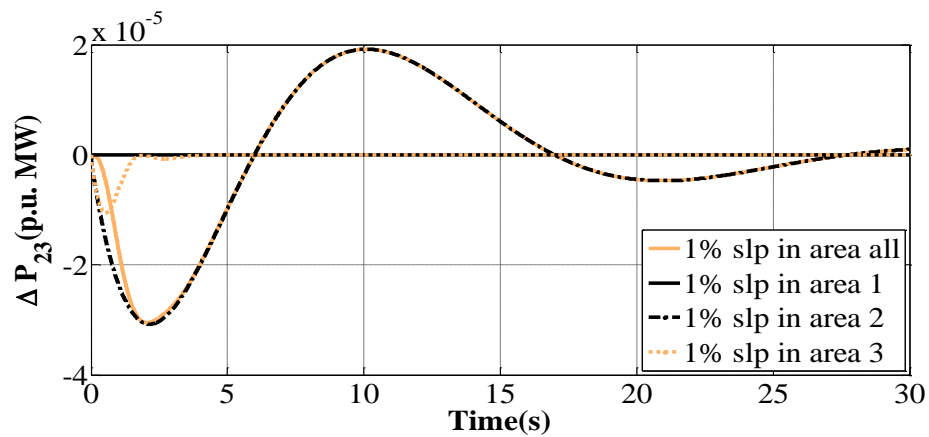
(e)

(f)

Fig.8. 11: Dynamic response of non-reheat thermal, hydro and non-reheat thermal interconnected power system with BESS at 1% slp (a)Frequency deviation of area-1(b)Frequency deviation of area-2 (c)Frequency deviation of area-3(d)Tie line power deviation between area-1 and area-2(e)Tie line power deviation between area-2 and area-3(f)Tie line power deviation between area-1 and area-3, Vs Time.

174

A similar analysis has been discovered for frequency deviation of area-2 and area-3 when power system is under 1 % slp in area-2 and area-3 respectively. It has been analyzed that when power system is under 1 % slp in area-1, tie-line power deviation between area-2 and area-3 are drive to transients although there is no contribution from area-2 and area-3 and it gives FPu value less, ST value more and FPt value more in area-1 among other tie-line power deviation of the same case. Similar trend can be seen for power system with BESS at 1 % slp in area-3.

8.5.5 Comparison of AGC of three area interconnected multi source power system with BESS

AGC of interconnected power system with sources as non reheat thermal, hydro and gas sources are further compounded. Case 2 is named as THG, Case 3 is named as TTT and Case 4 is named as THT for comparison. Comparison of dynamic responses in terms of frequency deviation for three cases of interconnected multi area multi source power system including BESS at 1% slp in all control areas is shown in Fig. 8.8.

Three parameters of IC for each power system with SMES are designed to minimize objective function is given in Table 8.6. It has been detected that FPu and ST of dynamic responses for case 2 is quite less as compared to other two cases. The sluggishness of responses in case of hydro sources is significantly improved with the use of BESS.
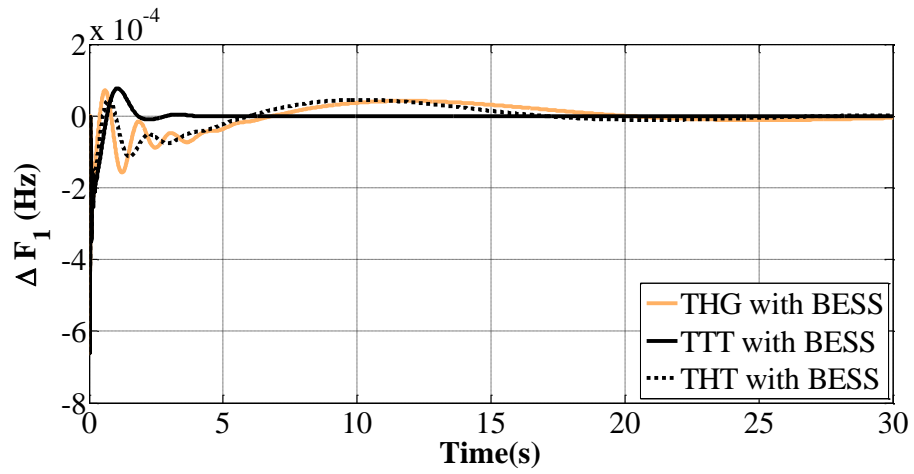
(a)
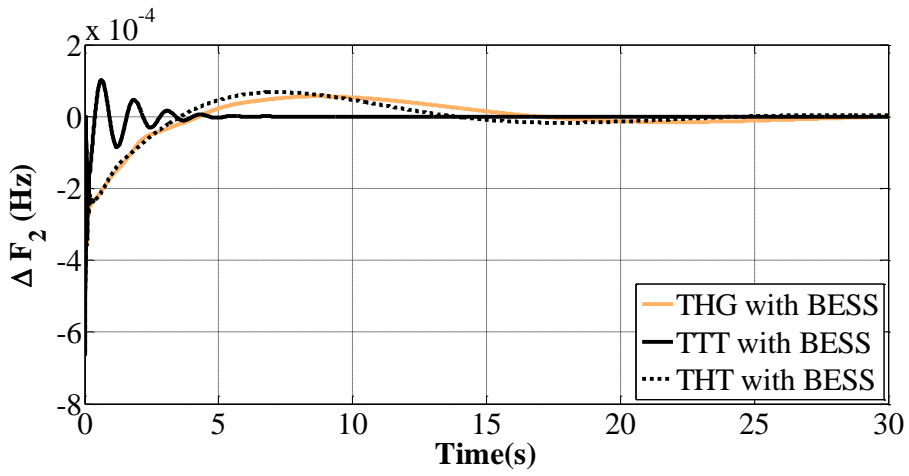
(b)
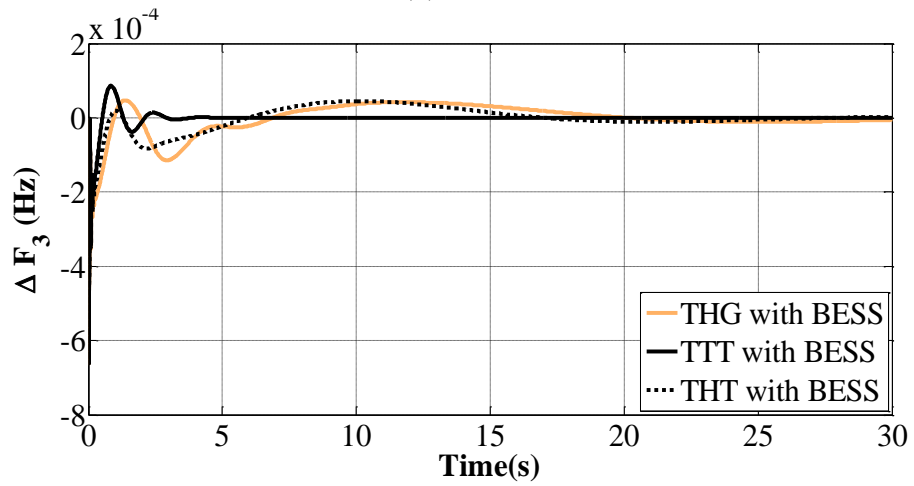
(c)

Fig.8. 12: Dynamic response of AGC of multi area interconnected power system with BESS at 1% slp in area-all (a) Frequency deviation of area-1 (b) Frequency deviation of area-2 (c) Frequency deviation of area-3, Vs Time.

TABLE 8. 6   Optimum parameter values for power systems with BESS at 1% slp in different areas

IC		K_{IC1}	K_{IC2}	K_{IC3}
THG with BESS	area-1	6	0.75	3
	area-2	9	3.7	2.9
	area-3	9.4	2.3	3
	area-all	8.9	2	3.1
TTT with BESS	area-1	3	0.9	20
	area-2	9	9	9
	area-3	0.9	60	3
	area-all	3	8.9	0.5
THT with BESS	area-1	6	2	3.7
	area-2	9	2.5	3
	area-3	9	2.5	3.2
	area-all	6	2.5	3

8.6   Conclusion

Effect of BESS is exhibited in PSO tuned IC for AGC of interconnected multi area multi source power system. Initially, reheat thermal, hydro and gas are considered as sources in PSO tuned IC for AGC strategy. Frequency deviation responses of each area and percentage improvement of frequency deviation responses in terms of ST assisted the criterion for judgment of betterment of proposed approach of PSO tuned IC power system with BESS than PSO tuned IC power system without BESS. This clearly reveals that application of BESS in power system certainly helps the power system to achieve AGC objectives in astonishingly quick response time even with reneweable sources. The study is further extended to three area non-reheat thermal, hydro and gas interconnected power system with BESS, three area non-reheat thermal interconnected power system with BESS and three area non-reheat thermal, hydro and non-reheat thermal interconnected power system with BESS. Moreover, effect of 1% slp in

177

different control areas is analyized. Significant improvement in the dynamic responses of power system has been observed in case of thermal and gas power sources. Degradation of system due to the presence of hydro sources in interconnected multi source power system at 1% slp in all areas as compared to 1% slp in individually areas is remarkably diminished by considering BESS in each area.

CHAPTER 9

CONCLUSIONS

9.1 Overview of the work

This chapter presents an outline of the commitments made in the current proposal. In this study, an endeavor is made to introduce different approaches on AGC of interconnected multi area power system with diverse sources. To take care of AGC issue, some new control procedures have been proposed in this thesis. To analyze and in this way approve the consequences of the proposed regulators, the simulation is directed on different AGC of interconnected multi area power systems with different artificial techniques. Also, optimal AGC regulators have been designed by using different structures of cost weighting matrices (Q and R) and then performance of all three types of regulators has been compared in each power systems. in the thesis. The following conclusions of the works done in this thesis are expressed as follows:

A. Jaya based AGC of two-area interconnected diverse source power system with varying participation

Jaya is employed to optimize PID controller for AGC of two-area multi-source power system models at 1% slp and random load disturbances. Each area of diverse sources like thermal, hydro and gas are interconnected by tielines. From the system results, it is concluded Jaya based PID controller outperforms better responses having less numerical values of settling time, first peak undershoot, first peak time , first rise time and performance indices. Jaya based PID controller outsmarts even the

intelligent control approaches prevalent in the literature. Further, comparative study of varying participation of diverse power sources in Jaya based AGC strategy for interconnected two area power system has been done. It has been seen that by decreasing the participation of hydro power source as compared to combine participation of thermal and gas power sources improves the dynamic responses.

B. Jaya based AGC of two area interconnected thermal-hydro-wind and thermal-hydro-diesel power system with/ without nonlinearities

Jaya based PID controller is proposed to solve AGC problem of two-area thermal-hydro-diesel and thermal-hydro-wind interconnected power systems with/without non linearity. The efficacy of novel Jaya based approach in two area interconnected power system without nonlinearities at 1% slp and random varying load is proved by comparing with bio-inspired evolutionary based AI techniques like IPSO, PSO and BFA on same system.

Dyanamic responses and performance values of power sysem at 1% slp and random varying load with nonlinearities like GRC in thermal and hydro sources, GDB in thermal and hydro sources and boiler dynamics in thermal source are studied. It is observed from the system outcomes on MATLAB platform that Jaya tuned PID outperforms TLBO tuned PID and various other intelligent algorithms tuned PID/PIDD controller available in the recent literature.

C. Optimal AGC of three area interconnected multi source power systems

Optimal AGC regulators has been designed by considering various structures of cost weighting matrices for three area interconnected multi source power systems. Power systems have different combination of non reheat thermal, hydro and gas

180

sources. Investigation of eigen values, dynamic responses and performance values ensures the stability of power system. The investigation carried out reveal that optimal AGC regulator based on structures of control and state cost weighting matrices with scaling method offer remarkable improvement in dynamic stability as compared to other designed regulators based on minimum performance index and by giving equal importance to each variable.

D. AGC of three area interconnected multi source power systems with superconducting magnetic energy storage

PSO tuned integral controller is designed for AGC of interconnected three area multi source power system with SMES. Power systems have different combination of non reheat thermal, hydro and gas sources. Comparative analysis portray potential benefits of proposed approach when compared with different bio-inspired artificial technique for tuning of AGC of interconnected thermal-hydro-gas power system including and excluding SMES.

E. AGC of three area interconnected multi source power systems with Battery energy storage system

PSO tuned integral controller is designed for AGC of interconnected three area multi source power system with BESS. Power systems have different combination of non reheat thermal, reheat thermal, hydro and gas sources. Comparative analysis portray potential benefits of proposed approach when compared with different bio-inspired artificial technique for tuning of AGC of interconnected thermal-hydro-gas power system including and excluding BESS. It is observed that proposed PSO tuned IC controller with BESS show superior performance in comparison to other AI techniques in terms of least values of settling time, first peak undershoot and

performance indices. Dynamic responses are significantly improved by using this approach.

9.2   Scope for the future research

In the present study it has been tried to propose some good designs of AGC controllers for AGC of multi area interconnected multi source power system. The proposed controllers have demonstrated very promising results. However, there are various areas, which need further research to provide better AGC controller designs for various types of power system structures. These areas are stated as follows:

1. In this study, the design of IC or PID controller is carried out employing GA, JAYA and other bio-inspired intelligent techniques but more fruitful results may be obtained by using some other new intelligent optimization techniques. Hybrid of some AI techniques in conjunction with some new tuning techniques may be implemented in future studies on multi source power systems with renewable sources.

2. In the present study, it is assumed that control areas of power system have combinations of multi- sources of power generations like thermal and hydro or thermal or gas or wind or diesel in each area. However, further studies may be done by considering diverse sources like bio diesel, PV etc. in each control area of multi-area power system.

3. In the present study, the impact of various energy storing devices like SMES and BESS has been studied for solving AGC problem of multi-area multi-source power systems. Further, studies may be done by considering CES or different types of battery like redox battery in system.

4. To secure the system we can add cybersecurity in power system.

5. In present study, only AC tie lines are considered between multi areas. DC tie line or both AC/DC tie lines can be implemented in power systems.

REFERENCES

[1]   Kundur P. Power system stability and control. Edited by Neal J. Balu, and Mark G. Lauby. 1994;4(2).

[2]   Elgerd OI. Electric energy systems theory: an introduction. McGraw-Hill Book Company, New York, NY1982.

[3]   Grigsby LL. Power system stability and control. CRC press; 2012.

[4]   IEEE Committee Report.IEEE Standard Definition of Terms for Automatic Generation Control of Electric Power Systems.IEEE Trans. Power Apparatus and Systems, 1970 Jul; 89:1358-1364.

[5]   Jalleli N, Vanslyck LS, Ewart DN, Fink LH, Hoffman AG. Understanding AGC, IEEE Trans. Power system. 1992;7(3): 1106-1112.

[6]   Wood AJ, Wollenberg BF, Sheblé GB. Power generation, operation, and control. John Wiley & Sons; 2013 Dec 18.

[7]   Concordia C, Kirchmayer LK. Tie-Line Power and Frequency Control of Electric Power Systems-Part II. Transactions of the American Institute of Electrical Engineers. Part III: Power Apparatus and Systems. 1954 Apr;73(2):133-146.

[8]   Cohn N. Some aspects of tie-line bias control on interconnected power systems. Transactions of the American institute of electrical engineers. Part III: power apparatus and systems. 1956 Jan;75(3):1415-1436.

[9]   Cohn N, Control of generation and power flows in interconnected systems, Wiley, USA, 1968.

[10]   Bevrani H. Robust power system frequency control. New York: Springer; 2009.

[11]   Green RK. Transformed automatic generation control. IEEE Transactions on Power Systems. 1996 Nov;11(4):1799-1804.

[12]   Kim JS, Edgar TF. Optimal scheduling of combined heat and power plants using mixed-integer nonlinear programming. Energy. 2014 Dec 1;77:675-690.

[13] Hasanien HM, Matar M. A fuzzy logic controller for autonomous operation of a voltage source converter-based distributed generation system. IEEE Transactions on Smart grid. 2014 Aug 5;6(1):158-165.

[14] Kumar A, Anwar MN, Kumar S. Sliding mode controller design for frequency regulation in an interconnected power system. Protection and Control of Modern Power Systems. 2021 Dec;6(1):1-12.

[15] Abrazeh S, Parvaresh A, Mohseni SR, Zeitouni MJ, Gheisarnejad M, Khooban MH. Nonsingular Terminal Sliding Mode Control With Ultra-Local Model and Single Input Interval Type-2 Fuzzy Logic Control for Pitch Control of Wind Turbines. IEEE/CAA Journal of Automatica Sinica. 2021 Feb 3;8(3):690-700.

[16] Suganthan PN, Katuwal R. On the origins of randomization-based feedforward neural networks. Applied Soft Computing. 2021 Jul ;105:107239.

[17] Bevrani H, Hiyama T. Intelligent automatic generation control. Boca Raton: CRC press; 2011 Apr.

[18] Kirchmayer LK. System optimization techniques. Electrical Engineering. 1962 Aug;81(8):618-622.

[19] Kothari ML, Nanda J, Kothari DP, Das D. Discrete-mode automatic generation control of a two-area reheat thermal system with new area control error. IEEE Transactions on power systems. 1989 May;4(2):730-738.

[20] Long CE, Polisetty PK, Gatzke EP. Deterministic global optimization for nonlinear model predictive control of hybrid dynamic systems. International Journal of Robust and Nonlinear Control: IFAC-Affiliated Journal. 2007 Sep 10;17(13):1232-1250.

[21] Mallesham G, Mishra S, Jha AN. Maiden application of Ziegler-Nichols method to AGC of distributed generation system. In2009 IEEE/PES Power Systems Conference and Exposition 2009 Mar 15 (pp. 1-7). IEEE.

[22] Ghosh A, Ray AK, Nurujjaman M, Jamshidi M. Voltage and frequency control in conventional and PV integrated power systems by a particle swarm optimized Ziegler–Nichols based PID controller. SN Applied Sciences. 2021 Mar;3(3):1-13.

[23]   Hajiaghaei-Keshteli M, Fathollahi-Fard AM. A set of efficient heuristics and metaheuristics to solve a two-stage stochastic bi-level decision-making model for the distribution network problem. Computers & Industrial Engineering. 2018 Sep 1;123:378-395.

[24]   Lee KY, El-Sharkawi MA, editors. Modern heuristic optimization techniques: theory and applications to power systems. John Wiley & Sons; 2008.

[25]   Glover F. Heuristics for integer programming using surrogate constraints. Decision sciences. 1977 Jan;8(1):156-166.

[26]   Kumawat M, Gupta N, Jain N, Shrivastava V, Sharma G. Applications of Meta-heuristics in Renewable Energy Systems. InMetaheuristic and Evolutionary Computation: Algorithms and Applications 2021 (pp. 253-282). Springer, Singapore.

[27]   Parouha RP, Verma P. State-of-the-Art Reviews of Meta-Heuristic Algorithms with Their Novel Proposal for Unconstrained Optimization and Applications. Archives of Computational Methods in Engineering. 2021 Feb 25:1-67.

[28]   Parouha RP, Verma P. Design and applications of an advanced hybrid meta-heuristic algorithm for optimization problems. Artificial Intelligence Review. 2021 Feb 13:1-80.

[29]   Marchand A, Gendreau M, Blais M, Emiel G. Efficient tabu search procedure for short-term planning of large-scale hydropower systems. Journal of Water Resources Planning and Management. 2019 Jul 1;145(7):04019025.

[30]   Niyomsat T, Puangdownreong D. Novel cooperative FPA-ATS algorithm and its application to optimal FOPID controller design for load frequency control. International Journal of Innovative Computing, Information and Control. 2020;16(6):1877-1894.

[31]   Xi L, Yu T, Yang B, Zhang X. A novel multi-agent decentralized win or learn fast policy hill-climbing with eligibility trace algorithm for smart generation control of interconnected complex power grids. Energy Conversion and Management. 2015 Oct 1;103:82-93.

[32]   Siddique N, Adeli H. Nature inspired computing: an overview and some future directions. Cognitive computation. 2015 Dec 1;7(6):706-714.

[33]   Kumar SR, Singh KD. Nature-Inspired Optimization Algorithms: Research Direction and Survey. arXiv preprint arXiv:2102.04013. 2021.

[34] Yang XS, Karamanoglu M. Swarm intelligence and bio-inspired computation: an overview. Swarm intelligence and bio-inspired computation. 2013 Jan :3-23.

[35] Prajapati Y, Kamat V, Patel J, Kher R. A Comprehensive Survey on Use of Soft Computing and Optimization Techniques for Load Frequency Control. Journal of Electrical and Electronic Engineering. 2020 Jun 20;8(2):64-70.

[36] Molina D, Poyatos J, Del Ser J, García S, Hussain A, Herrera F. Comprehensive Taxonomies of Nature-and Bio-inspired Optimization: Inspiration Versus Algorithmic Behavior, Critical Analysis Recommendations. Cognitive Computation. 2020 Sep;12(5):897-939.

[37] Kalavani F, Zamani-Gargari M, Mohammadi-Ivatloo B, Rasouli M. A contemporary review of the applications of nature-inspired algorithms for optimal design of automatic generation control for multi-area power systems. Artificial Intelligence Review. 2019 Feb;51(2):187-218.

[38] Alabool HM, Alarabiat D, Abualigah L, Heidari AA. Harris hawks optimization: a comprehensive review of recent variants and applications. Neural Computing and Applications. 2021 Feb 3:1-42.

[39] Man KF, Tang KS, Kwong S. Genetic algorithms: concepts and applications [in engineering design]. IEEE transactions on Industrial Electronics. 1996 Oct;43(5):519-534.

[40] Guha D, Roy PK, Banerjee S. Study of differential search algorithm based automatic generation control of an interconnected thermal-thermal system with governor dead-band. Applied Soft Computing. 2017 Mar 1;52:160-175.

[41] Storn R, Price K. Differential evolution–a simple and efficient heuristic for global optimization over continuous spaces. Journal of global optimization. 1997 Dec;11(4):341-359.

[42] Mohanty P, Sahu RK, Sahoo DK, Panda S. Adaptive differential evolution and pattern search tuned fractional order fuzzy PID for frequency control of power systems. International Journal of Modelling and Simulation. 2021 Feb 26:1-5.

[43] Beyer HG, Schwefel HP. Evolution strategies–a comprehensive introduction. Natural computing. 2002 Mar;1(1):3-52.

[44] Wang GG, Deb S, Coelho LD. Earthworm optimisation algorithm: a bio-inspired metaheuristic algorithm for global optimisation problems. International Journal of Bio-Inspired Computation. 2018;12(1):1-22.

[45]   Khan A, Mushtaq N, Faraz SH, Khan OA, Sarwar MA, Javaid N. Genetic algorithm and earthworm optimization algorithm for energy management in smart grid. InInternational Conference on P2P, Parallel, Grid, Cloud and Internet Computing 2017 Nov 8 (pp. 447-459). Springer, Cham.

[46]   Jagatheesan K, Anand B, Samanta S, Dey N, Ashour AS, Balas VE. Particle swarm optimisation-based parameters optimisation of PID controller for load frequency control of multi-area reheat thermal power systems. International Journal of Advanced Intelligence Paradigms. 2017;9(5-6):464-489.

[47]   Eberhart R, Kennedy J. A new optimizer using particle swarm theory. InMHS'95. Proceedings of the Sixth International Symposium on Micro Machine and Human Science 1995 Oct 4 (pp. 39-43). IEEE.

[48]   Yang XS. A new metaheuristic bat-inspired algorithm. InNature inspired cooperative strategies for optimization (NICSO 2010) 2010 (pp. 65-74). Springer, Berlin, Heidelberg.

[49]   Khooban MH, Niknam T. A new intelligent online fuzzy tuning approach for multi-area load frequency control: Self Adaptive Modified Bat Algorithm. International Journal of Electrical Power & Energy Systems. 2015 Oct 1;71:254-261.

[50]   Dash P, Saikia LC, Sinha N. Automatic generation control of multi area thermal system using Bat algorithm optimized PD–PID cascade controller. International Journal of Electrical Power & Energy Systems. 2015 Jun 1;68:364-372.

[51]   Alsattar HA, Zaidan AA, Zaidan BB. Novel meta-heuristic bald eagle search optimisation algorithm. Artificial Intelligence Review. 2020 Mar;53(3):2237-2264.

[52]   Das S, Biswas A, Dasgupta S, Abraham A. Bacterial foraging optimization algorithm: theoretical foundations, analysis, and applications. InFoundations of computational intelligence volume 3 2009 (pp. 23-55). Springer, Berlin, Heidelberg.

[53]   Yadav A. AEFA: Artificial electric field algorithm for global optimization. Swarm and Evolutionary Computation. 2019 Aug 1;48:93-108.

[54]   Hatamlou A. Black hole: A new heuristic optimization approach for data clustering. Information sciences. 2013 Feb;222:175-184.

[55] Gorripotu TS, Pilla R. Black hole optimised cascade proportional derivative-proportional integral derivative controller for frequency regulation in hybrid distributed power system. International Journal of Swarm Intelligence. 2019;4(2):155-174.

[56] Tzanetos A, Dounias G. A new metaheuristic method for optimization: sonar inspired optimization. InInternational Conference on Engineering Applications of Neural Networks 2017 Aug 25 (pp. 417-428). Springer, Cham.

[57] Erol OK, Eksin I. A new optimization method: big bang–big crunch. Advances in Engineering Software. 2006 Feb ;37(2):106-111.

[58] Jain C, Verma HK, Arya LD. Big Bang-Big Crunch based optimized controller for automatic generation control and automatic voltage regulator system. International Journal of Engineering, Science and Technology. 2011;3(10):12-19.

[59] Yesil E, Savran AI, Guzay C. Load frequency controller design using new Big Bang-Big Crunch 2 algorithm. In2014 IEEE International Symposium on Innovations in Intelligent Systems and Applications (INISTA) Proceedings 2014 Jun 23 (pp. 7-13). IEEE.

[60] Kaveh A, Dadras A. A novel meta-heuristic optimization algorithm: thermal exchange optimization. Advances in Engineering Software. 2017 Aug ;110:69-84.

[61] Alhato MM, Bouallègue S. Thermal exchange optimization based control of a doubly fed induction generator in wind energy conversion system. Indones. J. Electr. Eng. Comput. Sci. 2020 Dec;20:1-8.

[62] Kirkpatrick S, Gelatt CD, Vecchi MP. Optimization by simulated annealing. science. 1983 May; 220(4598):671-680.

[63] Chandrakala KV, Balamurugan S. Simulated annealing based optimal frequency and terminal voltage control of multi source multi area system. International Journal of Electrical Power & Energy Systems. 2016 Jun 1;78:823-829.

[64] Ghoshal SP. Application of GA/GA-SA based fuzzy automatic generation control of a multi-area thermal generating system. Electric Power Systems Research. 2004 Jul ;70(2):115-127.

[65] Murase H. Finite element inverse analysis using a photosynthetic algorithm. Computers and Electronics in Agriculture. 2000 Oct ;29(1-2):115-123.

[66]   Chuang CL, Jiang JA. Integrated radiation optimization: inspired by the gravitational radiation in the curvature of space-time. In2007 IEEE congress on evolutionary computation 2007 Sep 25 (pp. 3157-3164). IEEE.

[67]   Rao RV, Savsani VJ, Vakharia DP. Teaching–learning-based optimization: a novel method for constrained mechanical design optimization problems. Computer-Aided Design. 2011 Mar 1;43(3):303-315.

[68]   Bodaghi M, Samieefar K. Meta-heuristic bus transportation algorithm. Iran Journal of Computer Science. 2019 Mar;2(1):23-32.

[69]   Moghdani R, Salimifard K. Volleyball premier league algorithm. Applied Soft Computing. 2018 Mar 1;64:161-185.

[70]   Murali S, Shankar R. A True Event-Based Metaheuristic Algorithm Optimized AGC Mechanism for a Multi-area Power System. InSoft Computing: Theories and Applications 2020 (pp. 391-401). Springer, Singapore.

[71]   Atashpaz-Gargari E, Lucas C. Imperialist competitive algorithm: an algorithm for optimization inspired by imperialistic competition. In2007 IEEE congress on evolutionary computation 2007 Sep 25 (pp. 4661-4667). IEEE.

[72]   Kumar N, Tyagi B, Kumar V. Multiarea deregulated automatic generation control scheme of power system using imperialist competitive algorithm based robust controller. IETE journal of Research. 2018 Jul 4;64(4):528-537.

[73]   Gunduz M, Aslan M. DJAYA: A discrete Jaya algorithm for solving traveling salesman problem. Applied Soft Computing. 2021 Jul 1;105:107275.

[74]   Singh SP, Prakash T, Singh VP, Babu MG. Analytic hierarchy process based automatic generation control of multi-area interconnected power system using Jaya algorithm. Engineering Applications of Artificial Intelligence. 2017 Apr 1;60:35-44.

[75]   Panwar A, Sharma G, Nasiruddin I, Bansal RC. JAYA-Evaluated Frequency Control Design for Hydroelectric Power System Using RFB and UPFC. InIntelligent Computing Techniques for Smart Energy Systems 2020 (pp. 863-871). Springer, Singapore.

[76]   Cheraghalipour A, Hajiaghaei-Keshteli M, Paydar MM. Tree Growth Algorithm (TGA): A novel approach for solving optimization problems. Engineering Applications of Artificial Intelligence. 2018 Jun 1;72:393-414.

[77]   Khasanov M, Xie K, Kamel S, Wen L, Fan X. Combined Tree Growth Algorithm for Optimal Location and Size of Multiple DGs with Different Types in Distribution Systems. In2019 IEEE Innovative Smart Grid Technologies-Asia (ISGT Asia) 2019 May 21 (pp. 1265-1270). IEEE.

[78]   Abdel-Baset M, Wu H, Zhou Y. A complex encoding flower pollination algorithm for constrained engineering optimisation problems. International Journal of Mathematical Modelling and Numerical Optimisation. 2017;8(2):108-126.

[79]   Subramanian GG, Chidambaram IA, Manoharan JS. Flower Pollination Algorithm for Automatic Generation Control in Interconnected Power Systems under Restructured Market–A Survey. Asian Journal of Research in Social Sciences and Humanities. 2017;7(3):371-381.

[80]   Premaratne U, Samarabandu J, Sidhu T. A new biologically inspired optimization algorithm. In2009 international conference on industrial and information systems (ICIIS) 2009 Dec 28 (pp. 279-284). IEEE.

[81]   Moez H, Kaveh A, Taghizadieh N. Natural forest regeneration algorithm: a new meta-heuristic. Iranian Journal of Science and Technology, Transactions of Civil Engineering. 2016 Dec;40(4):311-326.

[82]   Punnathanam V, Kotecha P. Yin-Yang-pair Optimization: A novel lightweight optimization algorithm. Engineering Applications of Artificial Intelligence. 2016 Sep 1;54:62-79.

[83]   Song D, Liu J, Yang J, Su M, Wang Y, Yang X, Huang L, Joo YH. Optimal design of wind turbines on high-altitude sites based on improved Yin-Yang pair optimization. Energy. 2020 Feb;193:116794.

[84]   Civicioglu P. Artificial cooperative search algorithm for numerical optimization problems. Information Sciences. Elsevier, 2013 Apr; 229:58-76.

[85]   Selvaraju RK, Somaskandan G. ACS algorithm tuned ANFIS-based controller for LFC in deregulated environment. Journal of applied research and technology. 2017 Apr ;15(2):152-166.

[86]   Tanyildizi E, Demir G. Golden sine algorithm: A novel math-inspired algorithm. Advances in Electrical and Computer Engineering. 2017;17(2):71-80.

[87]   Rawa M, Abusorrah A, Bassi H, Mekhilef S, Ali ZM, Aleem SH, Hasanien HM, Omar AI. Economical-technical-environmental operation of power networks with wind-solar-hydropower generation using analytic hierarchy process and improved grey wolf algorithm. Ain Shams Engineering Journal. 2021 Mar 4.

[88]   Mishra D, Nayak PC, Bhoi SK, Prusty RC. Grey Wolf Optimization algorithm based Cascaded PID controller for Load-frequency control of OFF-Grid Electric Vehicle integrated Microgrid. In2020 IEEE International Symposium on Sustainable Energy, Signal Processing and Cyber Security (iSSSC) 2020 Dec 16 (pp. 1-6). IEEE.

[89]   Elgerd OI, Fosha CE. Optimum megawatt-frequency control of multiarea electric energy systems. IEEE Transactions on Power Apparatus and Systems. 1970 Apr(4):556-563.

[90]   Fosha CE, Elgerd OI. The megawatt-frequency control problem: a new approach via optimal control theory. IEEE Transactions on Power Apparatus and Systems. 1970 Apr(4):563-577.

[91]   Vournas CD, Dialynas EN, Hatziargyriou N, Machias AV, Souflis JL, Papadias BC. A flexible AGC algorithm for the Hellenic interconnected system. IEEE Transactions on Power Systems. 1989 Feb;4(1):61-80.

[92]   Premakumaran N, Parthasarathy K, Khincha HP, Chidambara MR. Some aspects of multilevel load-frequency control of a power system. InIEE Proceedings C (Generation, Transmission and Distribution) 1982 Nov 1 (Vol. 129, No. 6, pp. 290-294). IET Digital Library.

[93]   Singh O, Singh M. A Comparative Analysis on Economic Load Dispatch Problem Using Soft Computing Techniques. International Journal of Software Science and Computational Intelligence (IJSSCI). 2020 Apr 1;12(2):50-73.

[94]   Hlalele TG, Naidoo RM, Zhang J, Bansal RC. Dynamic economic dispatch with maximal renewable penetration under renewable obligation. IEEE Access. 2020 Feb 21;8:38794-38808.

[95]   Glover JD, Schweppe FC, Advanced load frequency control, *IEEE Trans. Power appar. and syst.*, 1972, Vol. PAS-91(5), 2095-2103.

[96]   Badal FR, Nayem Z, Sarker SK, Datta D, Rahman Fahim S, Muyeen SM, Islam Sheikh M, Das SK. A Novel Intrusion Mitigation Unit for Interconnected Power Systems in Frequency Regulation to Enhance Cybersecurity. Energies. 2021 Jan;14(5):1401.

[97]   Bevrani H, Golpîra H, Messina AR, Hatziargyriou N, Milano F, Ise T. Power system frequency control: An updated review of current solutions and new challenges. Electric Power Systems Research. 2021 May 1;194:107114.

[98]   Singh O. Current Philosophies of Intelligent Techniques based AGC for Interconnected Power Systems. International Journal of Energy Engineering. 2014 Jun 1;4(3):141.

[99]   Al-Ismail FS. DC microgrid planning, operation, and control: A comprehensive review. IEEE Access. 2021 Mar 1;9:36154-36172.

[100]   Alhelou HH, Hamedani-Golshan ME, Zamani R, Heydarian-Forushani E, Siano P. Challenges and opportunities of load frequency control in conventional, modern and future smart power systems: A comprehensive review. Energies. 2018 Oct;11(10):2497.

[101]   Singh B, Tiwari P, Singh SN. Enhancement of Power System Performances by Optimally Placed FACTS Controllers by using Different Optimization Techniques in Distribution Systems: A Taxonomical Review. In2018 5th IEEE Uttar Pradesh Section International Conference on Electrical, Electronics and Computer Engineering (UPCON) 2018 Nov 2 (pp. 1-7). IEEE.

[102]   Singh B, Pal C, Mukherjee V, Tiwari P, Yadav MK, Member IS. Distributed generation planning from power system performances viewpoints: A taxonomical survey. Renewable and Sustainable Energy Reviews. 2017 Aug 1;75:1472-1492.

[103]   Kumar P, Kothari DP. Recent philosophies of automatic generation control strategies in power systems. IEEE transactions on power systems. 2005 Jan 31;20(1):346-357.

[104]   Shayeghi HA, Shayanfar HA, Jalili A. Load frequency control strategies: A state-of-the-art survey for the researcher. Energy Conversion and management. 2009 Feb 1;50(2):344-353.

[105]   Gopi P, Reddy PL. A Critical review on AGC strategies in interconnected power system. InIET Chennai fourth international conference on sustainable energy and intelligent systems (SEISCON 2013) 2013 Dec 12 (pp. 85-92). IET.

[106]   Pandey SK, Mohanty SR, Kishor N. A literature survey on load–frequency control for conventional and distribution generation power systems. Renewable and Sustainable Energy Reviews. 2013 Sep 1;25:318-334.

[107]   Donde V, Pai MA, Hiskens IA. Simulation and optimization in an AGC system after deregulation. IEEE transactions on power systems. 2001 Aug;16(3):481-489.

[108]   Fini MH, Yousefi GR, Alhelou HH. Comparative study on the performance of many-objective and single-objective optimisation algorithms in tuning load frequency controllers of multi-area power systems. IET Generation, Transmission & Distribution. 2016 Sep 2;10(12):2915-2923.

[109]   Shankar R, Pradhan SR, Chatterjee K, Mandal R. A comprehensive state of the art literature survey on LFC mechanism for power system. Renewable and Sustainable Energy Reviews. 2017 Sep 1;76:1185-1207.

[110]   Ashmole PH, Battlebury DR, Bowdler RK. Power-system model for large frequency disturbances. InProceedings of the Institution of Electrical Engineers 1974 Jul 1 (Vol. 121, No. 7, pp. 601-608). IET Digital Library.

[111]   Hari L, Kothari ML, Nanda J. Optimum selection of speed regulation parameters for automatic generation control in discrete mode considering generation rate constraints. InIEE Proceedings C (Generation, Transmission and Distribution) 1991 Sep 1 (Vol. 138, No. 5, pp. 401-406). IET Digital Library.

[112]   VanSlyck LS, Jaleeli N, Kelley WR. Implications of frequency control bias settings on interconnected system operation and inadvertent energy accounting. IEEE transactions on power systems. 1989 May;4(2):712-723.

[113]   Prowse DC. Improvements to a standard automatic generation control filter algorithm. IEEE transactions on power systems. 1993 Aug;8(3):1204-1210.

[114]   Pan CT, Liaw CM. An adaptive controller for power system load-frequency control. IEEE Transactions on Power Systems. 1989 Feb;4(1):122-128.

[115]   Wang Y, Zhou R, Wen C. New robust adaptive load-frequency control with system parametric uncertainties. IEE Proceedings-Generation, Transmission and Distribution. 1994 May 1;141(3):184-190.

[116] Jiang L, Yao W, Wu QH, Wen JY, Cheng SJ. Delay-dependent stability for load frequency control with constant and time-varying delays. IEEE Transactions on Power systems. 2011 Nov 14;27(2):932-941.

[117] Saha A, Saikia LC. Renewable energy source-based multiarea AGC system with integration of EV utilizing cascade controller considering time delay. International Transactions on Electrical Energy Systems. 2019 Jan;29(1):e2646.

[118] Baghaee HR, Mirsalim M, Gharehpetian GB, Talebi HA. Eigenvalue, robustness and time delay analysis of hierarchical control scheme in multi-DER microgrid to enhance small/large-signal stability using complementary loop and fuzzy logic controller. Journal of Circuits, Systems and Computers. 2017 Jun 18;26(06):1750099.

[119] Doolla S, Bhatti TS, Bansal RC. Load frequency control of an isolated small hydro power plant using multi-pipe scheme. Electric Power Components and Systems. 2011 Jan 4;39(1):46-63.

[120] Foord TR. Step response of a governed hydrogenerator. InProceedings of the Institution of Electrical Engineers 1978 Nov 1 (Vol. 125, No. 11, pp. 1247-1248). IET Digital Library.

[121] Kusic GL, Sutterfield JA, Caprez AR, Haneline JL, Bergman BR. Automatic generation control for hydro systems. IEEE transactions on energy conversion. 1988 Mar;3(1):33-39.

[122] Tripathy SC, Kalantar M, Balasubramanian R. Dynamics and stability of wind and diesel turbine generators with superconducting magnetic energy storage unit on an isolated power system. IEEE Transactions on Energy Conversion. 1991 Dec;6(4):579-585.

[123] Bhatti TS, Al-Ademi AA, Bansal NK. Load-frequency control of isolated wind-diesel-microhydro hybrid power systems (WDMHPS). Energy. 1997 May ;22(5):461-470.

[124] Parmar KS, Majhi S, Kothari DP. Load frequency control of a realistic power system with multi-source power generation. International Journal of Electrical Power & Energy Systems. 2012 Nov 1;42(1):426-433.

[125] Ramakrishna KS, Bhatti TS. Sampled-data automatic load frequency control of a single area power system with multi-source power generation. Electric Power Components and Systems. 2007 May 31;35(8):955-980.

[126] Mohanty B, Panda S, Hota PK. Controller parameters tuning of differential evolution algorithm and its application to load frequency control of multi-source power system. International journal of electrical power & energy systems. 2014 Jan 1;54:77-85.

[127] Pradhan C, Bhende CN. Frequency sensitivity analysis of load damping coefficient in wind farm-integrated power system. IEEE Transactions on Power Systems. 2016 May 13;32(2):1016-1029.

[128] Shirai G. Load frequency control using a governor and voltage controls vis a new approach. Proceedings of the IEEE. 1978 Oct;66(10):1293-1295.

[129] Malek NG, Tan OT, Julich PM, Tacker EC. Trajectory-sensitivity design of load-frequency control systems. InProceedings of the Institution of Electrical Engineers 1973 Oct 1 (Vol. 120, No. 10, pp. 1273-1277). IET Digital Library.

[130] Moorthi VR, Aggarwal RP. Damping effects of excitation control in load-frequency control system. InProceedings of the Institution of Electrical Engineers 1974 Nov 1 (Vol. 121, No. 11, pp. 1409-1416). IET Digital Library.

[131] Kwatny HG, Kalnitsky KC, Bhatt A. An optimal tracking approach to load-frequency control. IEEE Transactions on Power Apparatus and Systems. 1975 Sep;94(5):1635-1643.

[132] Chintu JM, Sahu RK, Panda S. Design and analysis of two degree of freedom tilt integral derivative controller with filter for frequency control and real time validation. Journal of Electrical Engineering. 2020 Dec 1;71(6):388-396.

[133] Ibraheem KP, Hasan N. Nizamuddin. Sub-optimal automatic generation control of interconnected power system using output vector feedback control strategy. Electric Power Components and Systems. 2012 Jun;40(9):977-994.

[134] Bhagat SK, Saikia LC, Babu NR, Saha D. Impact of PLL and Virtual Inertia on Deregulated AGC System Integrated with Parallel AC/HVDC. IETE Journal of Research. 2021 Mar 11:1-4.

[135] Khanjanzadeh A, Soleymani S, Mozafari B, Fotuhi M. Integrated multi-area power system with HVDC tie-line to enhance load frequency control and automatic generation control. Electrical Engineering. 2020 Sep;102(3):1223-1239.

[136] Nanda J, Kaul BL. Automatic generation control of an interconnected power system. InProceedings of the Institution of Electrical Engineers 1978 May 1 (Vol. 125, No. 5, pp. 385-390). IET Digital Library.

[137] Nanda J, Mangla A, Suri S. Some new findings on automatic generation control of an interconnected hydrothermal system with conventional controllers. IEEE Transactions on energy conversion. 2006 Feb 21;21(1):187-194.

[138] Khodabakhshian A, Hooshmand R. A new PID controller design for automatic generation control of hydro power systems. International Journal of Electrical Power & Energy Systems. 2010 Jun 1;32(5):375-382.

[139] Panwar A, Sharma G, Nasiruddin I, Bansal RC. Frequency stabilization of hydro–hydro power system using hybrid bacteria foraging PSO with UPFC and HAE. Electric Power Systems Research. 2018 Aug 1;161:74-85.

[140] Bhatt P, Ghoshal SP, Roy R. Load frequency stabilization by coordinated control of thyristor controlled phase shifters and superconducting magnetic energy storage for three types of interconnected two-area power systems. International Journal of Electrical Power & Energy Systems. 2010 Dec 1;32(10):1111-1124.

[141] Nasiruddin, Ibraheem, Terlochan S. Bhatti, and Nizamuddin Hakimuddin. "Automatic generation control in an interconnected power system incorporating diverse source power plants using bacteria foraging optimization technique." Electric Power Components and Systems 43, no. 2 (2015): 189-199.

[142] Barakat M, Donkol A, Hamed HF, Salama GM. Controller parameters tuning of water cycle algorithm and its application to load frequency control of multi-area power systems using TD-TI cascade control. Evolving Systems. 2021 Feb 13(1):1-6.

[143] Kong F, Li J, Yang D. Multi-Area Load Frequency Control of Hydro-Thermal-Wind Power Based on Improved Grey Wolf Optimization Algorithm. Elektronika ir Elektrotechnika. 2020 Dec 18;26(6):32-39.

[144] Barisal AK. Comparative performance analysis of teaching learning based optimization for automatic load frequency control of multi-source power systems. International Journal of Electrical Power & Energy Systems. 2015 Mar 1;66:67-77.

197

[145] Abd-Elazim SM, Ali ES. Load frequency controller design of a two-area system composing of PV grid and thermal generator via firefly algorithm. Neural Computing and Applications. 2018 Jul 1;30(2):607-616.

[146] Bengiamin NN, Chan WC. Multilevel load-frequency control of interconnected power systems. InProceedings of the Institution of Electrical Engineers 1978 Jun 1 (Vol. 125, No. 6, pp. 521-526). IET Digital Library.

[147] Rerkpreedapong D, Hasanovic A, Feliachi A. Robust load frequency control using genetic algorithms and linear matrix inequalities. IEEE Transactions on Power Systems. 2003 May 13;18(2):855-861

[148] Daneshfar F, Bevrani H. Load–frequency control: a GA-based multi-agent reinforcement learning. IET generation, transmission & distribution. 2010 Jan 1;4(1):13-26.

[149] Davison E, Tripathi N. The optimal decentralized control of a large power system: Load and frequency control. IEEE Transactions on Automatic Control. 1978 Apr;23(2):312-325.

[150] Ram Babu N, Saikia LC. AGC of a multiarea system incorporating accurate HVDC and precise wind turbine systems. International Transactions on Electrical Energy Systems. 2020 Apr;30(4):e12277.

[151] Zhang Y, Liu X, Qu B. Distributed model predictive load frequency control of multi-area power system with DFIGs. IEEE/CAA Journal of Automatica Sinica. 2017 Jan 16;4(1):125-135.

[152] Jagatheesan K, Anand B, Dey KN, Ashour AS, Satapathy SC. Performance evaluation of objective functions in automatic generation control of thermal power system using ant colony optimization technique-designed proportional–integral–derivative controller. Electrical Engineering. 2018 Jun;100(2):895-911.

[153] Belkacemi R, Rimal AN. A novel NERC compliant automatic generation control in multi-area power systems in the presence of renewable-energy resources. Electrical Engineering. 2017 Sep;99(3):931-941.

[154] Alhelou HH, Golshan ME, Hatziargyriou ND. Deterministic dynamic state estimation-based optimal lfc for interconnected power systems using unknown input observer. IEEE Transactions on Smart Grid. 2019 Sep 9;11(2):1582-1592.

[155] Du X, Li P. Fuzzy logic control optimal realization using GA for multi-area AGC systems. International Journal of Information Technology. 2006;12(7):63-72.

[156] Oni B, Graham H, Walker L. Investigation of nonlinear tie line bias control of interconnected power systems. IEEE Transactions on Power Apparatus and Systems. 1981 May(5):2350-2356.

[157] Debbarma S, Saikia LC, Sinha N. AGC of a multi-area thermal system under deregulated environment using a non-integer controller. Electric Power Systems Research. 2013 Feb 1;95:175-183.

[158] Jagatheesan K, Samanta S, Choudhury A, Dey N, Anand B, Ashour AS. Quantum inspired evolutionary algorithm in load frequency control of multi-area interconnected thermal power system with non-linearity. InQuantum Computing: An Environment for Intelligent Large Scale Real Application 2018 (pp. 389-417). Springer, Cham.

[159] Abdelaziz AY, Ali ES. Cuckoo search algorithm based load frequency controller design for nonlinear interconnected power system. International Journal of Electrical Power & Energy Systems. 2015 Dec 1;73:632-643.

[160] Sudha KR, Raju YB, Sekhar AC. Fuzzy C-Means clustering for robust decentralized load frequency control of interconnected power system with Generation Rate Constraint. International Journal of Electrical Power & Energy Systems. 2012 May 1;37(1):58-66.

[161] Hiyama T. Optimisation of discrete-type load-frequency regulators considering generation-rate constraints. InIEE Proceedings C (Generation, Transmission and Distribution) 1982 Nov 1 (Vol. 129, No. 6, pp. 285-289). IET Digital Library.

[162] Doraiswami R. A nonlinear load-frequency control design. IEEE Transactions on Power Apparatus and Systems. 1978 Jul(4):1278-1284.

[163] Tripathy SC, Saha N. Stability of load frequency control system for interconnected power systems with governor dead-band nonlinearity. International Journal of Electrical Engineering Education. 1976 Jul;13(3):231-240.

[164] Tripathy SC, Bhatti TS, Jha CS, Malik OP, Hope GS. Sampled data automatic generation control analysis with reheat steam turbines and governor dead-band effects. IEEE Transactions on Power apparatus and systems. 1984 May(5):1045-1051.

[165]   Tsay TS. Load–frequency control of interconnected power system with governor backlash nonlinearities. International Journal of Electrical Power & Energy Systems. 2011 Nov 1;33(9):1542-1549.

[166]   Murali S, Shankar R. Impact of Inertia Emulation Based Modified HVDC Tie-Line for AGC Using Novel Cascaded Fractional Order Controller in Deregulated Hybrid Power System. Journal of Electrical Engineering & Technology. 2021 Feb 8:1-21.

[167]   Taylor CW, Lee KY, Dave DP. Automatic generation control analysis with governor deadband effects. IEEE Transactions on Power Apparatus and Systems. 1979 Nov(6):2030-2036.

[168]   Haes Alhelou H, Hamedani Golshan ME, Hajiakbari Fini M. Wind driven optimization algorithm application to load frequency control in interconnected power systems considering GRC and GDB nonlinearities. Electric Power Components and Systems. 2018 Jul 21;46(11-12):1223-1238.

[169]   Jena NK, Sahoo S, Sahu BK. Fractional order cascaded controller for AGC study in power system with PV and diesel generating units. Journal of Interdisciplinary Mathematics. 2020 Feb 17;23(2):425-434.

[170]   Gashti A, Akbarimajd A. Designing anti-windup PI controller for LFC of nonlinear power system combined with DSTS of nuclear power plant and HVDC link. Electrical Engineering. 2020 Jun;102(2):793-809.

[171]   Nayak PC, Prusty RC, Panda S. Grasshopper optimisation algorithm of multistage PDF+(1+PI) controller for AGC with GDB and GRC nonlinearity of dispersed type power system. International Journal of Ambient Energy. 2020 Jan 9:1-13.

[172]   Mohanty B. TLBO optimized sliding mode controller for multi-area multi-source nonlinear interconnected AGC system. International Journal of Electrical Power & Energy Systems. 2015 Dec 1;73:872-881.

[173]   Nanda J, Mishra S, Saikia LC. Maiden application of bacterial foraging-based optimization technique in multiarea automatic generation control. IEEE Transactions on power systems. 2009 Apr 14;24(2):602-609.

[174]   Panda S, Mohanty B, Hota PK. Hybrid BFOA–PSO algorithm for automatic generation control of linear and nonlinear interconnected power systems. Applied Soft Computing. 2013 Dec 1;13(12):4718-4730.

[175]   Dash P, Saikia LC, Sinha N. Comparison of performances of several Cuckoo search algorithm based 2DOF controllers in AGC of multi-area thermal system. International Journal of Electrical Power & Energy Systems. 2014 Feb 1;55:429-436.

[176]   Hsu YY, Chan WC. Optimal variable structure controller for the load-frequency control of interconnected hydrothermal power systems. International Journal of Electrical Power & Energy Systems. 1984 Oct 1;6(4):221-229.

[177]   Patel R, Li C, Yu X, McGrath B. Optimal automatic generation control of an interconnected power system under network constraints. IEEE Transactions on Industrial Electronics. 2018 Jan 22;65(9):7220-7228.

[178]   Fan GW, Nelson HD, Crouch PE, Mignolet MP. LQR-Based Least-Squares Output Feedback Control of Rotor Vibrations Using the Complex Mode and Balanced Realization Methods. InTurbo Expo: Power for Land, Sea, and Air 1992 Jun 1 (Vol. 78972, p. V005T14A004). American Society of Mechanical Engineers.

[179]   Carpentier J. Optimal power flows. International Journal of Electrical Power & Energy Systems. 1979 Apr 1;1(1):3-15.

[180]   Anderson BD, Moore JB. Optimal control linear quadratic methods Prentice Hall international. Inc. Englewood Cliffs NJ. 1989;7632.

[181]   Carpentier J. 'To be or not to be modern' that is the question for automatic generation control (point of view of a utility engineer). International journal of electrical power & energy systems. 1985 Apr 1;7(2):81-91.

[182]   Saif, M., Optimal linear regulator pole-placement by weight selection. International Journal of Control, 1989,50(1), pp.399-414.

[183]   Hasan N. Design and analysis of pole-placement controller for interconnected power systems. Int J Emerg Technol Adv Eng. 2012 Aug;2(8):212-217.

[184]   Das S, Pan I, Halder K, Das S, Gupta A, LQR based improved discrete PID controller design via optimum selection of weighting matrices using fractional order integral performance index, Applied Mathematical Modelling,Elsevier, 2013,37(6):4253-4268.

[185]   Habib M, Khoucha F, Harrag A. GA-based robust LQR controller for interleaved boost DC–DC converter improving fuel cell voltage regulation. Electric Power Systems Research. 2017 Nov 1;152:438-456.

[186]   Sharma G, Nasiruddin I, Niazi KR, Bansal RC. Optimal AGC of a multi-area power system with parallel AC/DC tie lines using output vector feedback control strategy. International Journal of Electrical Power & Energy Systems. 2016 Oct 1;81:22-31.

[187]   Hasan N, Ibraheem, Kumar P. Optimal automatic generation control of interconnected power system considering new structures of matrix Q. Electric Power Components and Systems. 2013 Jan 15;41(2):136-156.

[188]   Sharma G, Panwar A, Krishnan N, Kumawat M. Integrating LQR with GRNN for LFC of energy delivery system interconnected via AC/DC tie-lines. IET Energy Systems Integration. 2020 Dec;2(4):355-361.

[189]   Nasiruddin I, Sharma G, Niazi KR, Bansal RC. Non-linear recurrent ANN-based LFC design considering the new structures of Q matrix. IET Generation, Transmission & Distribution. 2017 Jun 6;11(11):2862-2870.

[190]   Larsson PT, Ulsoy AG. Scaling the speed of response using LQR design. InProceedings of the 37th IEEE Conference on Decision and Control (Cat. No. 98CH36171) 1998 Dec 18 (Vol. 1, pp. 1171-1176). IEEE.

[191]   Larsson PT, Ulsoy AG. Fast control of linear systems subject to input constraints. J. Dyn. Sys., Meas., Control. 2000 Mar;122(1):18-26.

[192]   Aldeen M, Crusca F. Multimachine power system stabiliser design based on new LQR approach. IEE Proceedings-Generation, Transmission and Distribution. 1995 Sep 1;142(5):494-502.

[193]   Moore B. Principal component analysis in linear systems: Controllability, observability, and model reduction. IEEE transactions on automatic control. 1981 Feb;26(1):17-32.

[194] Cavin RK, Budge MC, Rasmussen P. An optimal linear systems approach to load-frequency control. IEEE Transactions on Power Apparatus and Systems. 1971 Nov(6):2472-2482.

[195] Kothari DP, Nagrath IJ. Modern power system analysis. Tata McGraw-Hill Education; 2003.

[196] Ballesteros F, De Arriaga F. Optimal control of power systems and the Riccati equation. Applied Mathematics and Computation. 1989 Sep 1;33(1):43-52.

[197] Srivastava S, Misra A, Thakur SK, Pandit VS. An optimal PID controller via LQR for standard second order plus time delay systems. ISA transactions. 2016 Jan 1;60:244-253.

[198] Priyanka EB, Maheswari C, Thangavel S. Remote monitoring and control of LQR-PI controller parameters for an oil pipeline transport system. Proceedings of the Institution of Mechanical Engineers, Part I: Journal of Systems and Control Engineering. 2019 Jul;233(6):597-608.

[199] He JB, Wang QG, Lee TH. PI/PID controller tuning via LQR approach. Chemical Engineering Science. 2000 Jul 1;55(13):2429-2439.

[200] Jha SK, Yadav AK, Gaur P, Gupta JR, Parthasarathy H. Robust and optimal control analysis of sun seeker system. Journal of Control Engineering and Applied Informatics. 2014 Mar 26;16(1):70-79.

[201] Khamies M, Magdy G, Ebeed M, Kamel S. A robust PID controller based on linear quadratic gaussian approach for improving frequency stability of power systems considering renewables. ISA transactions. 2021 Jan 28.

[202] Çalik AK, Kakilli A. The modelling of electric power systems on the state space and controlling of optimal LQR load frequency. IU-Journal of Electrical & Electronics Engineering. 2009;9(2):977-982.

[203] Naidu DS. Optimal control systems. CRC press; 2002.

[204] Naidu DS, Paul S, Rieger CR. A simplified SDRE technique for regulation in optimal control systems. In2019 IEEE International Conference on Electro Information Technology (EIT) 2019 May 20, 327-332.

[205] Rakhshani E. Intelligent linear-quadratic optimal output feedback regulator for a deregulated automatic generation control system. Electric Power Components and Systems. 2012 Mar 1;40(5):513-533.

[206] Pillai AG, Samuel ER. Minimal realized power systems for load frequency control using optimal theory based PID controller. IETE Journal of Research. 2020 Jul 28:1-13.

[207] El-Kashlan SA. Two-Level PI Controller Design for Interconnected Power System Using Eigenvalues Assignment Technique (Dept. E). MEJ. Mansoura Engineering Journal. 2020 Nov 9;36(4):79-87.

[208] Gbadega PA, Akindeji KT. Linear Quadratic Regulator Technique for Optimal Load Frequency Controller Design of Interconnected Linear Power Systems. In2020 IEEE PES/IAS PowerAfrica 2020 Aug 25 (pp. 1-5). IEEE.

[209] Joshi MK, Sharma G, Davidson IE. Investigation of Diverse Sampling Time for LFC of Hydro Power System using Discrete LQR with UPFC and RFB. In2020 International SAUPEC/RobMech/PRASA Conference 2020 Jan 29 (pp. 1-6). IEEE.

[210] Pradhan SK, Das DK. H∞ Performance-Based Sliding Mode Control Approach for Load Frequency Control of Interconnected Power System with Time Delay. Arabian Journal for Science and Engineering. 2021 Feb;46(2):1369-82.

[211] Jiang Y, Fan J, Gao W, Chai T, Lewis FL. Cooperative adaptive optimal output regulation of nonlinear discrete-time multi-agent systems. Automatica. 2020 Nov 1;121:109149.

[212] Liu S, Wang Z, Wang L, Wei G. H∞ Pinning Control of Complex Dynamical Networks Under Dynamic Quantization Effects: A Coupled Backward Riccati Equation Approach. IEEE Transactions on Cybernetics. 2020 Oct 7.

[213] Sharma G, Loji K. Critical Aspects of AGC Emerging from Optimal Control to Machine Learning Techniques. Indonesian Journal of Electrical Engineering and Informatics (IJEEI). 2020 Jun 16;8(2):230-241.

[214] Bilgic HH, Sen MA, Yapici A, Yavuz H, Kalyoncu M. Meta-Heuristic Tuning of the LQR Weighting Matrices Using Various Objective Functions on an Experimental Flexible Arm Under the Effects of Disturbance. Arabian Journal for Science and Engineering. 2021 Feb 10:1-14.

[215] Rao R. Jaya: A simple and new optimization algorithm for solving constrained and unconstrained optimization problems. International Journal of Industrial Engineering Computations. 2016;7(1):19-34.

[216]   Goldberg DE. Genetic algorithms. Pearson Education India; 2006.

[217]   Nayak N, Mishra S, Sharma D, Sahu BK. Application of modified sine cosine algorithm to optimally design PID/fuzzy-PID controllers to deal with AGC issues in deregulated power system. IET Generation, Transmission & Distribution. 2019 Jan 29;13(12):2474-2487.

[218]   Blaabjerg F, Ionel DM. Renewable energy devices and systems–state-of-the-art technology, research and development, challenges and future trends. Electric Power Components and Systems. 2015 Jul 21;43(12):1319-1328.

[219]   Choudhury S, Dash TP, Bhowmik P, Rout PK. A novel control approach based on hybrid Fuzzy Logic and Seeker Optimization for optimal energy management between micro-sources and supercapacitor in an islanded Microgrid. Journal of King Saud University-Engineering Sciences. 2020 Jan 1;32(1):27-41.

[220]   Hajiamoosha P, Rastgou A, Bahramara S, Sadati SM. Stochastic energy management in a renewable energy-based microgrid considering demand response program. International Journal of Electrical Power & Energy Systems. 2021 Jul 1;129:106791.

[221]   Mohseni S, Brent AC, Kelly S, Browne WN, Burmester D. Strategic design optimisation of multi-energy-storage-technology micro-grids considering a two-stage game-theoretic market for demand response aggregation. Applied Energy. 2021 Apr 1;287:116563.

[222]   Hemmati M, Mirzaei MA, Abapour M, Zare K, Mohammadi-ivatloo B, Mehrjerdi H, Marzband M. Economic-Environmental Analysis of Combined Heat and Power-Based Reconfigurable Microgrid Integrated with Multiple Energy Storage and Demand Response Program. Sustainable Cities and Society. 2021 Feb 26:102790.

[223]   Wang J, Li KJ, Liang Y, Javid Z. Optimization of Multi-Energy Microgrid Operation in the Presence of PV, Heterogeneous Energy Storage and Integrated Demand Response. Applied Sciences. 2021 Jan;11(3):1005.

[224]   Ahmad Hamidi S, Ionel DM, Nasiri A. Modeling and management of batteries and ultracapacitors for renewable energy support in electric power systems–an overview. Electric Power Components and Systems. 2015 Jul 21;43(12):1434-1452.

[225]   Zobaa AF, Bansal RC, editors. Handbook of renewable energy technology. World Scientific; 2011.

[226] Yao L, Yang B, Cui H, Zhuang J, Ye J, Xue J. Challenges and progresses of energy storage technology and its application in power systems. Journal of Modern Power Systems and Clean Energy. 2016 Oct;4(4):519-528.

[227] Nadeem F, Hussain SS, Tiwari PK, Goswami AK, Ustun TS. Comparative review of energy storage systems, their roles, and impacts on future power systems. IEEE Access. 2018 Dec 18;7:4555-4585.

[228] Adefarati T, Bansal RC, Naidoo R, Potgieter S, Rizzo R, Sanjeevikumar P. Analysis and optimisation of a diesel-PV-wind-electric storage system for a standalone power solution. IET Renewable Power Generation. 2020 Dec 18.

[229] Saha A, Saikia LC. Load frequency control of a wind-thermal-split shaft gas turbine-based restructured power system integrating FACTS and energy storage devices. International Transactions on Electrical Energy Systems. 2019 Mar;29(3):e2756.

[230] Chidambaram IA, Paramasivam B. Control performance standards based load-frequency controller considering redox flow batteries coordinate with interline power flow controller. Journal of power sources. 2012 Dec 1;219:292-304.

[231] Singh K. Enhancement of frequency regulation in tidal turbine power plant using virtual inertia from capacitive energy storage system. Journal of Energy Storage. 2021 Mar 1;35:102332.

[232] Nayak PC, Mishra S, Prusty RC, Panda S. Performance analysis of hydrogen aqua equaliser fuel-cell on AGC of Wind-hydro-thermal power systems with sunflower algorithm optimised fuzzy-PDFPI controller. International Journal of Ambient Energy. 2020 Oct 23:1-14.

[233] Tasnin W, Saikia LC. Comparative performance of different energy storage devices in AGC of multi-source system including geothermal power plant. Journal of Renewable and Sustainable Energy. 2018 Mar 16;10(2):024101.

[234] Kim JY, Kim HM, Kim SK, Jeon JH, Choi HK. Designing an energy storage system fuzzy PID controller for microgrid islanded operation. Energies. 2011 Sep;4(9):1443-1460.

[235] Tasnin W, Saikia LC. Performance comparison of several energy storage devices in deregulated AGC of a multi-area system incorporating geothermal power plant. IET Renewable Power Generation. 2018 Jan 26;12(7):761-772.

[236]   Mitani Y, Tsuji K, Murakami Y. Application of superconducting magnet energy storage to improve power system dynamic performance. IEEE Transactions on Power Systems. 1988 Nov;3(4):1418-1425.

[237]   Xue XD, Cheng KW, Sutanto D. Power system applications of superconducting magnetic energy storage systems. InFourtieth IAS Annual Meeting. Conference Record of the 2005 Industry Applications Conference, 2005. 2005 Oct 2 (Vol. 2, pp. 1524-1529). IEEE.

[238]   Ali MH, Wu B, Dougal RA. An overview of SMES applications in power and energy systems. IEEE transactions on sustainable energy. 2010 Mar 18;1(1):38-47.

[239]   Tripathy SC, Juengst KP. Sampled data automatic generation control with superconducting magnetic energy storage in power systems. IEEE Transactions on Energy Conversion. 1997 Jun;12(2):187-192.

[240]   Liu Y, Tang Y, Xu Y, Shi J, Shi X, Wang Z, Deng J, Ren L, Yan S. Status evaluation method for SMES used in power grid. IEEE Transactions on Applied Superconductivity. 2015 Jul 14;25(5):1-10.

[241]   Vengatesh RP, Rajan SE, Sivaprakash A. An intelligent approach for dynamic load frequency control with hybrid energy storage system. Australian Journal of Electrical and Electronics Engineering. 2019 Oct 2;16(4):266-275.

[242]   Demiroren A Automatic generation control for power system with SMES by using neural network controller. Electric Power Components and Systems. 2003 Jan 1;31(1):1-25.

[243]   Tripathy SC, Kalantar M, Balasubramanian R. Dynamics and stability of wind and diesel turbine generators with superconducting magnetic energy storage unit on an isolated power system. IEEE Transactions on Energy Conversion. 1991 Dec;6(4):579-585.

[244]   Said SM, Aly M, Mohamed EA, Hartmann B. Analysis and comparison of SMES device power losses considering various load conditions. In2019 IEEE Conference on Power Electronics and Renewable Energy (CPERE) 2019 Oct 23 (pp. 1-5). IEEE.

[245]   Banerjee S, Chatterjee JK, Tripathy SC. Application of magnetic energy storage unit as load-frequency stabilizer. IEEE Transactions on Energy Conversion. 1990 Mar;5(1):46-51.

[246] Pradhan PC, Sfahu RK, Panda S. Firefly algorithm optimized fuzzy PID controller for AGC of multi-area multi-source power systems with UPFC and SMES. Engineering Science and Technology, an International Journal. 2016 Mar 1;19(1):338-354.

[247] Abraham RJ, Das D, Patra A. Automatic generation control of an interconnected hydrothermal power system considering superconducting magnetic energy storage. International Journal of Electrical Power & Energy Systems. 2007 Oct 1;29(8):571-579.

[248] Bhatt P, Roy R, Ghoshal SP. Comparative performance evaluation of SMES–SMES, TCPS–SMES and SSSC–SMES controllers in automatic generation control for a two-area hydro–hydro system. International Journal of Electrical Power & Energy Systems. 2011 Dec 1;33(10):1585-1597.

[249] Devotta JB, Rabbani MG, Elangovan S. Effect of SMES unit on AGC dynamics. InProceedings of EMPD'98. 1998 International Conference on Energy Management and Power Delivery (Cat. No. 98EX137) 1998 Mar 5 (Vol. 1, pp. 61-66). IEEE.

[250] Peterson HA, Mohan N, Boom RW. Superconductive energy storage inductor-converter units for power systems. IEEE Transactions on Power Apparatus and Systems. 1975 Jul;94(4):1337-1348.

[251] Ngamroo I. Robust frequency control of wind-diesel hybrid power system using superconducting magnetic energy storage. International Journal of Emerging Electric Power Systems. 2009 Apr 29;10(2).

[252] Hemeida AM. A fuzzy logic controlled superconducting magnetic energy storage, SMES frequency stabilizer. Electric Power Systems Research. 2010 Jun 1;80(6):651-656.

[253] Sudha KR, Santhi RV. Load frequency control of an interconnected reheat thermal system using type-2 fuzzy system including SMES units. International Journal of Electrical Power & Energy Systems. 2012 Dec 1;43(1):1383-1392.

[254] Ngamroo I, Mitani Y, Tsuji K. Application of SMES coordinated with solid-state phase shifter to load frequency control. IEEE Transactions on applied superconductivity. 1999 Jun;9(2):322-325.

[255] Abraham RJ, Das D, Patra A. AGC study of a hydrothermal system with SMES and TCPS. European Transactions on Electrical Power. 2009 Apr;19(3):487-498.

[256]   Demiroren A. Automatic generation control using ANN technique for multi-area power system with SMES units. Electric Power Components and Systems. 2004 Feb 1;32(2):193-213.

[257]   Kumar A, Suhag S. Effect of TCPS, SMES, and DFIG on load frequency control of a multi-area multi-source power system using multi-verse optimized fuzzy-PID controller with derivative filter. Journal of Vibration and Control. 2018 Dec;24(24):5922-5937.

[258]   Pappachen A, Fathima AP. Load frequency control in deregulated power system integrated with SMES–TCPS combination using ANFIS controller. International Journal of Electrical Power & Energy Systems. 2016 Nov 1;82:519-534.

[259]   Mohamed EA, Ahmed EM, Elmelegi A, Aly M, Elbaksawi O, Mohamed AA. An optimized hybrid fractional order controller for frequency regulation in multi-area power systems. IEEE Access. 2020 Nov 25;8:213899-213915.

[260]   Lal DK, Barisal AK. Comparative performances evaluation of FACTS devices on AGC with diverse sources of energy generation and SMES. Cogent Engineering. 2017 Jan 1;4(1):1318466.

[261]   Zheng ZX, Chen XY, Xiao XY, Huang CJ. Design and evaluation of a mini-size SMES magnet for hybrid energy storage application in a kW-class dynamic voltage restorer. IEEE Transactions on Applied Superconductivity. 2017 Sep 4;27(7):1-11.

[262]   Nandi M, Shiva CK, Mukherjee V. Frequency stabilization of multi-area multi-source interconnected power system using TCSC and SMES mechanism. Journal of energy storage. 2017 Dec 1;14:348-362.

[263]   Saha A, Saikia LC. Performance analysis of combination of ultra-capacitor and superconducting magnetic energy storage in a thermal-gas AGC system with utilization of whale optimization algorithm optimized cascade controller. Journal of Renewable and Sustainable Energy. 2018 Jan 12;10(1):014103.

[264]   Rajbongshi R, Saikia LC. Coordinated performance of interline power flow controller and superconducting magnetic energy storage in combined ALFC and AVR system under deregulated environment. Journal of Renewable and Sustainable Energy. 2018 Jul 21;10(4):044102.

[265]   Mukherjee P, Rao VV. Effective location of SMES for power fluctuation mitigation of grid connected doubly fed induction generator. Journal of Energy Storage. 2020 Jun 1;29:101369.

[266]   Kinjo T, Senjyu T, Urasaki N, Fujita H. Terminal-voltage and output-power regulation of wind-turbine generator by series and parallel compensation using SMES. IEE Proceedings-Generation, Transmission and Distribution. 2006 May 1;153(3):276-282.

[267]   Wali SB, Hannan MA, Reza MS, Ker PJ, Begum RA, Abd Rahman MS, Mansor M. Battery storage systems integrated renewable energy sources: A biblio metric analysis towards future directions. Journal of Energy Storage. 2021 Mar 1;35:102296.

[268]   DelMonaco JL, Lewis PA, Roman HT, Zemkoski J. Advanced Batteries For Load-Leveling The Utility Perspective on System Integration. IEEE Transactions on Power Apparatus and Systems. 1982 Sep(9):3315-3321.

[269]   Mbungu NT, Naidoo RM, Bansal RC, Siti MW, Tungadio DH. An overview of renewable energy resources and grid integration for commercial building applications. Journal of Energy Storage. 2020 Jun 1;29:101385.

[270]   Ibrahim H, Ilinca A, Perron J. Energy storage systems—Characteristics and comparisons. Renewable and sustainable energy reviews. 2008 Jun 1;12(5):1221-1250.

[271]   Divya KC, Østergaard J. Battery energy storage technology for power systems—An overview. Electric power systems research. 2009 Apr 1;79(4):511-520.

[272]   Kumar A, Meena NK, Singh AR, Deng Y, He X, Bansal RC, Kumar P. Strategic allocation and energy management of BESS for the provision of ancillary services in active distribution networks. Energy Procedia. 2019 Feb 1;158:2972-2978.

[273]   Kunisch HJ, Kramer KG, Dominik H. Battery energy storage another option for load-frequency-control and instantaneous reserve. IEEE Transactions on Energy Conversion. 1986 Sep(3):41-46.

[274]   Lu CF, Liu CC, Wu CJ. Dynamic modelling of battery energy storage system and application to power system stability. IEE Proceedings-Generation, Transmission and Distribution. 1995 Jul 1;142(4):429-435.

[275]   Dubarry M, Baure G, Pastor-Fernández C, Yu TF, Widanage WD, Marco J. Battery energy storage system modeling: A combined comprehensive approach. Journal of Energy Storage. 2019 Feb 1;21:172-185.

[276]   Parlikar A, Hesse H, Jossen A. Topology and efficiency analysis of utility-scale battery energy storage systems. InThe 13th International Renewable Energy Storage Conference 2019 (IRES 2019) 2019 Nov (pp. 119-131). Atlantis Press.

[277]   Biroon RA, Pisu P, Schoenwald D. Large-Scale Battery Energy Storage System Dynamic Model for Power System Stability Analysis. In2020 IEEE Texas Power and Energy Conference (TPEC) 2020 Feb 6 (pp. 1-5). IEEE.

[278]   Majumder R, Chakrabarti S, Ledwich G, Ghosh A. Advanced battery storage control for an autonomous microgrid. Electric Power Components and Systems. 2013 Jan 15;41(2):157-181.

[279]   Gayen PK, Majumdar R, Mondal S. Development and implementation of adaptive solar module–and battery characteristics–based real-time power management for solar battery system under grid-connected and-islanded conditions. International Transactions on Electrical Energy Systems. 2020 Mar;30(3):e12240.

[280]   Hill CA, Such MC, Chen D, Gonzalez J, Grady WM. Battery energy storage for enabling integration of distributed solar power generation. IEEE Transactions on smart grid. 2012 May 11;3(2):850-857.

[281]   Lawder MT, Suthar B, Northrop PW, De S, Hoff CM, Leitermann O, Crow ML, Santhanagopalan S, Subramanian VR. Battery energy storage system (BESS) and battery management system (BMS) for grid-scale applications. Proceedings of the IEEE. 2014 May 7;102(6):1014-1030.

[282]   Nazaripouya H, Chu CC, Pota HR, Gadh R. Battery energy storage system control for intermittency smoothing using an optimized two-stage filter. IEEE Transactions on Sustainable Energy. 2017 Sep 20;9(2):664-675.

[283]   Aditya SK, Das D. Application of battery energy storage system to load frequency control of an isolated power system. International journal of energy research. 1999 Mar 10;23(3):247-258.

[284]   Parise G, Martirano L, Kermani M, Kermani M. Designing a power control strategy in a microgrid using PID/fuzzy controller based on battery energy storage. In2017 IEEE International Conference on Environment and Electrical Engineering and 2017 IEEE Industrial and Commercial Power Systems Europe (EEEIC/I&CPS Europe) 2017 Jun 6 (pp. 1-5). IEEE.

[285]   Parmar KS. Load frequency control of multi-source power system with redox flow batteries: an analysis. International Journal of Computer Applications. 2014 Jan 1;88(8).

[286]   Kalyani S, Nagalakshmi S, Marisha R. Load frequency control using battery energy storage system in interconnected power system. In2012 Third International Conference on Computing, Communication and Networking Technologies (ICCCNT'12) 2012 Jul 26 (pp. 1-6). IEEE.

[287]   Kottick D, Blau M, Edelstein D. Battery energy storage for frequency regulation in an island power system. IEEE transactions on energy conversion. 1993 Sep;8(3):455-459.

[288]   Betancourt OA, Sanchez ZG, Saleh SA, Hill EF, Zhao X, Sanchez FP. Battery Energy Storage Systems for Primary Frequency Regulation in Island Power Systems. In2020 IEEE/IAS 56th Industrial and Commercial Power Systems Technical Conference (I&CPS) 2020 Jun 29 (pp. 1-10). IEEE.

[289]   Aditya SK, Das D. Battery energy storage for load frequency control of an interconnected power system. Electric power systems research. 2001 Jul 20;58(3):179-185.

[290]   Biswas S, Bera P. GA Application to optimization of AGC in two-area power system using battery energy storage. In2012 International Conference on Communications, Devices and Intelligent Systems (CODIS) 2012 Dec 28 (pp. 341-344). IEEE.

[291]   Aditya SK, Das D. Load-frequency control of an interconnected hydro-thermal power system with new area control error considering battery energy storage facility. International journal of energy research. 2000 May;24(6):525-538.

[292]   Chatterjee K. Effect of battery energy storage system on load frequency control under deregulation. International Journal of Emerging Electric Power Systems. 2011 Jun 13;12(3).

[293]   dos Santos GS, Grandinetti FJ, Alves RA, de Queiróz Lamas W. Design and Simulation of an Energy Storage System with Batteries Lead Acid and Lithium-Ion for an Electric Vehicle: Battery vs. Conduction Cycle Efficiency Analysis. IEEE Latin America Transactions. 2020 Jun 9;18(08):1345-1352.

[294]   Mi Y, He X, Hao X, Li Z, Fu Y, Wang C, Wang J. Frequency control strategy of multi-area hybrid power system based on frequency division and sliding mode algorithm. IET Generation, Transmission & Distribution. 2019 Apr;13(7):1145-1152.

[295]   Sasaki T, Kadoya T, Enomoto K. Study on load frequency control using redox flow batteries. IEEE Transactions on Power Systems. 2004 Feb 19;19(1):660-667.

[296]   Siti MW, Tungadio DH, Sun Y. Optimal control and management of load frequency in microgrid. IET Renew. Power Gener. 2019;13(13):2376-2382.

[297]   Saikia LC, Das SK, Dash P, Raju M. Multi—Area AGC with AC/DC link and BES and Cuckoo Search optimized PID controller. InProceedings of the 2015 Third International Conference on Computer, Communication, Control and Information Technology (C3IT) 2015 Feb 7 (pp. 1-6). IEEE.

[298]   Dekaraja B, Saikia LC. Performance of redox flow battery in combined frequency and voltage control of multi-area multi-source system using CFOPDN-FOPIDN controller. International Transactions on Electrical Energy Systems.2021 Mar; 31(3):e12782.

[299]   Senapati MK, Pradhan C, Samantaray SR, Nayak PK. Improved power management control strategy for renewable energy-based DC micro-grid with energy storage integration. IET Generation, Transmission & Distribution. 2019 May 6;13(6):838-849.

[300]   Valvo M, Wicks FE, Robertson D, Rudin S. Development and application of an improved equivalent circuit model of a lead acid battery. InIECEC 96. Proceedings of the 31st Intersociety Energy Conversion Engineering Conference 1996 Aug 11 (Vol. 2, pp. 1159-1163). IEEE.

[301]   Rayguru MM, Madichetty S, Mishra S. Battery super-capacitor hybrid system for electrical vehicle transportation's systems–an energy integrated approach. IET Energy Systems Integration. 2020 Oct 5;2(3):282-288.

[302]   McKeon BB, Furukawa J, Fenstermacher S. Advanced lead–acid batteries and the development of grid-scale energy storage systems. Proceedings of the IEEE. 2014 May 1;102(6):951-963.

[303]   Torkashvand M, Khodadadi A, Sanjareh MB, Nazary MH. A Life Cycle-Cost Analysis of Li-ion and Lead-Acid BESSs and Their Actively Hybridized ESSs With Supercapacitors for Islanded Microgrid Applications. IEEE Access. 2020 Aug 18;8:153215-153225.

[304]   Bhattacharjee A, Verma A, Mishra S, Saha TK. Estimating State of Charge for xEV Batteries Using 1D Convolutional Neural Networks and Transfer Learning. IEEE Transactions on Vehicular Technology. 2021 Mar 8;70(4):3123-3135.

[305]   Singh Y, Singh B, Mishra S. Multifunctional Control for PV-Integrated Battery Energy Storage System With Improved Power Quality. IEEE Transactions on Industry Applications. 2020 Aug 31;56(6):6835-6845.

[306]   Sharma S, Singh B, Mishra S. Economic operation and quality control in PV-BES-DG-based autonomous system. IEEE Transactions on Industrial Informatics. 2019 Aug 15;16(4):2346-2356.

[307]   Singh Y, Singh B, Mishra S. Flexible control for PV integrated battery energy storage system. In2019 IEEE Energy Conversion Congress and Exposition (ECCE) 2019 (pp. 6686-6692). IEEE.

[308]   Jha S, Singh B, Mishra S. Performance Enhancement of PV–DG–BS Distributed Generation System in Islanded Mode. Journal of The Institution of Engineers (India): Series B. 2021 Apr;102(2):311-321.

[309]   Pathak N, Hu Z. Hybrid-peak-area-based performance index criteria for AGC of multi-area power systems. IEEE Transactions on Industrial Informatics. 2019 Mar 18;15(11):5792-5802.

[310]   Bhamu S, Bhatti TS, Pathak N. Modelling and dynamic stability study of interconnected system of renewable energy sources and grid for rural electrification. International Journal of Emerging Electric Power Systems. 2019 Feb 1;20(1).

[311]   Pathak N, Verma A, Bhatti TS, Nasiruddin I, Luo H, Hu Z. Generation rate constraints physical identification and modeling in AGC of multi-area power systems. Electric Power Components and Systems. 2019 Jul 21;47(11-12):966-984.

[312]   Liu L, Hu Z, Duan X, Pathak N. Data-Driven Distributionally Robust Optimization for Real-Time Economic Dispatch Considering Secondary Frequency Regulation Cost. IEEE Transactions on Power Systems. 2021 Feb 4.

[313] Kumar J, Verma A, Bhatti TS. An Optimization Algorithm for Unit Commitment Economic Emission Dispatch Problem. InApplications of Artificial Intelligence Techniques in Engineering 2019 (pp. 113-129). Springer, Singapore.

[314] Prakash S, Mishra S. Fast terminal sliding mode control for improved transient state power sharing between parallel VSCs in an autonomous microgrid under different loading conditions. IET Renewable Power Generation. 2020 Apr;14(6):1063-1073.

[315] Nougain V, Mishra S, Jena SS. Resilient Protection of Medium Voltage DC Microgrids against Cyber Intrusion. IEEE Transactions on Power Delivery. 2021 Apr 21.

[316] Basanez L, Riera J, Ayza J. Modelling and simulation of multiarea power system load-frequency control. Mathematics and computers in Simulation. 1984 Feb 1;26(1):54-62.

[317] Mudaliyar S, Duggal B, Mishra S. Distributed tie-line power flow control of autonomous dc microgrid clusters. IEEE Transactions on Power Electronics. 2020 Mar 16;35(10):11250-11266.

[318] Pathak N, Verma A, Bhatti TS, Nasiruddin I. Modeling of HVDC tie links and their utilization in AGC/LFC operations of multiarea power systems. IEEE Transactions on Industrial Electronics. 2018 May 10;66(3):2185-2197.

[319] Egido I, Fernández-Bernal F, Rouco L, Porras E, Sáiz-Chicharro Á. Modeling of thermal generating units for automatic generation control purposes. IEEE transactions on control systems technology. 2004 Feb 26;12(1):205-210.

[320] Pathak N, Verma A, Bhatti TS. Automatic generation control of thermal power system under varying steam turbine dynamic model parameters based on generation schedules of the plants. The Journal of Engineering. 2016 Aug;2016(8):302-314.

[321] IEEE PES committee Report. Dynamic models for steam and hydro turbines in power system studies. IEEE transactions on power apparatus and systems. 1973 Nov(6):1904-1915.

[322] Kishor N, Saini RP, Singh SP. A review on hydropower plant models and control. Renewable and Sustainable Energy Reviews. 2007 Jun 1;11(5):776-796.

[323] Singh VK, Singal SK. Operation of hydro power plants-a review. Renewable and Sustainable Energy Reviews. 2017 Mar 1;69:610-619.

215

[324] Hajagos LM, Berube GR. Utility experience with gas turbine testing and modeling. In2001 IEEE Power Engineering Society Winter Meeting. Conference Proceedings (Cat. No. 01CH37194) 2001 Jan 28 (Vol. 2, pp. 671-677). IEEE.

[325] Karamov D, Naumov I, Ivanov D, Podyachikh S. Modelling of diesel generator operating modes on the basis of the engine speed characteristic in autonomous photovoltaic systems. InICCS-DE 2020 (pp. 129-137).

[326] Kabir KM, Nath A, Mazumder S, Islam MO. Modelling & simulation of a grid connected hybrid power plant with photovoltaic, wind & diesel power for Cox's Bazar. In2016 2nd International Conference on Electrical, Computer & Telecommunication Engineering (ICECTE) 2016 Dec 8 (pp. 1-4). IEEE.

[327] Soder L, Holttinen H. On methodology for modelling wind power impact on power systems. International Journal of Global Energy Issues. 2008 Jan 1;29(1-2):181-198.

[328] Lund H, Münster E. Modelling of energy systems with a high percentage of CHP and wind power. Renewable Energy. 2003 Nov 1;28(14):2179-2193.

[329] Slootweg JG, Kling WL. Modelling and analysing impacts of wind power on transient stability of power systems. Wind Engineering. SAGE Publications Sage UK: London, England 2002 Jan;26(1):3-20.

[330] Sahu RK, Gorripotu TS, Panda S. Automatic generation control of multi-area power systems with diverse energy sources using teaching learning based optimization algorithm. Engineering Science and Technology, an International Journal. 2016 Mar 1;19(1):113-134.

[331] Sahu RK, Panda S, Padhan S. Optimal gravitational search algorithm for automatic generation control of interconnected power systems. Ain shams engineering journal. 2014 Sep 1;5(3):721-733.

APPENDIX A. State Cost Weighting Matrices:

Different approaches are applied to develop different structures of state cost weighting matrix (Q) as Qm, Ql and Qs for different power systems.

Nominal parameter of three area Non-reheat thermal hydro-gas power system

$$
Qm =
\begin{bmatrix}
0.18 & 0 & 0 & 0 & 0 & 0 & 0 & 0 & 0 & 0 & 0 & 0 & 0 & 0 & 0.42 & 0.42 & 0 & 0 & 0 & 0 \\
0 & 0 & 0 & 0 & 0 & 0 & 0 & 0 & 0 & 0 & 0 & 0 & 0 & 0 & 0 & 0 & 0 & 0 & 0 & 0 \\
0 & 0 & 0 & 0 & 0 & 0 & 0 & 0 & 0 & 0 & 0 & 0 & 0 & 0 & 0 & 0 & 0 & 0 & 0 & 0 \\
0 & 0 & 0 & 0.18 & 0 & 0 & 0 & 0 & 0 & 0 & 0 & 0 & -0.42 & 0 & 0.42 & 0 & 0 & 0 \\
0 & 0 & 0 & 0 & 0 & 0 & 0 & 0 & 0 & 0 & 0 & 0 & 0 & 0 & 0 & 0 & 0 & 0 & 0 & 0 \\
0 & 0 & 0 & 0 & 0 & 0 & 0 & 0 & 0 & 0 & 0 & 0 & 0 & 0 & 0 & 0 & 0 & 0 & 0 & 0 \\
0 & 0 & 0 & 0 & 0 & 0 & 0 & 0 & 0 & 0 & 0 & 0 & 0 & 0 & 0 & 0 & 0 & 0 & 0 & 0 \\
0 & 0 & 0 & 0 & 0 & 0 & 0 & 0.18 & 0 & 0 & 0 & 0 & 0 & -0.42 & -0.42 & 0 & 0 & 0 \\
0 & 0 & 0 & 0 & 0 & 0 & 0 & 0 & 0 & 0 & 0 & 0 & 0 & 0 & 0 & 0 & 0 & 0 & 0 & 0 \\
0 & 0 & 0 & 0 & 0 & 0 & 0 & 0 & 0 & 0 & 0 & 0 & 0 & 0 & 0 & 0 & 0 & 0 & 0 & 0 \\
0 & 0 & 0 & 0 & 0 & 0 & 0 & 0 & 0 & 0 & 0 & 0 & 0 & 0 & 0 & 0 & 0 & 0 & 0 & 0 \\
0 & 0 & 0 & 0 & 0 & 0 & 0 & 0 & 0 & 0 & 0 & 0 & 0 & 0 & 0 & 0 & 0 & 0 & 0 & 0 \\
0.42 & 0 & 0 & -0.42 & 0 & 0 & 0 & 0 & 0 & 0 & 0 & 0 & 2 & 1 & -1 & 0 & 0 & 0 \\
0.42 & 0 & 0 & 0 & 0 & 0 & -0.42 & 0 & 0 & 0 & 0 & 1 & 2 & 10 & 0 & 0 \\
0 & 0 & 0 & 0.42 & 0 & 0 & -0.42 & 0 & 0 & 0 & 0 & -1 & 1 & 2 & 0 & 0 & 0 \\
0 & 0 & 0 & 0 & 0 & 0 & 0 & 0 & 0 & 0 & 0 & 0 & 0 & 0 & 1 & 0 & 0 \\
0 & 0 & 0 & 0 & 0 & 0 & 0 & 0 & 0 & 0 & 0 & 0 & 0 & 0 & 0 & 1 & 0 \\
0 & 0 & 0 & 0 & 0 & 0 & 0 & 0 & 0 & 0 & 0 & 0 & 0 & 0 & 0 & 0 & 1
\end{bmatrix}
$$

$$
Ql =
\begin{bmatrix}
1 & 0 & 0 & 0 & 0 & 0 & 0 & 0 & 0 & 0 & 0 & 0 & 0 & 0 & 0 & 0 & 0 & 0 & 0 & 0 \\
0 & 1 & 0 & 0 & 0 & 0 & 0 & 0 & 0 & 0 & 0 & 0 & 0 & 0 & 0 & 0 & 0 & 0 & 0 & 0 \\
0 & 0 & 1 & 0 & 0 & 0 & 0 & 0 & 0 & 0 & 0 & 0 & 0 & 0 & 0 & 0 & 0 & 0 & 0 & 0 \\
0 & 0 & 0 & 1 & 0 & 0 & 0 & 0 & 0 & 0 & 0 & 0 & 0 & 0 & 0 & 0 & 0 & 0 & 0 & 0 \\
0 & 0 & 0 & 0 & 1 & 0 & 0 & 0 & 0 & 0 & 0 & 0 & 0 & 0 & 0 & 0 & 0 & 0 & 0 & 0 \\
0 & 0 & 0 & 0 & 0 & 1 & 0 & 0 & 0 & 0 & 0 & 0 & 0 & 0 & 0 & 0 & 0 & 0 & 0 & 0 \\
0 & 0 & 0 & 0 & 0 & 0 & 1 & 0 & 0 & 0 & 0 & 0 & 0 & 0 & 0 & 0 & 0 & 0 & 0 & 0 \\
0 & 0 & 0 & 0 & 0 & 0 & 0 & 1 & 0 & 0 & 0 & 0 & 0 & 0 & 0 & 0 & 0 & 0 & 0 & 0 \\
0 & 0 & 0 & 0 & 0 & 0 & 0 & 0 & 1 & 0 & 0 & 0 & 0 & 0 & 0 & 0 & 0 & 0 & 0 & 0 \\
0 & 0 & 0 & 0 & 0 & 0 & 0 & 0 & 0 & 1 & 0 & 0 & 0 & 0 & 0 & 0 & 0 & 0 & 0 & 0 \\
0 & 0 & 0 & 0 & 0 & 0 & 0 & 0 & 0 & 0 & 1 & 0 & 0 & 0 & 0 & 0 & 0 & 0 & 0 & 0 \\
0 & 0 & 0 & 0 & 0 & 0 & 0 & 0 & 0 & 0 & 0 & 1 & 0 & 0 & 0 & 0 & 0 & 0 & 0 & 0 \\
0 & 0 & 0 & 0 & 0 & 0 & 0 & 0 & 0 & 0 & 0 & 0 & 1 & 0 & 0 & 0 & 0 & 0 & 0 & 0 \\
0 & 0 & 0 & 0 & 0 & 0 & 0 & 0 & 0 & 0 & 0 & 0 & 0 & 1 & 0 & 0 & 0 & 0 & 0 & 0 \\
0 & 0 & 0 & 0 & 0 & 0 & 0 & 0 & 0 & 0 & 0 & 0 & 0 & 0 & 1 & 0 & 0 & 0 & 0 & 0 \\
0 & 0 & 0 & 0 & 0 & 0 & 0 & 0 & 0 & 0 & 0 & 0 & 0 & 0 & 0 & 1 & 0 & 0 & 0 & 0 \\
0 & 0 & 0 & 0 & 0 & 0 & 0 & 0 & 0 & 0 & 0 & 0 & 0 & 0 & 0 & 0 & 1 & 0 & 0 & 0 \\
0 & 0 & 0 & 0 & 0 & 0 & 0 & 0 & 0 & 0 & 0 & 0 & 0 & 0 & 0 & 0 & 0 & 1 & 0 & 0 \\
0 & 0 & 0 & 0 & 0 & 0 & 0 & 0 & 0 & 0 & 0 & 0 & 0 & 0 & 0 & 0 & 0 & 0 & 1 & 0 \\
0 & 0 & 0 & 0 & 0 & 0 & 0 & 0 & 0 & 0 & 0 & 0 & 0 & 0 & 0 & 0 & 0 & 0 & 0 & 1
\end{bmatrix}
$$

$$
Qs =
\begin{bmatrix}
0.06 & 0 & 0 & 0 & 0 & 0 & 0 & 0 & 0 & 0 & 0 & 0 & 0 & 0 & 0 & 0 & 0 & 0 & 0 & 0 \\
0 & 0.07 & 0 & 0 & 0 & 0 & 0 & 0 & 0 & 0 & 0 & 0 & 0 & 0 & 0 & 0 & 0 & 0 & 0 & 0 \\
0 & 0 & 0.08 & 0 & 0 & 0 & 0 & 0 & 0 & 0 & 0 & 0 & 0 & 0 & 0 & 0 & 0 & 0 & 0 & 0 \\
0 & 0 & 0 & 0.09 & 0 & 0 & 0 & 0 & 0 & 0 & 0 & 0 & 0 & 0 & 0 & 0 & 0 & 0 & 0 & 0 \\
0 & 0 & 0 & 0 & 0.11 & 0 & 0 & 0 & 0 & 0 & 0 & 0 & 0 & 0 & 0 & 0 & 0 & 0 & 0 & 0 \\
0 & 0 & 0 & 0 & 0 & 0.13 & 0 & 0 & 0 & 0 & 0 & 0 & 0 & 0 & 0 & 0 & 0 & 0 & 0 & 0 \\
0 & 0 & 0 & 0 & 0 & 0 & 0.16 & 0 & 0 & 0 & 0 & 0 & 0 & 0 & 0 & 0 & 0 & 0 & 0 & 0 \\
0 & 0 & 0 & 0 & 0 & 0 & 0 & 0.18 & 0 & 0 & 0 & 0 & 0 & 0 & 0 & 0 & 0 & 0 & 0 & 0 \\
0 & 0 & 0 & 0 & 0 & 0 & 0 & 0 & 0.22 & 0 & 0 & 0 & 0 & 0 & 0 & 0 & 0 & 0 & 0 & 0 \\
0 & 0 & 0 & 0 & 0 & 0 & 0 & 0 & 0 & 0.26 & 0 & 0 & 0 & 0 & 0 & 0 & 0 & 0 & 0 & 0 \\
0 & 0 & 0 & 0 & 0 & 0 & 0 & 0 & 0 & 0 & 0.31 & 0 & 0 & 0 & 0 & 0 & 0 & 0 & 0 & 0 \\
0 & 0 & 0 & 0 & 0 & 0 & 0 & 0 & 0 & 0 & 0 & 0.36 & 0 & 0 & 0 & 0 & 0 & 0 & 0 & 0 \\
0 & 0 & 0 & 0 & 0 & 0 & 0 & 0 & 0 & 0 & 0 & 0 & 0.43 & 0 & 0 & 0 & 0 & 0 & 0 & 0 \\
0 & 0 & 0 & 0 & 0 & 0 & 0 & 0 & 0 & 0 & 0 & 0 & 0 & 0.51 & 0 & 0 & 0 & 0 & 0 & 0 \\
0 & 0 & 0 & 0 & 0 & 0 & 0 & 0 & 0 & 0 & 0 & 0 & 0 & 0 & 0.60 & 0 & 0 & 0 & 0 & 0 \\
0 & 0 & 0 & 0 & 0 & 0 & 0 & 0 & 0 & 0 & 0 & 0 & 0 & 0 & 0 & 0.71 & 0 & 0 & 0 & 0 \\
0 & 0 & 0 & 0 & 0 & 0 & 0 & 0 & 0 & 0 & 0 & 0 & 0 & 0 & 0 & 0 & 0.84 & 0 & 0 & 0 \\
0 & 0 & 0 & 0 & 0 & 0 & 0 & 0 & 0 & 0 & 0 & 0 & 0 & 0 & 0 & 0 & 0 & 0 & 0 & 1
\end{bmatrix}
$$

Nominal parameter of three area Non-reheat thermal power system

$$Qm = \begin{bmatrix}
0.18 & 0 & 0 & 0 & 0 & 0 & 0 & 0 & 0 & 0.42 & 0 & -0.42 & 0 & 0 & 0 \\
0 & 0 & 0 & 0 & 0 & 0 & 0 & 0 & 0 & 0 & 0 & 0 & 0 & 0 & 0 \\
0 & 0 & 0 & 0 & 0 & 0 & 0 & 0 & 0 & 0 & 0 & 0 & 0 & 0 & 0 \\
0 & 0 & 0 & .18 & 0 & 0 & 0 & 0 & 0 & -0.42 & 0 & 0.42 & 0 & 0 & 0 \\
0 & 0 & 0 & 0 & 0 & 0 & 0 & 0 & 0 & 0 & 0 & 0 & 0 & 0 & 0 \\
0 & 0 & 0 & 0 & 0 & 0 & 0 & 0 & 0 & 0 & 0 & 0 & 0 & 0 & 0 \\
0 & 0 & 0 & 0 & 0 & 0 & 0.18 & 0 & 0 & 0 & -0.42 & 0.42 & 0 & 0 & 0 \\
0 & 0 & 0 & 0 & 0 & 0 & 0 & 0 & 0 & 0 & 0 & 0 & 0 & 0 & 0 \\
0 & 0 & 0 & 0 & 0 & 0 & 0 & 0 & 0 & 0 & 0 & 0 & 0 & 0 & 0 \\
0.42 & 0 & 0 & -0.42 & 0 & 0 & 0 & 0 & 0 & 2 & 1 & -1 & 0 & 0 & 0 \\
0 & 0 & 0 & 0 & 0 & 0 & -0.42 & 0 & 0 & 1 & 2 & 1 & 0 & 0 & 0 \\
-0.42 & 0 & 0 & 0.42 & 0 & 0 & 0.42 & 0 & 0 & -1 & 1 & 2 & 0 & 0 & 0 \\
0 & 0 & 0 & 0 & 0 & 0 & 0 & 0 & 0 & 0 & 0 & 0 & 1 & 0 & 0 \\
0 & 0 & 0 & 0 & 0 & 0 & 0 & 0 & 0 & 0 & 0 & 0 & 0 & 1 & 0 \\
0 & 0 & 0 & 0 & 0 & 0 & 0 & 0 & 0 & 0 & 0 & 0 & 0 & 0 & 1
\end{bmatrix}$$

$$Q1 = \begin{bmatrix}
1 & 0 & 0 & 0 & 0 & 0 & 0 & 0 & 0 & 0 & 0 & 0 & 0 & 0 & 0 & 0 \\
0 & 1 & 0 & 0 & 0 & 0 & 0 & 0 & 0 & 0 & 0 & 0 & 0 & 0 & 0 & 0 \\
0 & 0 & 1 & 0 & 0 & 0 & 0 & 0 & 0 & 0 & 0 & 0 & 0 & 0 & 0 & 0 \\
0 & 0 & 0 & 1 & 0 & 0 & 0 & 0 & 0 & 0 & 0 & 0 & 0 & 0 & 0 & 0 \\
0 & 0 & 0 & 0 & 1 & 0 & 0 & 0 & 0 & 0 & 0 & 0 & 0 & 0 & 0 & 0 \\
0 & 0 & 0 & 0 & 0 & 1 & 0 & 0 & 0 & 0 & 0 & 0 & 0 & 0 & 0 & 0 \\
0 & 0 & 0 & 0 & 0 & 0 & 1 & 0 & 0 & 0 & 0 & 0 & 0 & 0 & 0 & 0 \\
0 & 0 & 0 & 0 & 0 & 0 & 0 & 1 & 0 & 0 & 0 & 0 & 0 & 0 & 0 & 0 \\
0 & 0 & 0 & 0 & 0 & 0 & 0 & 0 & 1 & 0 & 0 & 0 & 0 & 0 & 0 & 0 \\
0 & 0 & 0 & 0 & 0 & 0 & 0 & 0 & 0 & 1 & 0 & 0 & 0 & 0 & 0 & 0 \\
0 & 0 & 0 & 0 & 0 & 0 & 0 & 0 & 0 & 0 & 1 & 0 & 0 & 0 & 0 & 0 \\
0 & 0 & 0 & 0 & 0 & 0 & 0 & 0 & 0 & 0 & 0 & 1 & 0 & 0 & 0 & 0 \\
0 & 0 & 0 & 0 & 0 & 0 & 0 & 0 & 0 & 0 & 0 & 0 & 1 & 0 & 0 & 0 \\
0 & 0 & 0 & 0 & 0 & 0 & 0 & 0 & 0 & 0 & 0 & 0 & 0 & 1 & 0 & 0 \\
0 & 0 & 0 & 0 & 0 & 0 & 0 & 0 & 0 & 0 & 0 & 0 & 0 & 0 & 1 & 0 \\
0 & 0 & 0 & 0 & 0 & 0 & 0 & 0 & 0 & 0 & 0 & 0 & 0 & 0 & 0 & 1
\end{bmatrix}$$

$$Qs = \begin{bmatrix}
0.06 & 0 & 0 & 0 & 0 & 0 & 0 & 0 & 0 & 0 & 0 & 0 & 0 & 0 & 0 & 0 \\
0 & 0.11 & 0 & 0 & 0 & 0 & 0 & 0 & 0 & 0 & 0 & 0 & 0 & 0 & 0 & 0 \\
0 & 0 & 0.20 & 0 & 0 & 0 & 0 & 0 & 0 & 0 & 0 & 0 & 0 & 0 & 0 & 0 \\
0 & 0 & 0 & 0.07 & 0 & 0 & 0 & 0 & 0 & 0 & 0 & 0 & 0 & 0 & 0 & 0 \\
0 & 0 & 0 & 0 & 0.13 & 0 & 0 & 0 & 0 & 0 & 0 & 0 & 0 & 0 & 0 & 0 \\
0 & 0 & 0 & 0 & 0 & 0.24 & 0 & 0 & 0 & 0 & 0 & 0 & 0 & 0 & 0 & 0 \\
0 & 0 & 0 & 0 & 0 & 0 & 0.09 & 0 & 0 & 0 & 0 & 0 & 0 & 0 & 0 & 0 \\
0 & 0 & 0 & 0 & 0 & 0 & 0 & 0.16 & 0 & 0 & 0 & 0 & 0 & 0 & 0 & 0 \\
0 & 0 & 0 & 0 & 0 & 0 & 0 & 0 & 0.30 & 0 & 0 & 0 & 0 & 0 & 0 & 0 \\
0 & 0 & 0 & 0 & 0 & 0 & 0 & 0 & 0 & 0.36 & 0 & 0 & 0 & 0 & 0 & 0 \\
0 & 0 & 0 & 0 & 0 & 0 & 0 & 0 & 0 & 0 & 0.44 & 0 & 0 & 0 & 0 & 0 \\
0 & 0 & 0 & 0 & 0 & 0 & 0 & 0 & 0 & 0 & 0 & 0.54 & 0 & 0 & 0 & 0 \\
0 & 0 & 0 & 0 & 0 & 0 & 0 & 0 & 0 & 0 & 0 & 0 & 0.67 & 0 & 0 & 0 \\
0 & 0 & 0 & 0 & 0 & 0 & 0 & 0 & 0 & 0 & 0 & 0 & 0 & 0.82 & 0 & 0 \\
0 & 0 & 0 & 0 & 0 & 0 & 0 & 0 & 0 & 0 & 0 & 0 & 0 & 0 & 0 & 1
\end{bmatrix}$$

Nominal parameter of three area Non-reheat thermal-hydro-non reheat thermal power system

$Qm =$

```
0.18 0 0 0 0 0 0 0  0 0 0.42 0.42 0 0 0  0
0 0 0  0 0  0 0 0 0  0 0 0 0  0 0 0
0 0 0  0 0  0 0 0  0 0 0 0  0 0 0
0 0 0 0.18 0 0 0 0 0  0 -0.42 0 0.42 0 0 0
0 0 0  0 0  0 0 0 0  0 0 0 0  0 0 0
0 0 0  0 0  0 0 0 0  0 0 0 0  0 0 0
0 0 0  0 0  0 0 0 0  0 0 0 0  0 0 0
0 0 0 0 0 0 0 0.18 0 0  0 -0.42 -0.42 0 0 0
0 0 0  0 0  0 0 0 0  0 0 0 0  0 0 0
0 0 0  0 0  0 0 0 0  0 0 0 0  0 0 0
0.42 0 0  -0.42 0 0  0 0 0 0 2 1 -1 0 0 0
0.42 0 0  0 0 0  0 -0.42 0  0 1 2 1 0 0 0
0 0 0 0.42  0 0 0 -0.42 0  0 -1 1 2  0 0 0
0 0 0  0 0  0 0 0 0  0 0 0 1 0  0
0 0 0  0 0  0 0 0 0  0 0 0 0 1  0
0 0 0  0 0  0 0 0 0  0 0 0 0 0 1
```

$Q1=$

```
1 0 0 0 0 0 0 0 0 0 0 0 0 0 0 0 0
0 1 0 0 0 0 0 0 0 0 0 0 0 0 0 0 0
0 0 1 0 0 0 0 0 0 0 0 0 0 0 0 0 0
0 0 0 1 0 0 0 0 0 0 0 0 0 0 0 0 0
0 0 0 0 1 0 0 0 0 0 0 0 0 0 0 0 0
0 0 0 0 0 1 0 0 0 0 0 0 0 0 0 0 0
0 0 0 0 0 0 1 0 0 0 0 0 0 0 0 0 0
0 0 0 0 0 0 0 1 0 0 0 0 0 0 0 0 0
0 0 0 0 0 0 0 0 1 0 0 0 0 0 0 0 0
0 0 0 0 0 0 0 0 0 1 0 0 0 0 0 0 0
0 0 0 0 0 0 0 0 0 0 1 0 0 0 0 0 0
0 0 0 0 0 0 0 0 0 0 0 1 0 0 0 0 0
0 0 0 0 0 0 0 0 0 0 0 0 1 0 0 0 0
0 0 0 0 0 0 0 0 0 0 0 0 0 1 0 0 0
0 0 0 0 0 0 0 0 0 0 0 0 0 0 1 0 0
0 0 0 0 0 0 0 0 0 0 0 0 0 0 0 1 0
0 0 0 0 0 0 0 0 0 0 0 0 0 0 0 0 1
```

$Qs=$

```
0.06 0 0 0 0 0 0 0 0 0 0 0 0 0 0 0 0
0 0.07 0 0 0 0 0 0 0 0 0 0 0 0 0 0 0
0 0 0.08 0 0 0 0 0 0 0 0 0 0 0 0 0 0
0 0 0 0.10 0 0 0 0 0 0 0 0 0 0 0 0 0
0 0 0 0 0.12 0 0 0 0 0 0 0 0 0 0 0 0
0 0 0 0 0 0.15 0 0 0 0 0 0 0 0 0 0 0
0 0 0 0 0 0 0.18 0 0 0 0 0 0 0 0 0 0
0 0 0 0 0 0 0 0.22 0 0 0 0 0 0 0 0 0
0 0 0 0 0 0 0 0 0.26 0 0 0 0 0 0 0 0
0 0 0 0 0 0 0 0 0 0.32 0 0 0 0 0 0 0
0 0 0 0 0 0 0 0 0 0 0.39 0 0 0 0 0 0
0 0 0 0 0 0 0 0 0 0 0 0.47 0 0 0 0 0
0 0 0 0 0 0 0 0 0 0 0 0 0.57 0 0 0 0
0 0 0 0 0 0 0 0 0 0 0 0 0 0.68 0 0 0
0 0 0 0 0 0 0 0 0 0 0 0 0 0 0.82 0
0 0 0 0 0 0 0 0  0 0 0 0  0 0 0 1
```

APPENDIX B - Power System Data

Chapter4

Nominal parameter of two-area interconnected diverse source power system with varying participation [141]

$\beta_1 = \beta_2 = 0.425$p.u.Mw/Hz, $K_P = 120$, $T_P = 20$s, $P_{tie12} = 200$MW, $T_{t1} = T_{t2} = 0.3$s, $T_{g1} = T_{g2} = 0.08$s, $K_{r1} = K_{r1} = 0.3$, $T_{r1} = T_{r1} = 10$s, $K_{t1} = K_{t2} = 0.6$, $T_{RH1} = T_{RH2} = 41.6$s, $T_{R1} = T_{R2} = 5$s, $T_{GH1} = T_{GH2} = 0.51$s, $T_{W1} = T_{W2} = 1$s, $K_{h1} = K_{h2} = 0.3$, $X_1 = X_2 = 0.6$, $Y_1 = Y_2 = 1$, $b_1 = b_2 = 0.05$, $c_1 = c_2 = 1$, $T_{F1} = T_{F2} = 0.23$s, $T_{CR1} = T_{CR2} = 0.01$s, $T_{CD1} = T_{CD2} = 0.2$s , $K_{g1} = K_{g2} = 0.1$

Chapter 5

Typical values of two area interconnected thermal-hydro-wind and thermal-hydro-diesel power system with nonlinearities [330]

$Pr_1 = Pr_2 = 2000$MW, $F_1^0 = F_2^0 = 60$Hz, $Kps_1 = Kps_1 = 120$Hz/puMW, $B_1 = B_2 = 0.425$puMW/Hz, $R_1 = R_2 = R_3 = R_4 = R_5 = R_6 = 2.4$Hz/puMW, $Tg_1 = Tg_2 = 0.08$s, $Tr_1 = Tr_2 = 10$s, $Kr_1 = Kr_2 = 0.33$s, $T_{t1} = T_{t1} = 0.3$s, $Tgh_1 = Tgh_2 = 48.7$s, $Trh_1 = Trh_1 = 10$s, $Trs_1 = Trs_1 = 0.513$s, $Tw_1 = Tw_2 = 1$s, $a_{12} = -1$, $T_{12} = 0.0866$pu, $Tp_1 = 6$, $Kp_1 = 1.25$s, $Kp_2 = 1.4$, $Tp_2 = 0.041$, $K_{diesel} = 16.5$, $K_3 = 0.92$.

Typical values of two area interconnected thermal-hydro-wind and thermal-hydro-diesel power system with nonlinearities [144]

$Pr_1 = Pr_2 = 2000$MW, $F_1^0 = F_2^0 = 60$Hz, $Kps_1 = Kps_1 = 120$Hz/puMW, $B_1 = B_2 = 0.425$puMW/Hz, $R_1 = R_2 = R_3 = R_4 = R_5 = R_6 = 2.4$Hz/puMW, $Tg_1 = Tg_2 = 0.08$s, $Tr_1 = Tr_2 = 10$s, $Kr_1 = Kr_2 = 0.33$s, $T_{t1} = T_{t1} = 0.3$s, $Tgh_1 = Tgh_2 = 0.2$s, $Trh_1 = Trh_1 = 28.75$s, $Trs_1 = Trs_1 = 5$s, $Tw_1 = Tw_2 = 1.1$s, $a_{12} = -1$, $T_{12} = 0.0545$pu, $Tp_1 = 0.6$, $Kp_1 = 1.25$, $Kp_2 = 1.3$, $Tp_2 = 0.041$, $K_{diesel} = 16.5$.

Chapter 6

Typical values of three area interconnected power system with thermal source, hydro sourceand gas source [141]

$Pr_1 = Pr_2 = Pr_3 = 2000$MW, $F_1^0 = F_2^0 = F_3^0 = 60$Hz, $R_1 = R_2 = R_3 = 2.4$Hz/p.u.MW, $B_1 = B_2 = B_3 = 0.42$ p.u.MW/Hz, $K_{p1} = K_{p2} = K_{p3} = 120$, $T_{p1} = T_{p2} = T_{p3} = 20$s, $P_{tie} = 200$MW, $T_t = 0.3$s, $T_g = 0.08$s, $2\Pi T_1 = 0.15$p.u.MW, $2\Pi T_{23} = 0.15$p.u.MW, $2\Pi T_{31} = 0.15$p.u.MW, $T_{RH1} = 41.6$s, $T_{RS} = 5$s, $T_{GH} = 0.51$ s, $T_W = 1$s, $X = 0.6$, $Y = 1$, $b = 0.05$, $c = 1$, $T_F = 0.23$s, $T_{CR} = 0.01$s, $T_{CD} = 0.2$s.

Chapter 7

Typical values of three area interconnected power system with thermal source, hydro source, gas source and SMES [122,141, 242, 256].

$Pr_1=Pr_2=Pr_3=2000MW, F_1{}^0=F_2{}^0=F_3{}^0=60Hz, R_1=R_2=R_3=2.4Hz/p.u.MW, B_1=B_2=B_3=0.42$ p.u.MW/Hz,$K_{p1}=K_{p2}=K_{p3}=120, T_{p1}=T_{p2}=T_{p3}=20s, P_{tie}=200MW, T_t=0.3s, T_g=0.08s, 2\Pi T_{12}$ $=0.15p.u.MW, 2\Pi T_{23}=0.15p.u.MW, 2\Pi T_{31}=0.15p.u.MW, T_{RH}=41.6s, T_{RS}=5s, T_{GH}=0.51s,$ $T_W=1s, X=0.6, Y=1, b=0.05, c=1, T_F=0.23s, T_{CR}=0.01s, T_{CD}=0.2s, SMES=30MJ, L=2.65H,$ $T_{dcs}=0.03s, K_{so}=100kV/unit ACE, K_{Ids}=0.2kV/kA, I_{dso}=4.5kA, I_{dsmin}=4kA, I_{dsmax}=4.9kA.$

Chapter 8

Typical values of three area interconnected power system with reheat thermal,non reheat thermal source, hydro source, gas source and BESS [141,156,283]

$Pr_1=Pr_2=Pr_3=2000MW, F_1{}^0=F_2{}^0=F_3{}^0=60Hz, R_1=R_2=R_3=2.4Hz/p.u.MW, B_1=B_2=B_3=0.42$ p.u.MW/Hz,$K_{p1}=K_{p2}=K_{p3}=120, T_{p1}=T_{p2}=T_{p3}=20s, P_{tie}=200MW, T_t=0.3s, T_g=0.08s, 2\Pi T_{12}$ $=0.15p.u.MW, 2\Pi T_{23}=0.15p.u.MW, 2\Pi T_{31}=0.15p.u.MW, T_{RH}=48.7s, T_{RS}=5s, T_{GH}=0.51s,$ $T_W=1s, X=0.6, Y=1, b=0.05, c=1, T_F=0.23s, T_{CR}=0.01s, T_{CD}=0.2s, Kr=0.5, Tr=10s, \alpha°=15, \beta°$ $=25, BESS=10MW/40MWh, Battery\text{-}voltage=1755\text{-}2925Vdc, K_{BESS}=100kV/puMW,$ $c_{bp}=52597F, r_{bp}=0.013ohm, X_{c0}=0.0274ohm, I^0{}_{BESS}=4.426kA, T_{BESS}=0.026s.$

BIODATA

Objective   To attain good position and maintain cordial relationship in Academic Institution by giving the practical knowledge which makes the student's career progressive.

Teaching Experience-19 years

Worked as a Lecturer in G.P.M.C.E. (15-01-2002 to 17-09-2007)
Worked as a Sr. Lecturer in G.P.M.C.E. (18-09-2007 to 06-01-2011)
Working as an Asst. Prof in Maharaja Surajmal Institute Of Technology, under I.P. University , Delhi (since 7th Jan. 2011).

Educational Qualification

PHD. (2011) - pursuing Phd in Power System from DTU , Delhi.
M.E.(2003-2006) in Power Apparatus And System from D.C.E.(71.4%)
B.Tech(1997-2001) in Electrical Engg. With 66.5% from A.I.E.T, Faridkot (Punjab) under Punjab Technical University, Jallandhar (Pb.)

School Happy Model School, New Delhi-58
Class12th (1997)-74.5%
Class10th(1995)-Maths 99%, Science 85%, Agg 69%

Software Exposure

Operating System- Win 2010, Dos,   Programming Language – C,C++,Core Java, Html, Auto Cad, Matlab

Personal Profile

Date Of Birth   09-03-1980

Husbands Name   Mr. Vikas Gupta

Marital Status   Married

Language Known   English, Hindi, Punjabi, Sanskrit

Hobbies

Solving Puzzles, Dancing, Listening Music, Reading mythological Books, Listening motivating lectures, learning latest Technology and encouraging students.

Professional memeber

I am a member of IEEE society.

LIST OF PUBLICATIONS

1. Nidhi Gupta, Narendra Kumar, B. ChittiBabu "JAYA Optimized Generation Control Strategy for Interconnected Diverse Source Power System with Varying Participation" Energy Sources, Part A: Recovery, Utilization, and Environmental Effects, Taylor and Francis, June 2019. SCI, Impact Factor-3.447, ISSN: 1556-7036 (Print) 1556-7230, 44, no. 1 (2022): 1813-1829.

2. Nidhi Gupta, Narendra Kumar "Particle Swarm Optimization based Automatic Generation Control of Interconnected Power System incorporating Battery Energy Storage System" Scopus indexed, Elsevier, Procedia Computer Science, Volume 132, 2018, Pages 1562-1569, ISSN: 1877-0509, UGC-46138, DOI:10.1016/ j.procs. 2018.05.12, April 2018.

3. Nidhi Gupta, Narendra Kumar, "AGC of Three Area Interconnected Power System Incorporating SMES" in International Journal of Industrial Electronics and Electrical Engineering , UGC- 43965, ISSN(p)- 23476982, ISSN(E): 2349204X, VOL.6 , Issue - 1, Jan 2018.

4. Nidhi Gupta, Narendra Kumar, Nisha Singh "PSO Tuned AGC Strategy of Multi Area Multi-Source Power System Incorporating SMES", International Conference on 2018 2nd IEEE International Conference on Power Electronics, Intelligent Control and Energy Systems (ICPEICES-2018), DTU Delhi, October 22nd -24th, 2018.

5. Nisha Singh, Narendra Kumar, Nidhi Gupta et. al "A Comparative Analysis of AGC of Two-area Hydro-Thermal Power System Interconnected by AC-DC Parallel Link in Restructured Power System" 2018 2nd IEEE International Conference on Power Electronics, Intelligent Control and Energy Systems (ICPEICES-2018) , DTU Delhi, October 22nd -24th, 2018.

6. Nidhi Gupta, Narendra Kumar presented the paper in the National Electrical Engineering Conference (NEEC-2011) held w.e.f. 16th -17th Dec, 2011 on "Power and Energy Systems for Tomorrow" at Delhi Technical University, Delhi.

nidhi gupta

Unknown affiliation

	All	Since 2016
Citations	10	10
h-index	2	2
i10-index	0	0

TITLE	CITED BY	YEAR
JAYA optimized generation control strategy for interconnected diverse source power system with varying participation N Gupta, N Kumar, CB Babu Energy Sources, Part A: Recovery, Utilization, and Environmental Effects, 1-17	5	2019
Particle swarm optimization based automatic generation control of interconnected power system incorporating battery energy storage system N Gupta, N Kumar Procedia computer science 132, 1562-1569	5	2018
A Comparative Analysis of AGC of Two-area Hydro-Thermal Power System Interconnected with AC-DC Parallel Link in Restructured Power System N Singh, N Kumar, Y Arya, N Gupta 2018 2nd IEEE International Conference on Power Electronics, Intelligent …		2018
PSO Tuned AGC Strategy of Multi Area Multi-Source Power System Incorporating SMES N Gupta, N Kumar, N Singh 2018 2nd IEEE International Conference on Power Electronics, Intelligent …		2018
Automatic generation control of three area interconnected thermal hydro thermal system by integral controller and optimal controller NGN Kumar Proceedings of National Electrical Engineering Conference, Power & Energy …		2011

224